

# **ELECTROKINETIC REMEDIATION OF METAL-CONTAMINATED SOILS**

**A Thesis Submitted  
in Partial Fulfillment of the Requirements  
for the Degree of**

**DOCTOR OF PHILOSOPHY**

**by**

**SONAM TANEJA  
(2K20/PHDEN/04)**

**Under the Supervision of**

**Prof. A.K. HARITASH  
Delhi Technological University  
India**

**Dr. ÖZNUR KARACA  
Çanakkale Onsekiz Mart University  
Turkey**



**Department of Environmental Engineering**

**DELHI TECHNOLOGICAL UNIVERSITY  
(Formerly Delhi College of Engineering)  
Shahbad Daultpur, Main Bawana Road, Delhi-110042. India**

**December, 2024**



# **DELHI TECHNOLOGICAL UNIVERSITY**

(Formerly Delhi College of Engineering)

Shahbad Daultpur, Main Bawana Road, Delhi-42

## **CANDIDATE'S DECLARATION**

I, Sonam Taneja, hereby certify that the work which is being presented in the thesis entitled “Electrokinetic Remediation of Metal-contaminated Soils” in partial fulfillment of the requirements for the award of the Degree of Doctor of Philosophy, submitted in the Department of Environmental Engineering Delhi Technological University is an authentic record of my own work carried out during the period from August, 2020 to September, 2024 under the supervision of Prof. A. K. Haritash, Department of Environmental Engineering, Delhi Technological University, and Dr. Öznur Karaca, Department of Geological Engineering, Çanakkale Onsekiz Mart University, Turkey.

The matter presented in the thesis has not been submitted by me for the award of any other degree of this or any other Institute.

**Sonam Taneja**



# DELHI TECHNOLOGICAL UNIVERSITY

(Formerly Delhi College of Engineering)

Shahbad Daulatpur, Main Bawana Road, Delhi-42

## CERTIFICATE BY THE SUPERVISORS

Certified that **Sonam Taneja** (2K20/PHDEN/04) has carried out the research work presented in this thesis entitled **“Electrokinetic Remediation of Metal-contaminated Soils”** for the award of **Doctor of Philosophy** from Department of Environmental Engineering, Delhi Technological University, Delhi, under our supervision. The thesis embodies results of original work, and studies are carried out by the student herself and the contents of the thesis do not form the basis for the award of any other degree to the candidate or to anybody else from this or any other University/Institution.

**Prof. A. K. Haritash**

Professor

Deptt. of Environmental Engineering

Delhi Technological University

India

**Dr. Öznur Karaca**

Associate professor

Deptt. of Geological Engineering

Canakkale Onsekiz Mart University,

Turkey

Date:

## ACKNOWLEDGEMENT

I would like to take this opportunity to express my deepest gratitude to all those who have supported me throughout the journey of completing my thesis. Firstly, I would like to express my sincere gratitude to my supervisor, Prof. A. K. Haritash, for his invaluable guidance, constant support, and encouragement throughout the research process. His unwavering support and expertise have been pivotal in shaping the direction and depth of this work. I would also like to thank my co-supervisor, Dr. Öznur Karaca, Çanakkale Onsekiz Mart University (ÇOMU), Turkey, for accommodating me in her lab and providing the necessary facilities required for the work.

I would like to extend my sincere thanks to the faculty and staff of the Department of Environmental Engineering, Delhi Technological University for providing the necessary resources and creating an environment conducive to research. I would also like to thank the members of Analytik Jena, Patparganj, Delhi, for letting me work in their lab.

I sincerely express my gratitude to the International Office at Delhi Technological University, DTU, and the International Office at ÇOMU, Turkey, especially Hakan Basaran, for facilitating my visit to Turkey, for the incredible opportunity to work at ÇOMU, and for making this cross-cultural experience possible. I would also like to thank Dr. Çetin Kantar and his scholars, Ms. Özlem, and Ms. Iremsu, for their unwavering guidance and support throughout my time at ÇOMU.

I am thankful to my colleagues and friends, for the shared experiences, and moral support, which have helped me stay motivated and focused during the challenging times. I am especially thankful to my family for their endless patience, love, and encouragement. Their belief in me has been my strength throughout this journey. To everyone who has contributed, directly or indirectly, to the successful completion of this thesis, I offer my heartfelt appreciation.

**Sonam Taneja**

## ABSTRACT

The issue of soil pollution has been recognized as a significant concern that poses a threat to human health and well-being. Remediating surface and sub-surface areas that have been contaminated, particularly with heavy metals, is a serious challenge due to the persistent and non-biodegradable nature of metals. The conventional treatment methods for soil cleanup have limitations pertaining to the labor-intensive nature, substantial costs, and time-consuming requirements. Therefore, it is imperative to come up with an innovative technique to overcome these limitations. Electrokinetic Remediation (EKR) is a developing technique to remediate metal-contaminated soils. The treatment method involves the application of direct current across the soil, which leads to the migration of contaminants through different transport mechanisms like electromigration, electro-osmosis, and electro-phoresis. EKR has gained much attention in the past decade due to the ability to remove contaminants *in situ* from a wide range of matrices irrespective of heterogeneity. Although, many researchers have proved its applicability to remove metals in laboratory experiments, and some field tests, there is still a lack of understanding of complicated electrochemical reactions and soil properties upon varying the operating conditions of EKR. Therefore, the present study aims to examine the feasibility of EKR to remediate metal-contaminated soils, particularly, Hexavalent Chromium, Lead, and Cadmium, and to investigate the effect of three main operating variables, applied voltage, electrolyte composition, and electrode material. In addition, the effect of different electrode configurations was also investigated on mixed metal-contaminated soils. The experiments were performed on a laboratory-scale EKR setup. The findings revealed that the application of high-voltage (2.5 V/cm) against the lower voltage (1.5 V/cm, as stated in earlier literature) had no significant effect on soil health. Periodic voltage application (Day-on, Night-off) yield better removal and save energy which is an essential factor to take into account for practical applications of EKR. A significant removal of metals was achieved with EKR in a shorter period of 10 h in the order Cr (77%) > Pb (65%) > Cd (30.2%) when a combination of electrolyte amendment with EDTA (0.1 M) with high voltage gradient was employed. The rate of removal only slightly increased when the concentration of EDTA increased from 0.1 M to 0.2 M,

but the extra input of chemicals added to the cost of the treatment. Thus, the optimum conditions were found to be the combination of high voltage application and 0.1 M EDTA amendment. The application of surfactant as an electrolyte did not improve the efficiency of soil EKR toward the removal of heavy metals. The formation of sharp pH zones in the soil was not found, instead, the pH remained neutral to slightly basic in all experiments. Upon the characterization of soil after EKR treatment for its physical and chemical properties, it was found that the treated soil resulted in improved plastic limit and liquid limit suggesting improved stability of the soil and reduced concentrations of sulphates, further enhancing the soil quality. EKR proved suitable for the treatment of soils contaminated with single metal as well as a multi-metal matrix with almost equal efficiency. The results obtained on comparison of different electrode configurations indicated that the square configuration was able to minimize the inactive electrical zones and yield maximum removal, followed by the trigonal configuration. Considering the efficiency and cost-benefit analysis, it is observed that EKR is suitable for treating the metal-contaminated soil, along with the removal of other organic contaminants, thereby bringing the environmental toxicity down in the soil. The optimization of regulating parameters can not only improve the efficiency of treatment but can also bring the cost of treatment down to a significant level.

## **List of Tables**

<b>Table No.</b>	<b>Title of the table</b>	<b>Page No.</b>
2.1	Maximum concentration (mg/kg) of selected heavy metals in the soil as reported in the literature	8
2.2	Maximum allowable levels of some selected heavy metals in soil and their potential effects on human health	9
2.3	Performance of EKR towards metal removal with variable power and electrode configurations	30-31
2.4	Summary of performance of EKR on different matrices using electrolyte enhancements	36-37
2.5	Summary of technological and economic feasibility, and major challenges of EKR-coupled technologies	47
2.6	Cost comparison of different remediation technologies as reported in previous literature studies	49-50
2.7	Some selected field scale studies of EKR	51
3.1	The selected voltage gradients (V/cm) at which EKR was run for different metal-contaminated soils	69
3.2	The selected electrode configurations used to run EKR for different metal-contaminated soil	70
3.3	The selected electrolyte solutions used to run EKR for different metal-contaminated soil	71
3.4	Selected values for the variables used in HHRA (USEPA, 1989)	87-88
3.5	Reference Dose and Slope Factor of the selected metals	88
4.1	Details of experimental conditions used for EKR of Cr (VI)-contaminated Soil	90
4.2	The variations in pH, EC, TDS, volume, and Cr (VI) concentration in anolyte and catholyte after EK treatment	95-96
4.3	The variations in pH, EC, TDS, moisture content, and Cr (VI) concentration in soil before and after EK treatment	97-99
4.4	Variations in Current (Amperes) with time during the EKR of Cr (VI)-contaminated soils	102

4.5	Removal percentage and mass balance of chromium metal in different fractions at the end of the electrokinetic test	106
4.6	Characterization of soil health before and after EKR treatment	111
4.7	Energy consumption and cost analysis for different combinations during EKR of Cr-contaminated Soil	114
4.8	The design of experiments for EKR of Pb-contaminated Soil under different operating conditions	115
4.9	The variations in pH, EC, TDS, volume, and Pb concentration in anolyte and catholyte after EK treatment	120-122
4.10	Variations in Current (Amperes) with time during the EKR process	126
4.11	The variations in pH, EC, TDS, moisture content, and Pb concentration in soil before and after EK treatment	129-132
4.12	The compartmentalization of Pb in soil, electrolyte (catholyte and anolyte), electrode material and filter during different sets of EKR	133
4.13	The characteristics of soil before and after EKR	140
4.14	The economic analysis of EKR to determine the cost of Pb removal (\$/g of Pb) from contaminated soil	141
4.15	Comparison of Pb removal of this study with previously published literature	142
4.16	Experimental Design for EKR of Cd-contaminated Soil using RSM	143
4.17	Experimental design for EKR of Cd-contaminated Soil using stainless steel as electrode	144
4.18	The variations in pH, EC, TDS, volume, and Cd concentration in anolyte and catholyte after EK treatment	147-149
4.19	Regression Analysis and ANOVA of response Electro-osmotic Volume	152
4.20	Regression Analysis and ANOVA of Response Removal Efficiency	155
4.21	Regression Analysis and ANOVA of Response Energy consumption per gram removal of Cd	158
4.22	Experimental conditions for EKR of mixed-metal contaminated Soil	159
4.23	pH, EC, and TDS values of electrolytes and soil sections after EK treatment	159



4.24	Experimental design for EKR of mixed-metal contaminated soil with varying electrode configuration	165
4.25	Variations in Current (Amperes) with time during the EKR process	170
4.26	Hazard Index categories given by USEPA	173
4.27	Total daily intake (mg/kg/day) via ingestion, inhalation, and dermal contact pathways, and HI for Cr (VI), Pb, and Cd in adults and children	174
4.28	Carcinogenic risks of adults and children under different exposure pathways	176
4.29	Score indicator set for each criterion selected on the basis of the experiments	177
4.30	A Weighted Decision Matrix (WDM) designed to select the optimized conditions for EKR	179

## List of Figures

<b>Figure No.</b>	<b>Caption of the figure</b>	<b>Page No.</b>
1.1	Sustainable Development Goals (SDGs) linked to Soil Pollution	6
2.1	The sources of metals in the environment, its interaction, and effects of soil, plants, and Human Health	11
2.2	Schematic diagram of Electrokinetic Remediation (EKR) and major transport processes	15
2.3	Assembly set-ups of some integrated-EKR technologies	38
2.4	An overview of enhancement strategies for major operating components of EKR, and the sustainable alternatives offered	56
3.1	Flowchart of the methodology adopted for this study	65
3.2	(a) Schematic diagram of EKR setup used in this study (1) soil cell (2) anode well (3) cathode well (4) DC Power Supply (5) anode (6) Cathode (7) Nylon Mesh (8) Electrolyte reservoirs (b) EKR assembly used for this study	67
3.3	Schematic representation of the soil cell setup for trigonal and square configuration	68
3.4	Flame photometer used for the analysis of cations ( $\text{Na}^+$ , $\text{K}^+$ , $\text{Ca}^{2+}$ )	75
3.5	Standard curve of concentration (mg/L) against absorbance obtained for Pb	79
3.6	Standard curve of concentration (mg/L) against absorbance obtained for Cd	80
3.7	Flame Atomic Absorption Spectrophotometer (AAS) at (a) Water lab, DTU (b) at Environment lab, ÇOMU, Turkey	84
4.1	Variations in pH of soil after EKR treatment under different conditions (a) controlled conditions at four different applied voltage (b) enhanced with EDTA at 20 V (c) enhanced with EDTA at 50V	93
4.2	Variations in Electrical conductivity (EC) of soil after EKR treatment under different conditions (a) controlled conditions at four different applied voltage (b) enhanced with EDTA at 20 V (c) enhanced with EDTA at 50V	94

4.3	Variations in current in soil during EKR treatment under different conditions (a) unenhanced with four different applied voltage (b) enhanced with EDTA at 20 V (c) enhanced with EDTA at 50V	100-101
4.4	Electro-Osmotic flow (EOF) in soil measured by change in volume (ml) in anolyte and catholyte post-EKR treatment	104
4.5	Percentage removal of chromium from soil after EKR treatment (a) under the applied voltage of 20V, 30V, 40V and 50V, and (b) under varying conditions of electrolyte and electrode material at low (20V) and high voltage (50V).	107
4.6	Distribution of residual chromium in soil sections S1-S4 from anode to cathode	109
4.7	Variations in pH of anolyte, catholyte, and soil after EKR treatment in experiments with distilled water, EDTA, and Tween 80 as electrolyte	117
4.8	Variations in Electrical conductivity (EC) of soil after EKR treatment under different conditions (a) unenhanced tests at applied voltages from 50 V to 20 V with Graphite and Stainless Steel electrode (b) enhanced with EDTA (c) enhanced with Tween 80	119
4.9	Variations in current in the soil during EKR treatment in experiments with DW, EDTA, and Tween 80 as electrolyte	124-125
4.10	Electro-osmotic Flow (EOF) (ml) in anolyte and catholyte at 50 V after EKR treatment	127
4.11	Distribution of residual Pb in soil sections S1-S4 from anode to cathode in EKR setup	134-135
4.12	Percentage distribution of (a) Pb-hydroxides complexes in unenhanced EKR (b) Pb-EDTA complexes in enhanced EKR against pH of soil using Visual Minteq Program (v 3.1)	138
4.13	Variations in pH of electrolytes and soil	145
4.14	Variations in electrical conductivity in soil sections	146
4.15	Variations in TDS in soil sections for all the runs	146
4.16	(a) 3-D and (b) Contour response surface plots of EOv against variables A and B	151

4.17	(a) 3-D and (b) Contour response surface plots of Removal Efficiency of EKR for Cd against variables A and B	154
4.18	(a) 3-D and (b) Contour response surface plots of Energy consumption per gram removal of Cd against variables A and B	156-157
4.19	Variation in current intensity (mA) during EK treatment of mixed metals	160
4.20	Removal rate and the normalized residual concentration of Cr (VI), Cd, and Pb in the soil	161
4.21	Removal efficiencies of metals in individual metal-contaminated soil and mixed-metal-contaminated soils	162
4.22	Percentage distribution of metals in different fractions from the sequential extraction procedure	164
4.23	Variations in pH and EC of soil for (a) linear (b) trigonal (c) square configuration	167
4.24	Experimental setups for electrode configurations, Linear, Trigonal, and Square marked with the nomenclature of soil sections taken. (Left to Right)	168
4.25	Variations in current intensity (mA) in experiments I, II, and III during EKR	169
4.26	Variations in Electro-osmotic Volume (EOF) in anolyte and catholyte for experiments I, II, and III after EKR	171
4.27	Normalized residual concentration of metals in soil in (a) Linear, (b) Trigonal, and (c) Square assemblies	172

## List of Abbreviations

AC	Alternate Current
ADD	Average Daily Dose
APHA	American Public Health Association
ASTM	American Society for Testing and Materials
AT	Average Exposure Time
BW	Body Weight
Cd	Cadmium
Cr (VI)	Hexavalent Chromium
DC	Direct Current
EC	Electrical Conductivity
ED	Exposure Duration
EDTA	Ethylenediaminetetraacetic Acid
EF	Exposure Frequency
EKR	Electrokinetic Remediation
EOF	Electro-osmotic Flow
ESA	Exposed Skin Surface Area
HDPE	High Density Polyethylene
HI	Hazard Index
HQ	Hazard Quotient
LDH	Layered Double Hydroxided
MFC	Microbial Fuel Cell
PAH	Polyaromatic Hydrocarbons
Pb	Lead
PEF	Particle Emission Factor
RfD	Reference Dose

SAF	Soil to Skin adherence
SDG	Sustainable Development Goals
SF	Slope factor
TCR	Total Carcinogenic Risk
TDS	Total Dissolved solids
TOC	Total Organic Carbon
USEPA	United States Environmental Protection Agency
WHO	World Health Organization

# CHAPTER 1

## INTRODUCTION

Soil is one of the essential resources available to mankind being the backbone of agriculture and the foundation for food security. It is the ultimate recipient of the contaminants, with its innate ability to filter, buffer, retain, and degrade contaminants. The components of soil, mainly organic matter, inorganic nutrients, air, and water govern the filtering capacity of soil. However, the increasing population, urbanization, and industrialization have led to increased consumption and subsequent waste generation that is ultimately dumped onto the land. This leads to the release of pollutants like toxic organic compounds and heavy metals into the soil and tampers with the natural attenuation capacity of the soil leading to soil pollution. The pollutants also tend to disrupt the physical structure and biological entities of soil. The degradation of soil quality significantly impacts the agricultural sector, adversely affecting crop yield and quality. Thus, the issue of soil pollution has been recognized as a significant concern that threatens human health, overall well-being, and the proper functioning of sub-surface environments. Hence, it is imperative to remediate contaminated soils to enhance their quality and safeguard human well-being.

### **1.1. Soil pollution due to heavy metals**

Over the decades, widespread soil contamination has increased due to excess waste generation, irresponsibly being dumped in water bodies and over the land areas. The complexity of pollution increases when the regions are contaminated with inorganic pollutants like heavy metals due to their non-biodegradable nature and prolonged persistence. Heavy metals are inorganic contaminants with high atomic mass and a density of more than  $5 \text{ g/cm}^3$ . The metals are generally introduced from a geogenic origin, for example, volcanic eruptions,

weathering of rocks, etc. (Hanfi et al., 2019). Metals like iron (Fe), zinc (Zn), manganese (Mn), copper (Cu), and nickel (Ni) serve as essential plant nutrients in low concentrations (Raffa et al., 2021). However, anthropogenic activities like mining, the use of fertilizers, transportation, waste disposal, etc. accelerate the release of toxic metals like Cadmium (Cd), Lead (Pb), Chromium (Cr), etc. in the environment (Karaca et al., 2019; Wuana & Okieimen, 2011).

According to Liu et al. (2018), more than 5 million sites, including over 20 million hectares of land worldwide, have been contaminated by various heavy metals. In the Indian context, the status of metal pollution in the soil is scarce due to the lack of soil contamination and pollution monitoring systems. However, based on a study by Kumar et al. (2019), trace element concentrations in Indian soils have exceeded the Indian national guideline values significantly over the past 20 years due to very rapid economic growth through industrial, agricultural, and mining activities. Metals once introduced into the environment persist in nature for prolonged periods in different chemical forms. The state in which the metal occurs influences its bioavailability and hence, its toxicity (Rajendiran et al., 2015; Wuana & Okieimen, 2011).

The increasing concentration of toxic metals in soil influences soil microbiology by changing its population, diversity, and growth, leading to reduced soil fertility, stunted plant growth, and necrosis (Krishna & Govil, 2007). Soil can also serve as a potential source for releasing contaminants into the aquatic systems, posing the risk of groundwater contamination. Metal toxicity in humans can cause serious chronic implications by affecting the central and peripheral nervous system, causing kidney failure, cardiovascular diseases, and intestinal damage (Silva et al., 2018; Taneja et al., 2024). It enters the human body via the dermal or oral route and can cause acute poisoning like dizziness, fatigue, headache, and memory loss (Raffa et al., 2021). Thus, heavy metal toxicity is a concern for the environment and public health, necessitating the need to remediate such soils. Remediating surface and sub-surface areas that have been contaminated poses significant challenges due to the labor-intensive nature, substantial costs, and time-consuming requirements.



## **1.2. Treatment of metal-contaminated soils**

Depending on the type of contaminant to be extracted, type of soil, and cost-effectiveness of methods, many traditional approaches for *in-situ* and *ex-situ* soil remediation have been used in the past such as soil flushing, bioremediation, phytoremediation, electrokinetic remediation, etc. (Cameselle et al., 2013; Liu et al., 2018; Naz et al., 2018; Rajendiran et al., 2015; Wuana & Okieimen, 2011). Physical methods such as vitrification, landfilling and drilling, soil excavation, and other engineering developments provide long-term solutions in a limited amount of time. However, these methods are energy and cost-extensive techniques and can only be used on a small area of land (Rajendiran et al., 2015). Solidification/stabilization technique immobilizes the contaminants which leaves the risk of future mobilization of contaminants. Chemical techniques such as soil washing and *in-situ* flushing employ chemical treatment of the soil, but this can lead to contamination of the soil due to the chemicals used in this treatment. Another drawback of this kind of technology is the insufficient delivery of chemicals in low-permeability soils and, therefore, low removal efficiency (Khalid et al., 2017). Biological approaches like bioremediation and phytoremediation are sustainable, low-cost, and environmentally friendly ways of removing contaminants from soils by natural processes with no significant modification of the properties and texture of the soil after the treatment (Cameselle et al., 2013). However, their applicability is limited to the treatment of low-concentration metals and for a single contaminant at a time. Besides, the remediation is restricted to surface soils accessible to plant roots (Zhou et al., 2005). These conventional techniques, although successful to some extent, have certain limitations in treating persistent and non-biodegradable heavy metals.

## **1.3. Electrokinetic Remediation**

Electrokinetic Remediation (EKR) is a developing technique that uses a low-voltage electric current between the electrodes to eliminate contaminants from the soil. Unlike soil flushing and washing, EKR can be used on both coarse and fine-grained soils since the removal mechanism is independent of pore size

(Yeung et al., 1997). Under the influence of an electric field, the ionic species present in the soil appear to move to the oppositely charged electrodes when the soil is positioned between two electrodes connected to an external power supply. A low direct current induces the key processes in the soil, that is electrolysis, electromigration, electro-osmosis, and electro-phoresis, which are responsible for the movement of metal ions within the soil (Alshawabkeh et al., 1999). EKR is a promising technique widely being used to remove heavy metals, organic compounds, and other inorganic compounds. Researchers have applied EKR to evaluate its efficiency in different soil types, sediments, acid mines, and groundwater.

*In-situ* application with minimal soil disruption, non-specificity of contaminants, and suitability for low permeable soils makes EKR a superior technology to conventional techniques like soil washing, vitrification, and bioremediation (Reddy & Shirani, 1997). The effective migration of metals in soil depends upon the solubility of metal ions into the soil pore fluid. The application of electric current has a slight effect on the geochemical properties of soil such as pH, redox, moisture content, etc. which influence the solubilization and mobility of metals in soil (Al-Hamdan & Reddy, 2008). EKR allows regulation of operating parameters like voltage, current, electrode material, electrolyte composition, etc. to increase metal solubility and thus, enhance its efficiency (Benamar & Baraud, 2011).

#### **1.4. Research gaps**

- I. Comprehensive studies on the characterization and identification of pollutants in contaminated soils on a national level are limited in most countries, including India.
- II. Conventional methods, mainly chemical treatment methods such as soil washing, are widely adopted due to higher removal rates. However, the technique being *ex-situ* increases the cost of transportation, disturbs the physical landscape, and poses a risk of secondary pollution to the environment.

- III. Biological methods like phytoremediation are sustainable and green remediation strategies. However, with a metal removal rate of 5-10%, the technique is unsuitable for highly contaminated soils such as mine tailings. The process, being dependent on the life span of the plants (sometimes in years), is time-consuming and extends the treatment duration.
- IV. Many researchers have proposed Electrokinetic Remediation as an alternative method for high-contaminated regions. However, most studies are conducted on commercial fine-grained soils, such as kaolinite. Though it is imperative to understand the behaviour of metals in low-permeable soil for effective removal, metal contamination usually occurs in heterogeneous soil. Thus, limited research is available on the feasibility of EKR for naturally-contaminated soils.

### **1.5. Objectives of the study**

Considering the knowledge gaps associated with the remediation of metal-contaminated soils, particularly EKR, the following objectives are devised for this study.

- I. Characterization of contaminated soil, spiking and sequential extraction of heavy metals.
- II. To assess the feasibility of EKR for heavy metal-contaminated soils.
- III. To study the effect of variables like electrolyte composition, electrode material, pH of soil, and current intensity on the efficiency of EKR.
- IV. To study the inter-ionic effects towards the efficiency of EKR.
- V. To optimize the efficiency of EKR with the help of Response Surface Methodology (RSM).

## 1.6. Scope and relevance of the study

The characterization and identification of the number of potentially contaminated sites specifically mine-tailings, industries, regions around the landfill, etc. are lacking in India. There is an urgent need for the characterization, identification, and treatment of such contaminated sites with cost-effective and efficient *in-situ* methods. The present study is aimed at overcoming the limitations of existing soil remediation strategies and devising an optimized EKR technique to remediate highly contaminated sites. Further to add scientific and engineering value, the operating conditions of EKR are to be analyzed and the cost of treatment is to be estimated, which is not reported in most of the studies in the literature. The social relevance of this study lies in the human health risk assessment which is performed to assess the efficacy of EKR to reduce toxicity and the subsequent adverse effects on public health. The improvement in soil quality and public health through EKR would help in achieving the Sustainable Development Goals (SDGs), specifically SDG 2: Zero Hunger, SDG 3: Good health and well-being, and SDG 15: Life on Land (FAO, 2021). The direct and indirect linkages of SDGs to soil remediation are given in Fig 1.1.

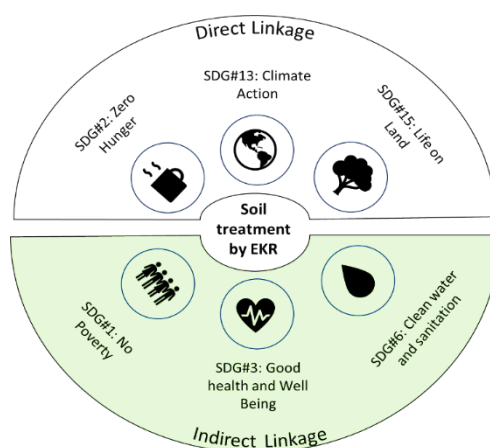


**Fig 1.1** Sustainable Development Goals (SDGs) linked to Soil Pollution

## CHAPTER 2

### REVIEW OF LITERATURE

Heavy metals are inorganic contaminants with high atomic mass and a density of more than 5 g/cm<sup>3</sup>. The metals are generally introduced from a geogenic origin, for example, volcanic eruptions, weathering of rocks, etc. (Hanfi et al., 2019). Metals like iron (Fe), zinc (Zn), manganese (Mn), copper (Cu), and nickel (Ni) serve as essential plant nutrients in low concentrations (Raffa et al., 2021). However, anthropogenic activities like mining, the use of fertilizers, transportation, waste disposal, etc. accelerate the release of toxic metals like Cadmium (Cd), Lead (Pb), Chromium (Cr), etc. in the environment (Bolan et al., 2014; FAO, 2021). The most metal-polluting activities have been identified to be plating industries, and mining and metallurgical processes (Table 2.1).

#### 2.1. Heavy metal contamination in soil

The rate of metal contamination in the soil has increased over the past decades. Higher concentration of heavy metals in soil is a grave concern due to the non-biodegradable nature and translocation through the food chain, which pose health risks to humans and animals (Liu et al., 2018). The maximum allowable levels of selected heavy metals in soil and their potential effects on human health are given in Table 2.2. In order to address the issue of metal contamination in soil, it is crucial to understand the mechanisms of metal interactions with the environment. Further, the soil-metal interaction is beneficial in selecting the most suitable treatment methods to remediate contaminated soils.

**Table 2.1** Maximum concentration (mg/kg) of selected heavy metals in the soil as reported in the literature

S. No.	Soil type	Cr	Pb	Cd	References
1	Coal mine waste	833	311	2.6	Chandra et al., 2024
2	Mine waste	7020	1435	87	Kumar et al., 2019
3	Mine waste	171	56	21	Yellishetty et al., 2009
4	Mine tailings	70	41	11	Yellishetty et al., 2009
5	Industrial waste	-	530	224	Moturi et al., 2004
6	Mine waste	-	783	59	Benvenuti et al., 1997
7	Pb-Zn mine	-	1655	10	Kasemodel et al., 2019
8	Pb-Zn mine	41.7	1435	41	Banerjee et al., 2023
9	Chromite Mine	3120	105	1.6	Kumar & Maiti, 2015
10	Industrial waste	2652	206	34	Kumar et al., 2019

## 2.2. Soil-metal interactions

The metals are introduced into the environment through various natural and anthropogenic activities (Fig. 2.1). Once the metal is in the atmosphere, it is partitioned into water and soil through different processes. In soil, metals exist in three forms, dissolved in soil solution, adsorbed on soil particles, or as precipitates. These three broad forms are dependent upon the soil characteristics like pH, cation exchange capacity (CEC), soil mineralogy, microbial and biological conditions, and the presence of soil inorganic and organic ligands which greatly influence the bioavailability and in turn, the toxicity of heavy metals in soil (Wuana & Okieimen, 2011).

**Table 2.2** Maximum allowable levels of selected heavy metals in soil and their potential effects on human health (as per WHO, 1993)

<b>Metal</b>	<b>Sources</b>	<b>Maximum allowable limits for soil (mg/kg)</b>	<b>Effects on Human Health</b>
Cd	Electroplating, Batteries, Fertilizers	<3	Renal dysfunction, coronary heart disease, osteomalacia, periphery artery disease (Genchi et al., 2020)
Pb	Batteries, Paints	<300	Kidney failure, intestinal damage, cardiovascular diseases (Silva et al., 2018)
Cr	Timber treatment, Leather tanning, Dyes	<150	Gastrointestinal haemorrhage, pulmonary fibrosis, DNA alteration, (Pavesi & Moreira, 2020)
Cu	Industrial waste, pipes, Additives, Fungicides	<140	Cystic fibrosis, insomnia, Wilson disease, kidney damage (Wuana & Okieimen, 2011)

The portioning of metals in these three forms is influenced by geochemical processes mainly, sorption/desorption, precipitation/dissolution, and oxidation/reduction (Bolan et al., 2014). Sorption refers to the partitioning of ion from soil pore fluid onto the soil particle through adsorption by electrostatic forces of attraction or ion-exchange (Yan et al., 2022). It depends upon type of contaminant, soil and pore fluid characteristics like pH. Sorption processes decrease the bioavailability of metal ions by immobilizing it temporarily. Desorption on the other hand, releases the adsorbed metal ions, increasing its bioavailability. Precipitation of metal cations occur at high pH in the presence of anions like carbonates, sulphates, hydroxides etc. Formation of metal precipitates leads to immobilization of metals like Pb and Cu. Metals are susceptible to microbial

oxidation/reduction, which influence their speciation and mobility (Liu et al., 2018). Oxidation of trivalent Cr to hexavalent Cr increases the solubility of metal, thus its bioavailability and toxicity (Pavesi & Moreira, 2020). On the other hand, oxidation of Arsenic (As) from As (III) to As (V) causes immobilization as As (V) is retained strongly by soil (Taneja et al., 2023). The solubility of metals may also lead to leaching posing a risk of groundwater contamination. When the metals are present in higher concentrations, they tend to accumulate in the soil or are taken up by plants, impairing the health of the ecosystem. Due to this, alleviating the metal concentration is essential to prevent adverse effects on soil and living beings.

### **2.3. Remediation technologies for metal-contaminated soils**

The selection of suitable remediation alternatives can be done based on their ability to alleviate metal-associated risks. The removal of metals from soil depends mainly on the properties of the soil which influence the degree of soil-metal binding (Bolan et al., 2014). In case of fine-grained soil, techniques like soil washing are not successful due to the low permeability of such soils which does not allow the washing agents to uniformly act upon (Yeung et al., 1997). Similarly, alkaline soils with high pH promote adsorption and complexation of metals with soil rendering it difficult (Al-Hamdan & Reddy, 2008). Various site remediation technologies can be employed for reclamation, which can be divided into physical, chemical, and biological methods, as discussed below.



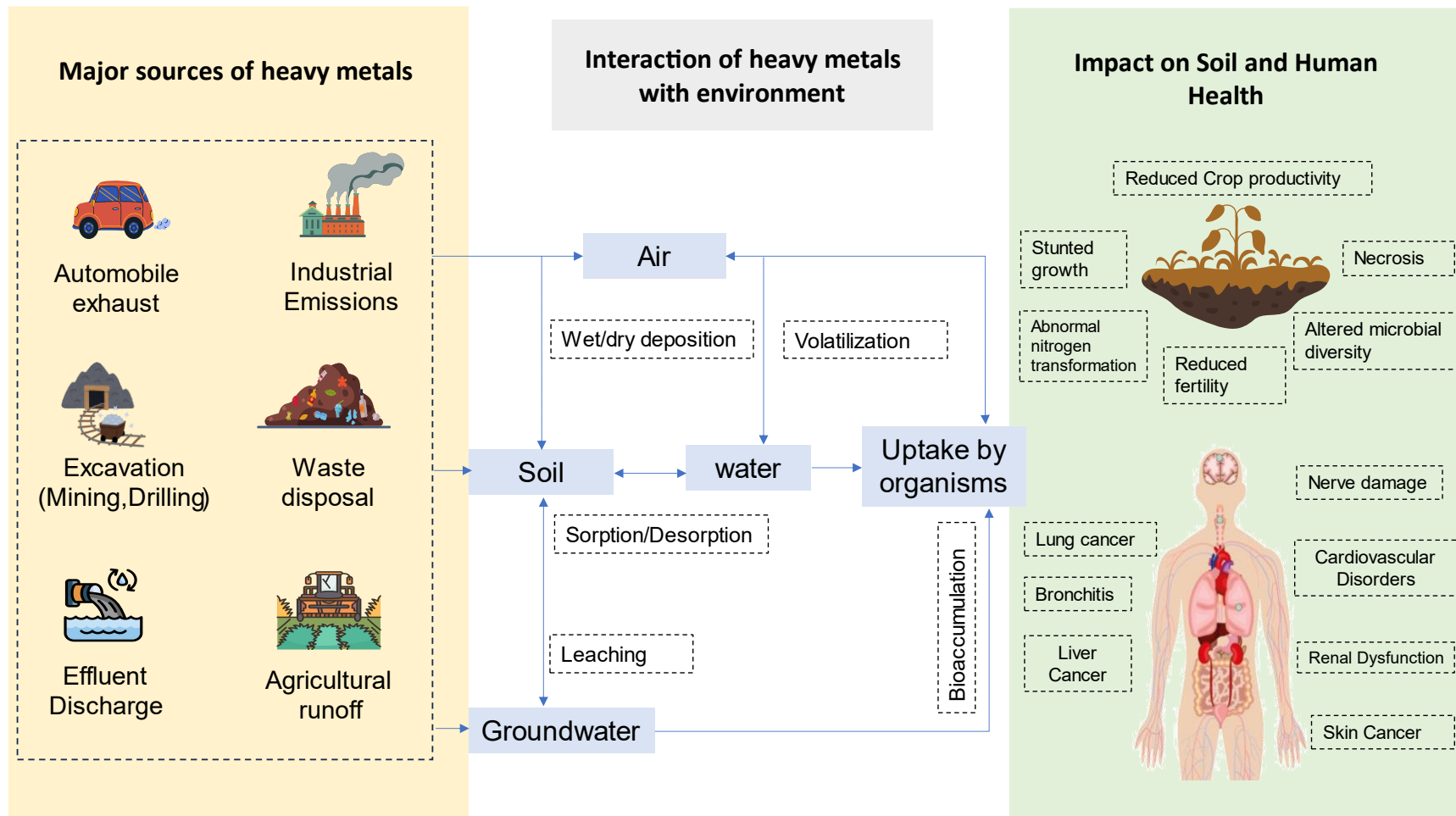


**Fig 2.1** The sources of metals in the environment, its interaction, and effects of soil, plants, and Human Health

### 2.3.1. Immobilization Strategies

Physical methods like surface capping, solidification/stabilization (S/S), and vitrification focus on immobilizing or containing the metals in the soil itself (Wuana & Okieimen, 2011). The surface capping method effectively mitigates the potential hazards associated with direct contact with contaminated soil, such as skin exposure or unintentional ingestion. The surface cap functions as an impermeable barrier that hinders the infiltration of surface water, hence preventing the diffusion of soil pollutants into the surface water and groundwater. The soil that has been capped, however, experiences a loss of its inherent environmental functions, particularly in its ability to support plant development (Liu et al., 2018). The solidification method is a process that entails introducing binding agents to a contaminated substance to confer physical and dimensional stability. This stability serves to confine the contaminants within a solid product and minimize their exposure to external agents. This is achieved through a combination of chemical reactions, encapsulation, and the reduction of permeability and surface area (Tajudin et al., 2016). The process of stabilization, also known as fixing, entails the introduction of specific reagents into the soil that is polluted to generate elements that are chemically more stable. The binding agents most frequently employed in the S/S technique are typically inorganic, including clay minerals like bentonite, fly ash, calcium carbonate, cement, iron/manganese oxides, blast furnace slag, charcoal, and zeolite. Additionally, organic stabilizers such as compost, bitumen, and manures may be used, either individually or in conjunction with inorganic amendments. The primary means by which metals are rendered immobilized is by the process of hydroxide precipitation occurring inside the solid matrix (Shen et al., 2019).

Vitrification, akin to S/S, employs thermal treatment rather than chemical amendments to decrease the mobility of metals with a high-temperature treatment, typically over 1500°C. Ballesteros et al., (2017) conducted vitrification of industrial waste that transformed  $\text{Cr}^{6+}$  to  $\text{Cr}^{3+}$  and achieved effective immobilization of the highly toxic waste. Vitrification is a technology that exhibits high efficiency; nonetheless, this method is not suitable for soils with high organic

matter content, and high moisture content, and if polluted by volatile or combustible organic substances. The bioavailability of metals can be reduced using immobilization techniques, although it is important to note that long-term stability cannot be assured and may potentially result in future re-contamination. Hence, it is imperative to devise a removal method that can effectively and permanently extract metals from soil.

### **2.3.2. Mobilization/extraction strategies**

The remediation techniques employed for soil contaminated with metals mostly involve the mobilization of metals, followed by extraction. These include soil washing/flushing, phytoextraction, and electrokinetic remediation. Soil washing/flushing method is employed for the permanent extraction of metals from coarse-grained soils, particularly those that are significantly contaminated, such as abandoned smelting and electroplating-affected soils (Reddy et al., 2010). Soluble metal ions contained in the pore fluid are effectively extracted from soil by passing a suitable extraction fluid through it. The selection of the optimal concentration and volume of extraction is a crucial factor to be taken into consideration to prevent any potential toxicity. This approach is exclusively suitable for homogeneous soils with coarse textures and high permeability (Popescu et al., 2017).

Phytoextraction is a treatment technique that utilizes the natural capabilities of green plants to extract heavy metals from contaminated environments (Deepika & Haritash, 2023). To achieve this objective, it is advantageous to utilize hyperaccumulator plants such as sunflower and tobacco, among others (Cameselle, et al., 2013). The aforementioned technology, which is derived from plant sources, exhibits operational simplicity, aesthetic desirability, economic viability, and widespread acceptance. In contrast to physical and chemical interventions that cause permanent modifications to soil characteristics, phytoremediation typically enhances the physical, chemical, and biological attributes of polluted soils. Nevertheless, this technique has several drawbacks concerning extended processing time and a relatively low rate of elimination (Siyar et al., 2020).

Electrokinetic remediation is a physicochemical technique that utilizes the application of an electric field to facilitate the movement of metal pollutants from the soil matrix (Taneja et al., 2024). Due to its capacity to be employed on soils with varying compositions and low permeability, the application of EKR exhibits extensive practical utility. It is a well-suited *in-situ* remediation method that yields excellent removal efficiency with moderate cost inputs (Taneja *et al.*, 2023).

#### **2.4. Electrokinetic Remediation**

The electrokinetic remediation (EKR) technique has garnered much attention in the past decade due to its wide applications in treating wastewater (Kadhun et al., 2022), sludge (Tang et al., 2021), groundwater (H. Xu et al., 2022), sediments (Benamar et al., 2019), acid mine tailings (Karaca et al., 2017), and soil (Taneja et al., 2023b). The technique exploits the potential of electric field to cause movement of contaminants toward the electrodes, especially in fine-grained soils which are relatively difficult to treat by other conventional techniques owing to their low permeability (Zhang et al., 2022). The suitability of EKR as a remediation strategy for low permeability soils is attributed to its dependence on path length rather than permeability (Yeung et al., 1997). The optimal procedure of EKR encompasses three distinct stages: Firstly, the electric field is generated using an externally applied power supply. Secondly, the contaminant species migrate and transport towards the electrodes that have an opposite charge. This migration occurs through various transport processes (Fig. 2.2). Lastly, the contaminants are removed from the electrode reservoirs through post-treatments, such as electrodeposition or chemical precipitation (Acar & Alshawabkeh, 2002).

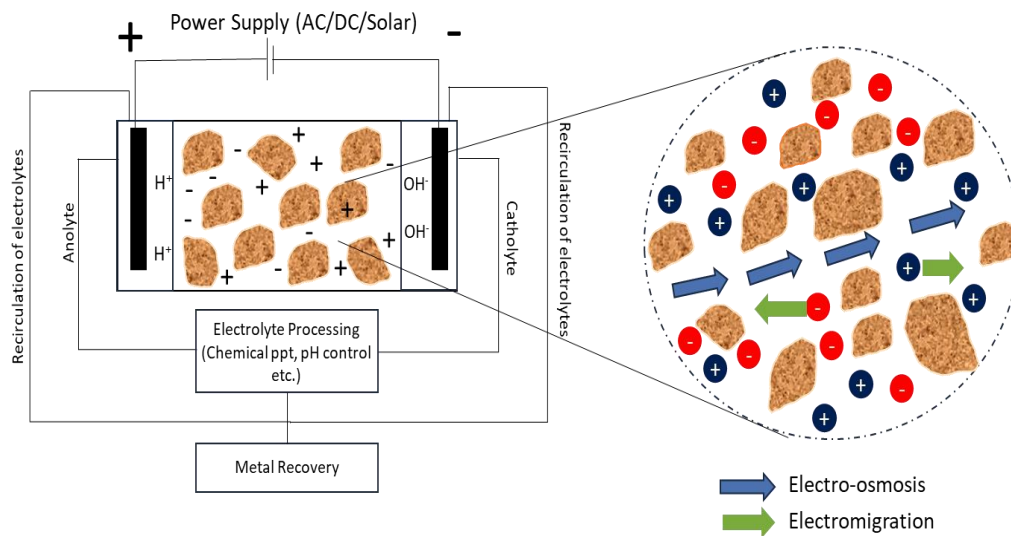


**Fig 2.2** Schematic diagram of Electrokinetic Remediation (EKR) and major transport processes

### 2.4.1. Transport Mechanisms

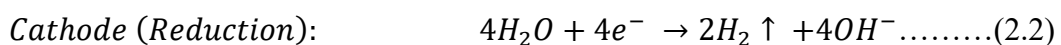
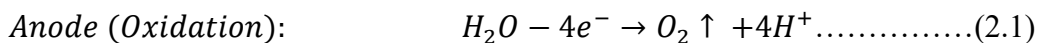
When an electric current is applied, the dissolved ions exhibit migration towards the electrodes with opposite charges. Specifically, positively charged ions migrate toward the negatively charged cathode, whereas negatively charged ions migrate toward the positively charged anode. The phenomenon is referred to as electromigration (Reddy & Shirani, 1997). Non-charged contaminant species within a soil column are moved toward the electrodes in conjunction with the electro-osmotic flow of pore water, which is initiated by the presence of an electric field. The phenomenon in which water moves in relation to the charged solid soil particles due to the presence of an electric field is referred to as electro-osmosis (Yeung et al., 1997). Due to the prevalent negative charge of soil particles, cations exhibit great affinity for them due to electrostatic interactions. This attraction leads to the formation of a double diffused layer (DDL), wherein additional cations are drawn towards the soil particles. The establishment of a potential difference, known as the Zeta Potential, between the two layers, is responsible for determining the magnitude and direction of electro-osmotic flow (Al-Hamdan & Reddy, 2008). The

direction of water flow is from the anode to the cathode when an electric field is applied, since the double layer of ions migrates towards the cathode along with the surrounding pore water due to viscous drag. The zeta potential is commonly observed to have a negative value, but it transitions to a positive value as the distance between soil particles and the dispersed layer grows. The phenomenon of electro-osmotic flow is mainly regulated by the conductivity and characteristics of the pore fluid, and the surface charge of the soil (Reddy & Shirani, 1997).

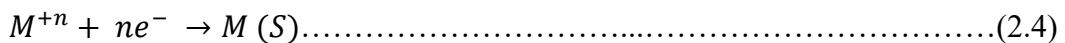
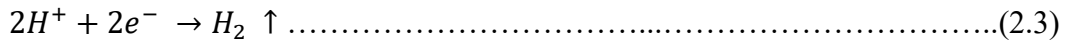
Electrophoresis refers to the phenomenon wherein charged particles, such as soil particles, microorganisms, and colloids exhibit movement in response to an applied electric field. Colloidal soil particles have a propensity to adsorb heavy metals and other contaminants, which can then be transferred by electrophoresis. Nevertheless, the efficacy of this transportation mechanism is limited when it comes to the removal of heavy metals due to the restricted movement of larger colloidal particles in densely packed soils. The process of diffusion, which involves the transfer of pollutants from areas of high concentration to areas of low concentration driven by a hydraulic gradient, plays a role in the migration of ions through the soil column (Acar et al., 1995).

The predominant mechanism for ion transport in low permeability soils is electromigration rather than electroosmosis (Pamukcu & Kenneth Wittle, 1992; Reddy & Shirani, 1997). The effectiveness of both processes relies on the presence of free metal ions in the pore fluid. The phenomenon of metal ion migration in response to an electric field has facilitated the effective elimination of heavy metals, including Cd, Co, Zn, Pb, among others, achieving a removal efficiency ranging from 85% to 95% (Yeung et al., 1997).

As the DC supply is initiated, the water in the immediate vicinity of electrode undergoes electrolytic decomposition. The primary reactions (oxidation and reduction) that occur at the electrodes are:



When excess metal ions ( $M^{+n}$ ) are available, secondary reactions might occur at cathode causing metal deposition (M). Primary reactions are dominant at the initial stage; however, once the ions start to migrate towards cathode, secondary reactions are dominant.



The electrolysis process leads to the production of hydroxyl ( $OH^-$ ) and hydrogen ( $H^+$ ) ions at the cathode and anode, respectively. This results in the establishment of alkaline conditions with a pH range of 10-12 at the cathode, and acidic conditions with a pH range of 2-4 at the anode. The presence of these ions has an impact on the soil's pH, as well as its ability to allow sorption-desorption and precipitation-dissolution interactions between the soil and pollutants (Reddy & Shirani, 1997). The EKR process is influenced by various factors, including the nature and concentration of contaminants, the presence of co-contaminants, and the presence of reducing agents. These factors play a role in determining the initial speciation of contaminants in the soil before undergoing electrokinetic treatment (Al-Hamdan & Reddy, 2006).

**2.4.2. Limitations of EKR**

The technology has several notable advantages compared to other conventional technologies, including its ease of operation, wide range of applicability, and better rate of removal (Reddy, et al., 2001). Nevertheless, the operation of EKR encounters certain technical difficulties. The metal ions have a tendency to form complexes with hydroxides and precipitate close to the cathode as a result of the electrolysis reactions at the electrodes, forming a focusing zone (Li et al., 2012). This phenomenon obstructs the soil pore structure, impacting the transport of ions into the aqueous phase and subsequently reducing the overall efficiency of metal removal. In order to achieve efficient removal, it is imperative to dissolve all ions present in the soil pore fluid, as the electric field effect

exclusively targets mobile ions (Yeung et al., 1997). The resistance of soil to electrical current is heightened as a result of the generation of gas bubbles on the surface of the electrode, hence reducing the conductivity of metal ions (Virikutyte et al., 2002). The use of electrical energy and the incorporation of electrode installations contribute to the augmentation of the overall expenditure associated with this process (Alshawabkeh et al., 1999; Kim et al., 2021). However, the flexible nature of the EKR provides the potential to address these constraints. Numerous researchers have made adjustments to the operational parameters of electrokinetic remediation (EKR) in order to enhance the technique's cost-effectiveness and removal efficiency, which are discussed in the next section.

### **2.4.3. Innovative Modifications in Power Supply**

The movement of pollutants through the soil in EKR is primarily facilitated by the electric field, often provided by an external direct current (DC) source. The utilization of electrical potential must be adequate in order to surpass the ohmic resistance produced by the soil, which has the potential to result in a gradual decrease in potential over time (Sun & Ottosen, 2012). According to Reddy and Shirani (1997), there is evidence suggesting that the effectiveness of EKR is enhanced with higher current densities, and that can be achieved by increasing the voltage gradient between the two electrodes.

#### *Effect of increasing voltage gradient*

The study conducted by Saleem et al. (2011) demonstrated that the removal of Ni exhibited an increase as the voltage gradient was elevated from 1 V/cm (38.5%) to 2 V/cm (54.3%). According to Taneja et al. (2023a), the removal of Cr (VI) from soil exhibited an increase from 22% to 55% when the voltage gradient was raised from 1 V/cm to 2.5 V/cm. The study conducted by Zhou et al. (2005) revealed that the increase of the applied voltage resulted in higher rates of Cu transport towards the cathode, leading to enhanced Cu removal performance. Nevertheless, a study conducted by Qui (2020) revealed that increasing the voltage gradient from 0.5 to 1.0 V/cm resulted in a 13% enhancement in the overall removal rate of Cd. Conversely, elevating the voltage gradient from 1.0 to 1.5 V/cm merely



led to a 3% increase in the Cd removal rate. A similar study by Song et al. (2018) observed an increase in metal removal with the increase in voltage gradient from 0.5 to 1 V/cm, however, no significant improvement in removal was observed with an increase in voltage from 1 to 1.5 V/cm. The findings of the study indicated that increased voltage gradients have a positive effect on the rate of both electrolysis and electromigration processes. This phenomenon results in the premature depletion of mobile ions from the soil into the electrolytes. In contrast, electrolysis results in an elevation of OH<sup>-</sup> ion generation at the cathode, which subsequently triggers the formation of precipitates, thus diminishing the overall efficiency. Additionally, the challenge of increased energy consumption and elevated costs represents a significant constraint to EKR. Hence, it is imperative to optimize the utilization of power supply in order to provide an effective remediation procedure while simultaneously reducing energy consumption (Wang et al., 2019).

#### *Effect of Periodic Voltage*

The efficacy of the periodic application of current also referred to as pulse current application, has been investigated in comparison to the use of continuous current supply in order to reduce energy usage. The process involves the implementation of "POWER ON" and "POWER OFF" intervals during the treatment cycle. According to Sun et al. (2013), the pulse mode is often determined by the ratio of the duration of current flow ("ON" time) to the duration of no current flow ("OFF" time). It is hypothesized that the implementation of an ON/OFF cycle can mitigate the impact of polarization at the cathode by reducing power inputs and facilitating the diffusion of ions. This, in turn, results in an elevation of metal solubility for subsequent ON cycles (Cameselle & Reddy, 2013; Sun et al., 2013). According to the findings of Hassan et al. (2015), it was noted that the pH levels in soil sections were lower and there was higher removal of metals during intermittent current compared to tests conducted using a continuous current, despite both methods having the same energy usage. According to Sun and Ottosen (2012), the pulsed current studies resulted in a greater removal rate (ranging from 51% to 76%) for the metals Cu and As, compared to the continuous current experiments (ranging from 17% to 31%).

Additionally, the pulsed current experiments were found to save approximately 60% to 67% of energy consumption. The percentage of total Cd removal increased to 38% while using interval or pulsed current, in comparison to a 28% removal rate observed under continuous current application. The results were found to be associated with the elevated electric current and electrical conductivity observed in the soil when a pulsed current was applied. This phenomenon facilitated the desorption and movement of metals, leading to an enhancement in the efficiency of their removal. Nevertheless, it is anticipated that a high frequency of ON/OFF ratio may hinder the acidification process in soil, resulting in a decrease in the solubility of metals. Hence, it is recommended to employ a comparatively reduced pulse frequency, such as 30 cycles per day, while implementing the pulsed electric field technique to enhance the solubility of metal (Cai et al., 2022).

#### *Effect of super-imposed electric field*

The superimposed electric field EK (SE-EK) method is a potential solution to mitigate the focusing effect. In a study conducted by Sun et al. (2019), the superimposed electric field was generated through the manipulation of two distinct sets of stationary electrodes positioned at varying locations. The authors reported 87.60% Cd removal, which demonstrated a significant improvement of 6.13 times compared to standard EKR methods. It was found that the energy utilization efficiency in SE-EK was 6.38 times higher compared to traditional EK.

#### *Effect of Polarity Reversal*

The process of polarity exchange modification involves the reversal of the electric field's polarity, resulting in the neutralization of the  $H^+$  and  $OH^-$  ions produced. This phenomenon contributes to the mitigation of soil acidity near the anode and the buffering effect near the cathode region, thus enhancing the effectiveness of removal. A challenge encountered in polarity exchange electrokinetic remediation is the diminished efficacy of the remediation process resulting from the repetitive migration of contaminants. A study conducted by Sun et al. (2021), concluded that in conventional EKR, removal was maximum but had

an adverse effect on soil pH as compared to tests with exchange polarity, where minimum adverse effect was observed on soil pH resulting in low removal rate.

### *Effect of Approaching Electrodes*

The Approaching Anode (AA-EKR) technique is an advanced strategy that entails the successive movement of an approaching electrode toward the fixed electrode. It is observed that the majority of metal ions exhibit migration towards the cathode and subsequent accumulation in the high pH region. Consequently, the anode is typically repositioned in proximity to the cathode, resulting in a gradual acidification of the soil and a reduction in the spatial extent of metal precipitation. Several studies have examined the differences between approaching and fixed anodes and have found that the AA-EK method leads to a higher rate of metal removal. This is attributed to an increased current and a drop in soil pH (Li et al., 2012; Shen et al., 2007; Tang et al., 2021; Zhang et al., 2014). In a study conducted by Zhang et al. (2016), it was observed that the removal rate of Cd and Pb was significantly greater when anode enhancement was employed, with values of 25.93% and 31.27% respectively. In comparison, the traditional electrokinetic method yielded removal rates of 17.96% for Cd and 30.40% for Pb. The AA-EK approach has the capacity to generate a significant quantity of H<sup>+</sup> ions, resulting in the acidification of sludge and a subsequent fall in pH.

According to Tang et al. (2021), the metals Cu, Zn, Cr, Pb, Ni, and Mn demonstrated the maximum extraction efficiencies as  $52.2 \pm 2.57\%$ ,  $56.8 \pm 3.62\%$ ,  $60.4 \pm 3.62\%$ ,  $47.2 \pm 2.35\%$ ,  $53.0 \pm 3.48\%$ , and  $54.2 \pm 3.43\%$ , respectively when EDDS was used as the purging solution along with AA. According to Cai et al. (2022), the application of a voltage gradient of 1 V/cm over a duration of 48 hours results in a remarkable maximum removal efficiency of Cu, reaching as high as 61.98%. This is in contrast to the significantly lower removal efficiency of 38.97% seen when employing the typical electrokinetic remediation method with a single fixed anode (FA). The study conducted by Zhao et al. (2022) examined the improved electrokinetic removal of Cr (VI) in soil using a novel cathode strategy. This was driven by the tendency of Cr (VI) to generate anions in aqueous solutions

and migrate towards the anode. The utilization of the cathode technique in the EDTA test demonstrated the achievement of soil alkalization. However, this approach did not yield a substantial improvement in the electromigration of Pb and Cr. According to Ng et al. (2016), there was a reduction of 22.5% in power usage for the electrokinetic process. The studies indicate that AA-EK has the potential to significantly mitigate the concentration gradient near areas with high pH (Li et al. 2012).

The optimal remediation was achieved through the combined use of the array adsorption zone and polarity exchange techniques, resulting in an average removal efficiency of 83% for Cd. Furthermore, the re-entry of Cd resulting from the exchange of polarity is no longer considered a side effect. The energy usage for 30 days is recorded as 7.72 kWh/m<sup>3</sup>, indicating a much lower value compared to conventional treatment (Zhao et al., 2022).

#### **2.4.4. Influence of Electrode and its modifications**

Electrodes are the components responsible for regulating the magnitude and strength of the electric field produced throughout the soil column. The area activated by an electric field over the soil and the duration of the remediation process is influenced by electrode specifications, namely design, material, number, and spacing/arrangement (Liu et al., 2018; Turer & Genc, 2005). The output voltage is a function of both, power and electrode variables. Table 2.3 summarizes some of the studies on enhancements of power and electrode variables.

##### *Electrode material*

According to Benamar and Baraud (2011), electrodes that have minimal voltage loss at the interface between soil and electrode, while also exhibiting resistance to corrosion, are capable of achieving the highest level of removal. The electrodes that are most frequently employed include graphite, platinum, titanium, silver, and stainless steel (Virikutyte et al., 2002). Stainless steel electrodes are generally favoured over graphite electrodes due to the higher susceptibility of graphite to corrosion, despite both materials demonstrating equivalent removal efficiency for Pb (Taneja et al., 2023b). According to Zhou et al. (2005), titanium

alloys demonstrate superior removal capabilities compared to carbon electrodes due to their higher surface area, which leads to a significant enhancement in the rate of electrolysis. The rate of electrolysis is additionally influenced by the specific purging solution employed. The use of an iron anode is not recommended in the presence of EDTA as a cathode-purging solution due to the significant depletion of EDTA caused by the formation of ferric ions through the anodic reaction. According to a study conducted by W.-S. Kim et al. (2014), the utilization of an inert electrode has the potential to improve the elimination of Cu and Pb contaminants. Kim et al. (2021) employed titanium (Ti) electrodes that were coated with iridium (Ir) in order to mitigate the potential corrosion resulting from the electrolytic reaction occurring at the surface of the electrodes.

The distance between the anode and cathode plays a crucial role in regulating both the intensity of the electric field applied and the duration of the process (Kim et al., 2014). The quantity of electrodes needed is dependent upon the arrangement of electrodes with same polarity (Alshwabkeh et al., 1999; Kim et al., 2021). According to a study conducted by Kim et al. (2021), it has been observed that an increase in the distance between electrodes leads to a reduction in the number of electrodes installed. Consequently, this decrease in the number of electrodes results in a reduction in additional expenditures. Nevertheless, it has been observed that the electrode density is comparatively lower in cases where longer electrode spacing is employed, in contrast to shorter electrode spacing (Bunditboondee et al. 2023). The study conducted by Johar and Embong (2015) investigated the impact of altering the distance between the anode and cathode on the removal of metals. The findings indicated that a spacing of 22.0 cm was the most effective in attaining substantial removal of metals at 90 volts. Notably, Pb exhibited the highest removal ratio when the electrode distance was set at 14 cm. The results of the studies indicated that the effectiveness of EKR is reliant upon the specific metal being targeted and its partitioning behavior.

### *Electrode Arrangement*

In a typical one-dimensional (1D) electrokinetic system, two electrodes, namely the anode and cathode, are positioned within the soil. The migration of pollutants towards their corresponding electrodes is observed during soil remediation processes. However, this phenomenon gives rise to a localized area characterized by the absence of electric fields (inactive area) between electrodes of the same polarity, resulting in the accumulation of pollutants that cannot be efficiently eliminated (Alshwabkeh et al., 1999). In order to address this constraint, some researchers have advocated for increasing the number of electrodes, hence enhancing the overall efficacy of removal. Nevertheless, this would result in supplementary expenses for installation as well as increased energy use. In order to enhance the efficiency by employing many electrodes, various configurations of electrodes in a two-dimensional (2D) space have been proposed, including trigonal, rectangular, square, and hexagonal arrangements. In a study conducted by Kim et al. (2021), a comparison was made between the arrangement of electrodes in 1D and 2D configurations. The findings indicated that both rectangular and hexagonal electrode configurations exhibited significant active areas and demonstrated high efficiency in removing metal. However, it was observed that the hexagonal configuration outperformed the rectangular configuration in terms of mercury removal due to its larger active surface area (Bunditboondee et al., 2023).

In a study conducted by Kim et al. (2014), it was found that the hexagonal configuration exhibited an effective area of 79%, but the square configuration demonstrated a lower effective area of 50%. Turer and Genc (2005) argued that the efficacy of the 2D Multiple anode-arrangement in comparison to the conventional 2-plate electrode configuration for the elimination of Pb, Zn, and Cu was not significantly superior. However, Kim et al. (2021) observed an enhancement in removal efficiencies of Cd, Cu, Pb, and Zn by approximately 10-15% when transitioning from a 1D to a 2D configuration. This discrepancy can be attributed to the fact that the soil pH saw a more substantial drop in the 2D process compared to the 1D process, as observed by a comparative analysis of the findings obtained using an equivalent number of electrodes.

Previous studies have indicated that the adoption of a 2D configuration is more effective in the remediation of contaminated soil compared to a 1D configuration and is considered to be a more economically viable option (Kim et al., 2021; Kim et al., 2014). Based on a cost-benefit analysis, it is probable that the most optimal approach would involve the implementation of a 1D configuration with a minimum of three pairs of electrodes. In the study conducted by (Kim et al., 2021), it was observed that when the primary focus is on the final removal efficiency, disregarding energy costs, the hexagonal 2D array demonstrates comparable or superior results compared to the 1D configuration consisting of five pairs of electrodes. Conversely, the trigonal 2D configuration was found to be less effective than the aforementioned configurations. Hence, the quantity and positioning of electrodes play pivotal roles in determining the overall viability of EKR.

The three-dimensional (3D) cell is derived from a conventional 2D cell through the incorporation of an additional electrode possessing a significantly larger surface area (Duduković et al., 2023). This modification serves to improve both the mass transfer and electroactivity of the cell. 3D electrodes serve as microelectrodes inside the soil, producing additional  $H^+$  and  $OH^-$  ions that create a localised acidic or alkaline environment surrounding the electrode. This localised environment effectively counteracts the migration of  $H^+$  and  $OH^-$  ions originating from the main electrodes, thereby neutralising their impact. Consequently, the alterations in pH exhibit a more moderate nature, the distribution of voltage becomes more uniform, and the magnitude of current increases. Hence, it can be observed that the 3D cell exhibits superior current efficiency and elimination rate in comparison to the conventional 2D cell (Bunditboondee et al., 2023; He et al., 2021; Xue et al., 2017). Previous research has examined the use of various materials, such as graphite, polypyrrole (PPy) (Qu et al., 2023), polyaniline (PANI) (L. Wang et al., 2019), and activated carbon (AC) (Yan et al., 2018), as three-dimensional (3D) electrodes for the purpose of remediating soil contaminated with metals. The AC-Fe particles were employed as a supplementary electrode to remediate Cr (VI) -contaminated soil due to their ability to undergo polarisation

upon the application of a voltage. The excessive addition of electrode particles resulted in the proliferation of many tiny electric fields within the electrolyzer, leading to accumulation. This effect impeded the overall electromigration of ions, thereby diminishing the efficacy of Cr (VI) removal. Furthermore, the incorporation of electrode particles can potentially give rise to a short-circuit current and elevate resistance during particle mass transfer. Consequently, this could result in a diminished removal ratio of Cr (VI) (Yan et al., 2018).

#### *Electrode Placement*

The positioning of the electrode plays a crucial role in affecting the effectiveness of metal extraction or the movement of metals. The technique of array arrangement, as employed by Zhou et al. (2022), effectively reduces the spatial separation between the cathode and anode through the placement of several anodes surrounding the cathode. This arrangement results in enhanced remediation efficiency. In addition, it is possible to move and secure the electrodes in the radial direction within the adjacent anodic chambers. One aspect to consider is the adjustable range of the distance between the cathode and anode, as highlighted in the study conducted by Zhou et al. (2020). Conversely, it is also worth investigating the impact of this distance on the effectiveness of the remediation process. The experimental results indicated that positioning the secondary anode at a distance of 15 mm from the cathode resulted in a more effective removal of Cu compared to placing it at a distance of 50 mm from the cathode.

#### *Use of Composite polymers*

In recent years, there has been a significant increase in the interest surrounding the use of composite polymer materials as electrodes or reactive media. It can be attributed to their enhanced adsorption capacities and improved efficiency in the removal process. Polypyrrole (PPy) is a highly conductive substance that exhibits exceptional adsorption capabilities, making it extensively employed as an auxiliary electrode in various applications (L. Wang et al., 2019). The utilisation of Ppy with Linen Fibre (Ppy-LF) as a supporting material led to a Cr (VI) removal rate of 91.7% at an applied voltage of 1 V/cm. This removal rate was comparatively



higher than that achieved using simply graphite electrodes, which resulted in a removal rate of 80.8% (Wang et al., 2019). According to Qu et al. (2023), the utilisation of PPy-MF (Melamine foam) auxiliary electrode resulted in a significant enhancement in the removal rates of total Cr and Cr (VI) at various voltage conditions. Specifically, the removal rates of total Cr and Cr (VI) were observed to increase by 34.5% and 11.5%, 26.1% and 10.1%, and 25.2% and 9.9% at 1, 1.5, and 2 V/cm gradient, respectively, when compared to the traditional EKR method. Furthermore, the implementation of PPy-MF auxiliary electrode also led to an improvement in the overall reduction rate of soil Cr (VI). A study by Wang et al. (2022), examined three different PPy materials, magnetic PPy (Fe<sub>3</sub>O<sub>4</sub>@PPy), arginine modified PPy (Arg@PPy), and arginine modified magnetic PPy (Arg/Fe<sub>3</sub>O<sub>4</sub>@PPy). The utilization of Fe<sub>3</sub>O<sub>4</sub>@PPy, Arg@PPy, and Arg/Fe<sub>3</sub>O<sub>4</sub>@PPy resulted in significantly improved efficiency in removing Cr (VI) near the anode compared to PPy. The removal efficiency increased by 74.60%, 26.04%, and 68.64% for Fe<sub>3</sub>O<sub>4</sub>@PPy, Arg@PPy, and Arg/Fe<sub>3</sub>O<sub>4</sub>@PPy, respectively. It was observed that the removal effectiveness of Cr (VI) was significantly enhanced by 74.16% when compared to the use of a single EKR.

A composite of polyaniline with non-woven fabric (PANI/NF) was created and utilised as an auxiliary electrode in the construction of a multi-electrode system for EKR. The optimisation of auxiliary electrode designs was conducted in order to improve the efficacy of soil remediation for Cr (VI) contamination. In contrast to the conventional multi-electrode system, the utilisation of PANI auxiliary electrodes with metal ion adsorption properties enables the absorption of heavy metals during the electrolysis process. This advantageous feature eliminates the need for additional power, resulting in enhanced removal efficiency without any supplementary energy consumption. The removal exhibited a 5-20% improvement compared to the standard EKR method (Wang et al., 2019).

#### *Use of nanomaterials*

The integration of EKR with nanotechnology, specifically nanomaterials and nanoparticles, has emerged as a novel strategy attracting

significant interest. The material that is most commonly employed in various applications include nano-Zero valent Iron (nZVI) (Kadhun et al., 2022). The inclusion of sulfidated nano-scale zerovalent iron (S-nZVI) in 3D electrode structure of EKR has been shown to be an effective strategy for metal removal. The S-nZVI material exhibits a notable layer of iron sulphides that possesses a reduced band gap and enhanced electrical conductivity. In comparison to alternative 3D electrodes, the S-nZVI has resulted in enhanced removal efficiencies for total Cr and Cr (VI) by at least 15.4% and 22.6%, respectively (He et al., 2021). Another study by Huang et al. (2018) employed graphite-supported nZVI (GP-nZVI) as a microelectrode to improve Cr migration from chromated mine residues.

Carbon based nanomaterials as auxiliary electrodes, for example, porous and reduced graphene oxide (PRGO) has shown to effectively enhance the migration of Cd ions. The surface of PRGO is characterised by a substantial presence of oxygen-containing functional groups, such as hydroxyl (OH) and carboxyl (COOH) groups. These groups possess the potential to effectively adsorb  $\text{Cd}^{2+}$  ions and subsequently release  $\text{H}^+$  ions, which can then react with  $\text{OH}^-$  ions produced at the cathode. According to a study conducted by Xu et al. (2020), the use of the PRGO auxiliary electrode resulted in a 12% increase in Cd removal efficiency compared to the traditional electrode. This improvement can be primarily attributed to the fall in soil pH caused by the PRGO.

Yuan et al. (2016) conducted an assessment on the impact of a newly developed material, carbon nanotube coated polyethylene terephthalate yarns (PET-CNT), when used as a cathode electrode in the simultaneous EK remediation of kaolin polluted with multiple heavy metals (Cu, Cd, Pb, Ni, and Zn). The utilisation of a cathode PET-CNT composite material resulted in a substantial augmentation of both electric current and electroosmotic flow. Additionally, this cathode exhibited the ability to decrease soil pH, thus leading to improved efficiency in the extraction of heavy metals. The findings of this study revealed a descending trend in the effectiveness of heavy metal removal, with Ni exhibiting the highest removal efficiency, followed by Cd, Zn, Cu and Pb. These results suggest that Ni, Cd, and Zn are generally more readily extractable compared to Cu

and Pb. In contrast, it was observed that the removal of Cu and Pb posed greater challenges.

A porous nanofiber composite material, known as aminated electrospun nanofiber membrane (ENFM), was successfully synthesised by a thermal treatment process. This involved subjecting a polyacrylonitrile (PAN) ENFM enriched with hyperbranched polyethylenimine (HPEI) to a brief thermal treatment. The PAN/HPEI ENFM exhibited a notable capacity for adsorbing Cr (VI) at around 206 mg/g, along with a high level of reusability exceeding 9 cycles. The findings showed that the PAN/HPEI ENFM employed in the remediation process successfully immobilised and eliminated the Cr (VI) present in the soil due to high specific surface area ranging from 10 to 20 m<sup>2</sup>/g, making it suitable for adsorption applications. Additionally, ENFM offers the advantages of convenience in terms of recycling and replacement (Wang et al., 2021).

Green nanoparticles possess the capacity to effectively diminish concentrations of pollutants within a brief timeframe. A study was conducted to explore the feasibility of integrating green nano-zero-valent iron (nZVI) with electrokinetics for the remediation of sediment contaminated with Cd and Zn. In the context of green synthesis, the utilization of extracts derived from desiccated mulberry leaves (ML-nZVI) and oak leaves (OL-nZVI) was employed. Upon comparing the results, it was seen that OL-nZVI exhibited superior efficacy as a nanomaterial, even when administered in lesser quantities. This finding has significance in terms of attaining enhanced economic advantages. This combination not only enhances the lifespan of green nZVI, but also improves its migratory capabilities (Duduković et al., 2023).

**Table 2.3** Performance of EKR towards metal removal with variable power and electrode configurations

<b>Matrix</b>	<b>Power Source</b>	<b>Enhancement</b>	<b>Voltage Output/current density</b>	<b>Duration</b>	<b>Metal (% Removal)</b>	<b>Energy/power consumption</b>	<b>References</b>
Soil	MFC	-		108 d	Cd (31), Pb (44)	-	Habibul et al., 2016
Sediment	DC	Approaching anode	1 V/cm	24 h	Pb (62)	27 kWh/m <sup>3</sup>	Rajić et al., 2012
Soil	Solar	-	18.8 V	48 h	Cd	500 kWh/m <sup>3</sup>	Yuan et al., 2009
Soil	DC	2D Hexagonal	100 V	6234 h	As (61), Cu (11), Pb (0.9)	25.5 kWh/m <sup>3</sup>	Kim et al., 2014
Soil	DC	2D hexagonal	100 V/m	6 d	Cd (80), Cu (83), Ni (34), Zn (81)	22 kWh/ton	Kim et al., 2021
Sludge	DC	Approaching anode	1 V/cm	50 h	Cu (52), Zn (56), Cr (60), Pb (47), Ni (53), Mn (54)	-	Tang et al., 2021

Soil	DC	Approaching anode	1 V/cm	240 h	Pb (84)	-	Zhang et al., 2014
Soil	DC	Polarity reversal	1 V/cm	168 h	Cr (40-60)	47.9 kWh/m <sup>3</sup>	Sun et al., 2021
Soil	DC	Pulsed current	0.2 mA/cm <sup>2</sup>	240 h	Cu (54), Cd (17), as (30)	42 Wh	Sun & Ottosen, 2012

#### **2.4.5. Influence of Electrolyte solution and its modifications**

The presence of an electrolyte solution is crucial for facilitating the movement of dissolved ions from the soil toward the electrodes. The pH conditions of soil, which in turn regulate the sorption/desorption of metal ions on soil particles, are influenced by the composition of the electrolyte. Therefore, the introduction of an electrolyte solution leads to an increase in conductivity and facilitates the removal of metal. Several studies have employed various processing fluids as electrolytes for the purpose of pH regulation and mobilization of metal ions for their subsequent removal, summarized in Table 2.4.

##### *Enhancements by acids*

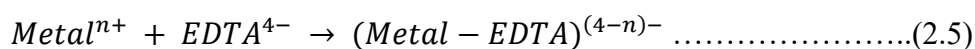
There are primarily two commonly used agents for the extraction of heavy metals from soils. The initial category of agents encompasses both inorganic and organic acids, whereas the subsequent category consists of chelating agents (Suzuki et al., 2014). In the study conducted by Figueroa et al. (2016), it was shown that inorganic or mineral acids have demonstrated the highest extraction ratios of more than 80% for a majority of metals, particularly for Co, Zn, Cd, and Cu. Nitric acid (HNO<sub>3</sub>) is commonly chosen as the electrolyte solution of choice due to higher solubility of nitrates. Hydrochloric acid (HCl) has also been employed as an anode purging solution. But, the increase in chloride ion concentration hinders the electrolysis reaction at the anode by generating Cl<sub>2</sub> gas (S.-O. Kim et al., 2021).

Organic acids are classified as weak acids due to their propensity to readily dissociate, hence facilitating the desorption mechanism of metals. They make an excellent electrolyte because they are biodegradable and environmentally friendly. In a study conducted by Cameselle and Pena (2016), an investigation was carried out to assess the efficacy of sulphuric acid, acetic acid, and citric acid in terms of their ability to reduce pH levels and facilitate the mobilisation of heavy metals in the vicinity of the cathode. The utilisation of citric acid, due to its capacity to enhance electro-osmotic flow, yielded the most favourable outcomes. The use of citric acid as a processing agent in anolyte and catholyte solutions promoted soil acidification, enhanced metal solubility, facilitated electro-osmotic transport and

electromigration towards the cathode. The mobilization of Cd, Co, Cu, and Zn in the soil was shown to be significantly enhanced in the presence of citric acid, resulting in removal rates exceeding 70%. In contrast, the mobilization of Cr and Pb exhibited poor removal efficiencies below 12%. According to the research conducted by Qiu (2020), it was shown that acetic acid demonstrated a 12% higher removal efficacy for Cd as compared to citric acid. Conversely, Li et al. (2012) found that citric acid facilitated the conversion of Cr (total) fractions more readily. In a study conducted by Cameselle et al. (2021), it was shown that increasing the concentration of citric acid to 0.5 M facilitated the removal of various metals. Specifically, the removal efficiencies were found to be 78.7% for Cd, 78.6% for Co, 72.5% for Cu, 73.3% for Zn, 11.8% for Cr, and 9.8% for Pb. The utilization of a mixture of lactic acid and calcium chloride demonstrated a significant efficacy in the elimination of 63% Cu and 65% Zn. According to Zhou et al. (2005), the desorption of metal ions was facilitated by lactic acid, which helped maintain the pH, while the presence of CaCl<sub>2</sub> assisted in sustaining the electric current.

*Enhancements by Chelating agents*

The use of acidic substances results in a decrease in soil pH, hence facilitating the desorption of metallic elements. Nevertheless, the possibility of soil acidification is enhanced. Chelators are employed as means to mitigate the occurrence of highly acidic or alkaline pH conditions. Chelating agents have the ability to create metal complexes that exhibit stability under typical soil pH conditions (Eqn. 2.5). This property enhances the effectiveness of chelating agents in removing target metals when compared to salts and surfactants, as demonstrated by Sun et al. (2023). Additionally, it has been observed that chelating compounds have a lesser impact on soil structure compared to very acidic substances. In recent years, there has been a prevalent utilization of ethylenediamine tetraacetic acid (EDTA), citric acid (CA), and oxalic acid (OA) as widely employed chelating agents (Yang et al., 2020).



EDTA is widely employed as a chelating agent due to its robust coordination capabilities towards cationic heavy metals, lack of selectivity towards pollutants, and effective treatment efficacy across a diverse array of soil compositions (Giannis et al., 2008). In a study, Amrate et al. (2006) examined the viability of employing electrokinetic soil processing for the purpose of extracting Pb from a real-contaminated soil. They focused on the impact of EDTA, a suitable conditioning agent for the circulating fluids, in order to eliminate Pb from calcareous soil under a consistent voltage. The removal efficiency of the method exhibits a rise from 13% to 26% when the concentration of EDTA involved in the process varies from 0.05 M to 0.10 M. At a higher ligand concentration of 0.20 M, there appears to be a minimal impact on the enhancement of recovery efficiency. The minimal molar quantity of EDTA required for the extraction of lead from contaminated soil should ideally correspond to the molar quantity of metal present in the soil.

The authors Iannelli et al. (2015), and Reddy and Chinthamreddy (2004) conducted a comparative analysis between acids and chelating agents in order to determine the most appropriate electrolyte solution. On employing sulfuric acid, acetic acid, citric acid, and EDTA as the purging solution, it was found that 46% to 82% of Cr was successfully eliminated from the soil, with the maximum removal rates for Ni and Cd being 48% and 26% respectively, when a concentration of 1.0M acetic acid was employed. The application of sulphuric acid resulted in a notable rise in electrical resistivity and electroosmotic flow. However, it also caused substantial formation of sulphate precipitates, both inside the solid material and in the catholyte. Consequently, its suitability for large-scale implementation is severely limited.

EDTA is difficult to biodegrade, therefore chelators with relatively better degradability have been opted in some research studies, such as Ethylenediamine disuccinic acid (EDDS) (Tang et al., 2021). A study by Ge et al. (2022) compared the use of three chelating agents, EDTA, nitrilotriacetic acid (NTA) and diethylenetriamine pentaacetic acid (DTPA) as purging solution. It was shown that DTPA exhibited the highest removal values for Cd (53%), Cu (59%),



and Ni (47%), followed by EDTA and NTA. The reason for DTPA's enhanced soil metal extraction capability can be attributed to its elongated structure compared to EDTA.

The conventional chelators have certain limitations, including inadequate biodegradability, elevated cost, and limited complexation capabilities. The reactions at anode during EKR treatment have the potential to induce soil acidification and anodic breakdown of organic materials within the anode solution. Consequently, this can lead to the release of metal cations from the metal-chelate complexes through a process known as decomplexation. Hence, it is imperative to conduct a thorough examination of the migration and transformation patterns shown by metal-chelate complexes and un-chelated metals as distinct entities (Song et al., 2019).

**Table 2.4** Summary of performance of EKR on different matrices using electrolyte enhancements

<b>Matrix</b>	<b>Electrolyte enhancements</b>	<b>Contaminants</b>	<b>Removal efficiency (%)</b>	<b>Voltage gradient (V/cm)</b>	<b>Duration</b>	<b>Reference</b>
Sediments	EDTA (0.05M)	Cd, Pb, Ni, Cu, Zn	100, 94, 74, 55, 51	1	15 days	Ayyanar & Thatikonda, 2021
Sediments	EDTA (0.1M)	Ni, Pb, Zn	52.8, 60.1, 34.9	1	21 days	Song et al., 2016
Spiked Soil	EDTA (0.1M)	Cd	15.1	1	5 days	Gu et al., 2018
Mine Tailings	EDTA (0.1M)	Pb, Zn	27, 13.6	2	9 days	Asadollahfardi et al., 2021
Sediments	EDDS (0.1 M)	Cu, Zn, Cu	51, 26, 52	1	21 days	Song et al., 2016
Sediments	NTA (0.1 M)	Cr, Cd, Cu	43, 38, 34	1	21 days	Song et al., 2016
Spiked Soil	NTMP (0.1 M)	Cd	22.8	1	5 days	Gu et al., 2018
Spiked Soil	EDTMP (0.1 M)	Cd	22.4	1	5 days	Gu et al., 2018
Sediments	CA (0.1M)	Cd	40.2	1	21 days	Song et al., 2016

Electroplating sludge	CA (1 M)	Zn, Cu, Pb, Ni, Cr	64, 34, 34, 42, 69	1	5 days	Peng & Tian, 2010
Mine Tailings	CA (1 M)	Pb, Zn	51.31, 32.86	2	9 days	Asadollahfardi et al., 2021
Industrial Soil	CA (0.1 M)	Cr	36.5	1	18 days	Gao et al., 2020
Tannery Sludge	CA (0.1 M)	Cr	72.37	2	56 hours	Prakash et al., 2022
Industrial Soil	CA (0.1 M)	Cr	49.4	2	7 days	Fu et al., 2017
Electroplating sludge	SDS (0.02 M)	Zn, Cu, Pb, Ni, Cr	50, 31, 26, 37, 65	1	5 days	Peng & Tian, 2010
Industrial Soil	Humic acid	Cr	51.7	1	18 days	Gao et al., 2020
Industrial Soil	KCl (0.1 M)	Cr	40.4	1	18 days	Gao et al., 2020
Tannery Sludge	Saponin (0.1 M)	Cr	80	2	56 hours	Prakash et al., 2022
Industrial Soil	PASP (1%)	Cr	25.33	2	7 days	Fu et al., 2017

## 2.5. EKR-integrated technologies

Due to the influence of several factors such as soil properties, electrode material, and metal concentrations, relying solely on the optimization of EKR parameters may not yield removal effectiveness that meets the desired standards. The inclusion of additional elements, such as the implementation of chelates and the multiple electrodes, results in increased expenses and energy demands. Hence, it is recommended to integrate EKR technology with traditional methods in order to leverage the advantages offered by both approaches. The representation of the feasibility and challenges of the selected EKR-coupled technologies are given in Fig. 2.3 and Table 2.5.

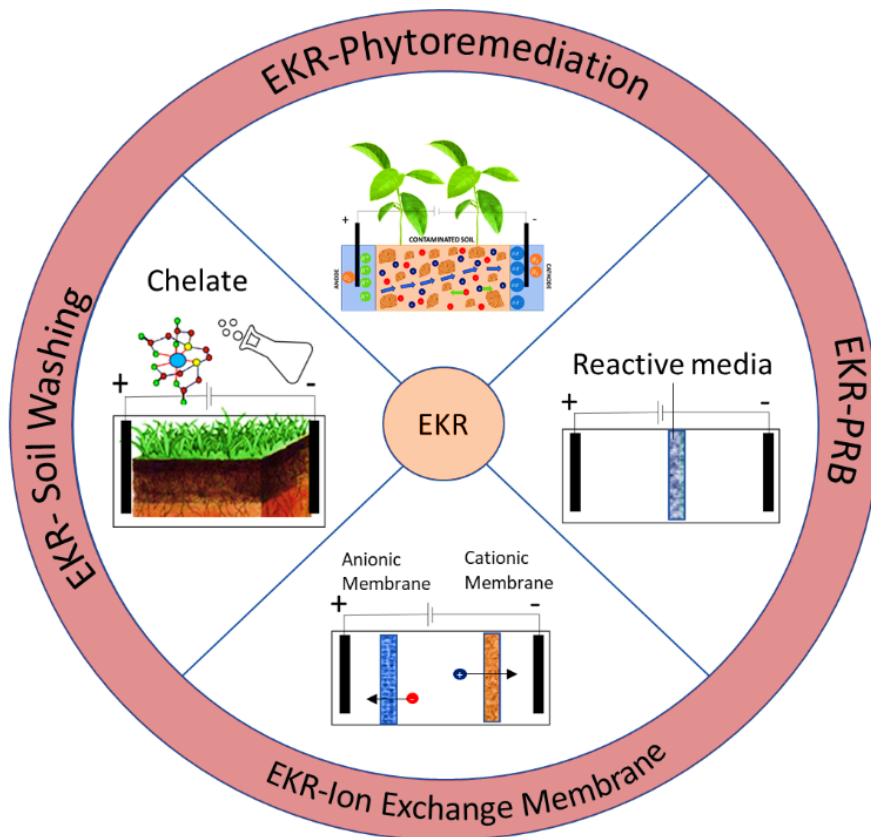


**Fig 2.3** Assembly set-ups of some integrated-EKR technologies

### **2.5.1. Ion-Exchange membrane**

The ion-exchange membrane (IEM) is a type of material that facilitates the selective transport of ions based on their charge and size (Pedersen et al., 2018). The IEMs employed in the EKR can be classified into two distinct categories: cation exchange membranes (CEMs), which selectively facilitate the passage of cations, and anion exchange membranes (AEMs), which exclusively permit the passage of anions. The application of IEM was employed for the remediation of red soil contaminated with both Pb-EDTA and Cd-EDTA. The results obtained in the study indicated that a fraction of free metal cations can be dissociated from the metal-EDTA complexes as a result of the acidic conditions and electrochemical degradation occurring at the anode. The cations underwent electromigration and subsequently aggregated at distinct sites within the soil, influenced by their hydrolysis capacity and the variation in soil pH across different sections. A significant reduction in the concentration of Cd (61%) and Pb (83%) was seen in the soil during a 7-day treatment, during which the electrolyte pH was maintained at a controlled level of 10. The removal efficiencies of metals in the treatment assisted by anion-exchange membranes were found to be superior to those in the treatment assisted by cation-exchange membranes. According to Song et al. (2019), the restriction of de-complexed free metal cations from returning to the soil during metal accumulation phenomena can be achieved through the utilisation of an anion-exchange membrane or pre-precipitation under alkaline conditions. This approach has been demonstrated to effectively mitigate the impact of metal accumulation. The utilisation of CEM has the potential to augment both energy consumption and expense due to the heightened resistance introduced by the membranes, necessitating regular replacement. However, fouling of IEM remains a significant constraint in the design and implementation of an EKR system. Fouling occurs as a result of the accumulation of contaminants on the surface of the membrane, leading to the decline in membrane performance characterised by a decrease in flow and an increase in resistance (Kim et al., 2005).

The adoption of dual cation-exchange membranes in conjunction with the circulation method-assisted EDTA-enhanced technique has been explored.

Using an innovative strategy to improving EK remediation, an aged electroplating-contaminated soil was treated. In contrast to conventional EK and EK-treatments boosted with EDTA, the use of this particular approach demonstrated a notable three to tenfold enhancement in the removal of Ni and Cu. Furthermore, this method effectively prevented the adverse metal buildup, resulting in a substantial reduction of the highly acidified region from 80% to 20%. Additionally, it exhibited a significantly low toxicity towards photobacterium *P. phosphoreum* T3. This exemplifies the increased efficacy in increasing performance and the environmentally conscious attributes of this procedure. In contrast to the impacts of acidification, it was observed that the use of EDTA did not yield a substantial chelating effect on Ni and Cu in this particular soil type when subjected to conventional EDTA-enhanced electrokinetic remediation conditions. Additional investigation into the optimisation of operating conditions and the recycling of chelating agents would be of significance in enhancing the cost-effectiveness of this innovative methodology (Song et al., 2020).

Numerous investigations have highlighted the phenomenon of EDTA depletion resulting from anodic oxidation. This results in a subsequent escalation of the overall expenditure associated with the aforementioned process (Pedersen et al., 2018). The Neosepta CMX cation-exchange membrane is a uniform film composed of a cross-linked sulfonated copolymer of vinyl compounds supported by a synthetic reinforcing fabric. Upon successful completion of the action of EDTA, the resulting complex underwent migration towards the anode, where it underwent oxidation. Furthermore, it was anticipated that the Pb that was released would re-enter the soil and cause contamination in the event of the complex's destruction. One approach to mitigate the destruction of the anionic complex at the anode was the implementation of a cation-exchange membrane. The findings pertaining to the dispersion of contaminants throughout the soil column indicate that lead was effectively transported towards the anode, despite the presence of a substantial quantity of calcite (25%) and the sample's considerable acid/base buffer capacity. The ability to recover both EDTA and lead from their chelated solutions

simultaneously was achieved by employing the same experimental arrangement and by monitoring the pH levels in the circulating fluids (Amrate et al., 2006).

The utilisation of ion exchange fibres has been investigated in a manner analogous to that of membranes. Nevertheless, fibres possess a cellulose structure that imparts hydrophilic characteristics to them. Therefore, fibres have demonstrated a favourable mechanical architecture and have improved the electro-osmotic flux while exhibiting superior selectivity towards ions that are less hydrated, such as lead. The removal efficiencies for Pb and Zn were found to be higher, with Zn exhibiting more retention within the cation exchange fibres. According to Souilah et al. (2012), fibres exhibit superior mechanical qualities compared to ion exchange membranes. Additionally, fibres possess a higher level of hydrophilicity relative to membranes due to their cellulose structure.

### **2.5.2. EKR-assisted Soil Washing**

The soil washing-assisted EKR technique involves the utilisation of additives to facilitate the mobilisation and migration of metal ions in the presence of an electric field. The efficacy of the method was assessed for the treatment of soils contaminated with a mixture of organic and inorganic pollutants. In order to improve the extractability and solubility of the pollutants, a sequential flushing approach was employed using two chemical agents: EDTA as a complexing agent and Igepal CA-720 as a surfactant. This was done due to the distinct chemical properties of the contaminants. The study determined that the application of a voltage gradient resulted in a decrease in the elimination of Pb and Cu. The efficacy of Igepal surfactant in the removal of polycyclic aromatic hydrocarbons (PAHs) from soil has been demonstrated, whereas the effectiveness of EDTA chelant in the removal of heavy metals from soil has also been established. The most favourable outcomes were achieved by implementing a two-stage flushing procedure using 0.2 M EDTA, first without and then with a voltage gradient of 1 VDC/cm. This was subsequently followed by a two-stage flushing process utilising 5% Igepal, first without and then with a voltage gradient of 1 VDC/cm. The primary method for the removal of heavy metals was through the process of EDTA flushing, resulting in

removal efficiencies of approximately 60% for Zn, 80% for Pb, and 30% for Cu (Reddy et al., 2010).

The effectiveness of pH control on coupling soil washing with cathodic reduction to remove multiple heavy metals from soil under various current densities was examined by Sun et al. (2023). The total removal rate of target metals exhibited a significant increase of 3 to 6 times when the pH of the soil suspension was maintained at a regulated value of  $7.0 \pm 0.2$ . The highest removal efficiencies for Cd, Pb, and Zn are 83.14%, 76.90%, and 50.22% respectively. The empirical findings indicate that altering of soil suspension pH can enhance the overall removal efficiency of target metals by a factor of 3-6. Furthermore, there is an observed enhancement of around 30% in the removal efficacy of residual Pb from the soil. The implementation of pH regulation has demonstrated the potential to decrease the solubility and mobility of metals by approximately 50%. This reduction in ecological risk is particularly notable for Zn, as its concentration has been effectively lowered from approximately 90 mg/kg to 50 mg/kg. Additional investigation is required to delve into the mechanism underlying the synergistic impact, and to enhance the efficacy of this technology in order to advance the coupling of soil washing with cathodic reduction.

### **2.5.3. EKR-assisted Permeable Reactive Barrier (EKR-PRB)**

The Permeable Reactive Barrier (PRB) is a passive methodology employed to eliminate pollutants from soil or water matrices by utilising a reactive medium. The media often employs several mechanisms such as ion-exchange, adsorption, precipitation, or redox reactions to effectively confine contaminants within the imposed barriers. The approach has been increasingly popular due to its cost-effectiveness and ability to be used on-site. When combined with EKR, it has been shown to enhance the rate of metal removal from soil and address the primary drawback of EKR, which is the focusing effect (Zhou et al., 2020). The PRB media effectively eliminates the  $\text{OH}^-$  ions generated in the vicinity of the cathode, hence impeding the precipitation of metals and subsequently hindering the movement of ions. The choice of PRB filling materials or reactive media is a matter of



consideration. The media can be classified into three distinct types based on the method of removal: absorbent materials (e.g., active carbon, zeolite, ion exchange resin), precipitant materials (e.g., limestone, phosphate, magnesium hydroxide), and reductant materials (e.g., zero-valent iron) (Yuan & Chiang, 2007; Zhang et al., 2022). Zeolite exhibits favourable adsorption and ion exchange capabilities, rendering it a commonly employed substance for applications involving filling and adsorption. The process has the ability to convert free heavy metal ions, specifically Cr (VI), into less mobile Cr (III), or induce the formation of precipitates.

Layered Double Hydroxides (LDH) exhibit significant potential as a PRB material due to their advantageous anionic exchange capability. LDHs, namely chloride hydrocalumite (CaAl-LDH), have been identified as a viable and economically efficient option for the removal of oxyanion pollutants due to their cost-effectiveness, long-term viability, and significant capabilities for anionic exchange (Ma et al., 2022). The substance is frequently utilised as an adsorption medium, referred to as anionic clay, and exhibits a diverse array of compositions. In the conducted experiment, a combination of reducing agents, ascorbic acid and citric acid, along with chelating agents, EDTA-2Na, were employed in conjunction with CaAl-LDH for the purpose of pre-treating soil contaminated with As and Cr. The optimal removal efficiencies for As and Cr were found to be 41.2% and 46.8%, respectively. The findings of the study revealed that the adsorption of As mostly occurred on the surface of CaAl-LDH, whereas the primary processes for the adsorption of Cr involved both surface adsorption and intercalation of CaAl-LDH. When combined with a hydrocalumite barrier, EKR exhibits significant promise and has the potential to be highly effective in remediating clay polluted with Cr (VI). According to a study conducted by Xu et al. (2016), it was observed that the removal efficiency of Cr (VI) and total Cr reached 96.6% and 67.3%, respectively, on using a combination of EKR-PRB based on calcined hydrotalcite. The notable efficiency in decontamination is believed to be a result of the synergistic effect, wherein EK concentrates anionic chromate towards the anode region, while calcined hydrotalcite absorbs and immobilises it (Zhang et al., 2012).

The initial study by Suzuki et al. (2014), introduced the application of Magnetite ( $\text{Fe}_3\text{O}_4$ ) as a reactive medium and conducted a comparative analysis of its effectiveness in removing Cr in comparison to the conventional Fe-PRB method. The reductant present in PRBs that are positioned near to the anode facilitates the reduction of Cr (VI) into Cr (III), which is both less toxic and less soluble. As a result, almost 70% Cr (III) species is retained within the PRB.

An iron-based amorphous alloy with a PRB was employed for the remediation of both simulated Cu-contaminated soil and actual contaminated soil. The findings of the study indicated that the augmentation of soil moisture content and voltage gradient throughout the remediation process exhibited a positive influence on the migration of  $\text{Cu}^{2+}$  ions towards the cathode. In the given experimental setup, wherein the soil moisture content is maintained at 40% and a voltage gradient of 3 V/cm is applied, the technique exhibits a better efficiency in removing copper from simulated copper-contaminated soil compared to the ZVI-EKR. This mechanism effectively prevents the accumulation of  $\text{Cu}^{2+}$  ions at the cathode with a removal rate of 42.37% (Pei et al., 2023).

Nanomaterials have been extensively used as reactive materials in integrated EKR-PRB processes, particularly nZVI, due to their high adsorption capabilities (Huang et al., 2018). The use of nZVI as reactive media has resulted in an enhancement of the reduction efficiency of Cr (VI) and the removal efficiency of total Cr to 88% and 19%, respectively (Shariatmadari et al., 2009). Yuan et al. (2016) conducted a study on the implementation of an EKR-PRB using a carbon nanotube coated with cobalt (CNT-Co) as the barrier material to remove As (V) from soil. The findings indicated that the system utilising EDTA as the processing fluid exhibited a removal efficiency of over 70% for As (V), surpassing the efficiencies observed in the EK and EK/CNT systems by a factor of 2.2. The application of EKR in conjunction with calcined hydrotalcite (CHT) as a filler material resulted in a notable improvement in the removal efficiency of Cr (III) ions (Zhang et al., 2012). These observations highlight the substantial synergy between PRB and EKR.

#### 2.5.4. EKR-assisted Phytoremediation

The integration of electrokinetics with phytoremediation has been suggested as a potential solution to address the significant drawback of phytoremediation, i.e., its prolonged treatment duration. The combined phytoremediation-electrokinetic technology (Phyto-EKR) involves the utilisation of a low intensity electric field in the polluted soil area where identified plants are being cultivated. According to Cameselle et al. (2013), the presence of an electric field has the potential to augment the elimination of pollutants by improving the bioavailability of those contaminants. The efficacy of Phyto-EKR treatment in reducing soil pH to around 1.5 in the vicinity of the anode has been seen to facilitate the dissolution of metal(loid)s, hence enhancing their solubility (Mao et al., 2016). Significant reductions in soil metal concentrations were seen through the implementation of experiments including hyperaccumulators such as vetiver (Siyar et al., 2020) and ryegrass (O'Connor et al., 2003). Nevertheless, the absence of any indication of metal toxicity in the plants implies that phytostabilization exerted a more significant influence than phytoextraction. The phytoextraction potential of *Eucalyptus globulus*, a plant species that does not possess hyperaccumulation properties, was found to be considerably lower when considering unit biomass (Luo et al., 2018). Additional plant species such as Indian mustard, spinach, and cabbage have also demonstrated proficiency in accumulating metals such as Pb, As, and Cs (Mao et al., 2016). The plant species *Brassica napus* (rapeseed) and *Nicotiana tabacum* (tobacco) were employed to investigate their potential of removing Cd and Zn. The removal efficacy of both rapeseed and tobacco was found to be comparable to that of *T. caerulescens* and other hyperaccumulator plants, such as *A. murale* and *T. ochroleucum* (Bi et al., 2011).

The application of chelators such as EDTA has been found to considerably enhance the capacity of plants to uptake metal complexes (Luo et al., 2018). In order to examine the impact of electric current application on plant growth and the transformation of soil heavy metals, Indian mustard (*Brassica juncea*) was utilised as the plant species, and the experiment was carried out over a period of 35 days. Four different voltage gradients were applied (0, 1, 2, and 4 V/cm DC) for a

duration of 16 days, with each day consisting of 8 hours of exposure. The application of Phyto-EKR resulted in an enhanced uptake of metals by plants. Among the voltage gradients tested, a medium voltage gradient of 2 V/cm exhibited the maximum efficacy in terms of metal accumulation in the plant tissues. A study by Cang et al. (2011) found that the root biomass of plant increased with increasing voltage gradient and vice-versa. The authors concluded that the primary determinant influencing plant growth, soil characteristics, and metal concentrations in both soil and plants is the voltage gradient.

In order to investigate the impact of various electric fields, three distinct voltage gradients (1, 2DCV/cm and 2ACV/cm) were administered to Vetiver grass over a period of 21 days, with an exposure duration of 8 hours each day, by applying the electric fields throughout the soil. The findings indicated that while the application of AC current resulted in minimal alterations, the application of DC current had a substantial impact on the Eh-pH values. The Vetiver grass exhibited the highest concentration of extractable metals at a rate of 2DCV/cm, resulting in a notable 50% increase compared to the AC. When examining the translocation rate and the overall health of plants, it is seen that the application of alternating current (AC) over an extended treatment duration may yield more favourable outcomes in the Phyto-EKR of Vetiver grass through the phytoextraction process (Siyar et al., 2020).

Aboughalma et al. (2008) conducted experiments on potato tubers to investigate the efficacy of DC and AC current application in removing Zn, Pb, Cu, and Cd metals. The plants exhibited a 72% increase in biomass output under the AC treatment, while a 27% decrease in biomass production was seen under the DC treatment, in comparison to the control. The metal uptake in plant shoots was shown to be significantly reduced under the DC treatment. A study conducted by Chirakkara et al. (2015) observed a marginal enhancement in the biomass of oat and sunflower plants when exposed to a 25 V AC current. However, this increase did not yield significant improvements in the phytoextraction of heavy metals when compared to the control group consisting of plants without electric current. The AC

electric field exhibited fewer adverse impacts on the growth of plants in comparison to the DC electric field.

In order to mitigate the impact of energy consumption, research was conducted to investigate into the utilisation of solar energy (Yang, et al., 2018; Mao et al., 2016). The findings indicated that the electric field generated by conventional power supply systems resulted in a decrease in soil moisture throughout all the layers of the soil profile, hence mitigating the potential for leaching. The utilisation of solar cells in the operation of a periodic running field has been found to significantly reduce the fluctuation of metals in each layer while also reducing the cost of electricity as compared to conventional AC/DC power supply methods.

**Table 2.5** Summary of technological and economic feasibility, and major challenges of EKR-coupled technologies

<b>EKR-coupled Technologies</b>	<b>Technological and economic Feasibility</b>	<b>Major Challenges</b>
EKR-Soil Washing	<ul style="list-style-type: none"> <li>• Efficient metal migration</li> <li>• High removal rate</li> <li>• Applicable to heterogenous soils</li> <li>• Relatively low cost</li> </ul>	Selection of ideal extraction fluid to avoid secondary contamination
EKR-Phytoremediation	<ul style="list-style-type: none"> <li>• Enhanced metal accumulation by plants</li> <li>• Feasible for large scale application</li> <li>• Highly economically feasible</li> </ul>	Selection and planning of appropriate plant species for faster removal.
EKR-PRB	<ul style="list-style-type: none"> <li>• High removal rate</li> <li>• Prevention of post treatment contamination</li> <li>• Low cost</li> </ul>	Selection of suitable reactive media Optimization to improve reuse of material

## **2.6. Economic consideration and scale-up of EKR**

An important aspect for selection of a technique is its economic viability. The cost of installation of electrodes, construction of wells, and electricity can challenge the economic feasibility of EKR. The contribution of electricity cost is only 17 % of the total cost. A comparison of cost of different techniques as reported in previous literature is presented in Table 2.6. From the comparison it can be inferred that EKR treatment of large volumes of soil/sediments or highly contaminated site can be prove to be cost effective as compared to other techniques. However, the selection criteria must also take into account the type of soil to treated.

Many researchers have conducted laboratory studies to assess the efficiency of EKR; however, field-scale studies are limited in the literature. The major factor for large-scale application of EKR is the pre-treatment of the site, installation of electrodes, power consumption, process operations, and post-EKR treatment for contaminant-enriched electrolytes and soil near the electrode wells. The complex nature of the field conditions (soil heterogeneity, unsaturated medium, large volume) and the inability to predict the field EK performance using selected laboratory operating parameters may restrict the efficiency of EKR on field (Benamar et al., 2020). Nevertheless, a few selected case studies on field have reported to successfully remove metals with 45-95% removal efficiencies (Table 2.7).

**Table 2.6** Cost comparison of different remediation technologies as reported in previous literature studies

Remediation technologies	Cost of treatment (US\$/ton)							Remarks
	Mulligan et al., 2001	Virkutyte et al., 2002a	Karachaliou et al., 2016	Khalid et al., 2017	Liu et al., 2018	Trentin et al., 2019	Akansha et al., 2024	
<b>Excavation/ Disposal</b>	-	-	74	270-460	300-500	25	270-460	<ul style="list-style-type: none"> <li>• High economic cost owing to transportation</li> <li>• Highly contaminated soils</li> <li>• Short time duration</li> </ul>
<b>Vitrification/ Soil heating</b>	-	65-123 \$US/yd <sup>3</sup>	-	300-500	330-425	-	700	<ul style="list-style-type: none"> <li>• Cost-efficient</li> <li>• Limited to low organic, low moisture soil</li> <li>• Low-moderately contaminated soils</li> <li>• Short time duration</li> </ul>

<b>Chemical oxidation</b>	-	130-200	-	-	520 US\$/m <sup>3</sup>	-	190-660	<ul style="list-style-type: none"> <li>• Cost-effective</li> <li>• High risk of secondary pollution</li> <li>• Medium time duration</li> </ul>
<b>Soil-flushing</b>	100-200	-	49-60	75-210	70-180 US\$/m <sup>3</sup>	-	50-80	<ul style="list-style-type: none"> <li>• Cost efficient</li> <li>• Limited to coarse-grained soil</li> <li>• Medium time duration</li> </ul>
<b>Phyto-remediation</b>	5000-20,000 US\$/acre	-	56-72	25-100		12-15	2000-5000 US\$/acre	<ul style="list-style-type: none"> <li>• Low cost</li> <li>• Low-moderately contaminated soils</li> <li>• Long time duration</li> </ul>
<b>Electro-kinetics</b>	-	50-120 US\$/m <sup>3</sup>	-	-	26-295 US\$/m <sup>3</sup>	32-35	150-180	<ul style="list-style-type: none"> <li>• Relatively low cost</li> <li>• Highly contaminated soils</li> <li>• Medium time duration</li> </ul>



**Table 2.7** Some selected field scale studies of EKR

Field Case Studies	Key Highlights	References
Removal of Cd from paddy soil, China	<ul style="list-style-type: none"> <li>• 20 V/m applied to 200m<sup>2</sup> area using 5 electrodes (graphite) in linear configuration</li> <li>• 74% removal after 14 days</li> <li>• 0.6 kWh energy consumption was reported</li> </ul>	Cai et al., 2021
Removal of metals from paddy soil, South Korea	<ul style="list-style-type: none"> <li>• 0.5 V/cm applied to 207.4 m<sup>2</sup> area using</li> <li>• Removal of As, Cu, and Pb was reported as 44%, 40%, and 46% after 24 weeks</li> <li>• 1.6 kWh/m<sup>3</sup> energy consumption reported</li> </ul>	Jeon et al., 2015
Removal of Cu from landfill soil using EKR-PRB, Korea	<ul style="list-style-type: none"> <li>• 1V/m was applied for 30 days</li> <li>• Zeolites as reactive media resulted in 93% removal</li> </ul>	Chung, 2009
Geokinetics International Inc., USA	<ul style="list-style-type: none"> <li>• Corrosion-resistant conductive material (EBONEX)</li> <li>• Estimated cost of treatment 120-200\$US/yd<sup>3</sup></li> </ul>	Virkutyte et al., 2002
Removal of Cu from electroplating waste soil, China	<ul style="list-style-type: none"> <li>• 15 V applied between electrodes 2m apart</li> <li>• 81% Cu removal was reported after 48 days</li> <li>• Energy consumption: 0.22-0.26 kWh/m<sup>3</sup></li> <li>• Remediation cost was estimated to be 27\$US/m<sup>3</sup></li> </ul>	Hui et al., 2016

## **2.7. Sustainability concerns and future roadmap**

From a sustainability standpoint, the primary objective of remediation is not solely the complete extraction of heavy metal cations from the soil matrix, but also the retrieval of the heavy metals that have been extracted from the polluted soil. One additional element to be considered in sustainable technology, or a combination thereof, is the potential for non-reversible harm to soil structure, the significant energy requirements involved, and the subsequent treatment of chelators. This section examines strategies for enhancing the sustainability of EKR while maintaining the optimal removal efficiency (Fig.2.8).

### **2.7.1. Use of renewable energy sources**

The application of solar cell panels in EKR offers the advantage of reducing costs associated with electrical transmission, minimising power loss in transmission lines, and alleviating the requirement for DC transformers. The amount of power produced by solar cell panels is dependent upon the duration of daylight and the prevailing climatic conditions at the specific location (Yuan et al., 2009). Typically, it is anticipated that there would be variations in power supply during the day, as well as periods of complete power outage throughout the night. These fluctuations have the potential to impact the EKR process. Nevertheless, the use of solar energy to power EKR could bring down the cost of treatment significantly (Hassan et al., 2015). According to Jeon et al. (Jeon et al., 2015), the application of solar-based EKR resulted in a 50% reduction in energy consumption compared to EKR powered by DC, while also demonstrating a 5% decrease in metal removal. Yuan et al. (2009) discovered that solar cells have the potential to facilitate the electromigration of Cd in soil contaminated with this element. The efficiency of Cd removal achieved by solar cells was shown to be comparable to that achieved by a DC power source, but with significantly decreased energy consumption. In an investigation conducted by Zhang et al. (2015), it was observed that the removal efficiency of Cr (VI) increased to 99.8% over a duration of 30 minutes. This improvement was achieved by subjecting the system to solar radiation with an irradiation intensity of  $650 \pm 20 \text{ W/m}^2$ , while utilising photovoltaic solar panels and

a DC-DC converter to provide a 1.5 V/cm voltage gradient. The electric energy consumption at a maximum voltage of 11.5 V was recorded at 156.1 kWh/m<sup>3</sup>.

The microbial fuel cell (MFC) is another innovative bio-electrochemical device that has the capability to produce electrical energy by harnessing the metabolic processes of bacteria using organic substrates (Chen et al., 2015). Within the MFC system, the generation of electrons occurs at the anode as a result of the oxidation of organic compounds by microbes. Subsequently, these electrons are transported to the cathode *via* the external circuit. Simultaneously, the oxygen molecule, acting as the terminal electron acceptor, underwent reduction to become water through the transfer of electrons at the cathode. A study was carried out to remove Cd and Pb by utilisation of MFC driving the electrokinetic remediation technology. The levels of Cd and Pb in the soils exhibited a gradual increase from the anode to the cathode regions during the remediation process. After approximately 143 days and 108 days of operation, the anode region demonstrated removal efficiencies of 31.0% and 44.1% for Cd and Pb, respectively. The redistribution of soil parameters, including pH and soil conductivity, was found to be significant between the anode and cathode zones. The findings suggest that MFC-driven EKR is both economically viable and environmentally sustainable, hence exhibiting considerable potential for its implementation in soil remediation practises (Habibul et al., 2016).

Chen et al. (2015) conducted a study whereby three-chambered MFCs were employed for the purpose of extracting Zn and Cd from paddy soil. The experiment was carried out for a duration of 78 days, during which a total of 12 mg of Zn and 0.7 mg of Cd were successfully removed. These findings indicated that the electrical current generated by the MFCs play a substantial role in enhancing the removal of these metals. Another study employed a solid phase MFC system utilising wheat straw as the substrate for the treatment of soil contaminated with Pb and Zn. After a period of 100 days, the anode region of the SMFC containing 3% straw exhibited removal efficiencies of 37.2% for Pb and 15.1% for Zn. When comparing the use of standard EKR with the implementation of soil remediation technology driven by MFCs, a reduction in energy requirements, the potential for

biomass energy reuse, and a decrease in the potential risk of harmful metal leaking into groundwater was observed (Song et al., 2018).

### **2.7.2. Use of biodegradable materials**

The incorporation of biodegradable materials as electrodes, electrolyte solutions, or reactive media has the potential to significantly mitigate the occurrence of secondary pollutants and, to some extent, cut down expenses. This section examines the utilisation of various bio-based materials in conjunction with EKR in order to enhance its sustainability.

#### *Biochelators*

The utilisation of biodegradable chelating agents can help reduce the production of secondary pollutants, as is observed in case of synthetic chelators. Biochelators, Sodium Alginate and Chitosan, as electrolyte solution demonstrated removal of Cu and Zn by up to 95%. Alginate is a type of polysaccharide polyelectrolyte that is derived from brown algae. It exhibits a strong affinity for divalent cations and possesses desirable characteristics such as biodegradability, biocompatibility, and cost-effectiveness. Alginate and chitosan are well acknowledged as electroactive biomaterials that possess notable electrical conductivities and electrochemical redox characteristics (Wang et al., 2021). The utilisation of pine needle extract (PNE) as an electrolyte presents a cost-effective and environmentally friendly option. PNE consists of a range of organic acids, including amino acids and shikimic acid, which contribute to its exceptional alkali buffering capabilities. On comparing performance of PNE and two other substances, Chitosan (CTS) and Fulvic acid (FA), in terms of their ability to remove Cd, Cu, and Ni, it was found that CTS exhibited the highest metal removal followed by PNE and FA. In comparison to alternative enhancers, the PNE has a comparatively lower cost and does not result in the accumulation of Cd, Cu, and Ni following treatment. Despite the PNE's suboptimal removal efficiency, its cost-effectiveness and environmental benefits provide it a superior option (Ge et al., 2022).

Tetrasodium N, N-bis(carboxymethyl) glutamic acid (GLDA) is a cost-effective and environmentally friendly chelating agent to improve the efficiency of EKR. Despite its relatively low affinity to form metal complexes, it possesses the advantage of being a cost-effective chelator with a low potential for environmental risk. The experiments conducted for GLDA enhanced EKR indicate that the extraction rates of Cu and Ni ranged from 39% to 48%, which were comparatively higher than the extraction rates achieved using citric acid (26% to 41%) and lactic acid (0.44% to 25%). Furthermore, it was observed that the pH of the solution had minimal impact on the extraction rate of GLDA (Yang et al., 2020).

### *Biosurfactants*

In contrast to synthetic surfactants, biosurfactants have superior biodegradability, enhanced ecological safety, and reduced toxicity, and thus, are deemed more appropriate for soil remediation. A variety of microbial species, including bacteria, fungi, and yeasts, have been observed to synthesise biosurfactants as a byproduct of their metabolic activities (Tsui et al., 2022). Saponin and rhamnolipid are widely used biosurfactants for the removal of pollutants from soil, particularly, organic pollutants (Benamar et al., 2019; Tang et al., 2017; Xu et al., 2022). However, some researchers have found promising results on application biosurfactants in conjunction with organic acids (Prakash et al., 2022; Tian et al., 2017). Combined use of citric acid and saponin as enhancers in the EK process facilitated the migration and removal of chromium through a combination mechanism of electromigration and electroosmosis. However, the authors observed relatively low overall removal rates ranging from 4.4% to 15.8%. (Prakash et al. 2022).

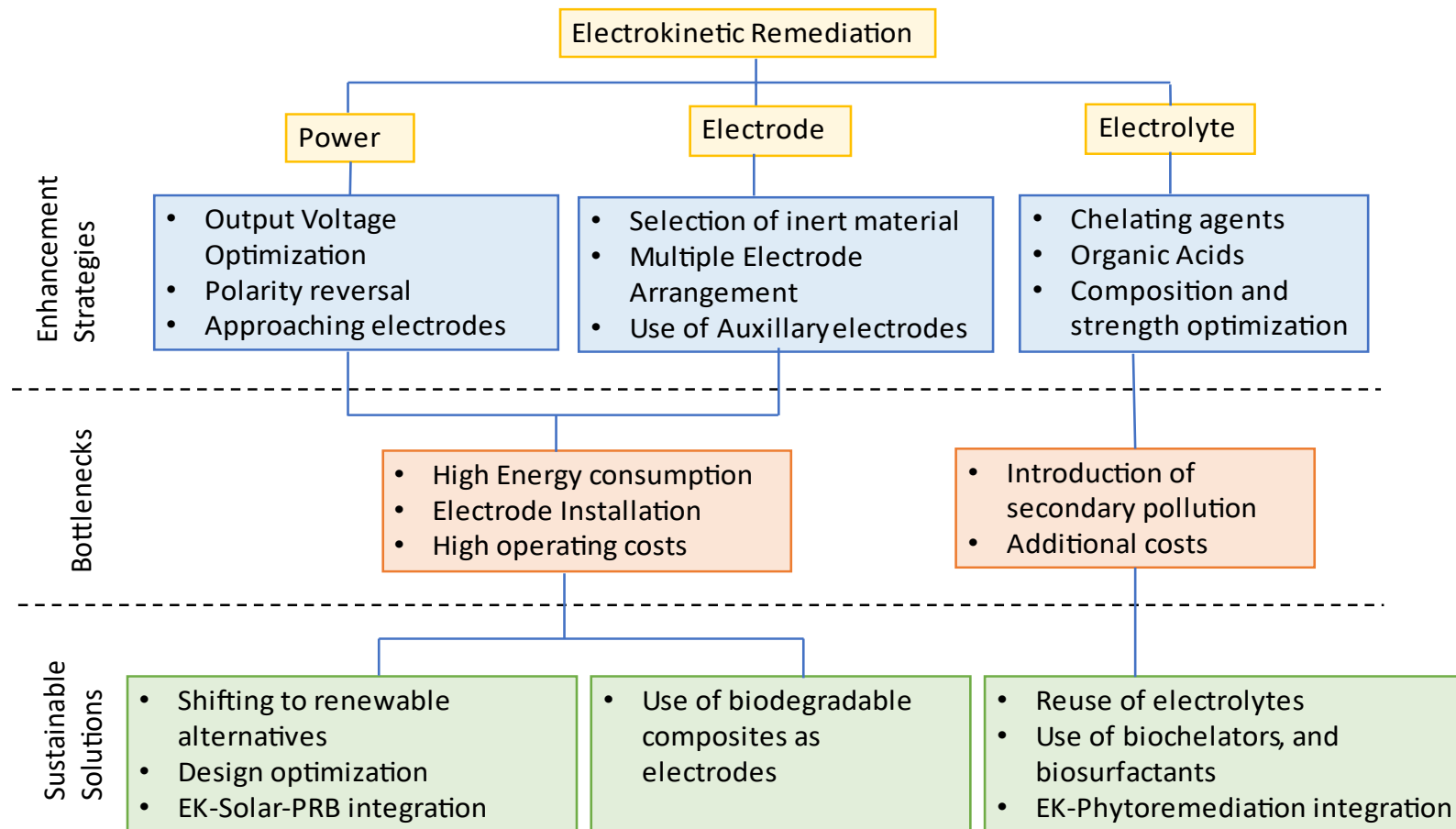


**Fig 2.4** An overview of enhancement strategies for major operating components of EKR, and the sustainable alternatives offered

The utilisation of GLDA as an electrolyte resulted in removal efficiencies of 53.2%, 67.4%, 59.2%, 45.4 %, 72.8 %, and 45.0 % for Cu, Zn, Cr, Pb, Ni, and Mn, respectively. However, substituting rhamnolipid as the electrolyte led to further enhancements in the removal efficiencies of these heavy metals, with values of 64.8%, 56.8 %, 49.4%, 46.6%, 60.4%, and 69.6% for Cu, Zn, Cr, Pb, Ni, and Mn, respectively. The combined use of GLDA and rhamnolipid in the electrokinetic process resulted in significantly higher removal efficiencies (Tang et al., 2017).

In a recent study by Tsui et al., (2022), the efficacy of using effective microorganisms (EM) in soil for Cd removal was evaluated and compared to the effectiveness of tap water, citric acid, and EDTA. The EM, being a mixed culture solution of a combination of yeasts, actinomycetes, photosynthetic bacteria, and lactic acid bacteria, acts as a biosurfactant. EM also has a variety of organic acids, which confer upon it the ability to function as a chelating agent. This property enhances its potential as an electrolyte for EK applications. EM resulted in a notable Cd removal efficiency of 90.5% over a period of 7 days, compared to citric acid (72.3%), EDTA (75.4%), and tap water (21.7%). The observed outcome can be partially be ascribed to the biosurfactant characteristic of EM, which facilitates their profound infiltration into the soil matrix, thereby leading to the dissolution of a substantial amount of contaminants. In general, the findings of this study suggest that EM can be utilised as a cost-effective and efficient biosurfactant in EK applications for the purpose of metal removal from soil.

#### *Biodegradable reactive media*

In recent studies conducted by Ghobadi et al., (2021), the effectiveness of the EK process has been enhanced through the use of a recyclable and environmentally sustainable reactive filter medium known as EK-RFM. This particular medium, which utilises compost as an adsorbent, has demonstrated promising results in the removal of heavy metals. The comparative efficacy of compost in mitigating soil pH fluctuations was found to surpass that of alternative soil amendments, including biochar, activated carbon, and a combination of biochar

and compost. However, the effectiveness of compost in removing other heavy metals from actual soil has not yet been assessed. Humus, a prospective eco-friendly agent, has the potential to augment the efficiency of EKR in the process of rehabilitating soil contaminated with As. Research has indicated that the utilisation of humus as a sustainable amendment can effectively enhance the removal efficiency of As by around 20% (Xu et al., 2021).

In order to enhance the overall performance of EKR, integrated bio-electrokinetics has been considered through the synergistic incorporation of humic substances (HS) with microbacteria into the systems. The utilisation of *Microbacterium* sp. Y2 in conjunction with electrokinetics has been found to significantly improve the efficiency of Cr (VI) treatment, resulting in a remediation rate of 90.67% during an 8-day period. The bacteria and humic substances possess inherent qualities that make them effective and environmentally-friendly agents for enhancing purposes (He et al., 2018). The use of yeast in the preparation of EKR-PRB employing immobilised microbial technology was employed for the purpose of remediating soil polluted with Cd. The embedding approach employed to create yeast pellets as PRB resulted in the lowest removal efficiency of approximately 34.12%. The use of fly ash-based yeast pellets made using the adsorption-embedding approach, as well as fly ash-adsorbed yeast prepared by the adsorption method, resulted in a significant increase of over 10% in the average removal of Cd when employed as PRB. From the findings, it is anticipated that the implementation of bio-electrokinetics will significantly mitigate the toxicity of soil contaminated with Cd, mitigate detrimental impacts on the soil environment, and decrease environmental concerns.

#### *Recycled waste as reactive media*

The usage of recycled waste to act as reactive media for heavy metals has shown great potential. The use of ash of recycled food waste, in conjunction with other enhancements such as acetic acid conditioning and electrode exchange demonstrated significant Cu and Pb removal efficiency of 87%, and 43%, respectively (Lee et al., 2021). The utilisation of carbonised food waste (CFW) was



employed as a material for PRBs by Han et al. (2010). The installation of the PRB in a region characterised by dynamic fluctuations in pH levels facilitated the processes of adsorption and precipitation of  $\text{Cu}^{2+}$  ions during the PRB's movement. The research findings indicate that the adsorption effectiveness of CFW, when utilised as a reactive material, was much higher compared to the Zeolite. The average removal efficiency achieved using CFW ranged from 53.4% to 84.6%, which was approximately 4 to 8 times more efficient than Zeolite.

### **2.7.3. Recycling of electrolytes and recovery of metals**

The aforementioned investigations primarily concentrated on the extraction of heavy metals from soil and sediments, resulting in the accumulation of elevated levels of heavy metals in the anolyte and catholyte solutions. Additionally, it contains a significant concentration of EDTA, which facilitates the solubilization of other earth elements found in the sediments. In the absence of appropriate treatment measures, the discharge of hazardous effluents into aquatic ecosystems, such as lakes and rivers, is not feasible. Also, the elevated expense associated with EDTA is a hindrance to the implementation of cleanup efforts on a larger scale.

Various approaches, including ion exchange, adsorption, precipitation, and electrolysis, have been suggested for the treatment of wastewater containing heavy metals. Adsorption is a frequently employed method for the treatment of wastewater that is contaminated with heavy metals. A variety of cost-effective adsorbents have been developed for the purpose of eliminating heavy metals from wastewater (Yang et al., 2020). However, the efficacy of adsorption is reliant upon the specific adsorbents employed, and subsequent storage of the adsorbent is a recurring challenge following the adsorption process. The precipitation technique commonly employed using sulphates or hydroxides is a simple and cost-effective method (Di Palma et al., 2003). However, its effectiveness may be limited in cases when the heavy metal concentration is low and tightly bound to ligands such as NTA, EDTA, and EDDS.

A study conducted by Gao et al. (2020) demonstrated the effective utilisation of an anion exchange resin in preventing the re-entry of Cd metal into the sludge. The utilisation of resins additionally augmented the removal efficacy through the enhancement of both current and electroosmosis rates. Nevertheless, these strategies possess certain drawbacks. For instance, while ion exchange is an appealing method, it necessitates the regeneration of exhausted resins through the addition of chemical reagents, hence potentially resulting in secondary pollution. Treating a substantial volume of wastewater with a low proportion of heavy metals poses a challenging undertaking. According to Yan et al. (2018) the use of ion exchange membrane not only hinder the interference of electrolysis byproducts during the treatment process, but also facilitate the retrieval and subsequent recycling of the ligand. Through the integration of selective membranes and controlled electrolysis, successful recovery of Pb and recovery of EDTA can be achieved (Amrate et al., 2006).

The usual approach employed for heavy metal complexes involves oxidative decomplexation or precipitation techniques by the inclusion of precipitants. However, the non-sustainability of these solutions arises from factors such as excessive consumption of oxidants and precipitants, the involvement of many processing steps, and the formation of secondary hazardous solid waste. Electrochemical decomplexation is a sophisticated and environmentally friendly approach for the decomposition of metal-EDTA complexes, enabling the retrieval of important metals through cathodic reduction or adsorption. Nevertheless, it has been observed that this method has a tendency to damage EDTA rather than facilitating its recovery (Lu et al., 2023). The precipitation of trace metals facilitated by the combination of  $\text{Na}_2\text{S}$  and  $\text{Ca}(\text{OH})_2$  enables the recycling of EDTA. During a 14-day timeframe, the EDTA reagent had losses ranging from 19.5% to 23.5% after being reused seven times (Zeng et al., 2005). The research conducted by Ayyanar and Thatikonda (2021) focused on the optimisation of EDTA dosage and the recovery and reuse of EDTA for the purpose of safe discharge. The optimal concentration of EDTA was determined to be 0.05 M. the authors reported that the application of  $\text{FeCl}_3$  and  $\text{Na}_2\text{PO}_4$  for the treatment of produced effluent resulted in

the effective recovery of EDTA. The recovered EDTA was subsequently reused for further testing, exhibiting removal efficiencies of 71%, 65%, and 52% in consecutive trials. The findings suggested that the use of recovered EDTA in EKR treatment effectively reduce the risk associated with heavy metals.

Based on the facts discussed in the literature, it has been established that EKR is a promising method for the treatment of heavy metal-contaminated soils/sediments/sludge *in-situ*. The removal efficiency is dependent on the nature and concentration of the metals present in the matrix, the interference posed by co-contaminants, the type of electrode and its material being used, and the nature of electrolyte being used/circulated. The integration of EKR with other methods like adsorption, phytoextraction/phytostabilization, ion exchange, chemical precipitation, membrane filtration, etc. Despite being highly efficient for the removal of contaminants from soil, EKR has gained much popularity and scientific recognition since the studies certifying its reliability, optimization, and cost-effectiveness are limited. Before making a decision for choice of method for soil decontamination, EKR must be given due priority owing to its application *in-situ*, supply of energy based on solar energy, rapid removal rates, and easy-to-operate nature. The EKR should necessarily be integrated with a suitable technique to minimize the generation of secondary pollution. Further, the optimization of regulating parameters shall be a way forward for bringing down the cost and duration of treatment, thus, addressing a larger scale for decontamination. It shall be of immense benefit to the environment and human health considering the risk assessment and reduction in toxicity of contaminated matrix. Therefore, active and scientifically sound studies on optimization of EKR and risk reduction shall be taken up on priority to address the issues involved in achieving the SDGs.



## **CHAPTER 3**

### **MATERIAL AND METHODS**

The methodology for this study was designed to fulfil the following broad objectives:

1. Treatment of single-metal contaminated soil by Electrokinetics.
2. Treatment of multi-metal contaminated soil by Electrokinetics.
3. Optimization of regulating parameters:
  - a. Applied voltage
  - b. Electrolyte composition
  - c. Electrode material
  - d. Electrode configuration
4. To explore the application of higher voltage for enhanced removal ( $> 2.5$  V/cm) without compromising the soil health.
5. To compare the environmental and economic benefits of optimized electrokinetics under high voltage application.

#### **3.1. Quality Control and Assurance**

In order to achieve the objectives stated above, the following SOPs were followed:

- All experiments were performed in triplicates and the results were confirmed using intra-lab investigations.
- Soil spiking was done using 04 wetting and drying cycles (Karaca et al., 2019)
- Ultrapure water was used in the analysis.
- ASTM and APHA standard methods were followed.

- Standard/reference materials for heavy metals with NIST traceability were used.
- All the chemicals and reagents used were of analytical grade.
- The variation in results was limited to  $\pm 3\%$ .

### **3.2. Materials and methods**

The flowchart for the methodology adopted for this study is depicted in Fig 3.1. The experimentation was done in two phases; first, the EKR was performed on the individual metal-contaminated soils to assess the optimal conditions for removal, and second, the EKR was performed on mixed metal-contaminated soil under the optimized conditions to assess the inter-ionic interferences. For this study, three metals of public concern were selected, Hexavalent chromium [Cr (VI)], Lead [Pb (II)], and Cadmium [Cd (II)]. The selection was based on their occurrence in the top 20 Priority Substances as per the ATSDR list and their extensive prevalence in nature.

#### **3.2.1. Chemicals and Reagents used**

The analytical grade potassium dichromate (99.9%) and cadmium metal (99%) were purchased from SRL Chemicals, India. The lead nitrate salt (99.5%) was purchased from Sarabhai Chemicals Ltd., under Merck. (Germany) and Synthetic solutions of metals were prepared using ultrapure Type-I water. Ethylenediaminetetraacetic acid disodium salt (98%), Sodium hydroxide (NaOH), and Sulphuric acid ( $H_2SO_4$ ) were purchased from Central Drug House (CDH) (P) Ltd., India.

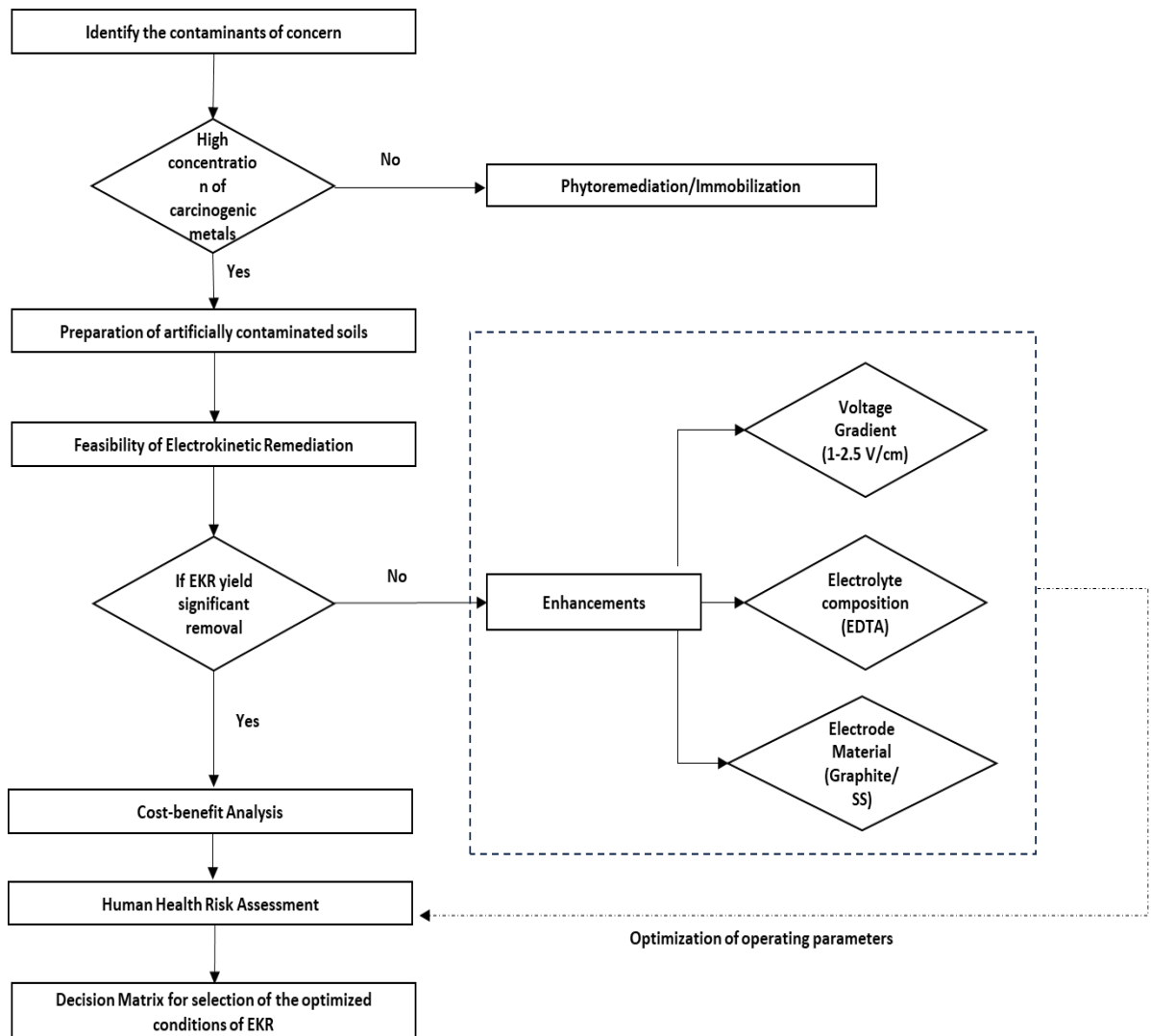


**Fig 3.1** Flowchart of the methodology adopted for this study

### 3.2.2. Soil collection and spiking

The soil was collected from the campus of Delhi Technological University, Delhi, for single-metal experiments, and from Kepez region, Canakkale, Turkey, for mixed-metal experiments. The soil was sampled at 0-20 cm depth after removing the surface cover, with the help of soil auger, and air dried. The dried soil was then crushed using a mortar and pestle and sieved through a 2 mm mesh to remove coarse particles. The characterization of soil for its physical and chemical properties was done using the sieved soil.

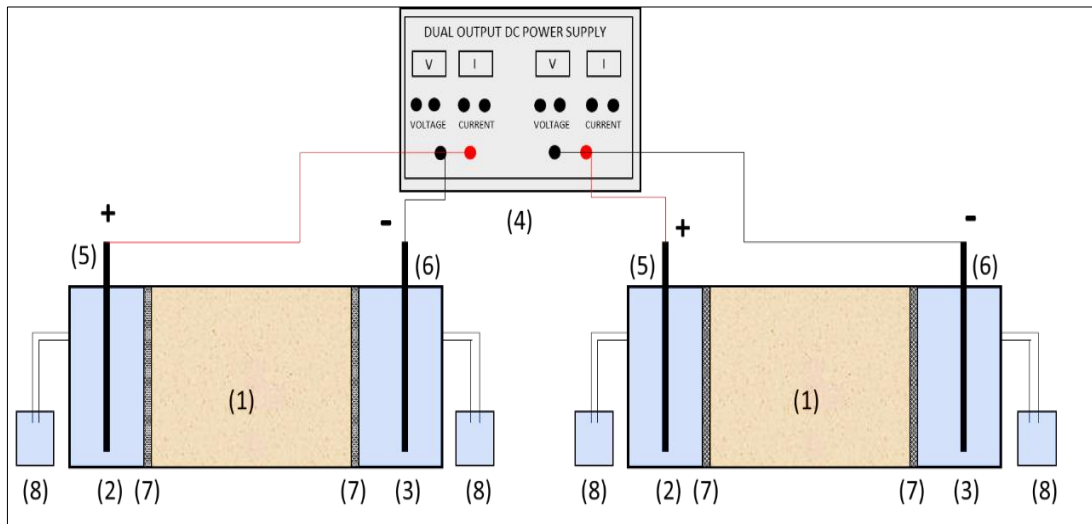
The sieved soil was spiked in the lab with the addition of metal salts. For the analysis of the EKR of individual metals, the concentration of  $\text{Cr}^{6+}$ ,  $\text{Pb}^{2+}$ , and  $\text{Cd}^{2+}$  were 1000 mg/kg, 1000 mg/kg, and 250 mg/kg, respectively. The concentrations were selected to simulate waste obtained from industries with high concentrations of metals such as electroplating, mining, etc. (Reddy and Chinthamreddy, 2004). For Cr (VI), 4.23 g of Potassium dichromate ( $\text{K}_2\text{Cr}_2\text{O}_7$ , 99.9% purity) was weighed for 1.5 kg soil (2.82g  $\text{K}_2\text{Cr}_2\text{O}_7$ /kg of soil) and was powdered before mixing with soil. For Pb (II), 1.59 g of Lead Nitrate  $\text{Pb}(\text{NO}_3)_2$  was weighed for 1 kg of soil. For Cd (II), 0.25 g of Cadmium metal was weighed and dissolved in nitric acid and the solution was used for spiking. For experiments with mixed metal-contaminated soils, the soil was spiked with 500 mg/kg of Cr (VI), 500 mg/kg Pb, and 250 mg/kg Cd.

The powdered metals was mixed with ground soil and mixed manually for 15 minutes. The spiked dry soil was then wetted using distilled water and mixed thoroughly to impart some moisture to the soil. The soil was then allowed to dry with periodic mixing at regular intervals and this cycle of wetting and drying was repeated 04 times. This process was done to ensure that metals are evenly distributed (through diffusion and dispersion), and subsequent adsorption onto soil particles, if any, to represent the soil under natural conditions, as suggested in earlier studies (Karaca et al., 2022). The spiked soil was stored in a plastic bag for a week before the experiment to avoid moisture loss.

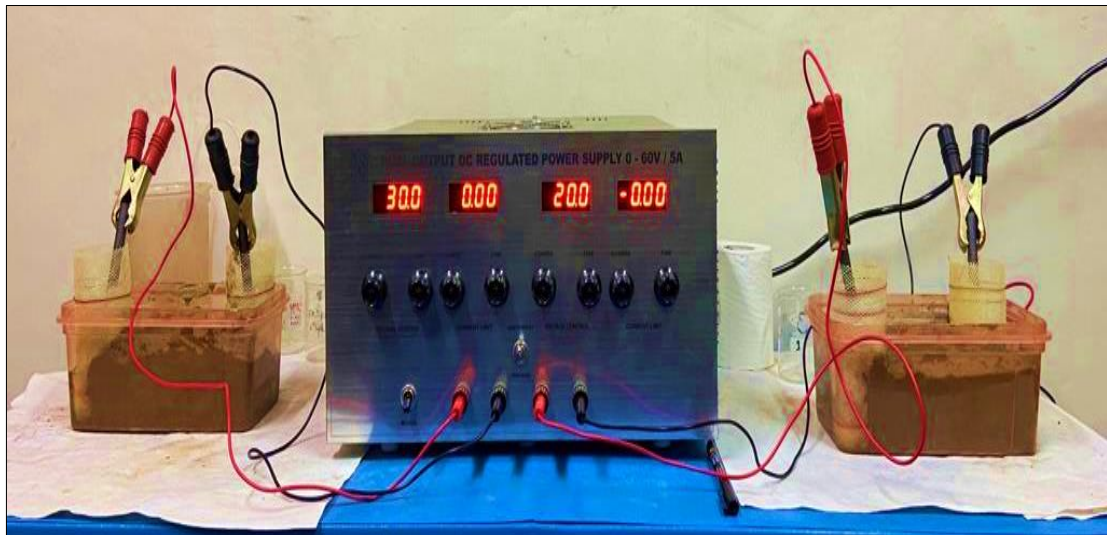


### 3.2.3. Electrokinetic Remediation Assembly

The experimental setup for EKR was assembled in the lab as shown in Fig. 3.2. The EK setup consists of four major components, soil cell, power supply, electrodes, and electrode wells.



(a)



(b)

**Fig. 3.2** (a) Schematic diagram of EKR setup used in this study (1) soil cell (2) anode well (3) cathode well (4) DC Power Supply (5) anode (6) Cathode (7) Nylon Mesh (8) Electrolyte reservoirs (b) EKR assembly used for this study

### ***Soil Cell***

Soil cell is the main component where the EKR transport processes occur. For this study, three different cells were selected. For the linear configuration, a rectangular HDPE container of dimension 19.5 cm x 5.5 cm x 4.5 cm was used as a soil cell. The soil cell was then filled with 1.5 kg of spiked and saturated soil. For trigonal configuration, a circular cell with a diameter of 20 cm was filled with 3 kg of spiked and saturated soil, and for square configuration, a soil cell of 39 cm x 5.5 cm x 4.5 cm was filled with 3 kg of spiked and saturated soil. The electrode wells were placed in the soil cell with electrodes suspended in them at a distance of 15 cm (Fig 3.3). Once the soil cell was filled with saturated soil, it was pressed with a lid to compact the soil and remove any possible air pockets that might be created.

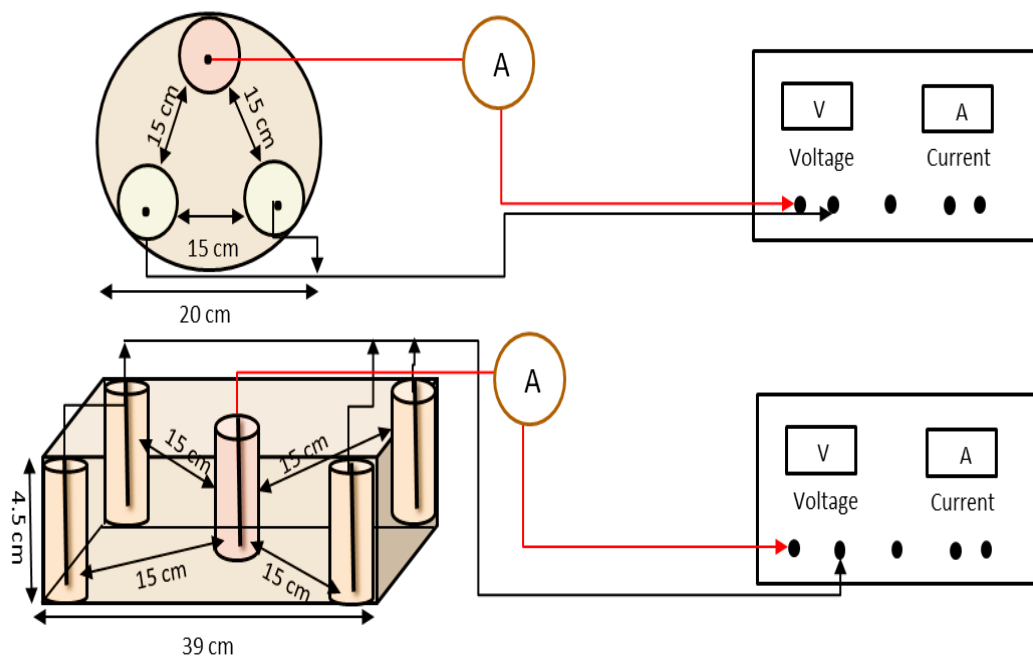


**Fig 3.3** Schematic representation of the soil cell setup for trigonal and square configuration

### ***Power Supply***

For individual metal-contaminated soils, a dual-output regulated variable DC power supply (VKS, 0-60V, 0-5A) was used to supply a direct current of desired voltage, and a milli-ampere meter (MASTECH, MAS830) was used for

measuring the current passing through the soil. For mixed metal-contaminated soils, a variable DC power supply (Sunline, SL-605D) was used to supply a direct current of desired voltage, and a milli-ampere meter cum data logger (ECAY Lab, Turkey) was used for measuring and recording the current passing through the soil. The experiments were performed over a range of four different voltage gradients to identify the most suitable voltage that yields maximum removal (Table 3.1).

**Table 3.1** The selected voltage gradients (V/cm) at which EKR was run for different metal-contaminated soils

S. No.	Chromium (VI)	Lead	Cadmium	Mixed
1.	1	1	0.5	-
2.	1.5	1.5	1.5	-
3.	2	2	-	-
4.	2.5	2.5	2.5	2.5

### ***Electrodes and electrode wells***

This study employed two commercially available electrodes, Graphite, and Stainless Steel (SS 504) of size 10 mm diameter x 150 mm length. The distance between the electrodes in the soil cell was kept constant at 15 cm in all configurations and arrangements. The electrode wells were prepared using perforated cylinders (5.5 cm diameter x 12 cm depth) covered with a nylon cloth of 200 mesh size to avoid clogging and entry of soil into the wells. The electrodes were suspended in the electrode wells filled with electrolytes and connected to the DC power supply with wires and clamps. Electrode wells were connected to the electrode reservoirs *via* tubings to collect the overflow of electrolytes. The following configuration of electrodes were adopted for different set of experiments (Table 3.2).

**Table 3.2** The selected electrode configurations used to run EKR for different metal-contaminated soils

S. No.	Chromium (VI)	Lead	Cadmium	Mixed
1.	Linear (2 electrodes)	Linear (2 electrodes)	Linear (2 electrodes)	Linear (2 electrodes)
2.	-	-	-	Linear (3 electrodes)
3.	-	-	-	Trigonal (3 electrodes)
4.	-	-	-	Square (5 electrodes)

### ***Electrolyte composition***

The removal of metal pollutants from soil under EKR is effective under saturated conditions. For this reason, the soil was saturated with the enhancing solutions, referred to as the electrolyte solutions. In the present work, distilled water was used as the control electrolyte, and ethylenediaminetetraacetic acid (EDTA) solution was used as the enhanced electrolyte solution. EDTA is considered to be an excellent chelating agent that can mobilize metals by forming soluble complexes. For Pb-contaminated soils, Tween 80 was also employed as an electrolyte solution to investigate the efficiency of a surfactant in mobilizing metals. The spiked soil was first pre-treated with the selected electrolyte to attain a moisture content of 25%. The saturated soil was mixed properly and was let to equilibrate for 24 hours to ensure homogenous distribution. The soil cell was filled with saturated soil and the electrode wells were filled with 120 ml of the selected electrolyte solution (Table 3.3).

**Table 3.3** The selected electrolyte solutions used to run EKR for different metal-contaminated soils

S. No.	Chromium (VI)	Lead	Cadmium	Mixed Metals
1.	Distilled water	Distilled water	Distilled water	-
2.	EDTA (0.1 M)	EDTA (0.1 M)	EDTA (0.1 M)	EDTA (0.1 M)
3.	-	Tween 80	EDTA (0.2 M)	-

### 3.2.4. EKR Procedure

All the experiments were performed for two days, for the duration of 5.0 hours each day. The total duration of each test was 10 hours. The soil cell was filled with saturated soil 24 hours before the start of the experiment. After 24 hours, the electrodes were placed in the wells, and connected to the power supply. The wells were filled with the electrolyte (120 ml in each electrode compartment), and the DC voltage was applied. During the experiments, both the voltage and current variations were monitored continuously. At the end of the first cycle of 5.0 hours, the anolyte and catholyte were extracted using the syringe in a measuring cylinder to measure the volume change and then stored in a beaker for analysis. The second cycle was repeated the next day at the same time with fresh electrolytes in the electrode compartments. After the termination of the second cycle, the anolyte and catholyte were extracted. The soil was sectioned into equal divisions from the anode to the cathode (S1, S2, S3, S4,...Sn) and extruded into the containers. Three samples were taken from each section for analysis. Prior to each experiment, the soil cell and electrode wells were washed with diluted acid (0.1M sulphuric acid) to avoid cross-contamination. Electrodes were thoroughly cleaned to remove deposition and fresh nylon cloth was used for each test.

### 3.2.5. Characterization of soil

Raw, spiked, and treated soil were characterized for physical and chemical properties before and after EK treatment. The soil was first air-dried and then pulverized using a mortar and pestle.

#### 3.2.5.1. Physico-chemical analysis

##### *Particle size distribution*

The particle size distribution was performed using the sieve analysis method (**ASTM-D422**). The ground soil was passed through three sieves of different mesh sizes, sieve no. 4 (4.75 mm), sieve no. 10 (2.36 mm), and finally sieve no. 200 (0.075 mm). Based on the weight of soil passed through the sieve and retained on the sieve, the soil was classified into sand, and silt + clay fraction.

##### *Atterberg's limits*

Atterberg's limits were performed using the standard method **ASTM-D4318**. For the liquid limit, 4.75 mm of sieved soil was weighed at 120 g to prepare a paste using distilled water. The paste was placed in a Casagrande cup. It was then grooved using a Casagrande tool and dropped repeatedly until the groove closed back up. This experiment was performed three times, and the moisture content for the three samples was analyzed on a moisture balance.

For plastic limit, 50 g of sieve soil was weighed and mixed with distilled water till it resembled a dough ball. The ball was then rolled on a glass plate into a thread until the soil crumbled. The experiment was repeated thrice and the moisture content was determined for the three samples. The Plasticity Index (PI) was determined by calculating the difference between liquid limit and plastic limit.

Specific gravity was determined using a pycnometer following the **ASTM-D854** method. First, the weight of the empty pycnometer was noted ( $M_1$ ). The 100 g of oven-dried soil was added to the pycnometer and weighed again ( $M_2$ ). Then, the pycnometer was filled with water up to the brim and weighed ( $M_3$ ). Finally, the weight of only the pycnometer and water was noted ( $M_4$ ). The specific gravity was calculated using the following formula:

$$G = \frac{(M_2 - M_1)}{(M_2 - M_1) - (M_3 - M_4)} \dots\dots\dots(3.1)$$

***Moisture Content***

The moisture content of the soil samples was measured using the thermo-gravimetric method (**ASTM-D2216**). First, the weight of the empty crucible was noted ( $W_1$ ). Then, fresh soil was added to the crucible and weighed again ( $W_2$ ). The crucible with fresh soil was kept in a hot air oven at 105°C for 24 hours and weighed again ( $W_3$ ). The moisture content was calculated using the following formula:

$$M.C. (\%) = \frac{(W_2 - W_3)}{(W_3 - W_1)} \times 100 \dots\dots\dots(3.2)$$

***pH and Electrical Conductivity (EC)***

The chemical properties, pH and EC of soil were measured using the standard procedures as per the **ASTM-D1293**. A soil suspension was prepared in a 1:10 soil-to-water ratio in a conical flask and kept in a shaker for 4 hours. The suspension was then left undisturbed for 10 minutes and then analyzed for pH and EC using a bench-top multiparameter (Systronics, LMMP 30 model) through the probes.

***Sodium ( $Na^+$ )***

A soil suspension was prepared in a 1:10 soil-to-water ratio in a conical flask and kept in a shaker for 2 hours. The suspension was allowed to sit for 5 minutes and then the supernatant was collected and centrifuged at 5000 rpm for 10 minutes to obtain a clear sample for analysis. The clear supernatant was then analyzed for  $Na^+$  using the Flame Photometer instrument (Systronics, 128  $\mu$ C) conforming to **APHA 3500-Na** standards. The instrument was calibrated with standard solutions of 10 mg/L, 20 mg/L, 30 mg/L, 40 mg/L, and 50 mg/L of  $Na^+$  prepared from a stock solution of 100 mg/L as NaCl. The standard solutions are aspirated by the instrument to obtain a calibration curve, against which the measurement of emission intensities by the samples was measured.

### ***Potassium ( $K^+$ )***

A soil suspension was prepared in a 1:10 soil-to-water ratio in a conical flask and kept in a shaker for 2 hours. The suspension was allowed to sit for 5 minutes and then the supernatant was collected and centrifuged at 5000 rpm for 10 minutes to obtain a clear sample for analysis. The clear supernatant was then analyzed for  $K^+$  using the Flame Photometer instrument (Systronics, 128  $\mu$ C) as per the **APHA 3500-K** standards. The instrument was calibrated with standard solutions of 10 mg/L, 20 mg/L, 30 mg/L, 40 mg/L, and 50 mg/L of  $K^+$  prepared from a stock solution of 100 mg/L as KCl. The standard solutions are aspirated by the instrument to obtain a calibration curve, against which the measurement of emission intensities by the samples was measured.

### ***Calcium ( $Ca^{2+}$ )***

A soil suspension was prepared in a 1:10 soil-to-water ratio in a conical flask and kept in a shaker for 2 hours. The suspension was allowed to sit for 5 minutes and then the supernatant was collected and centrifuged at 5000 rpm for 10 minutes to obtain a clear sample for analysis. The clear supernatant was then analyzed for  $Ca^{2+}$  using the Flame Photometer instrument (Systronics, 128  $\mu$ C) as per the **APHA 3500-Ca** standards. The instrument was calibrated with standard solutions of 10 mg/L, 20 mg/L, 30 mg/L, 40 mg/L, and 50 mg/L of  $Ca^{2+}$  prepared from a stock solution of 100 mg/L as  $CaCl_2$ . The standard solutions are aspirated by the instrument to obtain a calibration curve, against which the measurement of emission intensities by the samples was measured.





**Fig 3.4.** Flame photometer used for the analysis of cations ( $\text{Na}^+$ ,  $\text{K}^+$ , and  $\text{Ca}^{2+}$ )

**Chlorides ( $\text{Cl}^-$ )**

To determine the concentration of chloride ions ( $\text{Cl}^-$ ), the argentometric method was adopted as per the **APHA 4500 B- $\text{Cl}^-$**  method. First, a soil suspension was prepared in a 1:10 ratio of soil to distilled water to extract water-soluble cations from the soil. The extract was then centrifuged at 4500 rpm for 10 minutes and a clear supernatant was obtained which was used for analysis. For  $\text{Cl}^-$  ion estimation, the titrimetric method was employed using Silver Nitrate ( $\text{AgNO}_3$ ) as a reagent, also known as Mohr’s Method. To prepare the  $\text{AgNO}_3$  solution, 5 g of the salt was dissolved in 1000 mL of ultrapure water. To prepare the potassium chromate indicator, 50 g of  $\text{K}_2\text{CrO}_4$  was dissolved in 1000 mL of ultrapure water. A burette was filled with  $\text{AgNO}_3$ . 20 ml of each sample was taken in a conical flask and 1 ml of  $\text{K}_2\text{CrO}_4$  indicator was added using a pipette. The samples were then titrated against the  $\text{AgNO}_3$  till the colour changed to brick red with precipitation. The readings of the burette were recorded and the ion concentration was calculated using equation 3.3,

$$\text{Cl}^- \text{ Concentration (mg/L)} = \frac{(V \times N \times 35.45)}{V_s \text{ (ml)}} \times 1000 \dots\dots\dots(3.3)$$

Where, V is the volume of  $\text{AgNO}_3$  used, N is the strength of  $\text{AgNO}_3$  and  $V_s$  is the volume of sample.

### ***Sulphates ( $\text{SO}_4^{2-}$ )***

The presence of sulphates in the soil samples was determined with the help of the turbidity method using a single-beam spectrophotometer (LABTRONICS, LT-290 Model). The analysis followed the standards given by **APHA 4500- $\text{SO}_4^{2-}$**  in which the absorbance is taken at 420 nm. Before the analysis, soil suspension was prepared in a 1:10 soil-to-water ratio in a conical flask and kept in a shaker for 2 hours. The suspension was allowed to sit for 5 minutes and then the supernatant was collected and centrifuged at 5000 rpm for 10 minutes to obtain a clear sample for analysis. The instrument was calibrated with standard solutions of 10 mg/L, 20 mg/L, 30 mg/L, 40 mg/L, and 50 mg/L as  $\text{SO}_4^{2-}$ . To prepare the standards through serial dilution, a stock solution of 100 mg/L as  $\text{SO}_4^{2-}$  was prepared with 147.9 mg of  $\text{Na}_2\text{SO}_4$  mixed in 1000 ml of Type-I water. For  $\text{SO}_4^{2-}$  analysis, a conditioning reagent and Barium Chloride ( $\text{BaCl}_2$ ) were used as standard reagents. The conditioning reagent was prepared by adding 75 g of NaCl and 30 mL of concentrated HCl in 100 mL of 95 % ethyl alcohol followed by 50 mL glycerol and a volume make up to 300 mL using distilled water. First, a blank solution was prepared by taking 10 mL of ultrapure water in a clean test tube, in which 0.4 mL of conditioning reagent and a pinch of  $\text{BaCl}_2$  were added and gently mixed. The blank sample was then fed into the spectrophotometer using a cuvette and the instrument was set at zero absorbance. For calibration, 10 mL of each standard solution was prepared by adding 0.4 mL of conditioning reagent and a pinch of  $\text{BaCl}_2$ , and the absorbance was taken to attain a standard curve. After the calibration was completed, the samples were analyzed following the same procedure, and the concentrations were noted in mg/L as provided by the instrument.

### ***Carbonates ( $\text{CO}_3^{2-}$ )***

Carbonate ions are the essential parameter that governs the pH and conductivity of soils. Thus, the ions were determined following the standard

methods as per **ASTM D4373**. To 1 g of soil sample, 20 mL of 1N hydrochloric acid was added and boiled for 5 minutes. The sample was then diluted to 100 mL using ultrapure water and 2 drops of phenolphthalein indicator was added. The sample was then titrated against 1 N sodium hydroxide (NaOH) and the volume was NaOH used was noted. The CO<sub>3</sub><sup>2-</sup> was calculated as CaCO<sub>3</sub> equivalent (%) using the formula:

$$CaCO_3 \text{ equiv. (\%)} = \frac{(V_{HCl}N_{HCl} - V_{NaOH}N_{NaOH})}{g \text{ of soil}} \times 0.05 \times 100 \dots\dots\dots(3.4)$$

**Total Organic Carbon (TOC)**

Total organic carbon was determined using the Walkley-Black’s Method. To 0.2 g of soil sample, 10 ml of 1 N potassium dichromate (K<sub>2</sub>Cr<sub>2</sub>O<sub>7</sub>) and 10 ml of sulphuric acid were added under a fume hood and waited for 30 minutes. Then, 2 mL of Ortho-phosphoric acid was added and the sample was diluted to 50 mL using ultrapure water. To the solution, 0.5 mL of Diphenylamine indicator was added and titrated against 0.5 N of Ferrous Ammonium Sulphate (FAS) till the colour of the solution changed from violet blue to sea green. The volume of the FAS consumed was recorded and TOC was calculated using the formula:

$$TOC (\%) = \frac{V_{FAS} \times N_{FAS}}{V_{K_2Cr_2O_7} \times g \text{ of soil}} \times 0.003 \times 100 \dots\dots\dots(3.5)$$

**3.2.5.2. Metal Analysis**

To analyze the metal concentrations in the soil, the soil samples were oven-dried for 24 hours at 105°C. After oven-drying, 5 g of soil sample was thermally oxidized at 500°C in a muffle furnace for 2 hours. The oxidized soil was used to prepare a soil-acid suspension with 50 ml nitric acid (10 %) in an orbital shaker for 30 minutes. The extract was then centrifuged and the clear supernatant was used for metal analysis.

### ***Cr (VI) Analysis***

The concentration of Cr (VI) was determined as per **USEPA standard 7196A** spectrophotometric method using Diphenylcarbazide (DPC). In this study, the Cr (VI) concentration was measured using a UV-VIS single-beam spectrophotometer (LABTRONICS, Model LT-290) at a wavelength of 540 nm. The instrument was calibrated with standard solutions of 0.1 to 1.0 mg/L concentrations. After calibration, a blank was set wherein 10 ml of ultrapure water was taken in a test tube to which 2 drops of 0.2 N sulphuric acid were added. After shaking, 2 ml of DPC solution (0.250 g DPC salt in 50 ml acetone) was added to the test tube and shaken. The sample was fed to the spectrophotometer and the absorbance was set to zero. After the calibration, the samples were analyzed following the same procedure until a pink-purple tint appeared, and the concentrations were noted in mg/L as provided by the instrument. The nylon filter used to wrap the electrode wells absorbed some concentration of metals and was analyzed for mass balance. The filter was acid-digested in 50 mL of 5% nitric acid and sonicated for 30 minutes. The extract was centrifuged and analyzed using the same procedure as mentioned above.

### ***Lead (Pb) analysis***

The Pb concentration in samples was determined over a Flame Atomic Absorption Spectrophotometer (AAS) (Analytik-Jena novAA 350), conforming to the testing procedure **APHA 3500-Pb**. The instrument was calibrated with the standard solutions of Pb ranging between 10 to 60 mg/L. The solutions were prepared from 1000 mg/L of Pb stock solution. The stock was prepared by mixing 0.15 g of  $\text{Pb}(\text{NO}_3)_2$  with 10 mL of 1:1  $\text{HNO}_3$  and the volume was made up to 500 mL. The instrument was turned on and the element-specific hollow cathode lamp was selected. The flame was ignited and a method was developed for Pb using the instrument software. The standard solutions were aspirated to obtain a calibration curve (Fig 3.5). After calibration, the samples were aspirated and the concentration of Pb in mg/L was recorded.

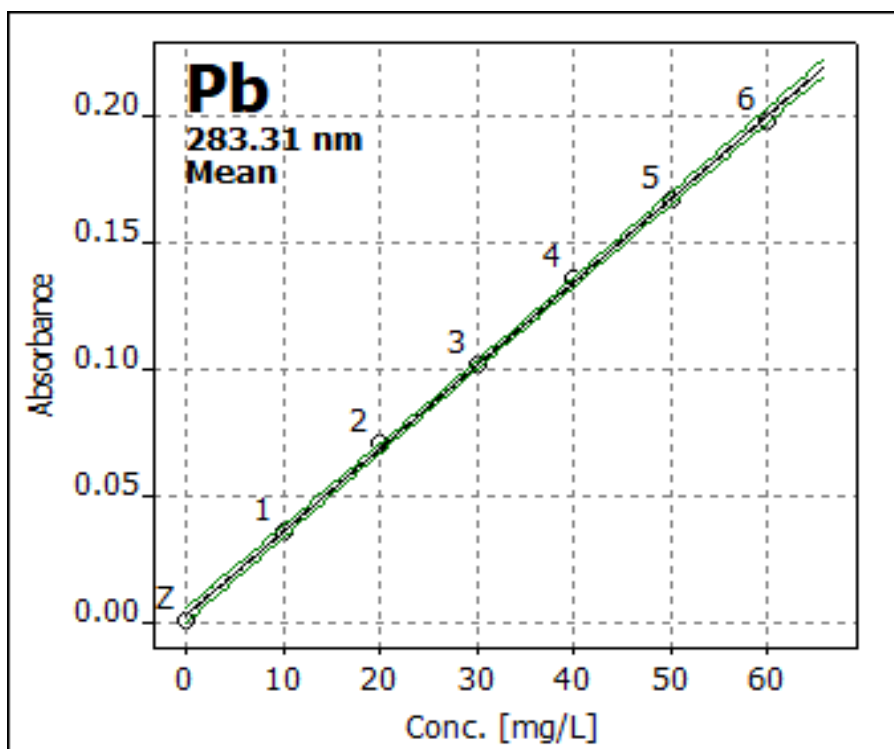


**Fig 3.5** Standard curve of concentration (mg/L) against absorbance obtained for Pb

### ***Cadmium Analysis***

The Cd concentration in samples was determined over a Flame Atomic Absorption Spectrophotometer (AAS) (Analytik-jena novAA 350), conforming to the testing procedure **APHA 3500-Pb**. The instrument was calibrated with the standard solutions of Cd ranging between 2.5 to 15 mg/L. The solutions were prepared from 1000 mg/L of Cd stock solution. The stock was prepared by mixing 163.1 mg of CdCl<sub>2</sub> with 20 mL of 1:1 HNO<sub>3</sub> and the volume was made up to 1000 mL. The instrument was turned on and the element-specific hollow cathode lamp was selected. The flame was ignited and a method was developed for Cd using the instrument software. The standard solutions were aspirated to obtain a calibration curve (Fig 3.6). After calibration, the samples were aspirated and the concentration of Cd in mg/L was recorded.

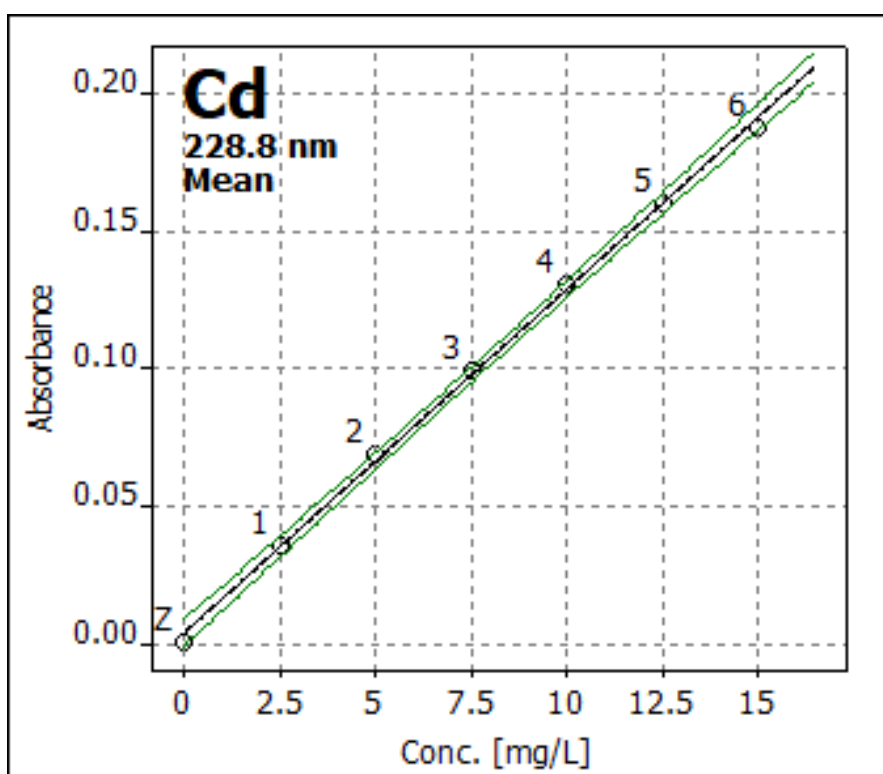


**Fig 3.6** Standard curve of concentration (mg/L) against absorbance obtained for Cd

### 3.2.5.3. Sequential extraction of metals

Sequential extraction analysis of metals was performed in order to determine the speciation of the metals in the soil before and after EK treatment. For this study, a widely used procedure given by Reddy et al. (2001), originally developed by Tessier et al. (1979), was used to determine the speciation of metals in five fractions, exchangeable and soluble form, carbonate bound, Fe-Mn oxide bound, organic matter bound, and residuals. The extraction procedure is as follows:

- I. Exchangeable: To 1 g of soil sample, 8 ml of 1 M Sodium Acetate solution is added at a pH of 8.2 and mixed continuously for 1 hour. 1 M Sodium Acetate solution was prepared by weighing 13.6 g of the salt in 1000 ml ultrapure water. After 1 hour, the suspension is centrifuged at 4500 rpm for 10 minutes and supernatant is collected for metal analysis.

- II. Carbonate bound: The residue from the above fraction is transferred to a conical flask and 8 mL of 1 M Sodium Acetate solution is added again, at a pH of 5. The solution is mixed thoroughly in a shaker for 5 hours. After 5 hours, the suspension is centrifuged at 4500 rpm for 10 minutes and supernatant is collected for metal analysis.
- III. Fe-Mn oxide bound: The residue from the above fraction is transferred to a conical flask and 20 mL of 0.04 M hydroxylamine hydrochloride (NH<sub>2</sub>OH.HCl) is added to the soil and heated at 96C for 6 hours with occasional stirring. 0.04 M NH<sub>2</sub>OH.HCl is prepared by adding 0.27796 g of the salt in 100 mL of ultrapure water and 25% of acetic acid. After heating, the suspension is centrifuged at 4500 rpm for 10 minutes and supernatant is collected for metal analysis.
- IV. Organic matter bound: The residue from the above fraction is transferred to a conical flask and 3 mL of 0.02 M nitric acid is added, followed by 5 mL of 30% hydrogen peroxide at a pH of 2. The mixture is heated at 85C for 2 hours with occasional stirring, after which again 3 mL of 30% hydrogen peroxide is added and kept in a shaker for 3 hours. The mixture is left to cool and then 5 mL of 3.2 M ammonium acetate in 20% nitric acid is added. The mixture is diluted to 20 mL and kept in a shaker for 30 minutes. After shaking, the suspension is centrifuged at 4500 rpm for 10 minutes and supernatant is collected for metal analysis.
- V. Residual: The sum of the above fractions is subtracted from the total concentration.

### **3.2.6. Characterization of electrolytes**

#### ***Electro-osmotic flow***

Volume change was measured For Cr (VI) analysis, electrolytes were centrifuged at 5000 rpm for 10 minutes and analyzed for Cr (VI) in the supernatant. Electrolytes collected from EDTA experiments were chemically oxidized to hexavalent chromium (APHA, 1992b) prior to chromium analysis.

### ***pH and Electrical Conductivity (EC)***

The electrolytes collected were analyzed for pH and EC using a bench-top multiparameter (Systronics, LMMP 30 model) through the probes.

### ***Cr (VI) analysis***

The concentration of Cr (VI) was determined as per **USEPA standard 7196A** spectrophotometric method using Diphenylcarbazide (DPC). In this study, the Cr (VI) concentration was measured using a UV-VIS single-beam spectrophotometer (LABTRONICS, Model LT-290) at a wavelength of 540 nm. The instrument was calibrated with standard solutions of 0.1 to 1.0 mg/L concentrations. After calibration, a blank was set wherein 10 ml of ultrapure water was taken in a test tube to which 2 drops of 0.2 N sulphuric acid were added. After shaking, 2 ml of DPC solution (0.250 g DPC salt in 50 ml acetone) was added to the test tube and shaken. The sample was fed to the spectrophotometer and the absorbance was set to zero. After the calibration, the samples were analyzed following the same procedure until a pink-purple tint appeared, and the concentrations were noted in mg/L as provided by the instrument.

When the treatment employed EDTA, the electrolytes were oxidized to convert the total chromium into Cr (VI) which might have reduced to Cr (III). The testing procedure conformed to **APHA-3500 Cr (B)**. To 5 mL of sample, 3 drops of methyl orange indicator were added, followed by 1 mL of ammonium hydroxide (NH<sub>4</sub>OH) solution till the colour changed to yellow. Then, 2 mL of 1:1 HNO<sub>3</sub> was added and the volume was made up to 40 mL using ultrapure water. The mixture was boiled on a heating mantle and 2 drops of potassium permanganate (KMnO<sub>4</sub>) were added and boiled for 2 more minutes. The solution develops a red colour. To the solution, 1 mL of sodium azide (NaN<sub>3</sub>) was added till the colour faded and the solution was then left to cool. Once the solution was cooled, 0.25 mL of orthophosphoric acid (H<sub>3</sub>PO<sub>4</sub>) was added. The solution was then analyzed over the spectrophotometer after adding DPC and acid.



### ***Lead (Pb) analysis***

The Pb concentration in electrolyte samples was determined over a Flame Atomic Absorption Spectrophotometer (AAS) (Analytik-jena novAA 350), conforming to the testing procedure **APHA 3500-Pb**. Electrolyte solutions were centrifuged at 5000 rpm for 10 minutes to remove suspended soil particles and then analyzed on AAS. The instrument was calibrated with the standard solutions of Pb ranging between 10 to 60 mg/L. The solutions were prepared from 1000 mg/L of Pb stock solution. The stock was prepared by mixing 0.15 g of  $\text{Pb}(\text{NO}_3)_3$  with 10 mL of 1:1  $\text{HNO}_3$  and the volume was made up to 500 mL. The instrument was turned on and the element-specific hollow cathode lamp was selected. The flame was ignited and a method was developed for Pb using the instrument software. The standard solutions were aspirated to obtain a calibration curve. After calibration, the samples were aspirated and the concentration of Pb in mg/L was recorded.

### ***Cadmium (Cd) analysis***

The Cd concentration in electrolyte samples was determined over a Flame Atomic Absorption Spectrophotometer (AAS) (Analytik-jena novAA 350), conforming to the testing procedure **APHA 3500-Cd**. Electrolyte solutions were centrifuged at 5000 rpm for 10 minutes to remove suspended soil particles and then analyzed on AAS. The instrument was calibrated with the standard solutions of Cd ranging between 2.5 to 15 mg/L. The solutions were prepared from 1000 mg/L of Cd stock solution. The stock was prepared by mixing 163.1 mg of  $\text{CdCl}_2$  with 20 mL of 1:1  $\text{HNO}_3$  and the volume was made up to 1000 mL. The instrument was turned on and the element-specific hollow cathode lamp was selected. The flame was ignited and a method was developed for Cd using the instrument software. The standard solutions were aspirated to obtain a calibration curve. After calibration, the samples were aspirated and the concentration of Cd in mg/L was recorded.



(a)



(b)

**Fig 3.7** Flame Atomic Absorption Spectrophotometer (AAS) (a) Analytik-jena novAA 350, Water lab, DTU (b) Environment lab, ÇOMU, Turkey

### 3.2.7. Experimental design

The experiments for this work were designed using two different approaches. First, OFAT approach, i.e., One Factor At a Time, was employed wherein, only one factor was varied while the rest were kept constant to assess the effects of the specific parameter and to optimize its conditions. This was done to achieve baseline data and the individual implications of each parameter over the removal efficiency of the EK technique. The selected variables were applied voltage, electrolyte composition, and electrode materials, which were varied for EKR of Cr (VI), Pb, and mixed metal contaminated soils.

The second approach for experimental design was the Design of Experiments (DOE). A Response Surface Methodology (RSM) was employed to develop the correlation between the parameters and their interspecific effects for effective EKR of Cd-contaminated soils. RSM helps in assessing relations between the variables for optimisation and design of experiments. Thus, the parameters for the removal of Cd from soil using EKR were optimized using the Central Composite design (CCD). Since the model takes into consideration the continuous factors, only two parameters that showed continuous variations were considered i.e., removal efficiency are voltage ( $X_1$ ) and electrolyte composition ( $X_2$ ). Minimum and maximum levels for the parameters were ranged as 0.5-2.5 V/cm for  $X_1$ , and 0.0-0.2 M EDTA for  $X_2$ . Considering the factorial structure of CCD, the total number runs were obtained using the formula:  $N = 2^K + 2K + n_c$ , where K is the number of factors ( $K=2$ ), and  $n_c$  is the replicate number of central point ( $n_c = 1$ ). The Design Expert software was used to design 09 experimental runs ( $N = 2^2 + 2(2) + 1 = 9$ ) for three responses, removal efficiency, electro-osmotic flow, and energy consumption. The following equation was used to derive the relation between dependent (Y) and independent variables ( $X_i$ ).

$$Y = b_0 + b_1X_1 + b_2X_2 + b_3X_3 + b_{12}X_1X_2 + b_{13}X_1X_3 + b_{23}X_2X_3 + b_{11}X_1X_1 + b_{22}X_2X_2 + b_{33}X_3X_3 \dots\dots\dots(3.6)$$

### Cost-benefit analysis

For each metal analysis, an economic evaluation of EKR was conducted, considering the energy consumption for each experiment, followed by cost estimation for the chemicals and electrodes used. Energy expenditure is an important factor to assess the economic viability of EKR technique, as it accounts for 10-15% of the total cost (Virkyute et al., 2002). In this study, energy consumption is calculated using Eqn. 3.7,

$$E = \frac{1}{V_s} \int VI(t) dt \dots \dots \dots (3.7)$$

Where, V is the average voltage, I is the average current measured during EKR in time t and  $V_s$  is the volume of soil. The total cost of the treatment was calculated as the sum of cost of electricity consumed, cost of electrodes and the cost of chemicals used for electrolyte conditioning. Based on the removal efficiency of the experiment, cost per gram of removal of metal from soil was also calculated to evaluate the cost-effectiveness of this technique.

### 3.2.8. Human Health Risk Assessment

Risk Assessment is a product of the outputs of exposure as well as toxicity assessment which depicts the overall health impact in terms of carcinogenic, non-carcinogenic, and radiological risks. Non-carcinogenic risk is estimated using the **USEPA 1989 method** by calculating the Average Daily Dose (ADD, mg/kg/day) of a contaminant through all three routes of exposure pertaining to the days of exposure (Eq. 3.8-3.10). The ADD is then calculated against the RfD to obtain the Hazard Quotient (HQ) (Eqn. 3.11). The sum of HQ from the three pathways is the Hazard Index (HI) (Eqn. 3.12), which determines the non-cancer risks associated with a contaminant, with  $HI < 1$  will have no adverse effects, and  $HI > 1$  will have potential adverse non-carcinogenic effects. Carcinogenic risks, on the other hand, is estimated through the product of ADD with the slope factor (SF) (Eq. 3.13-3.15). Total Carcinogenic Risk (TCR) is estimated from the sum of risks from the three pathways (Eq. 3.16). The normal value of TCR ranges from  $10^{-6}$  to  $10^{-4}$ , above which, the associated contaminant poses adverse carcinogenic risk (Adimalla et al., 2020).

$$ADD_{ing} = \frac{C \times IngR \times EF \times ED \times EF}{BW \times AT} \times 10^{-6} \dots\dots\dots (3.8)$$

$$ADD_{inh} = \frac{C \times InhR \times ED \times EF}{BW \times AT \times PEF} \dots\dots\dots (3.9)$$

$$ADD_{der} = \frac{C \times ESA \times AF \times ED \times EF}{BW \times AT} \times 10^{-6} \dots\dots\dots (3.10)$$

$$HQ = \frac{ADD_i}{RfD_i} \dots\dots\dots (3.11)$$

$$HI = \sum HQ \dots\dots\dots (3.12)$$

$$CR_{ing} = ADD_{ing} \times SF_{ing} \dots\dots\dots (3.13)$$

$$CR_{inh} = ADD_{inh} \times SF_{inh} \dots\dots\dots (3.14)$$

$$CR_{der} = ADD_{der} \times SF_{der} \dots\dots\dots (3.15)$$

$$TCR = \sum (CR_{ing} + CR_{inh} + CR_{der}) \dots\dots\dots (3.16)$$

Where, C is the soil heavy metal concentration (mg/kg); IngR (mg/day) and InhR (m<sup>3</sup>/day) are the ingestion and inhalation rates of soil particles, respectively; EF (day/year) and ED (year) are the exposure frequency and exposure duration, respectively; BW and AT are the average body weight of the exposed individual (Kg) and average exposure time (day), respectively; ESA is the exposed skin surface area (cm<sup>2</sup>); AFS is the skin adherence factor (mg/cm<sup>2</sup>); PEF is the particle emission factor (m<sup>3</sup>/kg). RfD is the reference dose (mg/kg/day), “i” is the number of exposure pathway.

**Table 3.4.** Selected values for the variables used in HHRA (USEPA, 1989)

Variables	Physical significance and units	Values	
		Adults	Children
<i>IngR</i>	Ingestion rate of soil (mg/day)	100	200
<i>InhR</i>	Inhalation rate of soil (m <sup>3</sup> /day)	12.3	7.6
<i>EF</i>	Exposure frequency (days/year)	365	365
<i>ED</i>	Exposure duration (years)	30	6

<i>BW</i>	Average body weight (kg)	70	20
<i>AT</i>	Average exposure time (non-carcinogenic, days)	8760	2190
<i>ESA</i>	Exposed skin surface area (cm <sup>2</sup> )	4359	1600
<i>SAF</i>	Soil to skin adherence factor (mg/cm <sup>2</sup> )	0.07	0.2
<i>PEF</i>	Particle emission factor (m <sup>3</sup> /kg)	1.36×10 <sup>6</sup>	1.36×10 <sup>6</sup>

**Table 3.5.** Reference Dose and Slope Factor of the selected metals (Adimalla et al., 2020)

Exposure pathway		Cr	Pb	Cd
<i>RfD</i>	Ingestion	3.00E-03	3.50E-03	4.00E-02
	Dermal absorption	6.00E-05	5.25E-04	1.20E-02
	Inhalation	2.86E-05	3.52E-03	1.00E-03
<i>SF</i>	Ingestion	5.01E-01	8.50E-03	0.38
	Dermal absorption	2.00E+01	-	0.38
	Inhalation	4.20E+01	4.20E-02	6.3

### 3.2.9. Laboratories used

The experiments and analysis for phase I, i.e., for single metal-contaminated soils were performed in the Environmental Microbiology and Bioremediation Lab of the Department of Environmental Engineering, DTU. The analysis for cadmium metal concentration was performed in the Analytik Jena Laboratory, Patparganj, Delhi. The experiments and analysis for Phase II, i.e., for mixed metal-contaminated soils were performed in the Geology and Environment lab of Department of Geological Engineering, Çanakkale Onsekiz Mart University, Turkey.

## CHAPTER 4

### RESULTS AND DISCUSSION

The EKR was studied for three metals i.e., chromium, lead, and cadmium individually present in spiked soil, and mixed metals present in spiked soil to understand the behaviour of EKR under the presence of individual metals or mixed-metals as contaminants. The metal-specific results are presented in the section given below.

#### 4.1. EKR for Cr (VI)-contaminated soil

EKR was carried out to assess the removal of Cr (VI) from fine-grained sandy soil. A total of ten (10) experiments were carried out in 3 parts (Table 4.1). First, a series of tests were performed to identify the optimum voltage for maximum removal of Cr (VI) from soil (tests EK1-EK4). Second, EDTA was used as electrolyte at the recommended low voltage (20V, EE1) and high voltage (50V, EE2) and the results were compared with control tests using distilled water. In the third step, stainless-steel electrode was used in controlled conditions with distilled water to compare the results with graphite electrode (20V, ET1; 50V, ET2) and also with EDTA to evaluate the combined effects of electrode and electrolyte conditioning (20V, ES1; 50V, ES2). All the experiments were operated for 10 hours in 2 cycles of 5 hours each for two days.

**Table 4.1** Details of experimental conditions used for EKR of Cr (VI)-contaminated Soil

S. No.	Experiment	Electrolyte	Electrode Material	Voltage (V)	Moisture Content (%)	Treatment time
1	EK1	Distilled water	Graphite	20	25	10 h (5h + 5h batch mode)
2	EK2	Distilled water	Graphite	30	25	10 h (5h + 5h batch mode)
3	EK3	Distilled water	Graphite	40	25	10 h (5h + 5h batch mode)
4	EK4	Distilled water	Graphite	50	25	10 h (5h + 5h batch mode)
5	EE1	EDTA (0.1M)	Graphite	20	25	10 h (5h + 5h batch mode)
6	EE2	EDTA (0.1M)	Graphite	50	25	10 h (5h + 5h batch mode)
7	ET1	Distilled water	Stainless steel	20	25	10 h (5h + 5h batch mode)
8	ET2	Distilled water	Stainless steel	50	25	10 h (5h + 5h batch mode)
9	ES1	EDTA (0.1M)	Stainless steel	20	25	10 h (5h + 5h batch mode)
10	ES2	EDTA (0.1M)	Stainless steel	50	25	10 h (5h + 5h batch mode)

#### 4.1.1. Variations in pH

The variations in pH of electrolyte and soil after EKR treatment are given in Fig 4.1. A typical pH profile was observed with all voltage gradients indicating low pH in anolyte and a high pH in catholyte (Table 4.2). As the voltage gradient increased (Fig 4.1a), pH values decreased at anode to pH less than 2, and pH more than 11 at cathode due to faster electrolysis reactions. The pH gradient is formed primarily due to production of hydrogen and hydroxyl ions. Oxidation of water at anode generates hydrogen ions, while reduction at cathode generates hydroxyl ions (Acar et al., 1993), resulting in variation of pH at the respective



electrode. Application of high voltage produces higher electrical current, which increases the rate of dissociation of electrolytes and generation of more hydrogen and hydroxide ions that migrate into the soil system (Cameselle & Gouveia, 2020; Prakash et al., 2022b). When EDTA was used as electrolyte (Fig. 4.1b and 1c), comparable results were obtained with low anolyte pH (3.0) and high catholyte pH (10.0) at both 20 and 50V, as has been reported by Reddy & Chinthamreddy, (2004b).

Soil pH was not much affected by the applied voltage and EDTA and remained almost neutral throughout the experiments (Table 4.3 and Fig 4.1). Similar findings were observed by Wu et al., (2016), where slightly acidic pH (6.1) was observed in the soil section close to anode, while slightly alkaline pH (7.2) was observed in soil close to cathode at high voltage gradient of 2.5 V/cm. This could be attributed to high buffering capacity of soil due to the presence of carbonates (~18%) that neutralized the acid front generated at the anode (Reddy et al., 1997; Song et al., 2016a).

#### **4.1.2. Variations in electrical conductivity**

Electrical conductivity (EC) determines the flow of current through soil which is affected by soil pH and applied voltage. The EC of electrolytes after EKR is given in Table 4.2. In experiments EK1 to EK4, EC of anolyte was relatively higher than catholyte indicating the movement of ions towards the anode. However, in experiments where EDTA is used as electrolyte (EE1 to ET2), EC was higher in catholyte as compared to anolyte. Whereas, in experiments with EDTA and stainless steel electrode, the EC was comparable in anolyte and catholyte. The findings suggested that the use of EDTA with graphite may lead to generation of more OH<sup>-</sup> ions at the cathode, causing the formation of hydroxides and thereby increasing the EC at the catholyte. Table 4.3 and Fig. 4.2 exhibits the EC in soil sections S1-S4 after EKR treatment. At low voltage, EC was high in soil section S2 and low near electrodes. As the voltage increased to 30 V, the peak shifted to S3 from S2, which indicates migration and accumulation of ions towards cathode. At the maximum

voltage, minimum EC was observed in all sections due to depletion of ions by electromigration to the electrolyte used, at high voltage. EC values in soil were higher in tests with EDTA as compared to distilled water as electrolyte, with maximum value in EDTA-Graphite (EE2) experiment at 50V, due to increase in ionic concentration in the soil (Fig. 4.2b and 4.2c). However, the values were relatively low in S3 and S4 sections as compared to S1 and S2, which indicates movement of ions towards anode. In EE1, inverse trend was observed, with lower EC in S1 and S2 sections as compared to S3 and S4. The reason could be corrosion of graphite electrode at the anode due to oxidizing conditions, which increased the electrical resistance and reduced electrical conductivity near anode, as has been reported by other authors (Sun et al., 2021b).

#### **4.1.3. Variations in current**

Stronger electromigration is observed at high current values, which leads to more removal of metal ions. Table 4.4 and Fig. 4.3a shows the current profile during EKR process with time at different voltage gradients. In experiments EK1-EK4 (with varying voltage gradients), the results showed that initially the current increased rapidly, achieved a peak at a maximum value and then stabilized. Even though the trend was same at every voltage gradient, the current increased with voltage. It attained peak early in case of stainless steel (experiment ET1-ET2) as compared to graphite (Fig. 4.3b). When EDTA was used as electrolyte (Fig. 4.3c), the trend was inversed. The current started with a peak which decreased with time till it stabilized. Considering the combination of EDTA with electrode material, EDTA-G exhibited higher current than EDTA-SS. The saturation of soil with EDTA provided higher ionic strength by solubilizing ionic species, which increased the initial current (Cameselle et al., 2021b).

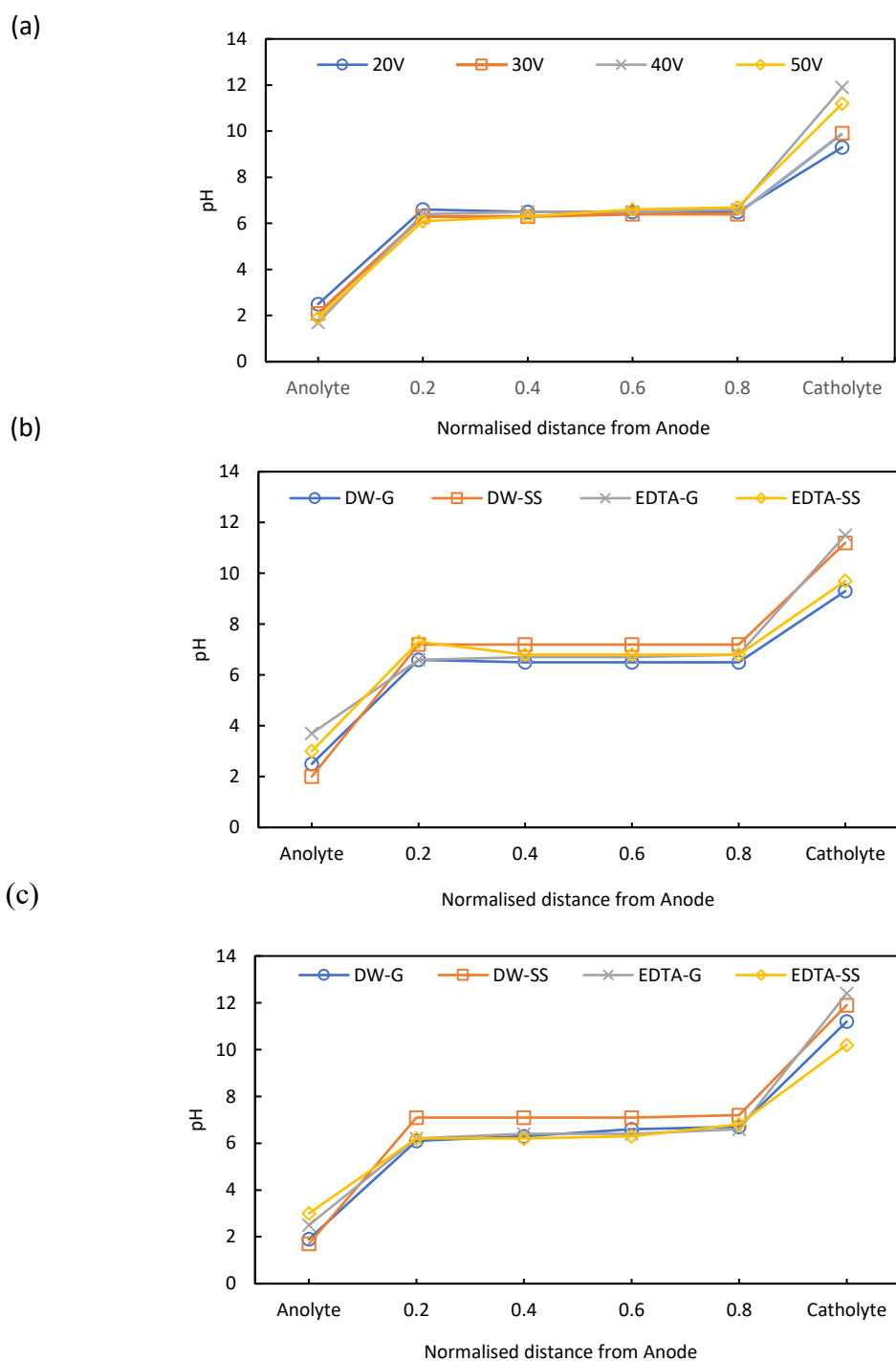


**Figure 4.1** Variations in pH of soil after EKR treatment under different conditions (a) controlled conditions at four different applied voltage (b) enhanced with EDTA at 20 V (c) enhanced with EDTA at 50V

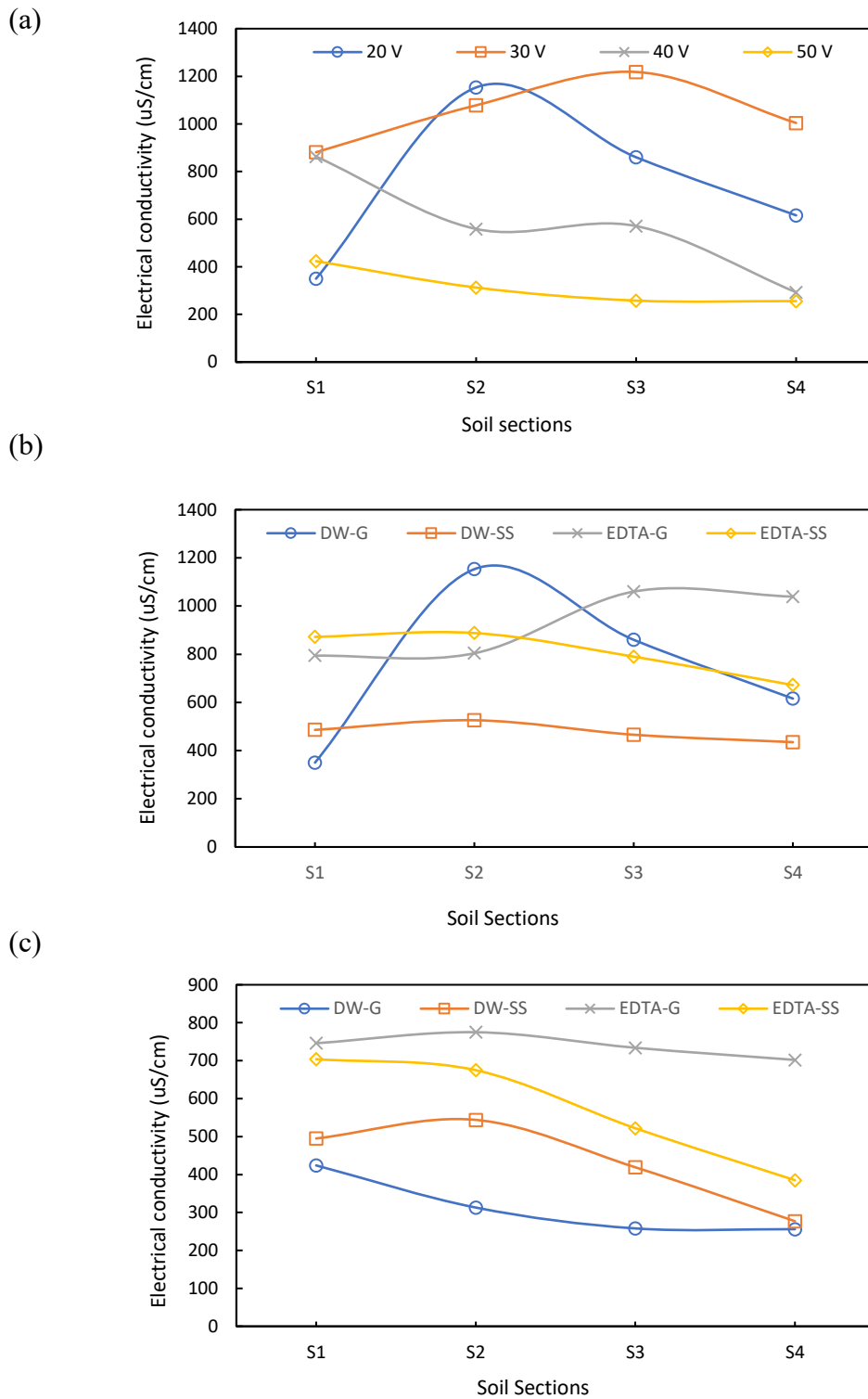


**Figure 4.2** Variations in Electrical conductivity (EC) of soil after EKR treatment under different conditions (a) controlled conditions at four different applied voltage (b) enhanced with EDTA at 20 V (c) enhanced with EDTA at 50V

**Table 4.2** The variations in pH, EC, TDS, volume, and Cr (VI) concentration in anolyte and catholyte after EK treatment

Experiment set	Cycle	Section	pH	EC (mS/cm)	TDS (ppm)	Volume change (mL)	Cr (VI) conc. (mg/L)
<b>EK1</b>	Day 1	A1	2.7	1.41	708	79	306
		C1	10.1	0.82	410	65.5	445
	Day 2	A2	2.2	2.83	1421	42	2.14
		C2	8.4	0.73	372	58	0.192
<b>EK2</b>	Day 1	A1	2.2	47.4	2360	78.5	720
		C1	10.7	2.49	1245	100.1	0.477
	Day 2	A2	1.9	7.09	3540	40	943.6
		C2	9.1	1.69	845	52	0.157
<b>EK3</b>	Day 1	A1	1.6	19.78	9870	28	3386
		C1	11.9	15.58	7800	59	3.72
	Day 2	A2	1.7	14.84	7570	27	2577.6
		C2	11.9	11.4	5700	35	3.008
<b>EK4</b>	Day 1	A1	1.9	13.25	6540	74	4008.3
		C1	10.9	4.02	1969	62	11.11
	Day 2	A2	1.8	14.82	7360	37	4020
		C2	11.5	6.3	3150	62	0.306
<b>EE1</b>	Day 1	A1	3.8	8.74	4360	65	805.6
		C1	10.8	19.43	9690	68	5.62
	Day 2	A2	3.6	8.47	4240	68	146.4
		C2	12.2	19.91	9960	77	1.89
<b>EE2</b>	Day 1	A1	2.6	5.91	2950	39	4629.6

		C1	12.2	21.8	10910	94	2.52
	Day 2	A2	2.3	6.15	3070	36	7697.6
		C2	12.5	22.4	11320	90	13.5
<b>ET1</b>	Day 1	A1	2.3	5.74	2860	25	2632
		C1	9.6	15.66	7850	68	80.62
	Day 2	A2	3.7	8.74	4370	50	1112
		C2	9.7	16	8020	69	35.77
<b>ET2</b>	Day 1	A1	3.5	8.46	4190	50	3744
		C1	10.1	18.58	9310	72	12.77
	Day 2	A2	2.4	4.98	2490	24	1532
		C2	10.2	17.83	8944	70	8.99
<b>ES1</b>	Day 1	A1	2	4.18	2230	28	1227
		C1	11.2	1.93	900	71	6.26
	Day 2	A2	1.9	4.09	2450	70	1172
		C2	11.2	3.86	2180	78	40.97
<b>ES2</b>	Day 1	A1	1.6	10.17	5070	66	2316.6
		C1	11.8	8.66	4310	85	7.374
	Day 2	A2	1.74	14.96	7500	55	4753.3
		C2	11.9	9.96	4780	79	5.076

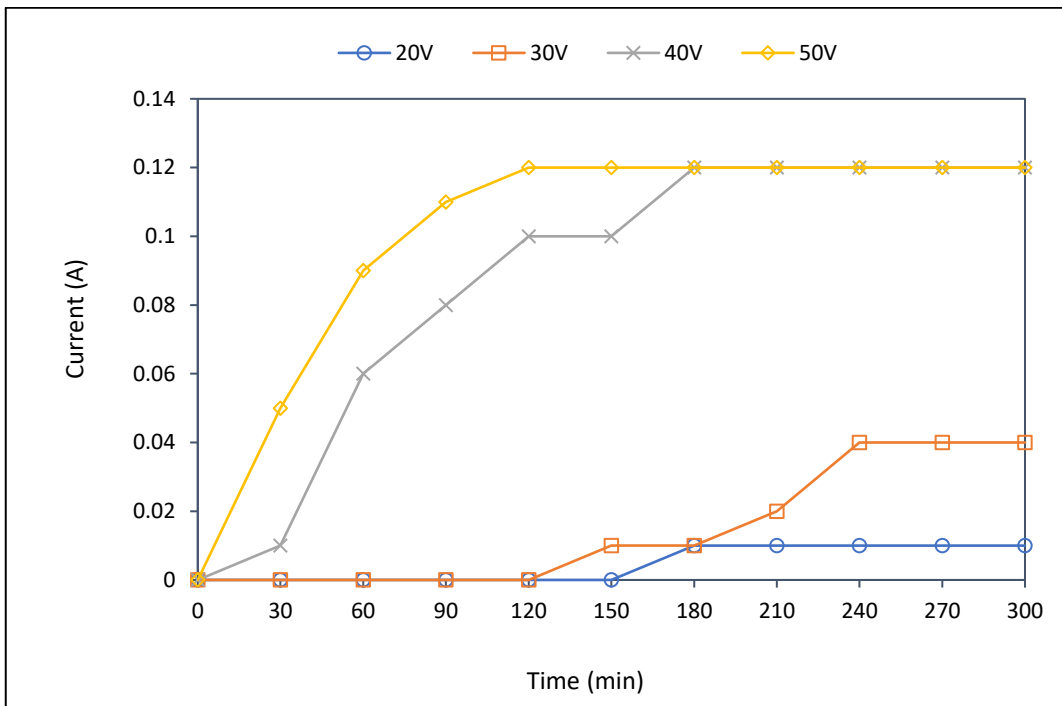
**Table 4.3** The variations in pH, EC, TDS, moisture content, and Cr (VI) concentration in soil before and after EK treatment

Experiment set	Sections	pH	EC (uS/cm)	TDS (ppm)	MC (%)	Cr (VI) (mg/kg)
<b>EK1</b>	Initial	6.4	749	376	25	370
	S1	6.6	350	176	21.9	450
	S2	6.5	1153	580	20.8	800
	S3	6.5	860	430	20.27	800
	S4	6.5	616	308	22.28	390
<b>EK2</b>	Initial	6.5	406	201	25	522
	S1	6.3	881	439	25.2	534
	S2	6.3	1078	538	21.8	1010
	S3	6.4	1218	613	23.13	540
	S4	6.4	1004	504	24.5	270
<b>EK3</b>	Initial	6.5	355	173.5	25	1750
	S1	6.4	863	345	21.8	1980
	S2	6.5	559	272	21.13	1320
	S3	6.5	571	287	20.95	1360
	S4	6.6	293	144.6	21.57	80.2
<b>EK4</b>	Initial	6.5	204	133.5	25.76	1340
	S1	6.1	424	211	22.9	1256
	S2	6.3	313	156.5	21.45	693

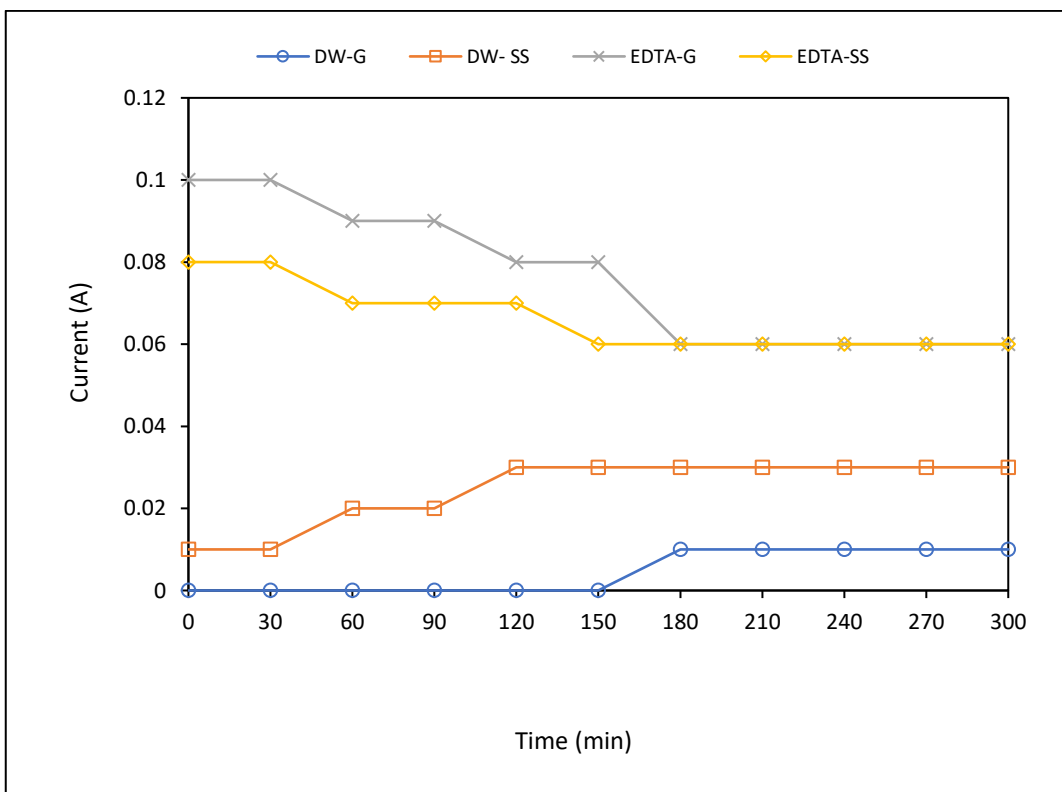
	S3	6.6	258	130.5	22.88	305
	S4	6.7	256	127.7	23.48	120
<b>EE1</b>	Initial	6.5	565	236	25	803
	S1	6.6	794	400	21.8	347
	S2	6.7	804	405	21.13	660
	S3	6.7	1060	531	20.95	582
	S4	6.8	1039	520	21.57	16.5
		Initial	6.5	580	285	25.76
<b>EE2</b>	S1	6.2	746	372	22.9	380
	S2	6.4	775	388	21.45	549
	S3	6.4	734	358	22.88	580
	S4	6.6	702	352	23.48	6
		Initial	6.5	548	275	24.3
<b>ET1</b>	S1	7.3	872	433	23.7	749
	S2	6.8	888	444	23.08	990
	S3	6.8	790	397	22.22	900
	S4	6.8	672	337	22.76	185
		Initial	6.5	512	256	24.8
<b>ET2</b>	S1	6.2	623	312	22.25	1155
	S2	6.2	675	336	21.8	650



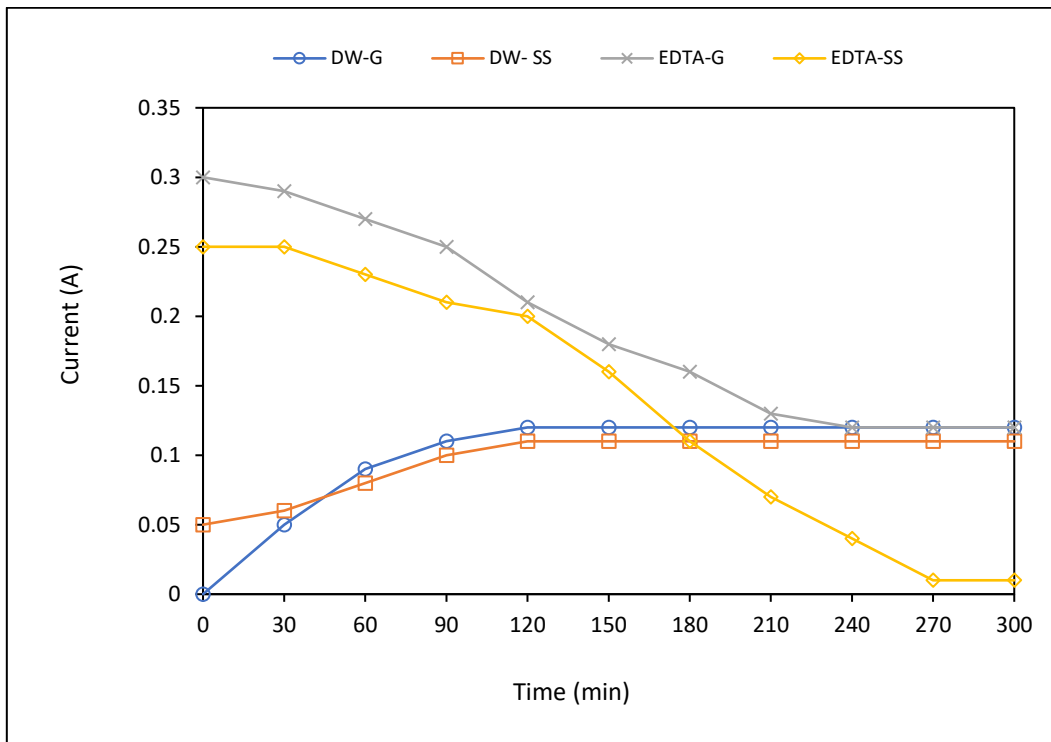
	S3	6.3	522	262	22.4	314
	S4	6.8	385	122	23.39	55.7
<b>ES1</b>	Initial	6.8	449	224	28.9	1174
	S1	7.2	486	242	27.38	1116
	S2	7.2	526	263	27.68	1060
	S3	7.1	466	238	23.8	476
	S4	7.2	435	215	25.23	595
	Initial	6.5	482	238	28.6	1217
<b>ES2</b>	S1	7.1	495	249	28.2	1010
	S2	7	544	271	27.8	810
	S3	7.1	419	210	24.6	600
	S4	7.2	277	138.8	26.24	3.7



(a)



(b)



(c)

**Figure 4.3** Variations in current in soil during EKR treatment under different conditions (a) unenhanced with four different applied voltage (b) enhanced with EDTA at 20V (c) enhanced with EDTA at 50V

**Table 4.4.** Variations in Current (Amperes) with time during the EKR of Cr (VI)-contaminated soils

<b>Time (mins)</b>	<b>EK1</b>	<b>EK2</b>	<b>EK3</b>	<b>EK4</b>	<b>EE1</b>	<b>EE2</b>	<b>ET1</b>	<b>ET2</b>	<b>ES1</b>	<b>ES2</b>
0	0	0	0	0	0.10	0.30	0.01	0.05	0.08	0.25
30	0	0	0.01	0.05	0.10	0.29	0.01	0.06	0.08	0.25
60	0	0	0.06	0.09	0.09	0.27	0.02	0.08	0.07	0.23
90	0	0	0.08	0.11	0.09	0.25	0.02	0.10	0.07	0.21
120	0	0	0.1	0.12	0.08	0.21	0.03	0.11	0.07	0.20
150	0	0.01	0.1	0.12	0.08	0.18	0.03	0.11	0.06	0.16
180	0.01	0.01	0.12	0.12	0.06	0.16	0.03	0.11	0.06	0.11
210	0.01	0.02	0.12	0.12	0.06	0.13	0.03	0.11	0.06	0.07
240	0.01	0.04	0.12	0.12	0.06	0.12	0.03	0.11	0.06	0.04
270	0.01	0.04	0.12	0.12	0.06	0.12	0.03	0.11	0.06	0.01
300	0.01	0.04	0.12	0.12	0.06	0.12	0.03	0.11	0.06	0.01

#### 4.1.4. Variations in electro-osmotic flow

Electro-osmotic flow (EOF) is the movement of pore fluid under the influence of electric field (Virkiute et al., 2002). Some ions and non-charged contaminants also migrate along with soil pore fluid due to EOF. In the present study, EOF was measured by volume change in the anolyte and catholyte after EKR treatment (Fig. 4.4). As the soil particles are negatively charged, the direction of EOF is usually from anode to cathode, which was also observed in all experiments of this study. Experiments with low voltage did not show much variation in volume (EK1). Maximum EOF was observed in EK4 due to higher applied voltage (50V). When EDTA was used as electrolyte, similar observations were made with respect to the direction of EOF. Maximum EOF was observed in case of EE2, followed by ET2, which shows that EOF is greatly influenced by applied voltage as it increases with increase in voltage gradient. The results confirm that voltage is directly proportional to EOF, as has also been reported by Gidudu and Chirwa (2020). Since the direction of EOF was opposite to the direction of electromigration, Cr migration towards anode was hindered and caused some migration of Cr into the cathode compartment in agreement to earlier reported studies (Reddy & Chinthamreddy, 2004b; Y. Song et al., 2016a). However, the effect of electromigration was higher than that of electroosmosis on the migration of Cr (VI).

#### 4.1.5. Removal of Cr (VI) and residual concentration

Analysis of anolyte and catholyte exhibited high concentration of Cr (VI) in anolyte, which suggests that Cr (VI) migrated and flushed into the anode-well through electromigration (Al-Hamdan & Reddy, 2008). Removal efficiency of all the tests was calculated using the formula

$$R\% = \frac{C_0 - C}{C_0} \times 100 \dots \dots \dots (4.3)$$

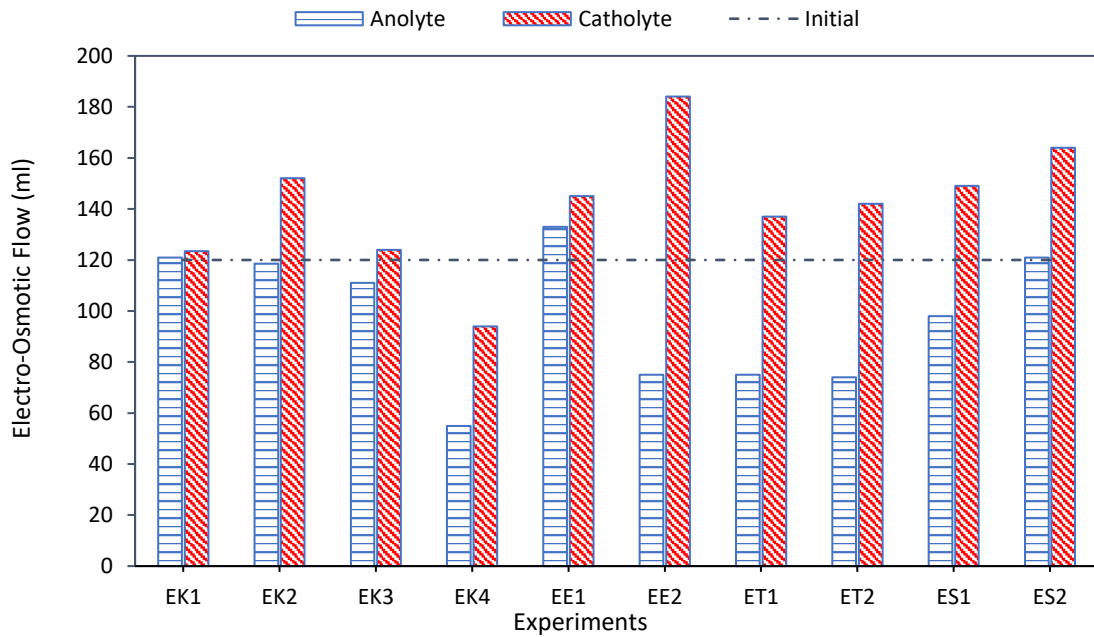


**Figure 4.4** Electro-Osmotic flow (EOF) in soil measured by change in volume (ml) in anolyte and catholyte post-EKR treatment

Where,  $C_0$  is the initial concentration of Cr in soil (mg) and  $C$  is the residual concentration of Cr in soil after EKR treatment (mg). Fig. 4.5a shows the percentage removal of chromium (VI) with increasing voltage. The findings showed that rapid removal was achieved at high voltage of 50V. Maximum removal was obtained with EDTA-enhanced EKR at 50V when graphite electrode was used (Fig. 4.5b). Same test when performed at low voltage of 20V, gave similar removal as obtained by unenhanced EKR at 50V with stainless-steel. This shows that the combination of both high voltage and enhancement with EDTA can significantly improve the efficiency of EKR. When EDTA was used as an electrolyte, Cr formed negatively charged soluble complexes with EDTA which then migrated towards anode. Similar observation have been reported by (Cameselle et al., 2021b).

The mass balance analysis of chromium was calculated (Eqn. 4.4) to account for the concentration of chromium in soil sections, anolyte and catholyte, and nylon filter ( $C_o$ ) and was compared with initial Cr in soil ( $C_i$ ).

$$\text{Mass Balance} = \frac{C_o}{C_i} \dots \dots \dots (4.4)$$

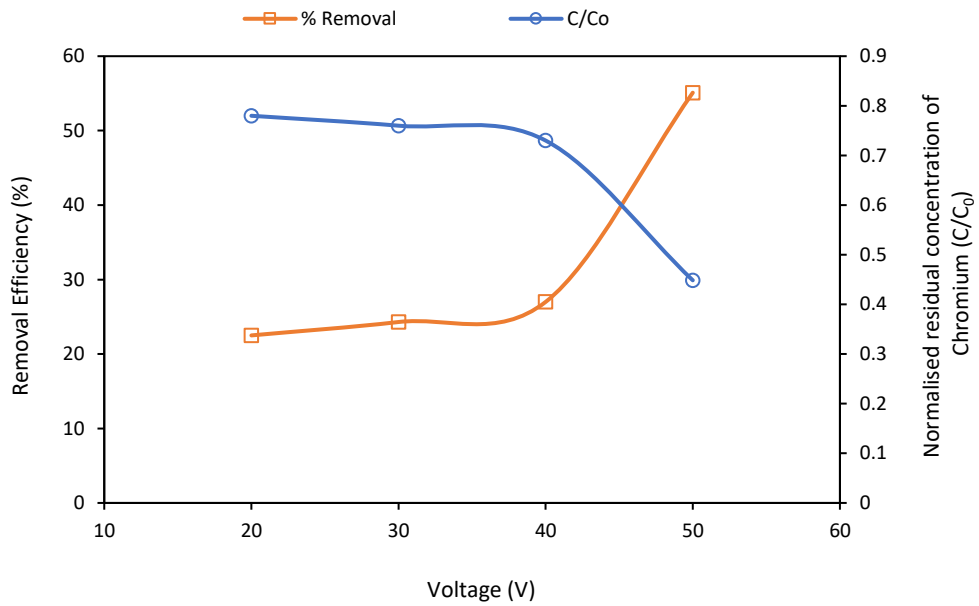
The results (Table 4.5) showed that significant fraction of Cr was accounted in all experiments performed (0.7-0.9) except for test EE2 with a value of 0.5. The possible reason for low mass balance in that experiment was adsorption of Cr on electrode and/or deposition of Cr-EDTA complex formed on the electrodes which was distinctly visible during the experiment. Similar findings were reported by (Reddy et al., 1997). The electrodes were not analyzed for adsorbed or trapped Cr for this study. Some studies have reported the reduction of Cr (VI) to Cr (III) that occurred near anode due to low pH. The analysis of Cr concentration was done after thermal oxidation of soil. Thus, even if the reduction of Cr (VI) to Cr (III) occurred during EKR, it was later oxidized thermally and was reported as Cr (VI).

Fig. 4.6 shows the fraction of residual Cr in different soil sections. The results revealed that at low voltage of 20V, the metal was accumulated in the centre of soil cell in soil sections S2 and S3. As the voltage increased to 30V, the concentration of residual Cr was increased in S2 as compared to S3. Similarly, when the voltage increased from 30 to 40V, Cr accumulation was maximum in section S1 close to anode. It was observed that mobility of Cr (VI) is greatly influenced by soil pH, current and voltage applied, electro-osmotic flow and type of electrolyte. Relatively low pH conditions near the anode resulted in some adsorption of Cr (VI). Other reasons for high concentration of Cr (VI) near anode section could be reflux of Cr (VI) from anolyte to soil by EOF and saturation of anolyte with metal. This trend shows that with increasing voltage, the migration of Cr increased from cathode to anode.

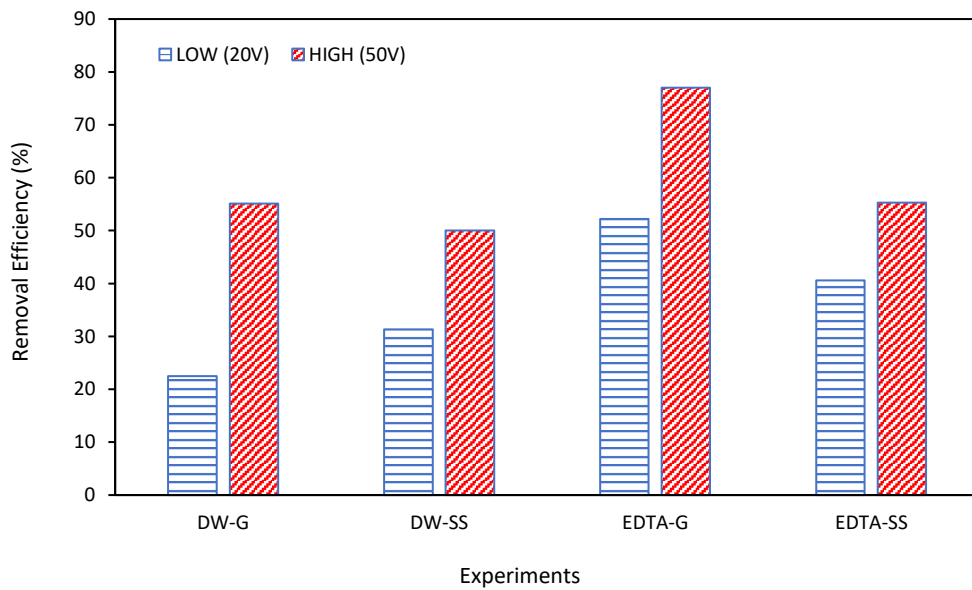
**Table 4.5** Removal percentage and mass balance of chromium metal (as Cr<sup>6+</sup>) in different fractions at the end of the electrokinetic test

S. No.	Test	Electrolyte	Electrode Material	Voltage gradient (V/cm)	Initial Cr content in soil (mg)	Residual Cr content in soil (mg)	Cr content in Anolyte (mg)	Cr content in catholyte (mg)	Cr content absorbed by filter (mg)	Cr Removal Percentage (%)	Mass Balance (C <sub>o</sub> /C <sub>i</sub> )
1	EK1	Distilled water	Graphite	1	1181	915	91	0.2	11	22.5	0.9
2	EK2	Distilled water	Graphite	1.5	1151	870	197	0.1	4	24.4	0.9
3	EK3	Distilled water	Graphite	2	2550	1860	328	0.6	12	27.1	0.9
4	EK4	Distilled water	Graphite	2.5	2010	902	892	1	13	55.1	0.9
5	EE1	EDTA (0.1M)	Graphite	1	1269	606	240	1	0.3	52.3	0.7
6	EE2	EDTA (0.1M)	Graphite	2.5	2519	581	638	1	1	77	0.5
7	ET1	Distilled water	Stainless steel	1	1761	1209	243	1.5	0.6	31.3	0.8
8	ET2	Distilled water	Stainless steel	2.5	1826	915	879	2	4.5	50	0.9
9	ES1	EDTA (0.1M)	Stainless steel	1	1788	1061	215	16	0.3	40.6	0.7
10	ES2	EDTA (0.1M)	Stainless steel	2.5	1860	830	390	3	0.7	55.3	0.7





(a)



(b)

**Figure 4.5** Percentage removal of chromium from soil after EKR treatment (a) under the applied voltage of 20V, 30V, 40V, and 50V, and (b) under varying

conditions of electrolyte and electrode material at low (20V) and high voltage (50V).

Soil section close to cathode had least metal accumulation as compared to other sections. Migration of residual Cr towards anode was higher when distilled water was used with graphite electrode (DW-G) as compared to when it was used with stainless steel electrode (DW-SS). That is why for test EK1-EK4, the maximum accumulation is at S2 and S3 sections, while for test ET1-ET2, maximum accumulation is at S1 and S2 sections. However, in both the tests, comparable Cr accumulation was present in S4 close to cathode. Similar results were obtained when EDTA was used with maximum Cr accumulation in section S2. From these results, it is concluded that if the treatment time of test was increased, the metal removal would also increase, as reported by Karaca et al. (2022).

#### **4.1.6. Properties of soil before and after treatment**

The characterization of raw soil, spiked soil and treated soil is given in Table 4.6. The properties of treated soil were analyzed after EKR treatment to detect the changes in soil properties when subjected to a high voltage of 50V for 10 hours. The results showed that physical properties like particle size and specific gravity did not change. However, the plastic limit and liquid limit of treated soil increased from 12.7% to 16.3% and 29.4% to 39.7%, respectively. Cations (K, Na, Ca) present in the raw soil moved towards cathode and decreased drastically in soil post-treatment due to electromigration, as was reported by Bessaim et al. (2020). Migration of anions ( $\text{Cl}^-$ ,  $\text{SO}_4^{2-}$ ,  $\text{CO}_3^{2-}$ ) towards anode was observed, however, was not removed from soil. This could be because of saturation of anolyte with Cr ions (Prakash et al., 2022b). The pH of soil did not change much from the initial value owing to the buffering capacity of soil, while the electrical conductivity of soil increased from 204 mS/cm to 312 mS/cm, due to the increased solubility of ions under increased voltage gradient.

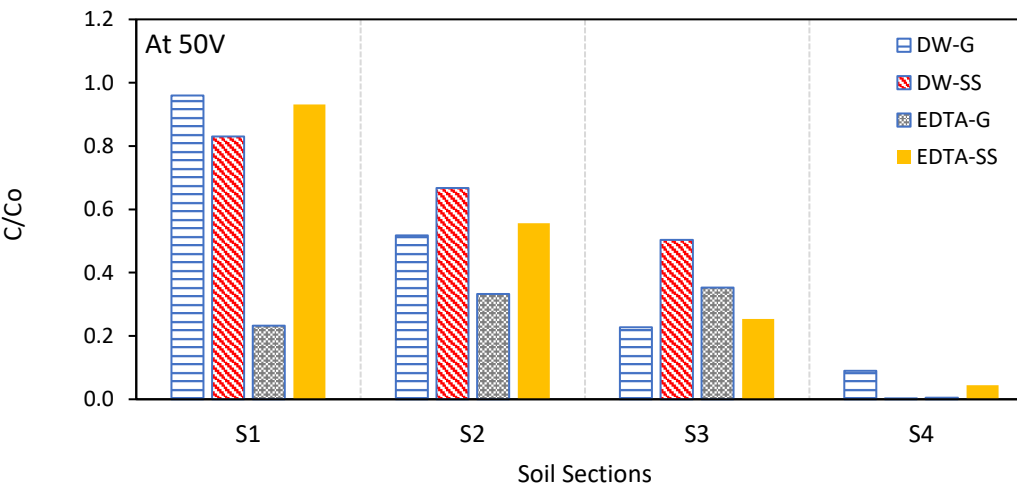
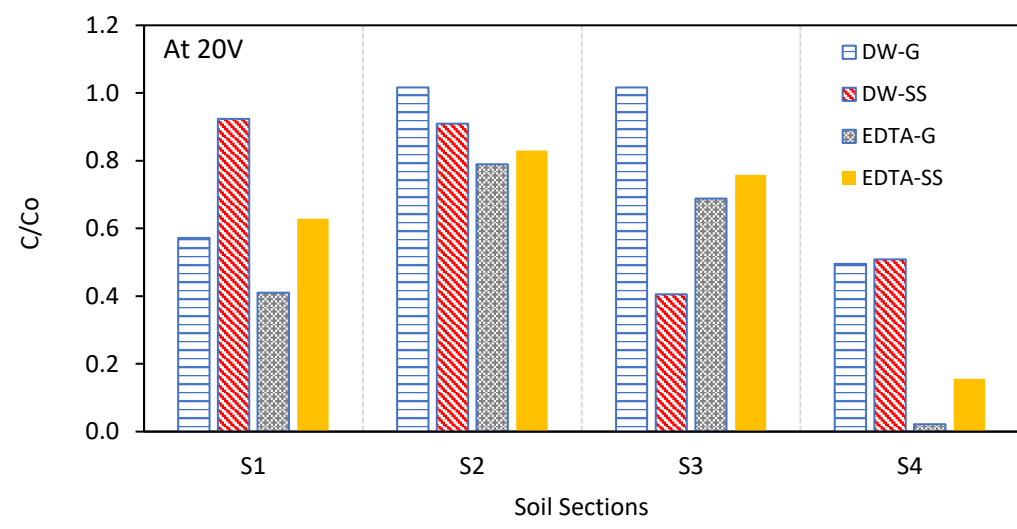
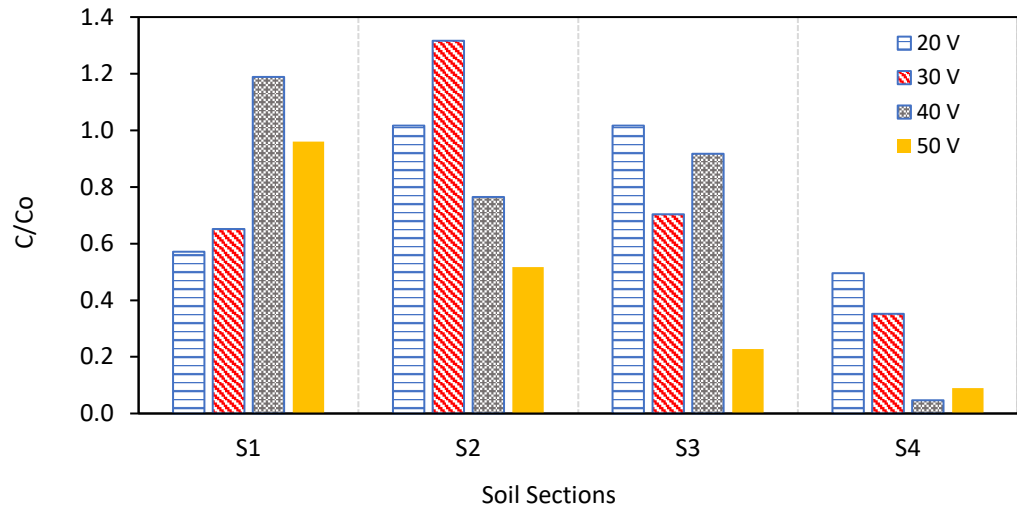


**Figure 4.6** Distribution of residual chromium in soil sections S1-S4 from anode to cathode

The application of 1.0 V/cm in most of the published literature has resulted in 30-40% removal of Cr (VI) in treatment period of 12-21 days using graphite electrode (Song et al., 2016; Gao et al, 2020) whereas, the present study reports removal of 55% of Cr (VI) within 10 hours, thus representing significantly higher removal rate compared to the earlier reports. In respect of soil health, the earlier studies reported changes in pH and EC alone. The pH is observed to slightly reduce in the treated soil even at 1.0 V/cm voltage gradient. The same has been reported (pH reduced to 6.5 from 6.7) in the present study carried at 2.5 V/cm. Apart from it, the parameters of soil health (Table 4.3) did not show any major adverse changes in properties of soil. The physical properties (plastic limit and liquid limit) were marginally affected since the electrolyte (EDTA) and EKR resulted in removal of cations. It was observed that the removal of divalent cations ( $\text{Ca}^{2+}$ ) was more than the monovalent cations ( $\text{Na}^+$ ) thereby resulting in relative abundance of negative ions. This may increase the thickness of double diffuse layer, thereby resulting in slightly higher liquid and plastic limits. Further, the decrease in organic carbon content may be attributed to removal of soluble organic carbon due to EDTA and subsequently its electro-osmotic flow towards cathode.

**Table 4.6** Characterization of soil health before and after EKR treatment

<b>Parameter</b>	<b>Raw Soil</b>	<b>Contaminated Soil</b>	<b>Treated Soil</b>	<b>Method</b>
Sand (%)	78 (31% medium, 47% fine grained)	78 (31% medium, 47% fine grained)	78 (31% medium, 47% fine grained)	ASTM D422
Silt and clay (%)	22	22	22	ASTM D422
pH (1:10 soil to water)	6.9	6.7	6.5	ASTM D1293
EC (1:10 soil to water) (mS/cm)	204	205	312	ASTM D1293
TDS (1:10 soil to water) (ppm)	255	276	189	ASTM D1293
Organic Content (%)	0.62	0.51	0.22	ASTM D2974
Plastic limit (%)	12.72	13.93	16.30	ASTM D4318
Liquid Limit (%)	29.40	31.17	39.77	ASTM D4318
Plasticity Index (%)	16.7	17.2	23.5	ASTM D4318
Specific Gravity	2.5	2.5	2.5	ASTM D854
Na (mg/kg)	5808	5808	3429	APHA 3111
K (mg/kg)	288	288	142	APHA 3111
Ca (mg/kg)	9560	9560	2549	APHA 3111
Chlorides (mg/kg)	200	280	280	EPA 9253
Sulphates (mg/kg)	152	6750	2013	EPA 9038
CaCO <sub>3</sub> equiv. (%)	17.5	18	18.7	ASTM D4373
Chromium (VI) (mg/kg)	0	1000	601	EPA 7196A

#### 4.1.7. Economic evaluation

Application of high voltage and amendment of electrolytes may contribute to energy and cost expenditure. The energy consumption in KWh and total cost of running EKR was evaluated to assess the feasibility of this technique. Total cost was calculated as the sum of cost of electricity consumed, cost of electrodes and the cost of chemicals used for electrolyte conditioning. Based on the energy consumption, cost per gram of removal of Cr from soil was also calculated to evaluate the cost-effectiveness of this technique (Table 4.8).

Maximum energy consumption was observed by test EE2 (0.1 KWh), followed by ES2 (0.07 KWh), EK4 (0.06 KWh) and ET2 (0.05 KWh). It is evident from the results, that application of high voltage showed relatively higher energy consumption. Amendment of EDTA decreased the resistance of soil by increasing mobility of ions and electrical conductivity, which increased the energy expenditure. Application of high voltage and EDTA together, increased the total cost of the experiment. However, as the removal of Cr was maximum in test EE2, followed by ES2, it showed minimum cost of running for per gram removal of Cr (0.8 and 0.7 US\$/g, respectively). Maximum cost of running EKR was calculated for control EK1 at 20 V (4.3 US\$/g). Addition of EDTA combined with high voltage gradient enhanced the removal rate of Cr and reduced the energy consumption. Stainless-steel electrode is relatively more cost-effective than graphite electrode as it does not show much corrosion effect and can be re-used.

Results of the present study indicated that a higher voltage gradient (2.5 V/cm) can be used to increase the removal efficiency, and shorten the duration of treatment. The application of higher voltage did not result in any significant change in health of the treated soil, thus, supporting the use of higher voltage gradient in treatment of sandy soil. On the other hand, most of the studies published show 30-50% removal (Gao et al., 2020; Ma et al., 2022). The current study shows 1.5 times relatively better removal. In respect of choice of electrode material and electrolyte, stainless steel with 0.1M EDTA proves to be more cost-

efficient towards removal of Cr (VI). The use of stainless-steel as electrode material under optimized conditions, results in relatively less corrosion of electrode as well, thus indicating the suitability of the configuration for EKR.

**Table 4.7** Energy consumption and cost analysis for different combinations during EKR of Cr-contaminated Soil

S. No.	Experiments	Energy Consumption (KWh)	Rate of electricity (₹/KWh)	Cost of Electricity (₹)	Cost of Electrodes (₹)	Cost of Chemicals (₹)	Total cost per gram removal of Cr	
							(₹/g)	(US\$/g)
1	EK1	0.002	8.5	0.017	88.90	0.00	334.3	4.3
2	EK2	0.012	8.5	0.102	88.90	0.00	316.7	4.1
3	EK3	0.032	8.5	0.272	88.90	0.00	129.2	1.7
4	EK4	0.06	8.5	0.51	88.90	0.00	80.7	1
5	EE1	0.016	8.5	0.136	88.90	28.6	177.4	2.3
6	EE2	0.1	8.5	0.85	88.90	28.6	61.1	0.8
7	ET1	0.004	8.5	0.034	25.00	0.00	45.4	0.6
8	ET2	0.05	8.5	0.425	25.00	0.00	27.9	0.4
9	ES1	0.014	8.5	0.119	25.00	28.6	73.9	1
10	ES2	0.07	8.5	0.595	25.00	28.6	52.6	0.7



#### 4.2. EKR for Pb-contaminated Soils

To assess the efficiency of EKR for the removal of Pb (II), fourteen experiments were performed under different operating conditions (Table 4.8). The tests were name-coded as P = Lead, G/S = electrode material, D/E/T = electrolyte solution used, and 1/2 = High/Low voltage.

**Table 4.8** The design of experiments for EKR of Pb-contaminated Soil under different operating conditions (DW= Distilled Water)

S. No.	Tests	Voltage (V)	Electrode	Electrolyte	Time Duration (hours)
1	PGD1	50	Graphite	DW	10
2	PGD2	40	Graphite	DW	10
3	PGD3	30	Graphite	DW	10
4	PGD4	20	Graphite	DW	10
5	PSD1	50	Stainless Steel	DW	10
6	PSD2	20	Stainless Steel	DW	10
7	PGE1	50	Graphite	EDTA (0.1M)	10
8	PGE2	20	Graphite	EDTA (0.1M)	10
9	PSE1	50	Stainless Steel	EDTA (0.1M)	10
10	PSE2	20	Stainless Steel	EDTA (0.1M)	10
11	PGT1	50	Graphite	Tween 80 (1%)	10
12	PGT2	20	Graphite	Tween 80 (1%)	10
13	PST1	50	Stainless Steel	Tween 80 (1%)	10
14	PST2	20	Stainless Steel	Tween 80 (1%)	10

#### 4.2.1. Variations in pH

In this study, pH was measured in anolytes, catholytes, and soil sections after EKR under varying operating conditions (Fig.4.7 and Table 4.9). Results indicated that in all experiments, the pH of anolyte was between 1 to 4 and that of catholyte was in the range of 8 to 12, which confirmed that oxidation of water led to acidification at the anode and reduction of water led to alkalization at the cathode. At high voltage, the pH of the anolyte was below 2, and the catholyte pH was above 10, compared to tests at a low voltage where the pH values ranged from 3-4 at the anode and 8-9 at the cathode. It was observed that the voltage gradient influenced the pH variations as the rate of electrolysis increased with increasing voltage.

The protons produced at the anode were expected to migrate across the soil toward the cathode, causing soil acidification and desorption of  $Pb^{2+}$  in the soil. However, in the present study, the soil pH did not show significant variations from the initial pH value (~8). The resistance of soil towards the advancement of an acidic front could be because of the high buffering capacity of soil owing to the presence of significant carbonate content (~18%), as has also been reported by Asadollahfardi et al. (2021). In the case of EDTA also, the soil pH showed negligible variations as EDTA can form a stable complex with metal at an alkaline pH without lowering the pH of the soil. Similar results were observed with Tween 80 as electrolytes, which showed that the voltage gradient has relatively more influence over the electrolysis reaction than the composition of the electrolyte solution.

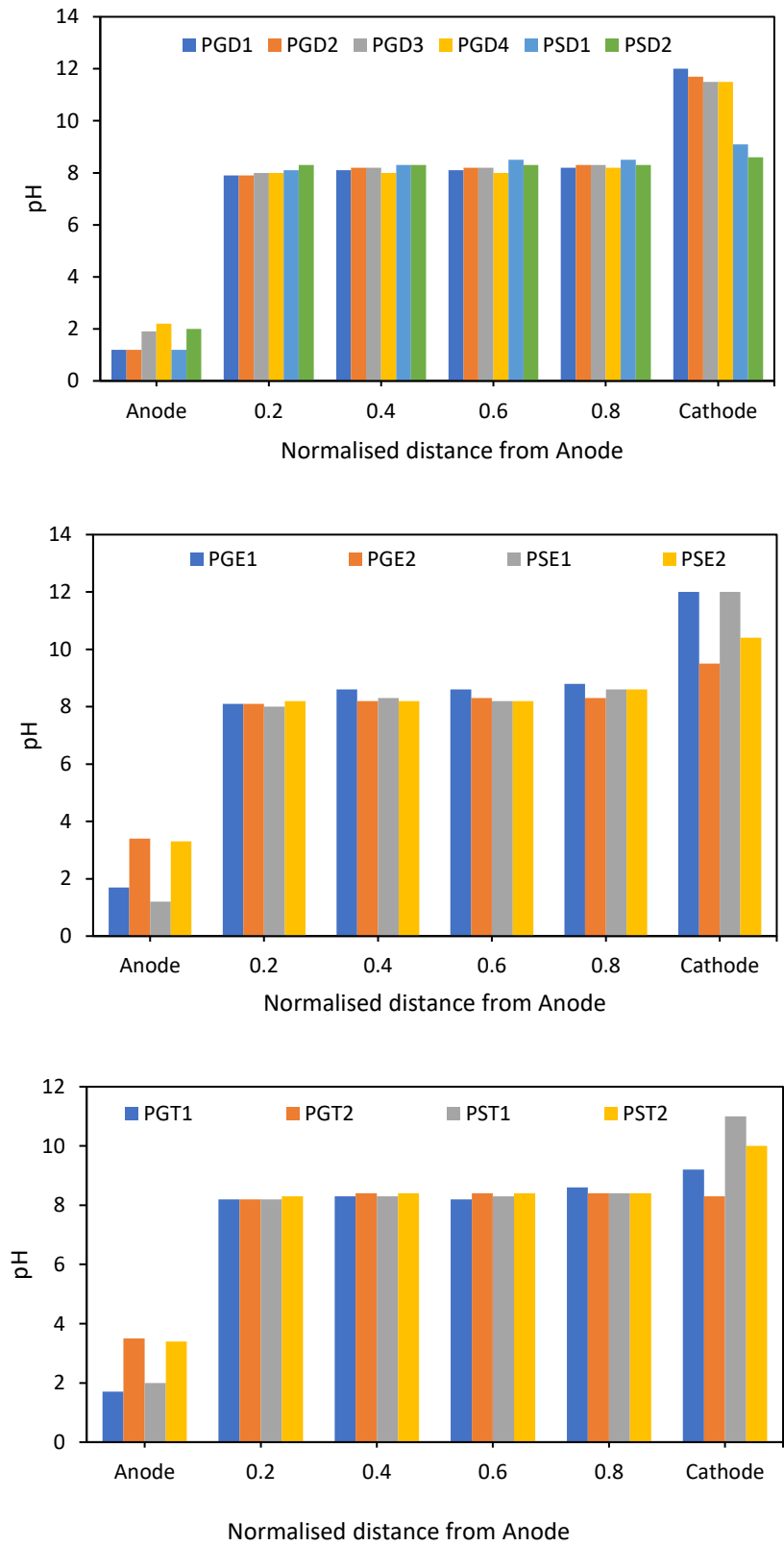


**Figure 4.7** Variations in pH of anolyte, catholyte, and soil after EKR treatment in experiments with distilled water, EDTA, and Tween 80 as electrolyte

#### 4.2.2. Variations in EC and current

The profile of EC ( $\mu\text{S}/\text{cm}$ ) soil sections after EKR is depicted in Fig 4.8 (Table 4.11). When DW was used as an electrolyte (PGD1-PSD2), a typical downward trend from the anode toward the cathode was observed (Fig 4.8a), which is the general trend for unenhanced experiments, as reported in earlier studies (Acar & Alshawabkeh, 1993). Relatively higher EC values in section S1 (0-3cm) from the anode could be attributed to the influx of solubilized ions from the low pH zone of anolyte or migration of negatively charged complex/precipitates toward the anode. The formation of insoluble metallic hydroxides in the soil at high pH regions increased electrical resistance and decreased the conductivity near the cathode. Maximum EC values were observed in PGD4 in all sections (342  $\mu\text{S}/\text{cm}$ - 253  $\mu\text{S}/\text{cm}$ ), while minimum EC was found in PSD1 (223-114  $\mu\text{S}/\text{cm}$ ). The trend indicated that EC decreased with an increase in voltage gradient due to decreased ionic strength in soil by increased electromigration of ions from soil into the electrolytes with voltage. In addition, there was a significant increase in the EC of electrolyte during the treatment. It increased from 0.096  $\text{mS}/\text{cm}$  (initial) to 17.2  $\text{mS}/\text{cm}$  (post-treatment), confirming that the soluble ions of soil are removed at the electrode wells.

In EDTA-enhanced experiments (Fig. 4.8b), EC values were relatively higher than in experiments with DW due to increase in ionic strength by the addition of electrolyte solution. EDTA increased the solubility of various ions present in soil which also aid in higher EC. Soil sections close to electrode wells (S1 and S4) had lower EC (247-616  $\mu\text{S}/\text{cm}$ ) than middle sections (S2 and S3) (532-1153  $\mu\text{S}/\text{cm}$ ). This was probably due to the movement of ions from soil sections close to the electrode wells into the electrolytes. In Tween 80-enhanced experiments, the final EC was similar to the initial EC values, and no significant change in EC was observed, which indicates almost negligible movement of ions within the soil column. EC trend was almost similar in the case of both, graphite and stainless-steel electrodes, with voltage being the prime parameter governing the conductivity within the soil cell.

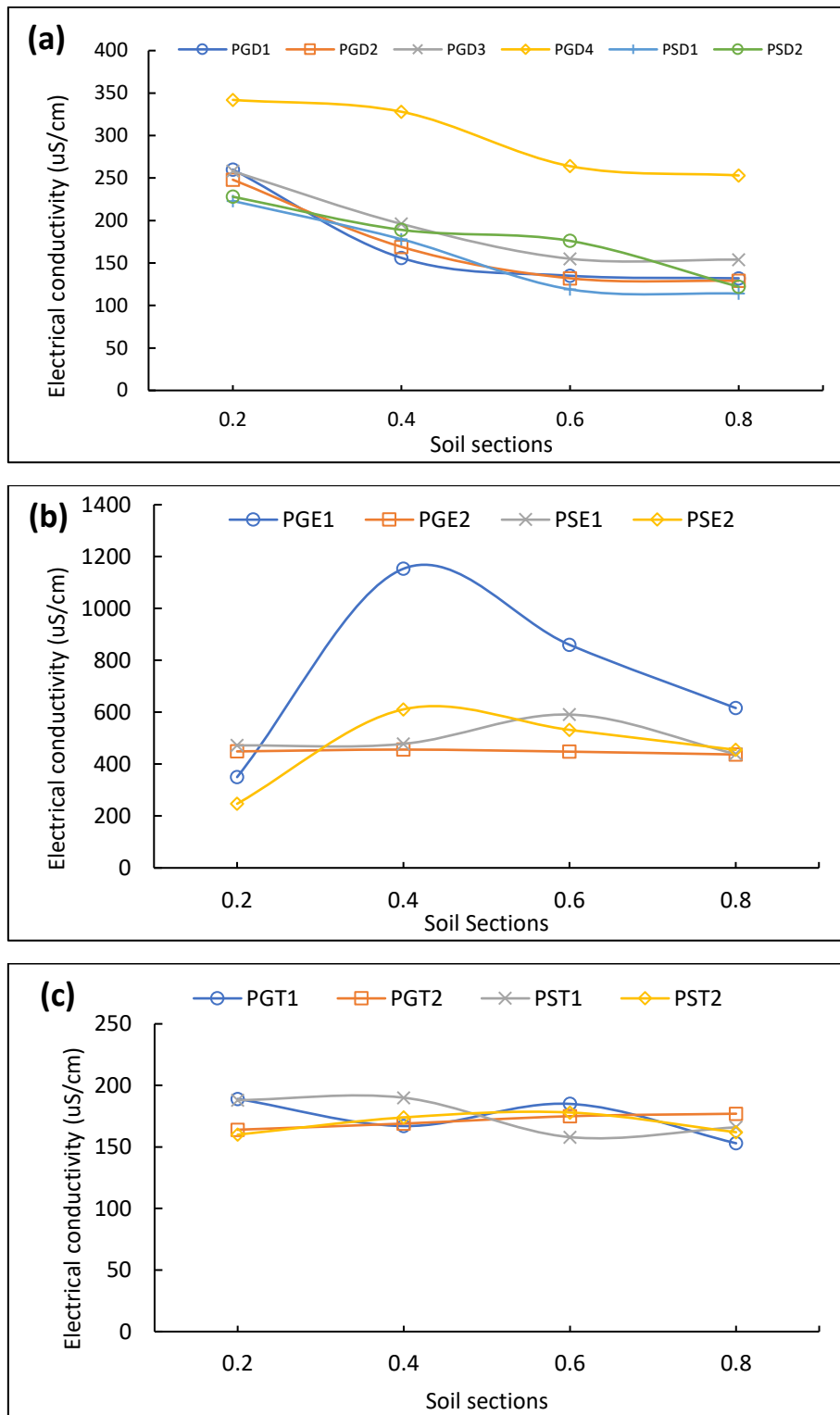


**Figure 4.8** Variations in Electrical conductivity (EC) of soil after EKR treatment under different conditions (a) unenhanced tests at applied voltages from 50 V to 20 V with Graphite and Stainless Steel electrode (b) enhanced with EDTA (c) enhanced with Tween 80

**Table 4.9** The variations in pH, EC, TDS, volume, and Pb concentration in anolyte and catholyte after EK treatment

Experiment	Cycle	Section	pH	EC (mS/cm)	TDS (ppt)	Volume change (mL)	Pb conc. (mg/L)
PGD1	Day 1	A1	1.2	17.3	86	61	5.113
		C1	12	5.3	2.6	110	6.091
	Day 2	A2	1.2	15.6	7.8	58	1.295
		C2	11.8	4.7	2.3	122	1.788
PGD2	Day 1	A1	1.2	14.7	7.4	57	1.354
		C1	11.8	4.7	2.3	92	3.688
	Day 2	A2	1.3	9.4	4.7	62	5.05
		C2	11.6	3.6	1.8	113	1.59
PGD3	Day 1	A1	1.9	5.9	2.9	74	20.38
		C1	11.3	1.5	0.7	102	21.48
	Day 2	A2	1.9	5.7	2.8	65	7.265
		C2	11.8	3.1	1.5	105	0.2848
PGD4	Day 1	A1	2.2	3.2	1.6	82	8.648
		C1	10.3	0.6	0.3	89	9.775
	Day 2	A2	2.4	2.6	1.3	72	1.924
		C2	11.5	1.5	0.7	88	4.314
PSD1	Day 1	A1	1.2	20	10	51	1.151

	Day 2	C1	9.1	1.7	0.8	97	50.43
		A2	1.4	14.5	7.2	46	14.06
		C2	9.1	9.1	0.8	102	4.309
PSD2	Day 1	A1	1.8	5.5	2.7	62	5.215
		C1	8.9	1.0	0.5	70	7.273
	Day 2	A2	2.1	2.9	1.4	74	45.95
		C2	8.6	8.6	0.3	80	15.75
PGE1	Day 1	A1	1.7	13.7	6.8	26	4843
		C1	11.8	19.5	9.7	31	2886
	Day 2	A2	1.0	20	10	95	28.74
		C2	12.1	20	10	102	12.88
PGE2	Day 1	A1	3.4	8.3	4.2	56	955.9
		C1	9.4	13.3	6.7	89	651.1
	Day 2	A2	3.4	7.3	3.6	62	2.683
		C2	9.6	13.5	6.7	88	48.24
PSE1	Day 1	A1	1.2	20	10	28	3670
		C1	12	20	10	84	5743
	Day 2	A2	1.3	18.4	9.3	21	40.36
		C2	11.8	22	11	87	29.32
PSE2	Day 1	A1	3.3	8.4	4.22	58	973.1

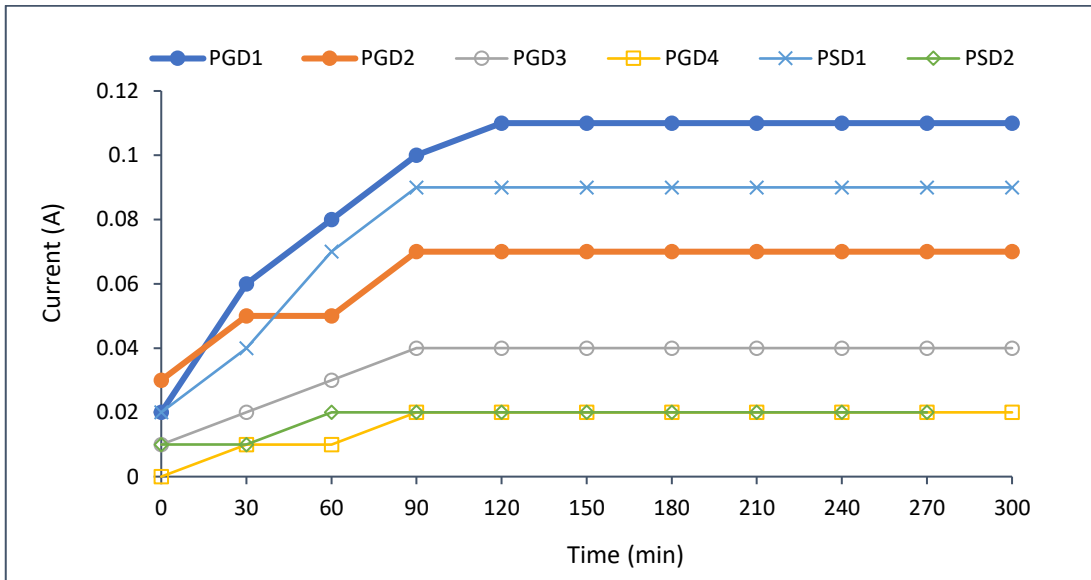
	Day 2	C1	10.3	12.5	6.3	84	773
		A2	3.2	10.2	5.0	53	111.2
		C2	10.1	14.6	7.4	76	133.8
PGT1	Day 1	A1	1.7	7.8	3.8	62	6.61
		C1	9.1	0.9	0.5	108	6.82
	Day 2	A2	1.7	7.4	3.7	65	6.28
		C2	9.2	0.9	0.4	112	0.052
PGT2	Day 1	A1	2.7	1.3	0.6	68	1.65
		C1	8.2	0.4	0.19	80	6.47
	Day 2	A2	3.8	0.8	0.39	72	0.807
		C2	8.3	0.3	0.17	82	6.049
PST1	Day 1	A1	2.1	4.4	2.2	61	7.26
		C1	10.2	0.8	0.4	92	1.503
	Day 2	A2	1.9	6.3	3.1	65	6.68
		C2	11.8	2.5	1.2	111	0.535
PST2	Day 1	A1	2.7	1	0.47	68	0.821
		C1	9.8	0.3	0.16	87	1.219
	Day 2	A2	5.4	0.2	0.08	82	5.548
		C2	10.2	0.2	0.12	85	2.199



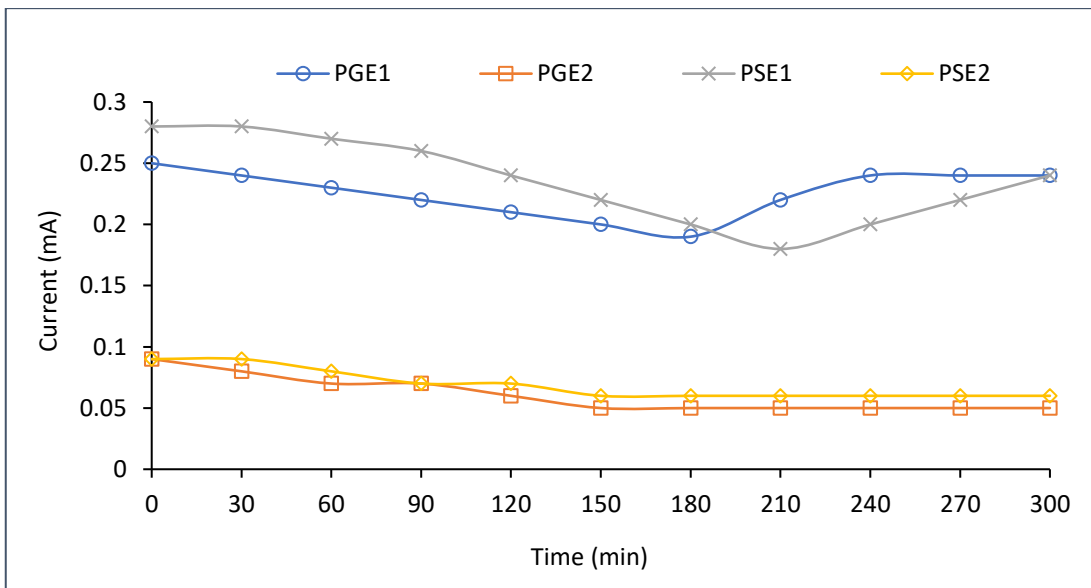
Electric current monitors the rate of electromigration as it is governed by the movement of ions within the soil. pH variations, electrical conductivity, and applied voltage have a profound effect on current (Ammami et al., 2015). Fig 4.9 (Table 4.10) indicates the electric current for experiments performed at a high voltage gradient of 2.5 V/cm. When DW was used as an electrolyte, current increased within the first 90-120 minutes and then stabilized. This could be attributed to the increased mobility of charged ions upon application of an electric field in the first few hours, however, when most of the ions were removed from the soil into the electrolyte, the current stabilized. PGD1 attained a peak with the highest current of 0.11A in 120 minutes of the experiment and then stabilized till the end of the experiment, which shows that increasing voltage would increase the current and thus, the rate of metal removal. The general trend of the current, as reported in previous studies, decreases after peak attainment and then stabilizes (Figuroa et al., 2016). However, it was not observed in this study since most of the elimination of ions could have happened at a higher applied voltage, due to which the current stabilized early. Another explanation could be the saturation of electrolytes with ions within 5 hours of treatment. Increasing treatment time and re-circulation of electrolytes could further improve the current and metal removal.

When EDTA was used as electrolyte in experiments PGE1 and PSE1, high current values were recorded. This could be correlated with the increase in the number of ionic species in the soil with the addition of EDTA, as was reported by Garcia-Blas et al. (2021). Many species were solubilized, forming complexes with EDTA to carry current, which decreased with time due to the depletion of mobile ions into electrolyte wells by electromigration. A dip in current was observed, after which the current increased. The Pb-EDTA complex dissociates into  $Pb^{2+}$  and  $EDTA^{4-}$  in acidic conditions, which causes the electro-deposition of EDTA salts on the anode (Amrate et al., 2005), as was observed in this study. The decrease in the reaction surface area of the anode by deposition of salts caused a dip in the current. Post removal of the scales the current flow increased again. The use of Tween 80 as electrolyte yielded a similar trend as obtained with DW, with an initial increase in current, followed by stabilization; however, the values reported were lower than

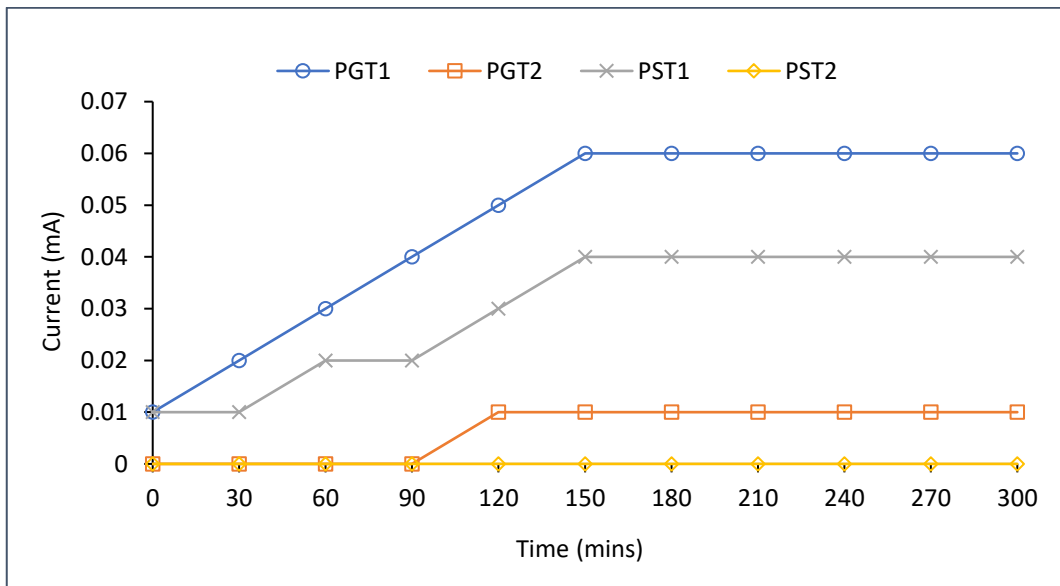
DW. Low current values could be attributed to the low solubilization of ions by Tween 80 and the migration of only the ions already present in the mobile fraction of soil. The probable reason may be confirmed against the values of EC as well.



(a)



(b)



(c)

**Figure 4.9** Variations in current during EKR treatment in experiments with DW, EDTA, and Tween 80 as electrolyte

**Table 4.10** Variations in Current (Amperes) with time during the EKR process

<b>Time (mins)</b>	<b>PGD1</b>	<b>PGD2</b>	<b>PGD3</b>	<b>PGD4</b>	<b>PSD1</b>	<b>PSD2</b>	<b>PGE1</b>	<b>PGE2</b>	<b>PSE1</b>	<b>PSE2</b>	<b>PGT1</b>	<b>PGT2</b>	<b>PST1</b>	<b>PST2</b>
0	0.02	0.03	0.01	0	0.02	0	0.25	0.09	0.28	0.09	0.01	0	0.01	0
30	0.06	0.05	0.02	0.01	0.04	0.01	0.24	0.08	0.28	0.09	0.02	0	0.01	0
60	0.08	0.05	0.03	0.01	0.07	0.01	0.23	0.07	0.27	0.08	0.03	0	0.02	0
90	0.1	0.07	0.04	0.02	0.09	0.02	0.22	0.07	0.26	0.07	0.04	0	0.02	0
120	0.11	0.07	0.04	0.02	0.09	0.02	0.21	0.06	0.24	0.07	0.05	0.01	0.03	0
150	0.11	0.07	0.04	0.02	0.09	0.02	0.2	0.05	0.22	0.06	0.06	0.01	0.04	0
180	0.11	0.07	0.04	0.02	0.09	0.02	0.19	0.05	0.2	0.06	0.06	0.01	0.04	0
210	0.11	0.07	0.04	0.02	0.09	0.02	0.22	0.05	0.18	0.06	0.06	0.01	0.04	0
240	0.11	0.07	0.04	0.02	0.09	0.02	0.24	0.05	0.2	0.06	0.06	0.01	0.04	0
270	0.11	0.07	0.04	0.02	0.09	0.02	0.24	0.05	0.22	0.06	0.06	0.01	0.04	0
300	0.11	0.07	0.04	0.02	0.09	0.02	0.24	0.05	0.24	0.06	0.06	0.01	0.04	0

### 4.2.3. Variations in electro-osmotic flow

Electro-osmotic flow (EOF) is the measurement of volume change in anolyte to catholyte from the initial volume due to the movement of soil pore water under electro-osmosis. EOF is mainly governed by pH and, in turn, the zeta potential of soil (Cameselle & Pena, 2016). Zeta potential is the potential difference developed between soil particles and the counteracting ions surrounding them. It is an essential property of soil which determines the charge on soil particles, and, thus, the direction of EOF. With higher negativity of zeta potential, the more fluid volume moves towards the cathode at a higher velocity (Altin & Degirmenci, 2005). From the results, it was evident that the direction of EOF was from the anode towards the cathode in all experiments. Fig. 4.10 shows the EOF in anolyte and catholyte after the EKR experiments were performed at a higher voltage since high voltage resulted in higher EOF. It was observed that EDTA amendments improved EOF better than DW, with maximum volume change in PGE1, followed by PSE1. Minimum EOF was observed in PST1, exhibiting a low effect of Tween 80 on EOF. The moisture content of soil also indicates the direction of EOF across the soil. The maximum moisture content was observed in experiment PGD1 (25%), while the minimum was observed in PGE1 (18%). Changes in the moisture content of the soil after EKR could be due to the flow of pore fluid into the electrode wells through electro-osmosis, or due to loss of water by electrolysis.

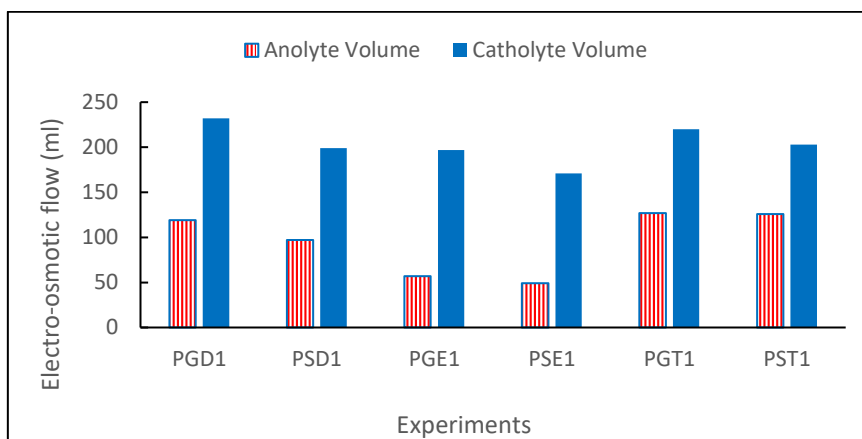


**Figure 4.10** Electro-osmotic Flow (EOF) (ml) in anolyte and catholyte at 50 V after EKR treatment

#### **4.2.4. Removal of Pb from soil**

In natural soils, heterogenous composition increases the sorption capacity of the soil, which can hinder the removal of metals using unenhanced EKR. In this study, such soil was subjected to EKR treatment with i) varying voltage gradient, ii) varying electrolytes, and iii) type of electrode material. Table 4.12 depicts the removal efficiency, mass balance, and concentration of Pb in different components of EKR. In experiments 1-4, the effects of applied voltage gradient on removal efficiency were investigated under control conditions using DW as an electrolyte and graphite electrode. In all cases, the concentration of Pb was higher in the catholyte than in the anolyte, with the highest in PGD1 (2.9 mg). The removal efficiency increased from 0.5% to 6.9% with an increase in voltage from 20V to 50V (Table 4.6). The results indicate that the removal rate increased with increasing the voltage gradient under unenhanced conditions, which could be attributed to the increased solubilization and movement of ions by DW in the soil-water system with voltage.

**Table 4.11** The variations in pH, EC, TDS, moisture content, and Pb concentration in soil before and after EK treatment

Experiment set	Sections	pH	EC (mS/cm)	TDS (ppt)	MC (%)	Pb (mg/kg)
<b>PGD1</b>	Initial	8.0	0.42	0.2	26.8	686
	S1	7.9	0.56	0.28	25.4	705.1
	S2	8.1	0.15	0.07	24.7	673.2
	S3	8.1	0.13	0.7	25.2	732.6
	S4	8.2	0.13	0.06	25.9	751
<b>PGD2</b>	Initial	8.0	0.18	0.09	25	673.9
	S1	7.9	0.24	0.12	26.3	664.8
	S2	8.2	0.16	0.08	25.5	689.2
	S3	8.2	0.13	0.07	24.4	652.5
	S4	8.3	0.13	0.06	25.8	750.8
<b>PGD3</b>	Initial	8.0	0.18	0.09	21.5	678.2
	S1	8.0	0.18	0.09	22.2	786.3
	S2	8.2	0.23	0.10	20.9	851.4
	S3	8.2	0.18	0.09	21.8	880.32
	S4	8.3	0.16	0.08	21.6	825.7
<b>PGD4</b>	Initial	8.0	0.19	0.09	24.9	730.9
	S1	8.0	0.21	0.10	21.1	747.4
	S2	8.0	0.17	0.08	21.4	783.3

	S3	8.0	0.17	0.08	20.3	843.2
	S4	8.2	0.13	0.07	20.1	796.9
<b>PSD1</b>	Initial	8.0	0.20	0.10	21.9	692
	S1	8.1	0.22	0.11	22.5	361.6
	S2	8.3	0.17	0.08	20.3	241.9
	S3	8.5	0.11	0.05	20.4	201.9
	S4	8.5	0.11	0.06	21.8	187.1
<b>PSD2</b>	Initial	8.0	0.19	0.09	23.3	725
	S1	8.3	0.22	0.11	23	343.6
	S2	8.3	0.18	0.09	20.3	250.6
	S3	8.3	0.17	0.08	22.2	495.8
	S4	8.3	0.12	0.06	21.6	373
<b>PGE1</b>	Initial	8.0	0.38	0.19	22.3	734.5
	S1	8.1	0.44	0.22	20.7	372.7
	S2	8.6	0.45	0.22	18.3	485
	S3	8.6	0.44	0.22	16.2	573.3
	S4	8.8	0.43	0.21	17.69	81.44
<b>PGE2</b>	Initial	8.0	0.56	0.28	21.1	703
	S1	8.1	0.62	0.31	20.84	573.9
	S2	8.2	0.60	0.30	19.5	722.9



	S3	8.3	0.52	0.26	19.3	736.9
	S4	8.3	0.5	0.25	19.4	689.7
<b>PSE1</b>	Initial	8.0	0.36	0.18	22.9	711.9
	S1	8.0	0.47	0.23	26	399.2
	S2	8.3	0.47	0.24	21.5	312.5
	S3	8.2	0.59	0.30	21	355.5
	S4	8.6	0.49	0.21	19.9	17.72
		Initial	8.0	0.38	0.19	23.7
<b>PSE2</b>	S1	8.2	0.42	0.25	22.4	225.7
	S2	8.2	0.61	0.30	21.3	419.6
	S3	8.2	0.53	0.26	20.1	863.1
	S4	8.6	0.45	0.23	21.8	142.4
		Initial	8.0	0.19	0.09	23.5
<b>PGT1</b>	S1	8.2	0.18	0.09	20.9	334.7
	S2	8.3	0.16	0.08	10.1	330.3
	S3	8.2	0.18	0.09	19.3	283.5
	S4	8.3	0.15	0.08	21.7	326.2
		Initial	8.0	0.19	0.09	23.1
<b>PGT2</b>	S1	8.2	0.16	0.08	21.5	343.6
	S2	8.4	0.16	0.08	19.8	281.5

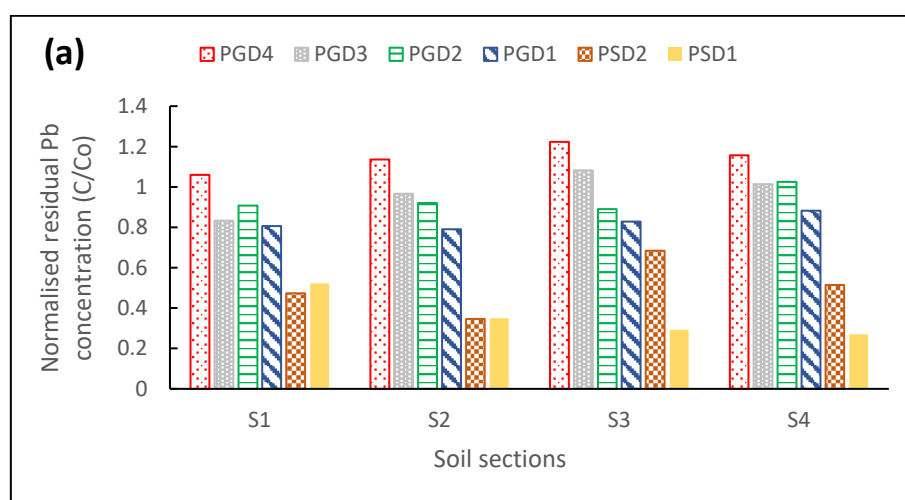
	S3	8.4	0.17	0.08	19.9	284.4
	S4	8.3	0.17	0.08	21.2	305.5
<b>PST1</b>	Initial	8.0	0.12	0.05	22.4	359.3
	S1	8.2	0.18	0.09	23.8	316
	S2	8.3	0.19	0.09	21.4	331.7
	S3	8.3	0.15	0.08	21.7	360.5
	S4	8.4	0.16	0.08	23.9	339.8
		Initial	8.0	0.1	0.05	24.2
<b>PST2</b>	S1	8.3	0.16	0.08	24.8	324.6
	S2	8.4	0.17	0.08	24.2	364.7
	S3	8.4	0.17	0.08	22.9	347.8
	S4	8.2	0.16	0.08	22.5	314.6

**Table 4.12** The compartmentalization of Pb in soil, electrolyte (catholyte and anolyte), electrode material, and filter during different sets of EKR

S. No.	Experiments	Voltage (V)	Initial Pb conc. in soil (mg)	Pb remaining in the soil (mg)	Anolyte (mg)	Catholyte (mg)	Filter (mg)	Removal (%)	Mass Balance (C/C <sub>0</sub> )
1	PGD1	50	1277.1	1188.9	0.8	2.9	1.9	6.9	0.94
2	PGD2	40	1098.9	1055.7	0.4	0.7	1.7	3.9	0.96
3	PGD3	30	1221.1	1182.9	0.6	1.4	2.2	3.1	0.97
4	PGD4	20	1033.8	1028.3	0.3	0.6	2.2	0.5	1.00
5	PSD1	50	1038.0	372.2	1.8	2.4	2.2	64.1	0.36
6	PSD2	20	1087.5	548.6	0.9	4.5	2.6	49.6	0.51
7	PGE1	50	1101.7	567.2	215.4	4.0	9.9	48.5	0.72
8	PGE2	20	1054.5	1021.3	93.9	4.5	5.2	3.1	1.07
9	PSE1	50	1067.9	407.6	223.4	5.9	8.3	65.1	0.55
10	PSE2	20	1162.8	619.1	97.4	19.5	4.1	46.8	0.64
11	PGT1	50	527.3	455.6	0.6	0.6	0.7	13.6	0.87
12	PGT2	20	502.1	471.8	0.9	0.7	1.1	6.0	0.95
13	PST1	50	579.9	506.9	0.2	0.7	0.9	12.6	0.88
14	PST2	20	538.9	505.5	0.5	0.7	1.3	6.2	0.94

Fig. 4.11 indicates the concentration of Pb that remained in different soil fractions after EKR. The maximum accumulation of Pb was observed in S3 and S4 sections close to the cathode in all experiments. This could possibly be due to the precipitation of Pb as hydroxides near the high pH zone of the cathode. With increasing voltage gradient, the precipitation of metal also increased. However, at the interval time when the current was in off-mode, depolarization of the cathode and diffusion of contaminants in the soil system occurred, which led to increased metal solubility for the next cycle, thereby increasing the net removal. A similar phenomenon was observed by Cameselle & Reddy (2013).

The formation of hydroxide complexes was confirmed with the simulation done by Visual Minteq v.3.1 program. Two important reactions that could occur in the EKR system, ionization of water and complex formation with Pb, were considered input parameters. From the predictions of this tool, it was found that three hydroxide complexes of Pb might have existed,  $Pb(OH)_2$ ,  $Pb(OH)^+$ , and  $Pb(OH)^{3-}$  at varying pH (Fig.4.12). However, because of the higher stability constant ( $\log K_s = -8.15$ ),  $Pb(OH)_2$  dominated the soil at  $pH \sim 8$ . The formation of these complexes reduced the overall removal efficiency. Pb is difficult to remove from the soil due to its high affinity to bind with organic matter to form a negatively charged complex that migrates to the anode, counteracting the movement of  $Pb^{2+}$ . This could be seen by the presence of some Pb content in anolyte.



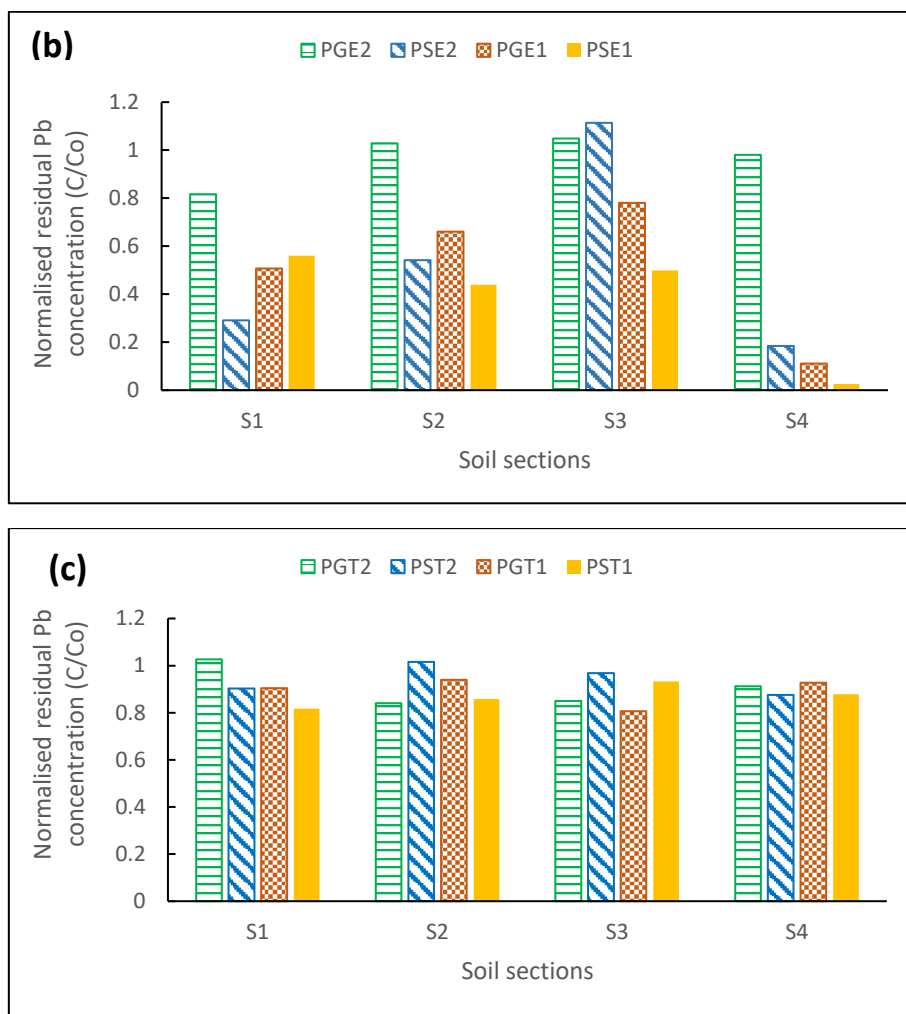
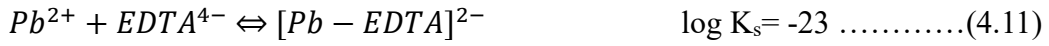


**Figure 4.11** Distribution of residual Pb in soil sections S1-S4 from anode to cathode in EKR setup

In experiments 7-14, the effects of varying electrolyte solutions to further mobilize Pb and improve metal extraction were investigated. When the soil was saturated with EDTA (0.1M), and as an electrolyte solution, the removal efficiencies were 3.1% (20V) and 48.5% (50V) when the graphite electrode was employed, which was better than DW. This was probably because EDTA forms soluble complexes with Pb at an alkaline pH >8, which migrates from the cathode to the anode in the soil pore water (Ayyanar & Thaikonda, 2021). From Fig. 4.11, residual Pb accumulation in soil was found to be maximum in S3 section in all experiments, except in PSE1, in which S1 section close to the anode had maximum accumulation. Since sections close to the cathode had relatively high pH, the Pb-

EDTA complexes were formed leading to solubilization. The majority of the complex migrated till S3 section and precipitated there. The variations in the residual concentration of Pb in soil sections show that electromigration was the dominant transport process in this case, which is in accordance with previous studies (Figueroa et al., 2016; Silva et al., 2018). However, the direction of EOF was opposite to the direction of electromigration, which reduced the overall efficiency of EKR process.

The pH of soil has a profound effect on the abundance of Pb-EDTA complex as plotted in Fig. 4.12. Two major EDTA complexes might have formed with Pb,  $[PbHEDTA]^-$  and  $[Pb-EDTA]^{2-}$ , with the former dominant at pH below 4 and the latter dominant at pH from 6-12. The formation of these complexes was confirmed with the simulation done by Visual Minteq program. The stability constants (log Ks) for different chemical species of Pb and EDTA are given below (Villen-Guzman et al., 2015; Figueroa et al., 2016). At high pH,  $Pb(OH)_2$  and  $[Pb-EDTA]^{2-}$  complexes might have competed, but  $[Pb-EDTA]^{2-}$  complex have a higher stability constant than  $Pb(OH)_2$  complex; thus, it dominated in tests PGE1 to PSE2.



When Tween 80 was employed as the electrolyte, the removal efficiencies were 6-13.6% from low to high voltage. The overall removal was not

significant when compared to DW and EDTA. This could be because Tween 80 could not solubilize much Pb and only a small amount of mobile Pb fraction was transported to the cathode by electromigration. As established in previous studies, Tween 80 effectively solubilizes organic matter, which is transported toward the cathode through electro-osmosis (Reddy & Saichek, 2003). Similar observations have been reported by Fardin et al. (2021). It is assumed in this study that Tween 80 led to the solubilization of organic matter, which got bound to Pb and formed negatively charged complexes. The direction of  $Pb^{2+}$  was counteracted by the direction of the Pb-organic matter complex, which led to low net removal. Pb concentration in anolyte and catholyte was comparable, which supports this reasoning. However, the effect of voltage was similar to other tests, with high removal at higher voltage application. The residual Pb concentration profile indicates that significant Pb was present in all soil sections after EKR due to limited mobility and removal of Pb with Tween 80 as electrolyte. Similar results were reported in a study by Paramkusam et al. (2015) that concluded low metal removal by non-ionic surfactants than by distilled water.

The effectiveness of applied voltage is greatly influenced by the conducting material used. When the electrode material was changed from graphite to stainless steel under unenhanced conditions, the removal efficiency increased to 49.6% and 64.1% at 20 V (PSD2) and 50 V (PSD1), respectively. Similar results were reported for EDTA-enhanced tests where the removal efficiencies increased to 46.8% (20V) and 65.1% (50V) when stainless-steel was employed. No significant difference was observed in Tween 80 enhancement tests with varying electrode material. In case of graphite as electrode, oxidation of carbon was observed at anode, which caused high corrosion effect. Whereas, in cathode, hydroxide precipitation over the surface of electrode caused high resistance in soil and reduced the flow of electric current. This could explain the low removal rate of Pb in experiments with graphite electrode. In case of stainless steel as electrode, relatively less corrosion and/or deposition was observed, which led to higher removal. The mass balance for all the experiments was calculated to account for metal loss and reported in Table 4.12. The average values were between 0.8-1.0,

which indicates that almost all Pb content was accounted for. Minimum value was for PSD1, which could possibly be due to deposition over the electrode which was not analyzed for this study.

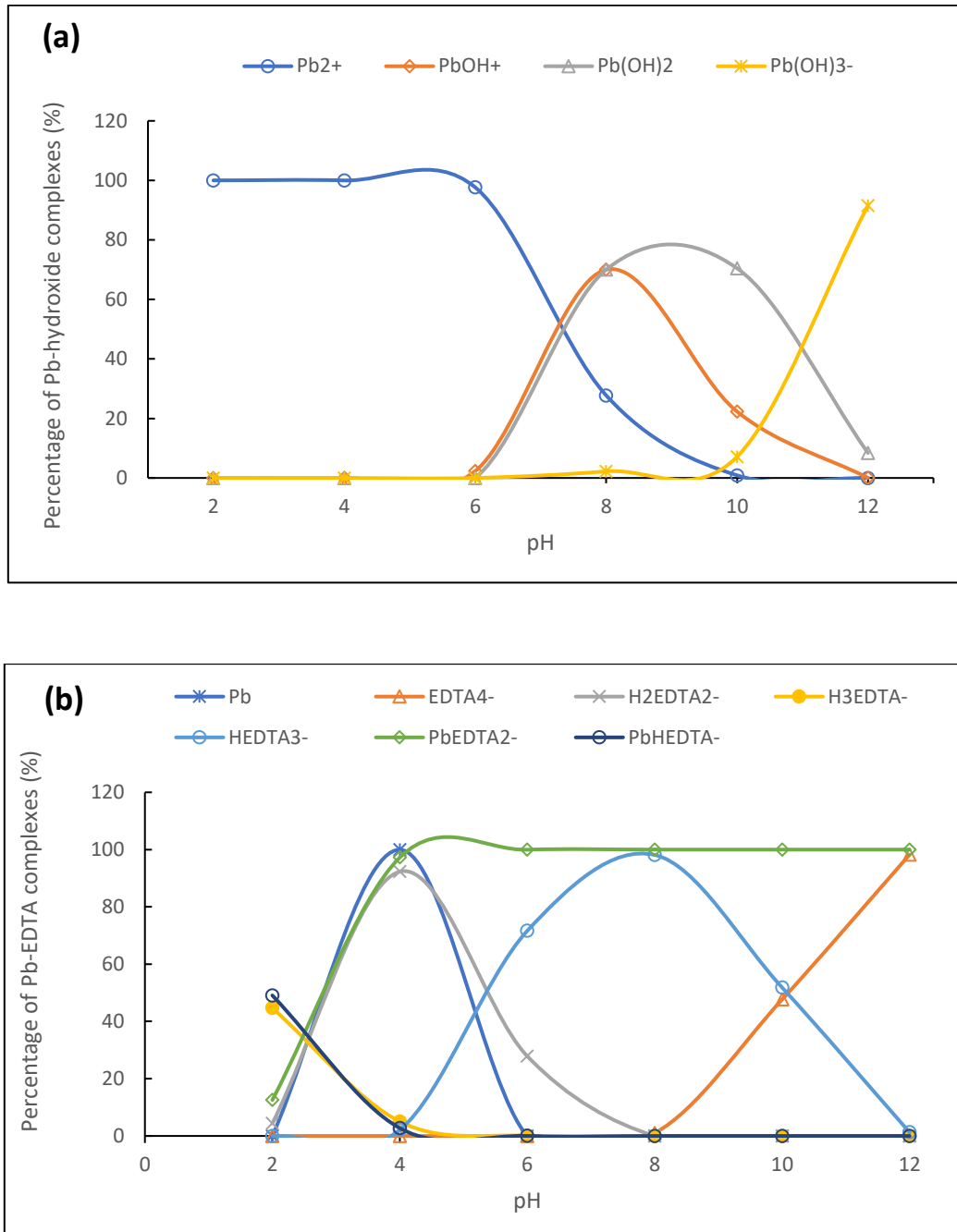


**Figure 4.12** Percentage distribution of (a) Pb-hydroxides complexes in unenhanced EKR (b) Pb-EDTA complexes in enhanced EKR against pH of soil using Visual Minteq Program (v 3.1)



It was hypothesized that electrolyte amendments with EDTA and Tween 80 would improve the solubilization of metal and aid in better removal. However, at high voltage, EDTA and DW tests yielded comparable removal rates, 65.1% and 64.1%, respectively, while Tween 80 did not yield significant removal (12.6%). The findings suggest that addition of electrolyte amendments was not much helpful in removal of Pb as compared to distilled water. Instead, factors like applied voltage and electrode material had more profound effect on the removal efficiency of EKR. Application of higher voltage yielded better removal, however, it also led to the corrosion of electrodes. Passivation or formation of oxides at the electrode surfaces increase the resistance and decrease the current flow, thereby decreasing overall removal. In this study, stainless steel exhibited better Pb removal with less passivation than graphite electrodes at higher voltage application. Therefore, electrode material plays an important role in the working of EKR and should be considered as an essential parameter for practical applications. Nevertheless, when the soil is subjected to low voltage gradient, EDTA amendments can prove to be helpful in further enhancing the metal removal.

#### **4.2.5. Properties of soil before and after EKR**

The characterization of initial and treated soil is given in Table 4.13. The properties of treated soil were analyzed after EKR treatment to detect the changes in soil properties when subjected to a high voltage of 50V for 10 hours. The results showed that the variations in physical properties like particle size, Atterberg's limits, and specific gravity were almost negligible. The migration of cations (K, Na, Ca) was observed towards the cathode and the concentration in the soil decreased post-treatment, as expected from the previous experiments. The migration of anions ( $\text{Cl}^-$ ,  $\text{SO}_4^{2-}$ ) did not result in significant removal from the soil, which could be attributed to the strong affinity of anions over the soil particles. The pH of soil did not change much from the initial value owing to the buffering capacity of the soil, while the electrical conductivity of the soil increased due to the increased solubility of ions under an increased voltage gradient.

**Table 4.13** The characteristics of soil before and after EKR

Properties	Contaminated Soil	Treated Soil	Method
Sand (%)	78	78	ASTM D6913
Silt and Clay (%)	22	22	ASTM D6913
pH	8.4	8.1	ASTM D4972-19
EC (mS/cm)	0.36	0.24	ASTM D4972-19
TDS (ppt)	0.12	0.07	ASTM D4972-19
K (mg/kg)	450	275	APHA 3111
Na (mg/kg)	5658	3266	APHA 3111
Ca (mg/kg)	3610	1592	APHA 3111
Chlorides (mg/kg)	300	360	EPA 9253
Sulphates(mg/kg)	3648	2142	EPA 9253
Organic Matter (%)	1.2	0.31	ASTM D2974
Plastic Limit (%)	12.8	13.7	ASTM D4318
Liquid limit (%)	29.6	32.7	ASTM D4318
Specific gravity	2.5	2.5	ASTM D854

#### 4.2.6. Economic evaluation

Table 4.14 indicates the energy consumption and total cost of the experiment. Maximum energy expenditure was observed in experiment PSE1 (78.3 KWh/m<sup>3</sup>), followed by PGE1 (73.3 KWh/m<sup>3</sup>). It was expected as both experiments were run at a higher voltage (50V) and with EDTA enhancement which increased current flow. Energy utilization was more in EDTA-enhanced tests than in Tween 80-enhanced tests (0-5.7 KWh/m<sup>3</sup>). Minimum energy consumption was seen in PGD4 and PSD2 (2.1 KWh/m<sup>3</sup>), which were run at low voltage (20V), without any enhancement liquid. Energy expenditure was not calculated for PST2 as no notable flow of current and removal of Pb was observed in this experiment.

**Table 4.14** The economic analysis of EKR to determine the cost of Pb removal (\$/g of Pb) from contaminated soil

Experiments	Pb removed from soil (g)	Energy Consumption (KWh/m <sup>3</sup> )	Total cost of experiment (₹)	Cost per gram of Pb removed	
				(₹/g)	(\$/g)
PGD1	0.088	30.0	178.9	2033.0	26.4
PGD2	0.043	16.0	136.9	318.4	4.1
PGD3	0.038	6.0	106.9	281.3	3.7
PGD4	0.006	2.1	95.3	15883.3	206.5
PSD1	0.170	25.7	194.6	1143.3	14.9
PSD2	0.539	2.1	124.0	230.1	3.0
PGE1	0.535	73.3	337.5	631.3	8.2
PGE2	0.033	8.0	141.5	4258.8	55.4
PSE1	0.622	78.3	381.2	612.6	8.0
PSE2	0.544	9.2	173.8	319.6	4.2
PGT1	0.072	40.4	228.7	3176.5	41.3
PGT2	0.030	5.7	124.9	4161.7	54.1
PST1	0.073	33.5	236.7	3242.6	42.2
*PST2	0.033	-	-	-	-

Experiments with higher energy expenditure showed higher operating costs. Applied voltage and addition of chemical electrolytes further increased the cost of EKR with a maximum of ₹381.2/- (US\$ 4.61) for EDTA-enhanced test run

at 50V with stainless steel electrode for 10 hours. However, when the cost was correlated with per gram removal of Pb, it was found that the cost was significantly less in experiments with high voltage applications and with EDTA enhancements (8.0 US\$/g and 8.2 US\$/g), as it yielded better removal of Pb from soil. Both, graphite and stainless-steel electrodes yield comparable results in terms of removal efficiency. However, corrosion was observed at graphite electrode, which can lead to additional maintenance costs, which makes stainless-steel electrode more cost-efficient. To further validate the results of this study, a comparison of the results obtained from this study was done with previous studies in Table 4.15, taking into account the factors like applied voltage gradient, electrolyte used, removal efficiency and energy expenditure. From the results obtained in the present study, it is suggested that combinations of high voltage application and use of additives like EDTA with EKR to remove Pb can be considered as economically viable than most conventional techniques.

**Table 4.15** Comparison of Pb removal of this study with previously published literature

S. No.	Voltage gradient (V/cm)	Electrolyte used	Duration	Pb Removal efficiency (%)	Energy Consumption (KWh/m <sup>3</sup> )	Reference
1	1	DW	4 d	15	-	Naidu et al., 2013
2	1	DW	9 d	20	-	Karaca et al., 2017
3	2	0.02M EDTA	4 d	24	-	Naidu et al., 2013
5	1	0.1M EDTA	360 h	47.8	-	Zhang et al., 2014
6	1	0.1 M EDTA	14 d	72	49	Silva at al., 2018
7	2	0.1M EDTA	240 h	11.19	140.3	Li et al., 2019
8	2	0.1M EDTA	9 d	26.36	486.38	Asadollahfar di et al., 2021
<b>9</b>	<b>2.5</b>	<b>DW</b>	<b>5 h</b>	<b>64.1</b>	<b>25.7</b>	<b>Present study</b>
<b>10</b>	<b>2.5</b>	<b>0.1 M EDTA</b>	<b>5 h</b>	<b>65.1</b>	<b>78.3</b>	<b>Present study</b>

### 4.3. EKR for Cd-contaminated soil

Response Surface Methodology (RSM) was used to design the experiments for EKR of Cd-contaminated soils. The interdependence of variables towards each other was plotted once the 3-dimensional response curves were generated over the CCD of RSM. To assess the interaction of the variables towards the response, 09 experimental runs were developed using Design Expert Software (Table 4.16). Since the model works better over continuous variables, two parameters were considered,  $X_1$ : Applied Voltage, and  $X_2$ : Concentration of electrolyte, and three responses were generated, (i) removal efficiency to assess the effective electro-migration phenomena, (ii) electro-osmotic flow to assess the electroosmosis process, and (iii) energy consumption for the economic estimation of the overall process.

**Table 4.16** Experimental Design for EKR of Cd-contaminated Soil using RSM

Run order	Factors		Responses		
	A: Voltage gradient (V/cm)	B: EDTA Conc. (mol/L)	Electro-osmotic Volume (ml)	Removal rate (%)	Energy consumed (KWh/g)
R1	0.5	0	156	4.45	0.1
R2	0.5	0.1	162	6.36	0.1
R3	0.5	0.2	169	5.91	0.4
R4	1.5	0	168	5.58	0.7
R5	1.5	0.1	191	8.43	1.4
R6	1.5	0.2	189	7.80	1.0
R7	2.5	0	183	19.73	0.8
R8	2.5	0.1	218	28.87	2.2

R9	2.5	0.2	193	26.74	1.3
----	-----	-----	-----	-------	-----

In addition, the effect of electrode material on the efficiency of EKR for Cd removal was also investigated. Since it is a discrete variable, it was not considered for the RSM model. Two additional experiments were performed using stainless steel as the electrode at two different electrolyte concentrations (Table 4.17).

**Table 4.17** Experimental design for EKR of Cd-contaminated Soil using stainless steel as electrode

Test No.	Voltage (V/cm)	Electrode	Electrolyte Conc.	Electro-osmotic volume	Removal rate	Energy consumed
R10	2.5	Stainless Steel	0 M	209	22.26	0.6
R11			0.1 M	170	30.16	1.8

#### 4.3.1. Variations in pH

The pH of electrolytes in different experiments is displayed in Fig 4.13. The results were consistent throughout with pH from 0.8-4 at the anode and from 8.5-12 at the cathode, due to the formation of H<sup>+</sup> and OH<sup>-</sup> ions at the anode and cathode respectively. The soil pH did not show significant variations from the initial value, as was observed in the previous experiments.

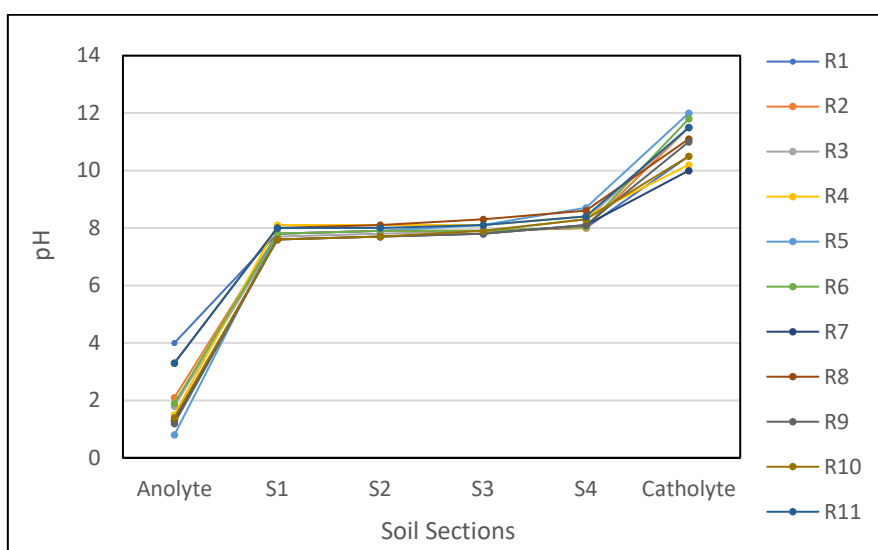


**Fig 4.13** Variations in pH of electrolytes and soil

#### 4.3.2. Variations in EC and TDS of soil

The variations in the conductivity of soil are shown in Fig 4.14. Among all the runs, EC was the maximum for R6. This was due to the addition of EDTA at 0.2 M concentration which increased the ionic strength in the soil. It was observed that EC decreased from the anode towards the cathode with maximum at S1 section for all the runs, except R4, in which a dip at S1 was observed. However, in experiments R5 and R6, EC decreased from the anode towards the cathode, and then increased at the S4 soil section, indicating higher EC at the soil sections close to the electrode wells. From the results, it can be inferred that as the voltage increased, EC was also increased, with higher values in EDTA-saturated soils. The TDS values of the soil displayed a similar trend as EC (Fig 4.15).

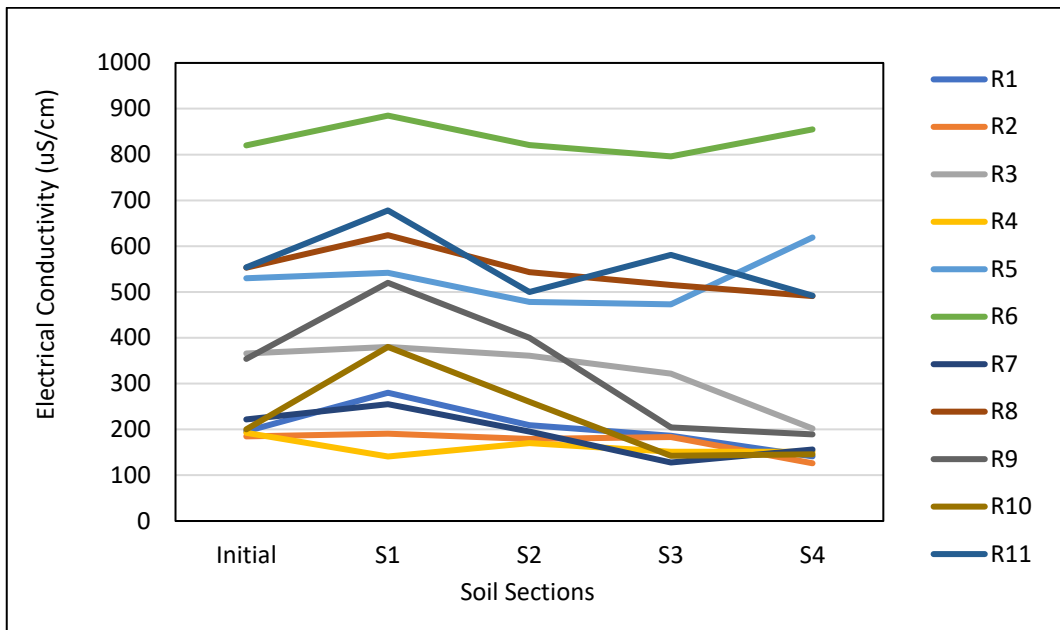


**Fig 4.14** Variations in electrical conductivity in soil sections

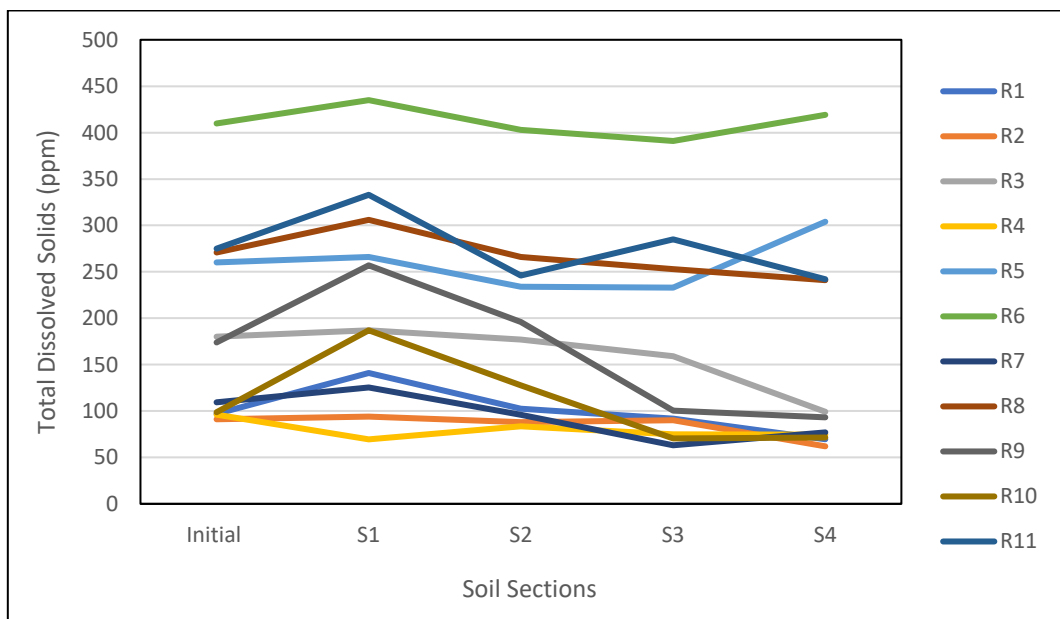


**Fig 4.15** Variations in TDS in soil sections for all the runs



**Table 4.18** The variations in pH, EC, TDS, volume, and Cd concentration in anolyte and catholyte after EK treatment

Experiment	Cycle	Section	pH	EC	TDS	Volume	Cd conc. (mg/L)
R1	Day 1	A1	3.5	0.37	0.18	87	0.11
		C1	10.5	0.35	0.17	80	0.0264
	Day 2	A2	4.6	0.39	0.19	89	0.3657
		C2	10.5	0.29	0.15	90.5	0.1766
R2	Day 1	A1	2.1	3.03	1.51	69	0.2057
		C1	11.6	1.22	0.62	95	0.1547
	Day 2	A2	2.1	2.9	1.45	69	0.0784
		C2	11.5	1.6	0.82	97	0.1756
R3	Day 1	A1	1.8	5.5	2.7	80	1.68
		C1	12	8.9	4.5	80	0.0705
	Day 2	A2	1.8	4.6	2.3	70.5	0.7658
		C2	11.5	4.9	2.4	76	0.0864
R4	Day 1	A1	1.5	28.5	13.9	17	128.2
		C1	10.4	28.1	13.7	80	4.041

	Day 2	A2	2.1	34	16.1	12	76.96
		C2	10.2	29.5	14.34	74	1.628
R5	Day 1	A1	0.8	14.9	7.4	22	92.98
		C1	12	14.9	7.4	95	5.337
	Day 2	A2	0.8	15	7.5	17	92.98
		C2	12	6.49	3.2	96	1.055
R6	Day 1	A1	1.9	4.09	2.04	75	1.9
		C1	11.8	3.28	1.64	91	0.1271
	Day 2	A2	1.9	3.8	1.91	72	1.079
		C2	11.7	2.5	1.28	98	0.1745
R7	Day 1	A1	1.3	10.34	5.16	65	2.106
		C1	9.5	2.1	1.06	115	0.1913
	Day 2	A2	1.5	9.95	4.87	48	0.0202
		C2	10.2	1.75	0.87	103	0.176
R8	Day 1	A1	3.3	6.57	3.28	65.5	63.14
		C1	11.4	7.11	3.55	89	9.472
	Day 2	A2	3.1	6.7	3.38	67	31.6

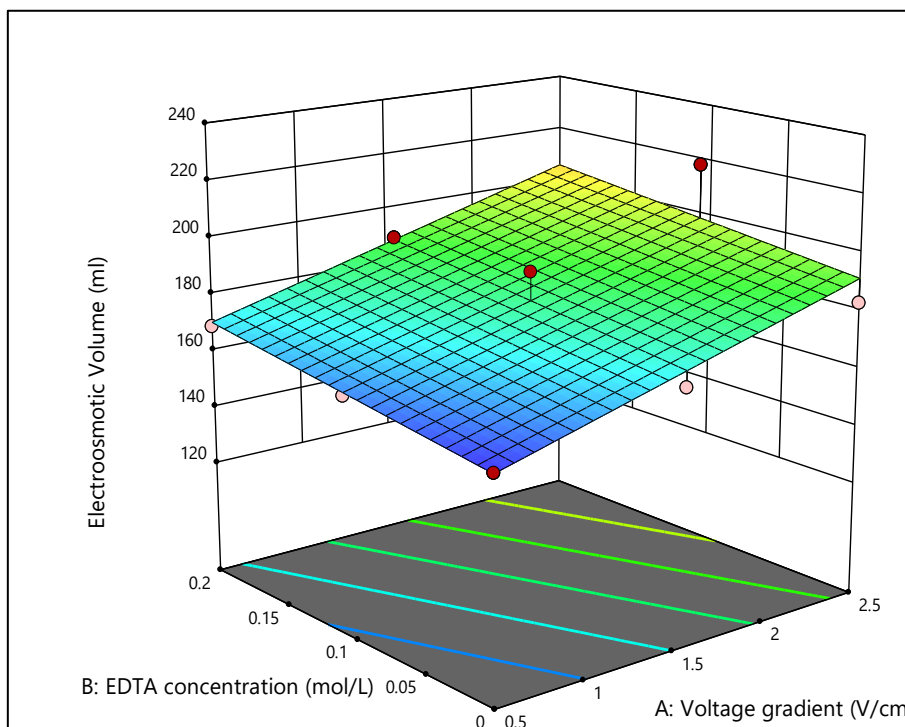
		C2	10.05	8.72	4.36	94	8.778
R9	Day 1	A1	1.2	10.6	5.3	52	4.466
		C1	10.9	2.21	1.1	91	0.0759
	Day 2	A2	1.3	9.03	4.5	35	1.233
		C2	11	2.09	1.04	102	0.0314
R10	Day 1	A1	1.3	7.6	3.8	63	1.035
		C1	9.7	2.33	1.17	118	0.12
	Day 2	A2	1.5	6.24	3.12	52	0.0543
		C2	11.7	3.3	1.65	91	0.1465
R11	Day 1	A1	3.3	8.3	4.2	67	74.93
		C1	10.2	11.7	5.8	84	10.66
	Day 2	A2	3.3	8.3	4.16	69	83.03
		C2	11.5	12.27	6.1	86	5.15

### 4.3.3. Variations in Electro-osmotic volume

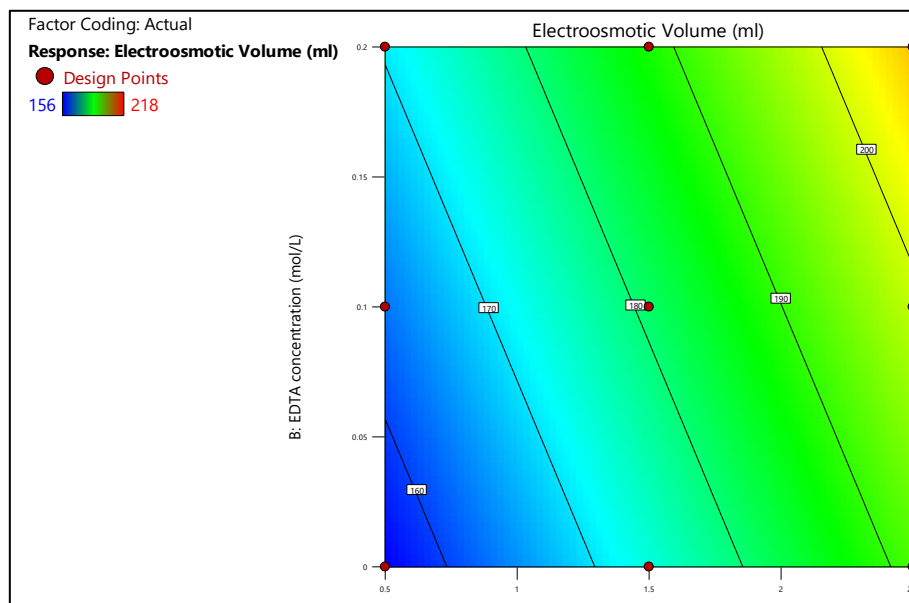
In order to determine the impact of voltage (A) and electrolyte solution (B) on the electro-osmotic volume accumulated at the cathode (Y), the following regression equation was achieved:

$$Y = 181.0 + 17.83 A + 7.33 B \dots\dots\dots(4.12)$$

The analysis of Variance (ANOVA) was done to determine the model accuracy (Table 4.19). The significance of the model was indicated by the F value and P value. The higher F-value of 8.9 for the model indicates that the model is efficient ( $P < 0.05$  for 95% confidence level). The regression coefficient ( $R^2$ ) of 74% indicates a good fit of the model. The interaction between each parameter was determined by using Response surface plots as shown in Fig 4.16. Higher EOVS indicates higher electro-osmosis, yielding better removal. Therefore, the optimized value for higher EOVS at 218 mL was achieved at 2.5 V/cm gradient, and 0.1 M EDTA as electrolyte solution.



(a)



(b)

**Fig 4.16** (a) 3-D and (b) Contour response surface plots of EOV against variables A and B

**Table 4.19** Regression Analysis and ANOVA of Response Electro-osmotic Volume

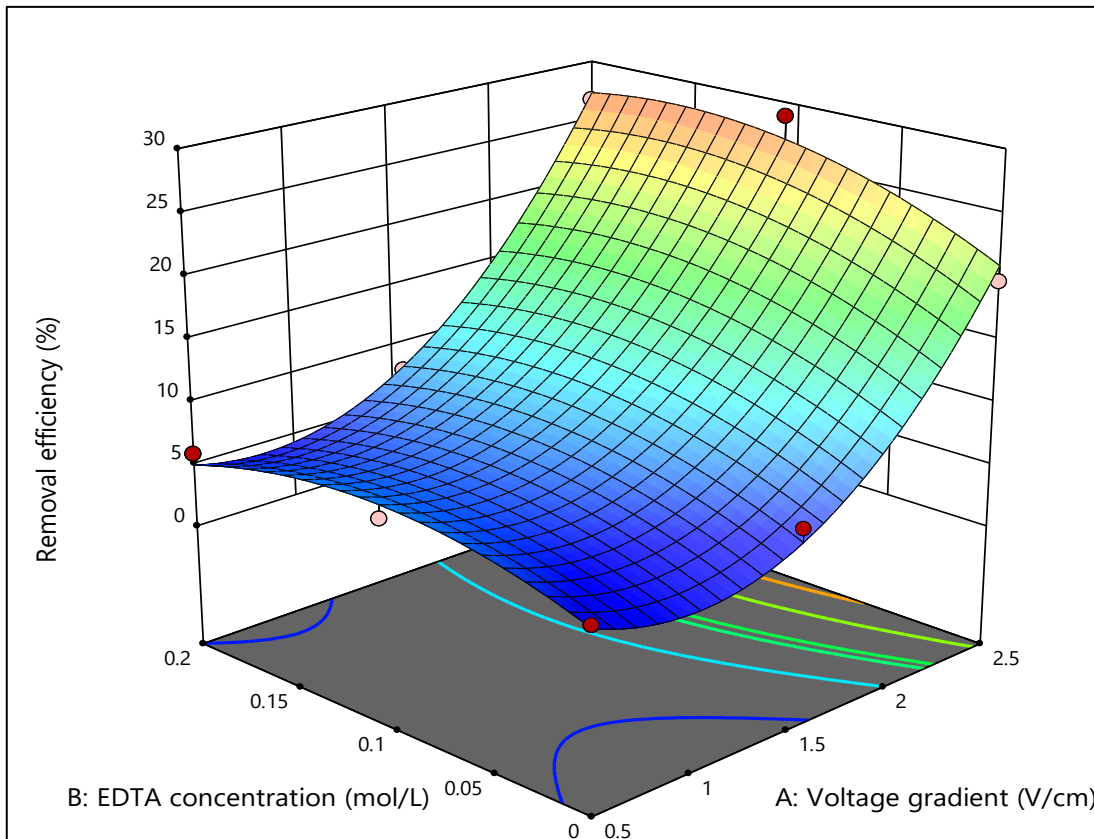
Source	Sum of Squares	df	Mean Square	F-value	p-value	
<b>Response 1: Electro-osmotic Volume (EOV)</b>						
<b>Model (Linear vs Mean)</b>	2230.83	2	1115.42	8.93	0.0159	Significant
A-Voltage gradient	1908.17	1	1908.17	15.28	0.0079	
B-EDTA Conc.	322.67	1	322.67	2.58	0.1591	
<b>Residual</b>	749.17	6	124.86			
<b>Cor Total</b>	2980.00	8		<b>R<sup>2</sup></b>	0.7486	
<b>Std. Dev.</b>	11.17			<b>Adjusted R<sup>2</sup></b>	0.6648	
<b>Mean</b>	181.00			<b>Predicted R<sup>2</sup></b>	0.4299	
<b>C.V. %</b>	6.17			<b>Adeq Precision</b>	7.8019	

#### 4.3.4. Removal efficiency

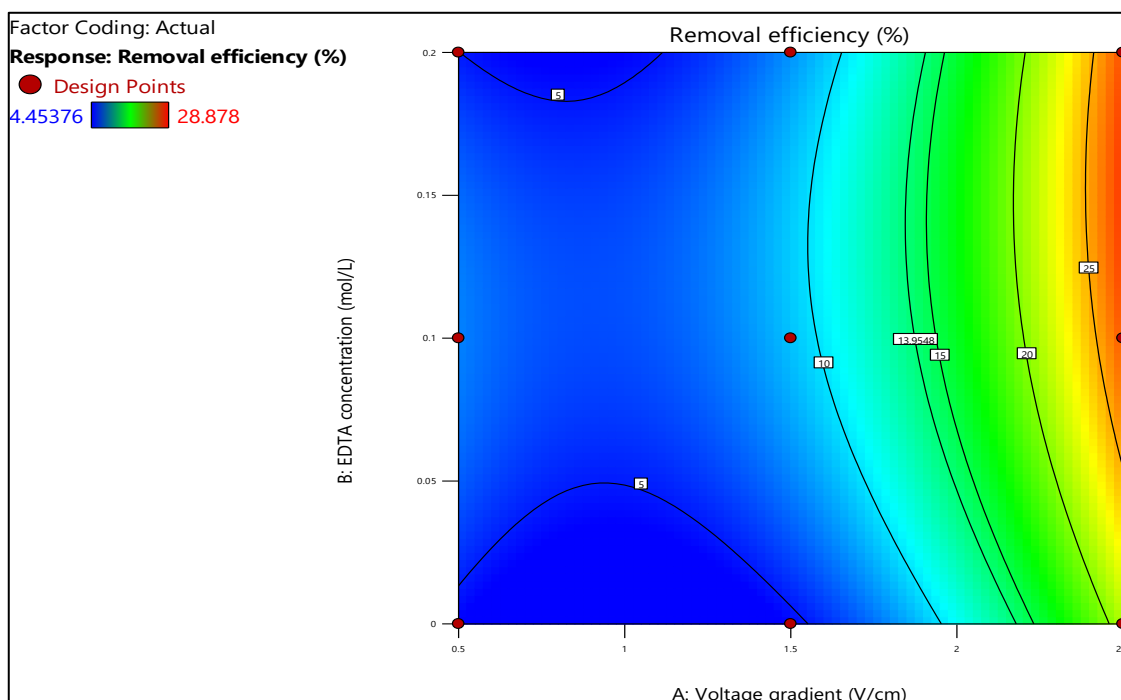
In order to determine the impact of voltage (A) and electrolyte solution (B) on the removal efficiency of EKR for Cd (Y), the following regression equation was achieved:

$$Y = 9.18 + 9.77 A + 1.78 B + 1.39 AB + 8.07 A^2 - 2.86 B^2 \dots\dots(4.13)$$

The analysis of Variance (ANOVA) was done to determine the model accuracy (Table 4.20). The significance of the model was indicated by the F value and P value. The higher F-value of 48.5 for the model indicates that the model is efficient ( $P < 0.05$  for 95% confidence level). The regression coefficient ( $R^2$ ) of 98% indicates a good fit of the model. The interaction between each parameter was determined by using Response surface plots as shown in Fig 4.17. The optimized value for maximum removal efficiency at 28.87% was achieved at 2.5 V/cm gradient, and 0.1 M EDTA as electrolyte solution.



(a)



(b)

**Fig 4.17** (a) 3-D and (b) Contour response surface plots of Removal Efficiency of EKR for Cd against variables A and B

From the results, it was observed that as the voltage gradient increased from 0.5 to 2.5 V/cm, the removal increased from 4.4 to 19.7 %. However, when the concentration of EDTA was increased from 0 M to 0.2 M, the removal rate increased to 28.87% and then decreased to 26.74%. Thus, no linear relationship could be derived from the removal rate with increasing the strength of the electrolyte, and the optimized condition was found to be 0.1 M of EDTA.

Additionally, R11 was found to yield a maximum removal of 30% when stainless steel was employed as the electrode. R10 also performed better with 22.26% removal as compared to R7 (similar conditions with Graphite electrode) with 19.7 % removal. Thus, Stainless-steel was found better suited for the remediation of Cd in terms of relatively higher removal efficiency in a short duration.



**Table 4.20** Regression Analysis and ANOVA of Response Removal Efficiency

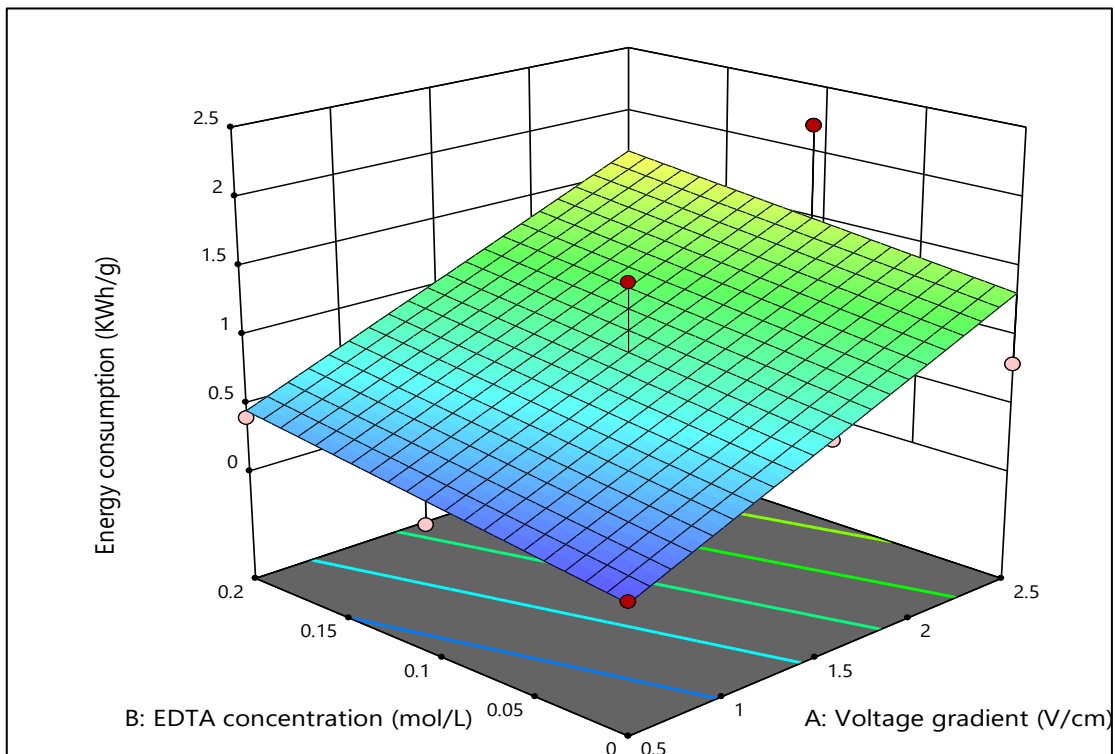
Source	Sum of Squares	df	Mean Square	F-value	p-value	
<b>Response 2: Removal Efficiency</b>						
<b>Model</b>	746.00	5	149.20	48.53	0.0045	Significant
A-Voltage gradient	572.63	1	572.63	186.27	0.0009	
B-EDTA conc.	19.03	1	19.03	6.19	0.0887	
AB	7.70	1	7.70	2.51	0.2116	
A <sup>2</sup>	130.33	1	130.33	42.40	0.0074	
B <sup>2</sup>	16.32	1	16.32	5.31	0.1046	
<b>Residual</b>	9.22	3	3.07			
<b>Cor Total</b>	755.23	8		<b>R<sup>2</sup></b>	0.9878	
<b>Std. Dev.</b>	1.75			<b>Adjusted R<sup>2</sup></b>	0.9674	
<b>Mean</b>	12.66			<b>Predicted R<sup>2</sup></b>	0.8589	
<b>C.V. %</b>	13.85			<b>Adeq. Precision</b>	16.1360	

#### 4.3.5. Energy consumption

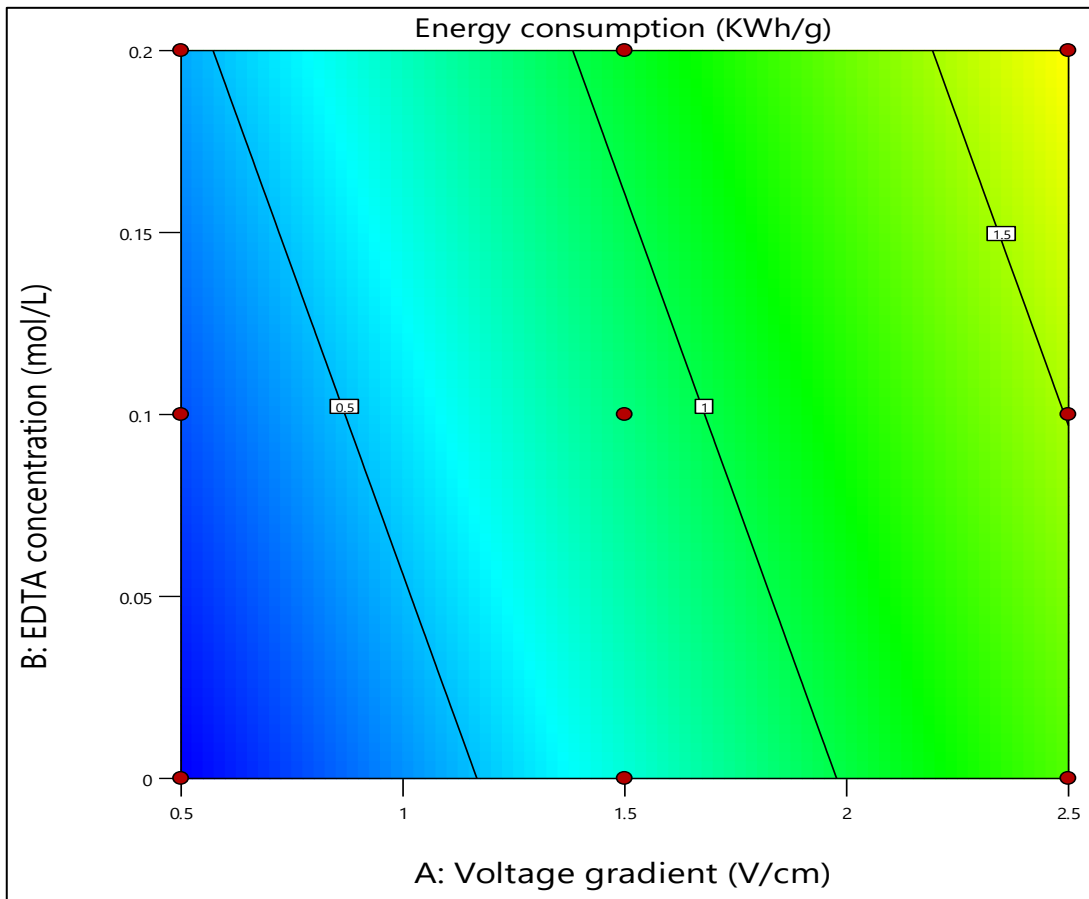
In order to determine the impact of voltage (A) and electrolyte solution (B) on the energy consumption per gram of metal removed (Y), the following regression equation was achieved:

$$Y = 0.8889 + 0.6167 A + 0.1833 B \dots\dots\dots(4.14)$$

The ANOVA was done to determine the model accuracy (Table 4.21). The significance of the model was indicated by the F value and P value. The higher F-value of 6.18 for the model indicates that the model is efficient ( $P < 0.05$  for 95% confidence level). The  $R^2$  was found to be of 67%. The interaction between each parameter was determined by using Response surface plots as shown in Fig 4.18. The energy consumption is directly dependent upon the voltage applied, which in turn is directly related to the removal of metal pollutants. Therefore, to determine the optimum conditions, energy consumption per gram removal of metal was considered.



(a)



(b)

**Fig 4.18** (a) 3-D and (b) Contour response surface plots of Energy consumption per gram removal of Cd against variables A and B

**Table 4.21** Regression Analysis and ANOVA of Response Energy consumption per gram removal of Cd

Source	Sum of Squares	df	Mean Square	F-value	p-value	
<b>Response 3: Energy Consumption per g removal</b>						
<b>Model (Linear vs Mean)</b>	2.48	2	1.24	6.18	0.0349	Significant
A-Voltage gradient	2.28	1	2.28	11.36	0.0150	
B-EDTA conc.	0.2017	1	0.2017	1.00	0.3551	
<b>Residual</b>	1.21	6	0.2009			
<b>Cor Total</b>	3.69	8		<b>R<sup>2</sup></b>	0.6732	
<b>Std. Dev.</b>	0.4482			<b>Adjusted R<sup>2</sup></b>	0.5643	
<b>Mean</b>	0.8889			<b>Predicted R<sup>2</sup></b>	0.2664	
<b>C.V. %</b>	50.43			<b>Adeq Precision</b>	6.1825	

#### 4.4. EKR for mixed-metal-contaminated Soils

The efficiency of EKR in mixed-metal contaminated soil was investigated. The operating variables of EK were set at the optimized values that were obtained from the results of individual metal-contaminated soils. The experimental conditions for this experiment are given in Table 4.22.

**Table 4.22** Experimental conditions for EKR of mixed-metal contaminated Soil

Metals used	Soil	Voltage	Electrolyte	Electrode	Duration
Cr (VI) (500 mg/kg) Pb (500 mg/kg) Cd (250 mg/kg)	1.5 kg	2.5 V/cm (50 V)	EDTA (0.1 M)	Stainless Steel	10 h

##### 4.4.1. Variations in pH, EC, and TDS

The variations in pH, EC, and TDS are given in Table 4.23. As expected, the pH of the soil increased from soil sections S1 to S4 due to the production of OH<sup>-</sup> ions at the cathode (pH = 13) that might have migrated into the soil raising the pH near the S4 section. The acidic front generated at the anode (pH = 1.9) could not lower the pH in the S1 section, possibly due to the resistance by the high buffering capacity of the soil and concentration of H<sup>+</sup> ions at the anode. The EC and TDS of soil decreased from the anode towards the cathode, indicating the movement of ions towards the anode, confirmed by the higher EC and TDS of the anolyte.

**Table 4.23** pH, EC, and TDS values of electrolytes and soil sections after EK treatment

Soil Sections	pH	EC (μS/cm)	TDS (ppm)
Initial	7.9	346	170
Anolyte	1.9	20960	13414
S1	7.9	368	181
S2	8.3	281	138

<b>S3</b>	8.3	255.6	125
<b>S4</b>	9.5	195.8	96
<b>Catholyte</b>	13.2	9480	6067

#### 4.4.2. Variations in Current

The current across the soil cell was continuously measured with the help of a milliamperere meter data logger (Fig. 4.19). The current increased with time till a maximum value of 118 mA, however, no peak was attained and the current did not stabilize, which could be correlated with the increase in the number of ionic species in the soil with the addition of EDTA, as was also reported by (Asadollahfardi et al., 2021).

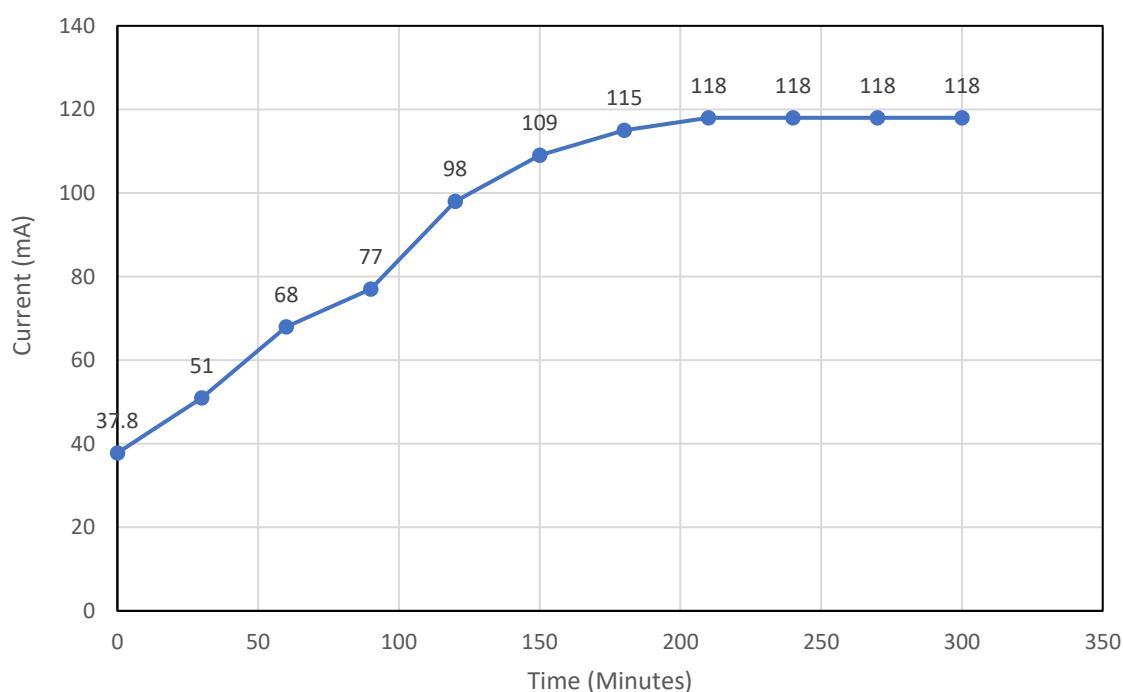


**Fig 4.19** Variation in current intensity (mA) during EK treatment of mixed metals

#### 4.4.3. Metal removal and residual concentrations in soil

The removal efficiency of EKR to remove the three selected metals simultaneously is given in Fig 4.20. The removal was in the order Cr (VI) > Pb > Cd. One of the reasons for higher Cr (VI) removal could be its relatively greater

ability to form complexes with EDTA as compared to Pb and Cd, which led to its effective removal. Another reason is the net movement of  $\text{CrO}_4^-$  ions and  $[\text{Cr-EDTA}]^-$  complexes towards the anode leading to higher removal. The same can also be confirmed from the residual concentration of Cr (VI) in the soil sections, with maximum accumulation at S1 near the anode.

In the case of Pb and Cd, the antagonistic movement of metal ions and metal-EDTA complexes led to the lower removal, as can also be seen from the residual concentration. In the case of Pb, the maximum accumulation was at the S4 section near the cathode, which suggests that movement of  $\text{Pb}^{2+}$  towards the cathode was dominant in this system, which later led to the precipitation of the ion due to the high pH zone near the cathode. The maximum accumulation of Cd was found in the middle of the soil column (S2 and S3 sections), due to the net movement of  $\text{Cd}^{2+}$  ions and Cd-EDTA complexes in the opposite direction.

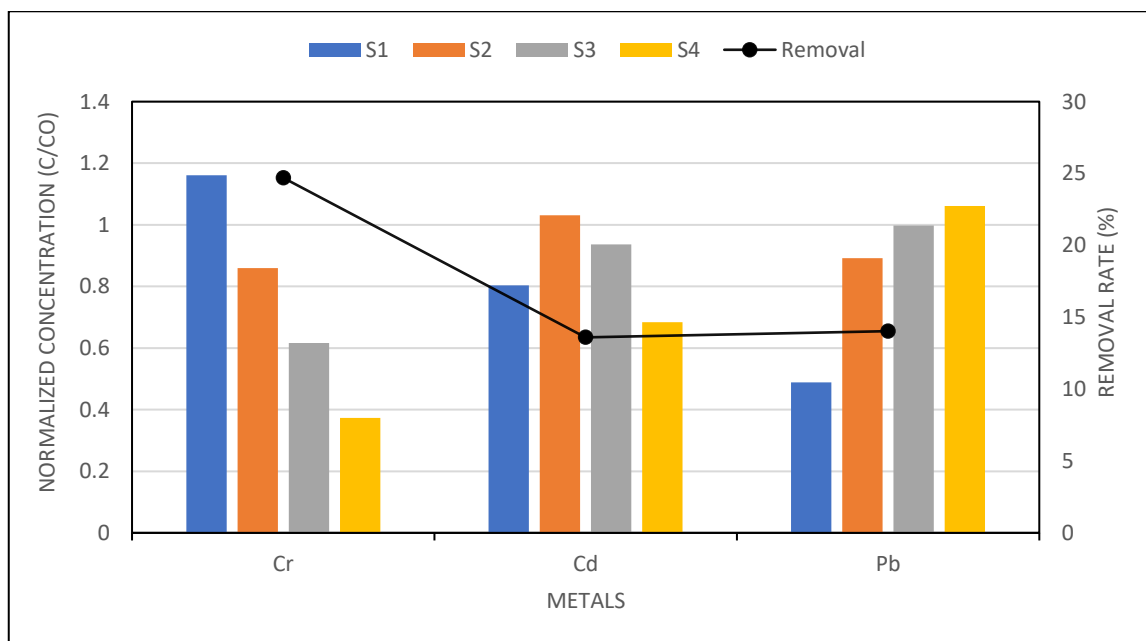


**Fig 4.20** Removal rate and the normalized residual concentration of Cr(VI), Cd and Pb in the soil

#### 4.4.4. Comparison of EKR for individual metals and mixed metal conditions

The trend of metal removal for individual metals was similar to the removal rate of metals in mixed conditions ( $\text{Cr (VI)} > \text{Pb} > \text{Cd}$ ). However, the increased ionic strength of the soil column upon the presence of multiple contaminants decreased the net removal of metals from the soil system. Since the electrolytes were not re-circulated during the experiment, the anolyte and catholyte were saturated with the ions, resisting the transfer of metals from the soil into the electrolyte. Due to this, the ions accumulated near the electrode wells in soil sections S1 and S4. From the results, it was found that Pb removal was less as compared to Cd (Fig 4.21). However, in the previous literature, it has been established that Pb has a stronger affinity with soil than Cd, and thus, a lower removal rate. One of the factors for this inverse trend could be the initial concentration of metals. For this study, the concentration of Pb was twice that of Cd which could result in higher removal of Pb. From these results, it was inferred that EKR yields better removal rates even in highly contaminated soil.

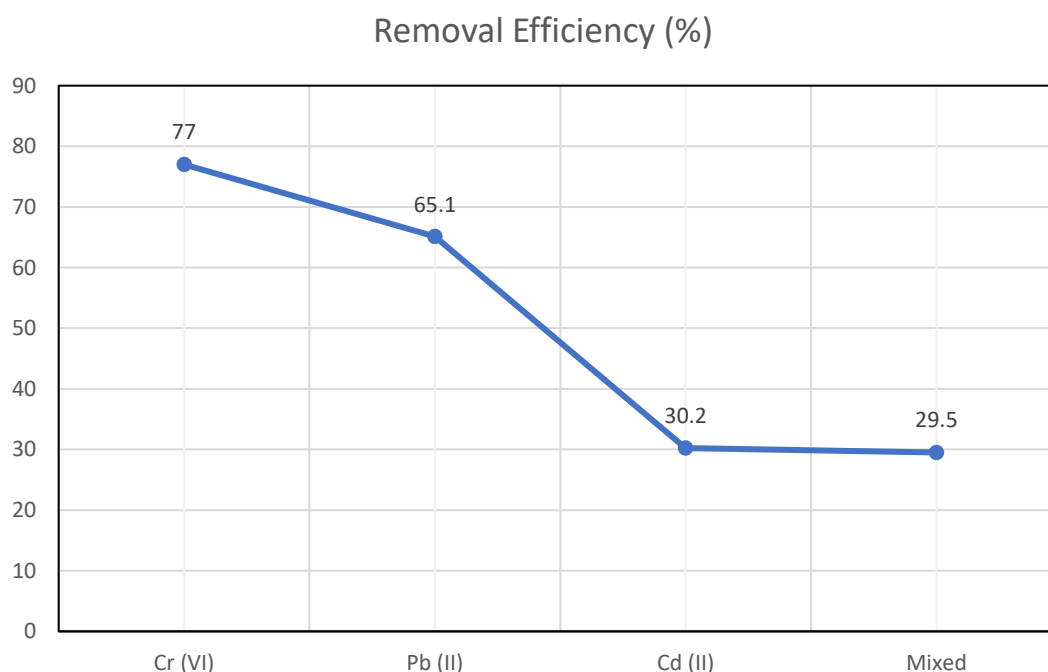


**Fig 4.21** Removal efficiencies of metals in individual metal-contaminated soil and mixed-metal-contaminated soils



#### **4.4.5. Mobilization of metals and toxicity removal**

The distribution of Cr (VI), Pb, and Cd in soil both before and after EK treatment was determined using the sequential extraction procedure analysis is summarized in Fig 4.22. With the help of sequential extraction, the different forms of metals in soil can be determined which serves as a useful tool to regulate soil-metal chemistry. In the case of Cr (VI), most of the fraction was in the exchangeable and soluble fraction. Due to this, the removal was relatively higher and faster. Upon EKR, the pH of the cathode increased which led to the partial reduction of Cr (VI) to Cr (III) and the precipitation of Cr as hydroxides or carbonates, preventing further migration (Reddy et al., 2001).

In the case of Pb, a major portion of the metal initially was present in the residual fraction resulting in the immobilization of metals. Upon EK treatment, the metals shifted to the exchangeable fraction which could be due to the development of an acidic front in the anolyte that led to solubilization of metal precipitates or hydroxides. The Cd distribution in the soil is similar to Cr (VI) with a major portion in the exchangeable form and soluble form, which migrated readily upon the induced electric field. The findings suggest that the metals when present in exchangeable and soluble form cause higher migration during EK treatment.

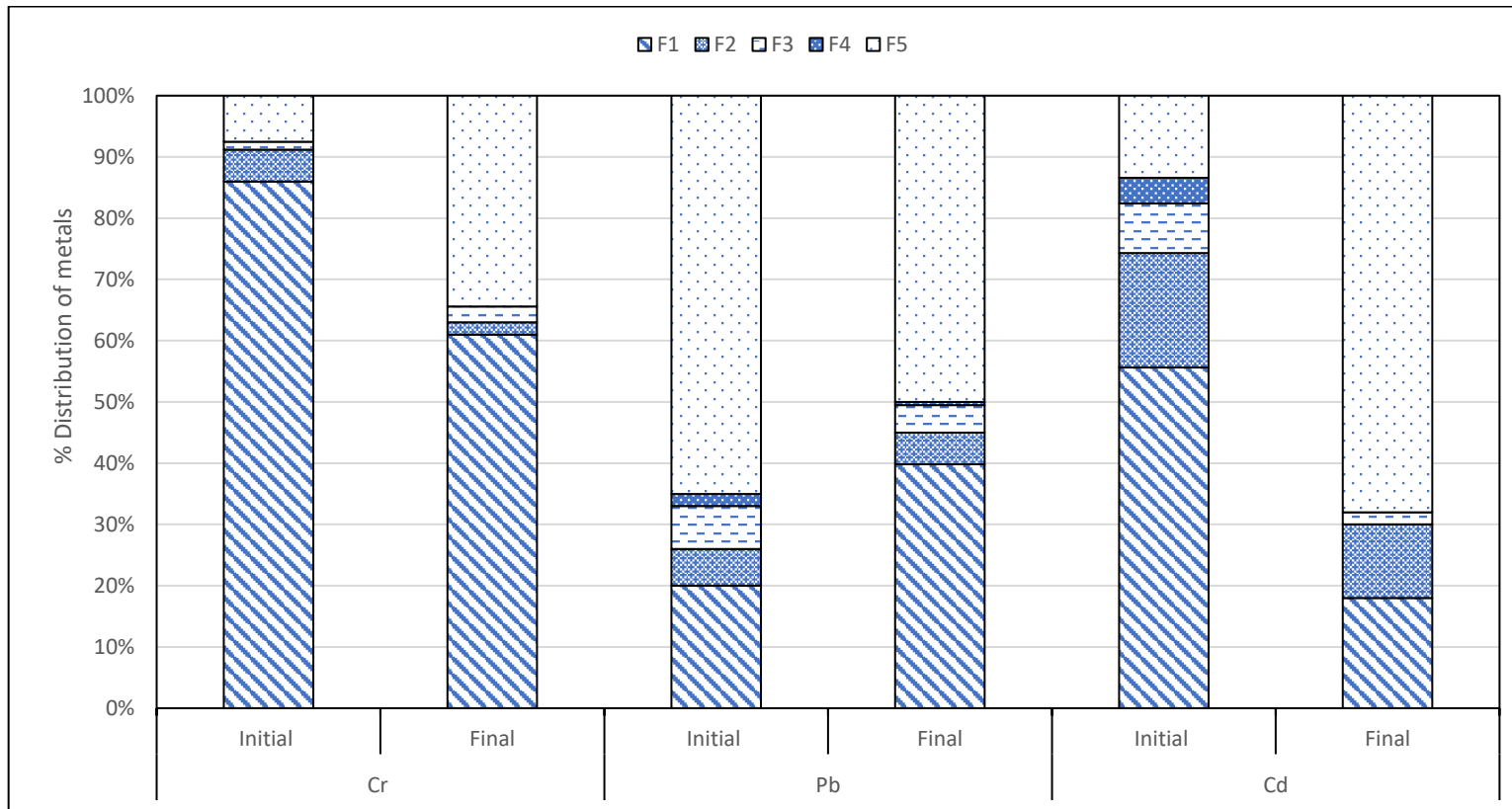


**Fig 4.22** Percentage distribution of metals in different fractions from the sequential extraction procedure

#### 4.5. Effect of Electrode Configuration on EKR

The electrodes play an important role in influencing the migration and transport of metals through pH regulation. Therefore, it is imperative to determine the most suitable placement of electrodes in the soil column for effective EKR. For this reason, the effect of electrode configuration on EKR efficacy was studied by varying the number and the arrangement of electrodes in linear, trigonal, and square configurations (Table 4.22). The electrodes were placed at a distance of 15 cm from each other in all the experiments. For each experiment, one anode was used against a variable number of cathodes.

**Table 4.22** Experimental design for EKR of mixed-metal contaminated Soil

S. No.	Electrode configuration	Electrode/ Electrolyte	Voltage Gradient	Time
1	Linear (1A-2C)	Stainless steel/ EDTA (0.1 M)	2.5 V/cm	10 h
2	Trigonal (1A-2C)			
3	Square (1A-4C)			

A= Anode; C= Cathode

##### 4.5.1. Variations in pH of soil

The results of pH in soil sections are given in Fig 4.23. It was observed that in all experiments, the pH of the anolyte ranged between 2-4, and the pH of the catholyte ranged between 8-12. The results were consistent with the previous observations and also the literature, confirming that the electrolysis reactions occurred at the electrodes leading to a decrease in pH at the anode, while an increase in pH at the cathode. The pH of the soil ranged from 7.9 to 8.5 in all experiments, with only a slight increase in the soil sections close to the cathode. It was observed that the acidic front created at the anode could not advance into the soil sections, which could have been due to the high buffering capacity of the soil that resisted the advancement of the acid front from the anode toward the cathode. The pH of soil is an important parameter that governs the mobilization of metals at low pH.

However, this work employed EDTA as an electrolyte that tends to form soluble metal complexes at a wide range of pH. Thus, it was expected that the pH of the soil would not hinder the removal of metals.

#### **4.5.2. Variations in electrical conductivity**

The electrical conductivity in the electrolytes is given in Fig 4.23. From the results, it was observed that in experiment I, the EC of anolyte ranged from 15-20.9 mS/cm, while in catholyte 2-9.4 mS/cm. Similarly, in experiment II, the EC of anolyte ranged from 9.7-12 mS/cm, while in catholyte it ranged from 0.2-2.3 mS/cm. In both experiments, EC was higher in the anolyte as compared to the catholyte, indicating the movement of ions toward the anolyte. However, in experiment III, the EC of anolyte ranged from 12-13.4 mS/cm, while in catholyte it ranged from 19-21 mS/cm, indicating the movement of ions toward the catholyte.

The distribution of EC in soil in all experiments showed a similar trend of a decrease in EC from the anode toward the cathode. In experiment I, EC was higher in soil sections close to the anode (S1 and S3) and minimum in soil sections (S5 and S6) which were lying at the corners perpendicular to cathodes. EC is an indicator of the movement of ions within the soil system, and in this case, due to the applied electric field. Thus, the higher EC implied a stronger electric field. Whereas, soil sections with low EC indicated the areas of low or almost negligible field and hence electrically inactive, for example, soil sections S5 and S6. The development of electrically inactive zones in soil can decrease the overall efficiency of EKR as processes like electromigration and electro-osmosis do not take place in those regions. In experiments II and III, EC was almost similar across all soil sections with slightly higher values near the anode, indicating uniform distribution of electric field in the soil column.

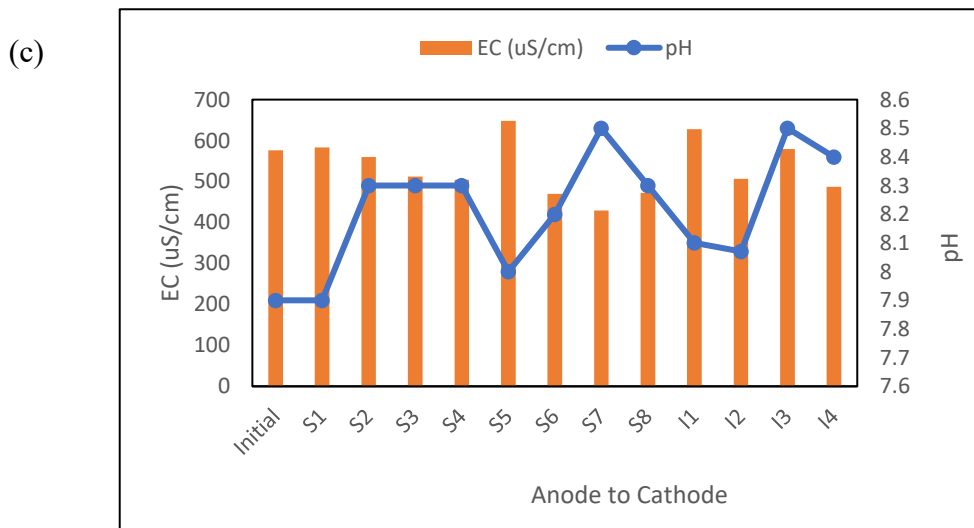
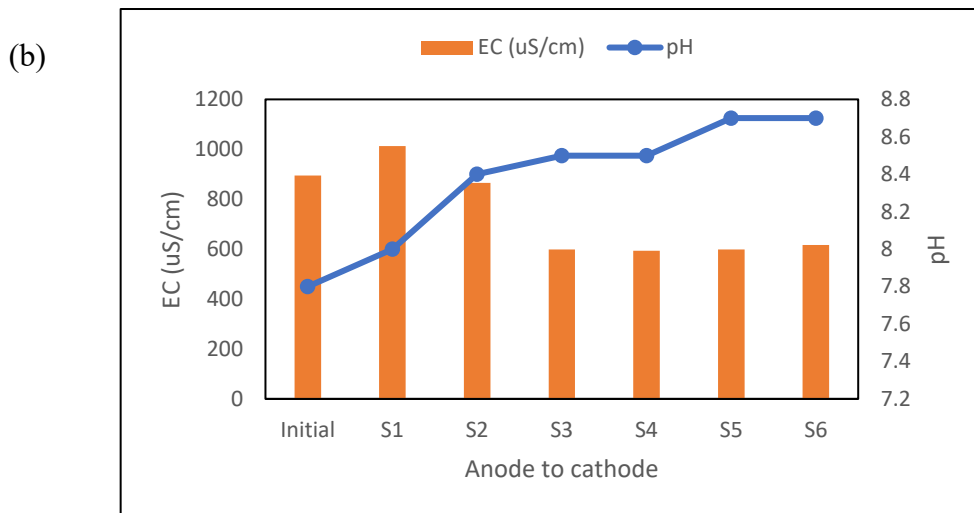
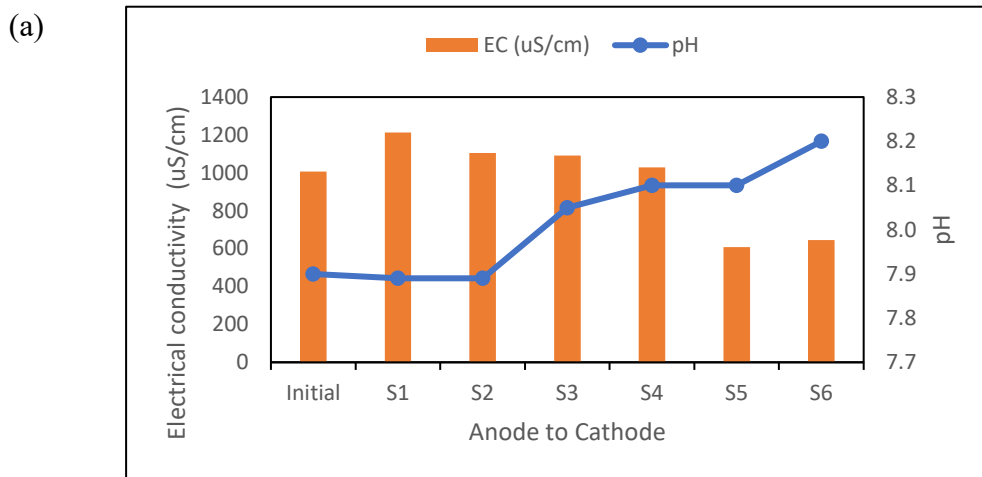


**Fig 4.23** Variations in pH and EC of soil for (a) linear (b) trigonal (c) square configuration

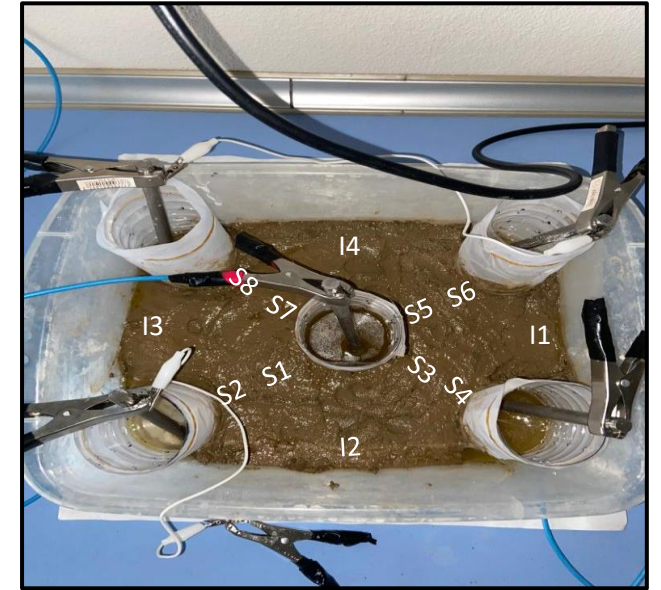
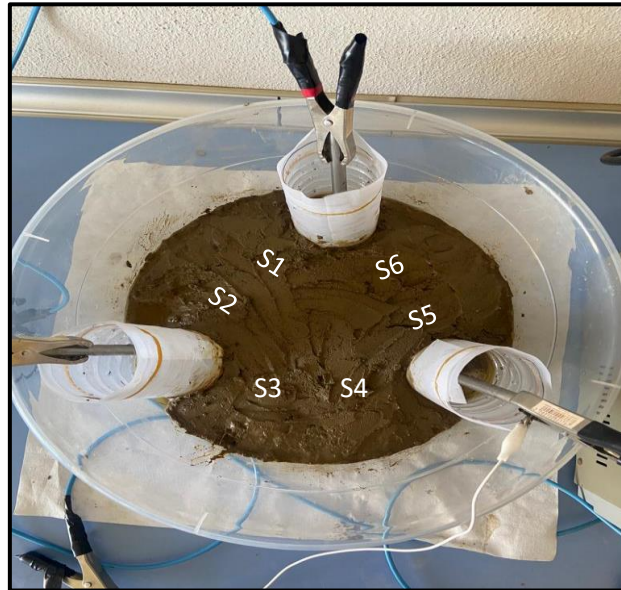
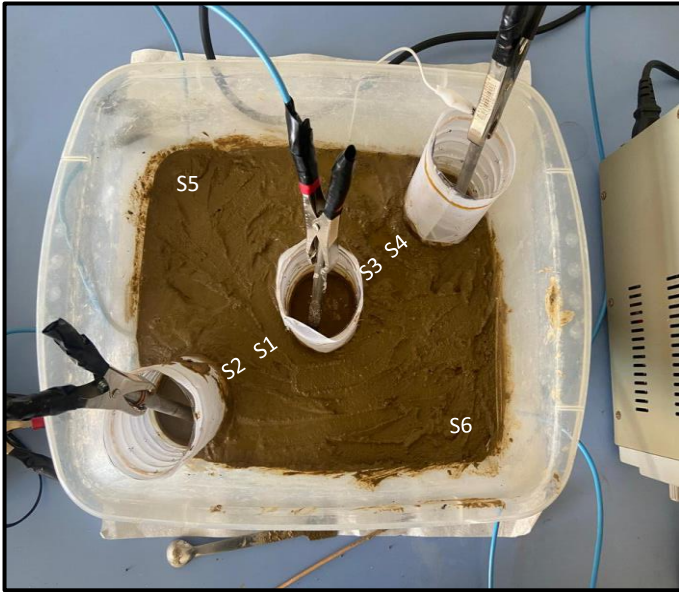


**Fig 4.24** Experimental setups for electrode configurations, Linear, Trigonal, and Square marked with the nomenclature of soil sections taken. (Left to Right)

### 4.5.3. Variations in current

The electric current across the soil cell was continuously measured with the help of a milliamperere meter data logger (Fig 4.25). In experiment I, the current increased, attained a peak and then decreased gradually. This could be attributed to the increased mobility of charged ions upon application of an electric field in the first few hours, however, when most of the ions were removed from the soil into the electrolyte, the current stabilized. In experiment III, the trend of current was similar with an increase in values with time. No peak was attained and the current did not stabilize, which could be correlated with the increase in the number of ionic species in the soil with the addition of EDTA, as reported by Asadollahfardi et al., (2021). However, experiment II exhibited an inverse trend with decreasing current with time. This trend could be observed because of higher ionic species in the mobile form at the start of the experiment which was readily available for migration. With time, the ions migrated toward electrode wells and hence the current decreased gradually.

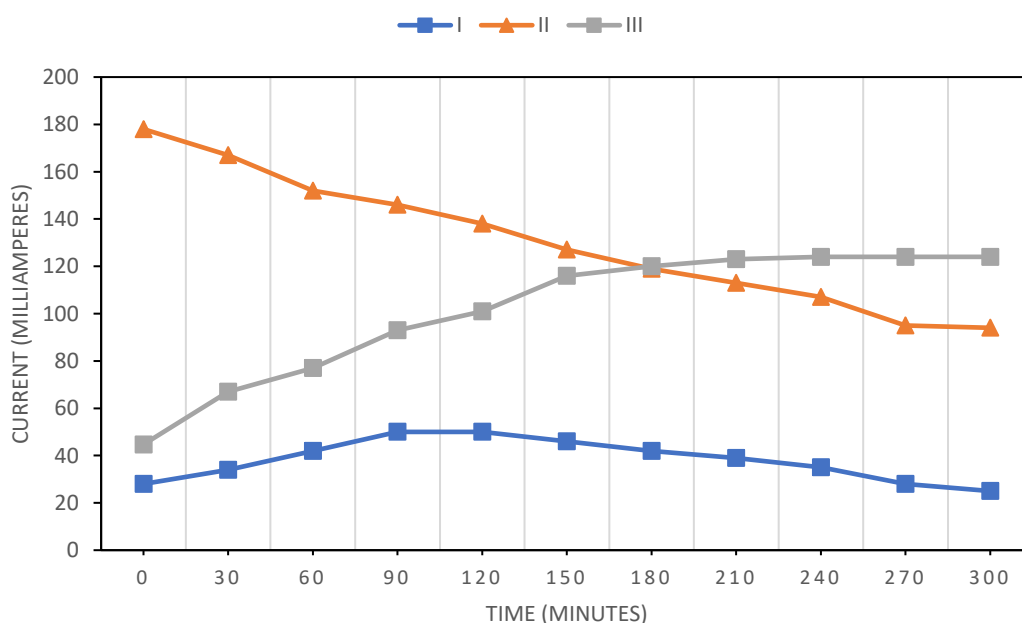


**Fig 4.25** Variations in current intensity (mA) in experiments I, II, and III during EKR

**Table 4.23** Variations in Current (Amperes) with time during the EKR process

<b>Time (mins)</b>	<b>Exp. I</b>	<b>Exp. II</b>	<b>Exp. III</b>
0	28	178	44.7
30	34	167	67
60	42	152	77
90	50	146	93
120	50	138	101
150	46	127	116
180	42	119	120
210	39	113	123
240	35	107	124
270	28	95	124
300	25	94	124

#### **4.5.4. Variations in electro-osmotic flow and moisture content**

The variations in Electro-osmotic Volume (EOF) in anolyte and catholyte after EKR are shown in Fig 4.26. From the results, it was evident that the direction of EOF was from anode to the cathode in all the experiments, with maximum EOF in experiment III. This could be attributed to a greater number of cathodes used in this experiment that led to higher accumulation. Minimum EOF was observed in experiment II, which suggests that more moisture loss took place in this setup.



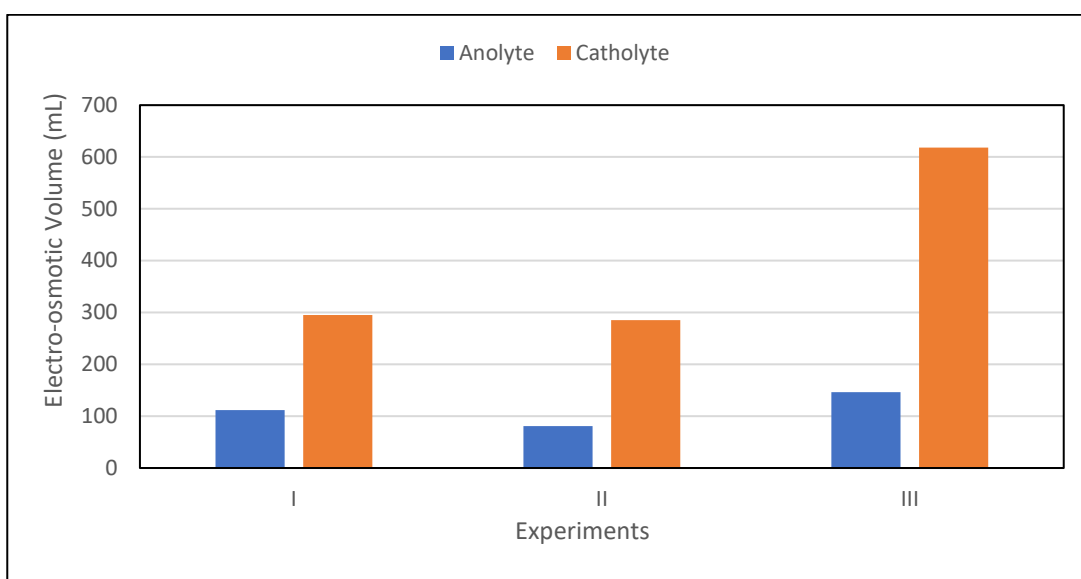
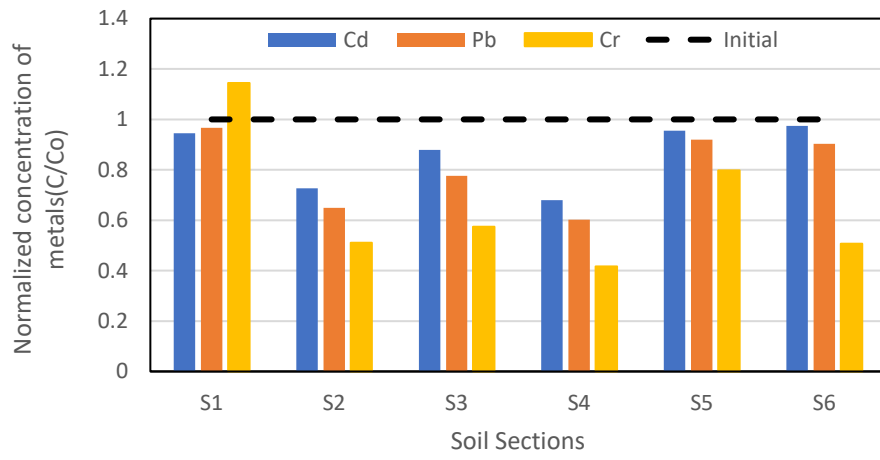


**Fig 4.26** Variations in Electro-osmotic Volume (EOF) in anolyte and catholyte for experiments I, II, and III after EKR

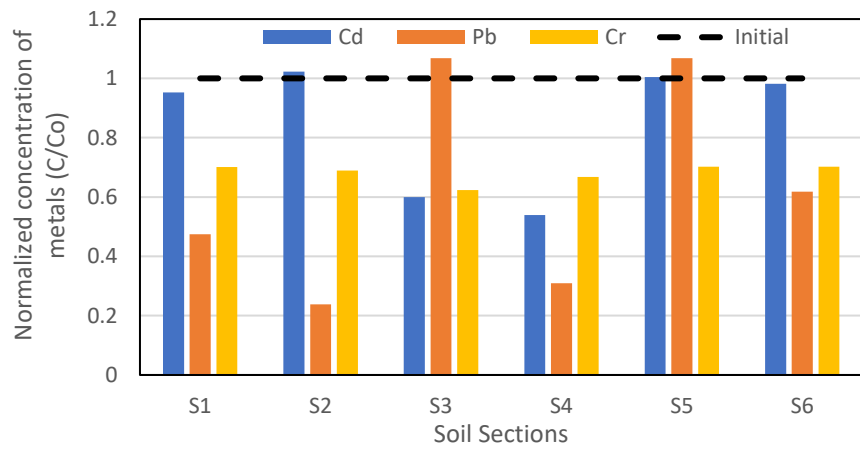
#### 4.5.5. Residual concentration of metals in soil

Fig. 4.27 indicates the concentration of metals that remained in different soil fractions after EKR. In experiment I, the concentration of metals decreased from S1 to S4 soil sections, accumulating at S1, close to the anode. Among the metals, Cr (VI) migration is higher as compared to Pb and Cd. The concentration of Pb and Cd was almost similar to the initial in soil sections S5 and S6. In experiment II, the reduced residual concentration of Cr (VI) against the initial indicates its effective removal. The accumulation of Cd in sections S1, S2, S5, and S6 confirms the migration of the ions towards the anode. The accumulation of Pb was observed in the S3 and S5 sections which are closer to the cathode, due to the formation of Pb-hydroxides in a high pH zone. In experiment III, the reduced residual concentration of metals indicated that maximum removal took place in this configuration. The distribution of Cr (VI) is almost similar throughout the soil column suggesting the uniform distribution of electric field. The residual concentration of Cd was found maximum in the S1, S3, S5, and S7 soil sections, which are closer to the anode. Pb, on the other hand, was accumulated in soil sections closer to the cathodes (S2, S6, S8). The results confirmed that the square configuration was better suited to overcome the formation of inactive zones within the soil cell.

(a)



(b)



(c)

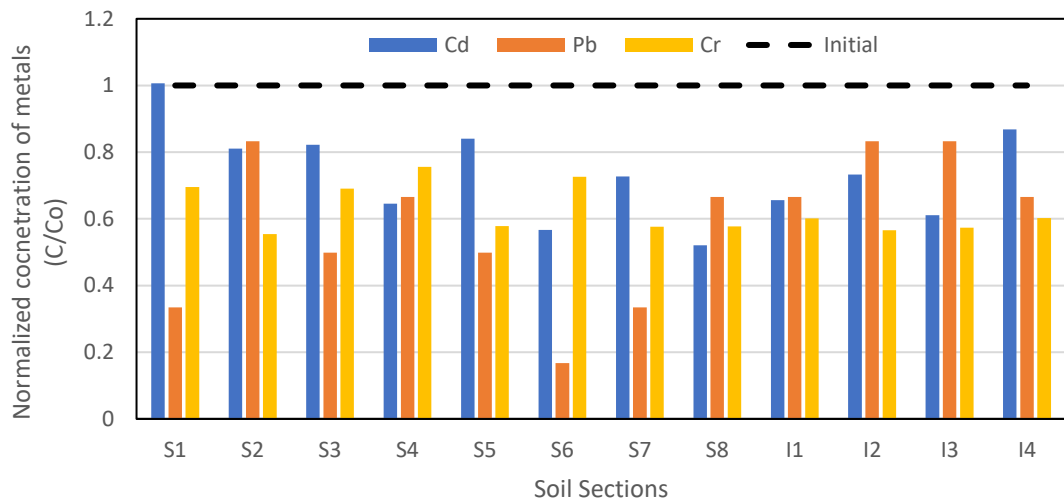


**Fig 4.27** Normalized residual concentration of metals in soil in (a) Linear, (b) Trigonal, and (c) Square assemblies

#### 4.6. Health Risk Assessment before and after EKR

The main goal of the removal of metals from soil is to reduce the toxicity in soil and to improve public health. In order to assess the EKR-induced toxicity reduction, a Human Health Risk Assessment (HHRA) was performed on the soil before and after the treatment. The exposure to the metals in soil was assessed taking into account, accidental ingestion, dermal contact, and inhalation. The daily dose through these exposure routes was calculated, using which the Hazard Index (HI) was determined (Table 4.24). Ideally,  $HI > 1$  is considered to pose no adverse non-carcinogenic effects. However, in this study, the non-carcinogenic effects based on HI have been categorized as follows:

**Table 4.24** Hazard Index categories given by USEPA.

HI range	Category
$HI < 0.1$	Negligible
$0 < HI < 1$	Low
$1 < HI < 4$	Medium
$HI > 4$	Very high risk

From Table 4.25, it was found that the HI index for untreated soils was under the very high risk to medium risk category for children, while only Cr (VI) and Pb soils were under the very high-risk category for adults. Upon treatment with EKR, the HI index reduced to the negligible and medium category for Cr (VI), Pb, and Cd-contaminated soils in adults and children respectively. The results indicate that Cr (VI) posed the most adverse non-carcinogenic health effects, followed by Pb when left untreated in soil. The non-carcinogenic effects can effectively be reduced through treatment with EKR.

**Table 4.25** Total daily intake (mg/kg/day) via ingestion, inhalation, and dermal contact pathways, and HI for Cr (VI), Pb, and Cd in adults and children

Metals	Conc. (mg/kg)	ADD <sub>ing</sub>		ADD <sub>inh</sub>		ADD <sub>der</sub>		HQ <sub>ing</sub>		HQ <sub>inh</sub>		HQ <sub>der</sub>		HI	
		Adult	Children	Adult	Children	Adult	Children	Adult	Children	Adult	Children	Adult	Children	Adult	Children
<b>Cd untreated</b>	246.45	0.0004	0.0025	0.0000	0.0001	0.0000	0.0000	0.4401	2.4645	0.0398	0.0691	0.0003	0.0002	0.4802	2.5339
<b>Cd treated</b>	171.875	0.0003	0.0017	0.0000	0.0000	0.0000	0.0000	0.3069	1.7188	0.0278	0.0482	0.0002	0.0002	0.3349	1.7671
<b>Pb untreated</b>	778.6	0.0014	0.0078	0.0001	0.0002	0.0000	0.0000	1.3904	7.7860	0.1257	0.2184	0.0010	0.0008	1.5171	8.0052
<b>Pb treated</b>	271.73	0.0005	0.0027	0.0000	0.0001	0.0000	0.0000	0.4852	2.7173	0.0439	0.0762	0.0003	0.0003	0.5295	2.7938
<b>Cr (VI) untreated</b>	2519.3	0.0045	0.0252	0.0004	0.0007	0.0000	0.0000	4.4988	25.1930	0.4069	0.7067	0.0031	0.0025	4.9088	25.9022
<b>Cr (VI) treated</b>	387.3	0.0007	0.0039	0.0001	0.0001	0.0000	0.0000	0.6916	3.8730	0.0625	0.1086	0.0005	0.0004	0.7546	3.9820

As the metals selected for this study are considered carcinogens, the assessment of Total Cancer Risk was also performed as per the U.S. EPA framework. The accepted level of cancer risk is generally one in a million ( $10^{-6}$ ). However, for this study, the acceptable cancer risk range of  $10^{-4}$  to  $10^{-6}$  was considered. TCR was calculated by multiplying the daily dose with the slope factor, given in Table 4.26. From the results, it was found that the maximum cancer risk was worst in Cr (VI)-contaminated soil without remediation, followed by cadmium. The children were at higher risk as compared to the adults, due to more exposure. However, the EK remediation of 10 hours showed a decrease in LCR from  $4.23 \times 10^{-2}$  to  $6.5 \times 10^{-3}$ , and from  $1.37 \times 10^{-3}$  to  $9.5 \times 10^{-4}$  in cadmium-contaminated soils. EKR was successful in bringing down the TCR due to cadmium within the acceptable range, while the TCR due to chromium decreased but not in line with the permissible limits, which could be due to relatively higher initial concentrations of chromium in soil. In the case of Pb-contaminated soil, the exposure through dermal contact was not established, thus the TCR due to oral ingestion and inhalation was in line with the acceptable range, before and after the treatment.

**Table 4.26** Carcinogenic risks of adults and children under different exposure pathways

	<b>CR<sub>ing</sub></b>		<b>CR<sub>inh</sub></b>		<b>CR<sub>der</sub></b>		<b>TCR</b>	
	<b>Adult</b>	<b>Children</b>	<b>Adult</b>	<b>Children</b>	<b>Adult</b>	<b>Children</b>	<b>Adult</b>	<b>Children</b>
<b>Cd untreated</b>	1.67E-04	9.37E-04	2.51E-04	4.36E-04	1.17E-09	9.37E-10	4.18E-04	1.37E-03
<b>Cd treated</b>	1.17E-04	6.53E-04	1.75E-04	3.04E-04	8.16E-10	6.53E-10	2.92E-04	9.57E-04
<b>Pb untreated</b>	1.18E-05	6.62E-05	5.28E-06	9.17E-06	-	-	1.71E-05	7.54E-05
<b>Pb treated</b>	4.12E-06	2.31E-05	1.84E-06	3.20E-06	-	-	5.97E-06	2.63E-05
<b>Cr (VI) untreated</b>	2.25E-03	1.26E-02	1.71E-02	2.97E-02	6.30E-07	5.04E-07	1.93E-02	4.23E-02
<b>Cr (VI) treated</b>	3.46E-04	1.94E-03	2.63E-03	4.56E-03	9.68E-08	7.75E-08	2.97E-03	6.50E-03

#### 4.1. Feasibility analysis of EKR and decision matrix for optimization

From the experimentations performed to test the efficiency of EKR, varied results were obtained for different metals. Therefore, to propose a standard EKR model that applies to a wide range of pollutants, it is important to sum up the various aspects of the EKR technique comprehensively. For this purpose, a weighted decision matrix (WDM) was developed to optimize EKR. To develop a WDM, the first step is to select the important criteria that are to be achieved based on design requirements. For this study, five criteria were selected: removal efficiency, cost of treatment, health risk reduction, environmental implications, and acceptability in terms of social wellness. The second step is to assign the criteria weights based on their relative importance, using the Eqn. 4.15, where n is the number of evaluations.

$$\sum_{i=1}^n W = 1 \dots\dots\dots(4.15)$$

In this study, the criteria weights were assigned considering two important aspects: technological efficiency and environmental sustainability. The score indicators were set on the basis of the results obtained from this study, as given in Table 4.27 for each criterion. The rating for each operating parameter was obtained by multiplying the score and the weight factor. Finally, each parameter was ranked according to the weighted score obtained.

**Table 4.27** Score indicator set for each criterion selected on the basis of the experiments

Score indicators	1	2	3	4	5
<b>Removal (%)</b>	<20	<40	<60	<70	>70
<b>Cost (US\$/g)</b>	>40	<40	<30	<20	<10
<b>Risk Reduction</b>	Very high	High	Medium	Low	Negligible
<b>Env. implications</b>	Very high	High	Moderate	Low	Very low
<b>Acceptability</b>	Not acceptable	Low	Moderate	High	Very High

**Table 4.28** A Weighted Decision Matrix (WDM) designed to select the optimized conditions for EKR

Design parameters		Criteria										Weighted score	Rank
		Removal efficiency		Treatment cost		Health risk reduction		Environmental implications		Acceptability			
Criteria weights →		0.15		0.15		0.25		0.35		0.1			
		Score	Rating	Score	Rating	Score	Rating	Score	Rating	Score	Rating		
<b>Applied voltage (V/cm)</b>	1	1	0.15	2	0.3	1	0.25	4	1.4	2	0.2	2.3	9
	2.5	4	0.6	4	0.6	4	1	3	1.05	3.5	0.35	3.6	3
<b>Electrolyte composition</b>	Distilled Water	2	0.3	3	0.45	1	0.25	5	1.75	4	0.4	3.15	8
	EDTA (0.1 M)	5	0.75	5	0.75	4.5	1.125	4	1.4	3	0.3	4.325	1
	EDTA (0.2 M)	4	0.6	4	0.6	3	0.75	3	1.05	2	0.2	3.2	7
<b>Electrode configuration</b>	2 electrodes	3	0.45	4	0.6	4	1	3.5	1.225	3	0.3	3.575	4
	3 electrodes (linear)	3.5	0.525	3	0.45	3	0.75	4	1.4	3.5	0.35	3.475	6
	3 electrodes (trigonal)	4	0.6	3	0.45	3	0.75	4	1.4	3.5	0.35	3.55	5
	5 electrodes (square)	5	0.75	2	0.3	4	1	4	1.4	3	0.3	3.75	2



The WDM for the selection of optimized conditions for EKR is shown in Table 4.28. On the basis of the ranking assigned to each operating condition, 0.1 M EDTA as an electrolyte solution was found to be the best enhancement technique, followed by the square configuration of electrodes, which fulfills both engineering, as well as environmental aspects of the EKR for practical applications. This comprehensive matrix provides quantitative knowledge based on the experiments performed and from the discussion with experts in this field. Moreover, the matrix incorporates social acceptance of the technique by the public which is an essential component for environmental remediation projects. The matrix is expected to be helpful in decision-making pertaining to the selection of the most suitable parameters for EKR or for addressing particular criteria.



## CHAPTER 5

# CONCLUSION, FUTURE SCOPE, AND SOCIAL IMPACT

### 5.1. Conclusion

Based on the outcomes of this study, the following conclusions are made.

- I. Electrokinetic Remediation is a potential and effective method for the removal of metals from highly contaminated soils. The application of high-voltage (2.5 V/cm) against the lower voltage (1.5 V/cm, as stated in earlier literature) can be employed for EKR without any significant effect on soil health. Periodic voltage application (Day-on, Night-off) yields better removal and saves energy which is an essential factor to take into account for practical applications of EKR in respect of cost and ease of operation.
- II. Electrolyte amendments with EDTA significantly improved the removal rates by solubilizing the metals. The rate of removal only slightly increased when the concentration of EDTA increased from 0.1 M to 0.2 M, but the extra input of chemicals added to the cost of the treatment. So, the optimum conditions were found to be the combination of high voltage application and 0.1 M EDTA amendment. The application of surfactant as an electrolyte does not improve the efficiency of soil EKR toward the removal of heavy metals. It rather imparts toxicity and mobilizes other pollutants.
- III. Variations of electrode material, and electrolyte composition can significantly improve the removal of metals in soil EKR, and a suitable combination in EKR can help treat the contaminated soils effectively. Thus, the optimization of regulating parameters is necessary to improve the efficiency of the treatment and to bring the cost of treatment down to a significant level.

- IV. EKR proves suitable for the treatment of soils contaminated with single-metal as well as a multi-metal matrix with almost equal efficiency and thus this technique can be used to remediate many different polluted sites such as mine tailings, areas around landfills, industrial sludge, etc.
- V. EKR, an in-situ technique, can significantly bring the secondary emissions and costs down, which can result in an environment-friendly technology with lower footprints. Further, it brings down the toxicity of metals in soil thereby adding to improved soil health and indirectly improved plant and animal health. It also brings down the risk to human health substantially.
- VI. Considering the efficiency and cost-benefit analysis, it is observed that EKR is suitable for treating the metal-contaminated soil, along with the removal of other organic contaminants, thereby bringing the environmental toxicity down in the soil. Further, optimization of EKR by RSM can significantly bring the cost of treatment and duration of treatment down, thereby making EKR potential technology to handle larger volumes of contaminated soils.

## **5.2. Future Scope and Recommendations**

Based on the outcomes of the present study, the following recommendations are suggested.

- I. EKR aids in improving the mobility of metals and, thus can be coupled with conventional technologies such as Phytoremediation, to further enhance the uptake of metals and ultimately the removal.
- II. Increasing voltage can result in higher energy consumption, and subsequently higher costs. Renewable energy sources as alternatives such as solar panels as a source of power supply are recommended to make EKR more sustainable.

- III. The electrolytes collected during EKR can be treated to re-circulate the enhancing agents, and recover metals. It would not only reduce wastewater generation but will also aid in resource recovery.
- IV. In the present study, two cycles were employed which yielded significant removal. It is recommended that the number of operating cycles be increased to achieve a better removal rate in a short period.
- V. Although there are some guidelines on the permissible limits of certain pollutants in soil. However, there are no standards laid in India for the identification of soil pollution and acceptable levels in different soil conditions. Hence, national standards and guidelines for soil quality in India should be developed.

### **5.3. Social Impact of the study**

Remediation of metal-contaminated soils through EKR have many positive impacts in terms of environmental and economic benefits, which contribute towards overall social wellness. Some of the impacts the present study can make are:

#### **5.3.1. Environmental Impacts**

- EKR is an *in-situ* treatment method that can be employed to remediate the contaminated site without disturbing the physical landscape or increasing the cost of transportation of contaminated soil. This also prevents the introduction of pollutants into the air and exposure of the community to the contaminated soil that might arise during excavation and transportation.
- The removal of metals from soil using EKR can reduce eco-toxicity in plants, animals, and humans, thereby reducing the human health risks associated with direct exposure to polluted soil.

- EKR of contaminated sites will improve the soil quality of the otherwise considered wasteland. Improved soil quality can help restore the degraded land, and also prevent leaching and cross-contamination of groundwater.

### **5.3.2. Economic impacts**

- Remediated soil with improved soil quality can improve the quality of crops in terms of nutrition and also crop yield, helping achieve food security with increased production.
- Soil with better quality improves biodiversity in terms of the diversity of crops, for example, medicinal plants and spices, which are otherwise sensitive to environmental stresses, like metal contamination.
- Soil remediation through EKR can generate job opportunities in terms of design, installation, and maintenance. It can also provide entrepreneurship opportunities to farmers by boosting agro-production over the reclaimed land.

### **5.3.3. Social Impacts**

- Along with increased production, improved food quality would indirectly lead to improved water quality, both surface and groundwater, promoting good health and well-being.
- Restoration of polluted sites, such as mining regions, or around landfills through EKR can help provide environmental equality to poor and marginal societies in terms of access to clean water and land and can improve the overall standard of living.
- For any remediation technique to be practically viable, its social acceptance and implications on public health are of utmost importance. From this study, it can be concluded that the EKR method is a promising technique that can

be upscaled for field applications, considering not only the engineering aspects but also its ability to cause minimum disruption to soil health, reduce human health risks, and improve environmental quality at low costs and treatment durations.

## REFERENCES

- Aboughalma, H., Bi, R., & Schlaak, M. (2008). Electrokinetic enhancement on phytoremediation in Zn, Pb, Cu and Cd contaminated soil using potato plants. *Journal of Environmental Science and Health, Part A*, 43(8), 926–933. <https://doi.org/10.1080/10934520801974459>
- Acar, Y. B., & Alshawabkeh, A. N. (2002). *Principles of electrokinetic remediation* (world) [Research-article]. ACS Publications; American Chemical Society. <https://doi.org/10.1021/es00049a002>
- Acar, Y. B., Alshawabkeh, A. N., & Gale, R. J. (1993). Fundamentals of extracting species from soils by electrokinetics. *Waste Management*, 13(2), 141–151. [https://doi.org/10.1016/0956-053X\(93\)90006-I](https://doi.org/10.1016/0956-053X(93)90006-I)
- Acar, Y. B., Gale, R. J., Alshawabkeh, A. N., Marks, R. E., Puppala, S., Bricka, M., & Parker, R. (1995). Electrokinetic remediation: Basics and technology status. *Journal of Hazardous Materials*, 40(2), 117–137. [https://doi.org/10.1016/0304-3894\(94\)00066-P](https://doi.org/10.1016/0304-3894(94)00066-P)
- Adimalla, N., Chen, J., & Qian, H. (2020). Spatial characteristics of heavy metal contamination and potential human health risk assessment of urban soils: A case study from an urban region of South India. *Ecotoxicology and Environmental Safety*, 194, 110406.
- Akansha, J., Thakur, S., Chaithanya, M. S., Gupta, B. S., Das, S., Das, B., Rajasekar, N., & Priya, K. (2024). Technological and economic analysis of electrokinetic remediation of



contaminated soil: A global perspective and its application in Indian scenario. *Heliyon*, *10*(2). <https://doi.org/10.1016/j.heliyon.2024.e24293>

Al-Hamdan, A. Z., & Reddy, K. R. (2006). Geochemical reconnaissance of heavy metals in kaolin after electrokinetic remediation. *Journal of Environmental Science and Health - Part A Toxic/Hazardous Substances and Environmental Engineering*, *41*(1), 17–33. <https://doi.org/10.1080/10934520500297475>

Al-Hamdan, A. Z., & Reddy, K. R. (2008). Transient behavior of heavy metals in soils during electrokinetic remediation. *Chemosphere*, *71*(5), 860–871. <https://doi.org/10.1016/j.chemosphere.2007.11.028>

Alshawabkeh, A. N., Gale, R. J., Ozsu-Acar, E., & Bricka, R. M. (1999). Optimization of 2-D Electrode Configuration for Electrokinetic Remediation. *Journal of Soil Contamination*, *8*(6), 617–635. <https://doi.org/10.1080/10588339991339504>

Amrate, S., Akretche, D. E., Innocent, C., & Seta, P. (2006). Use of cation-exchange membranes for simultaneous recovery of lead and EDTA during electrokinetic extraction. *Desalination*, *193*(1), 405–410. <https://doi.org/10.1016/j.desal.2005.06.071>

Asadollahfardi, G., Sarmadi, M. S., Rezaee, M., Khodadadi-Darban, A., Yazdani, M., & Paz-Garcia, J. M. (2021). Comparison of different extracting agents for the recovery of Pb and Zn through electrokinetic remediation of mine tailings. *Journal of Environmental Management*, *279*, 111728. <https://doi.org/10.1016/j.jenvman.2020.111728>

Ayyanar, A., & Thatikonda, S. (2021). Enhanced electrokinetic remediation (EKR) for heavy metal-contaminated sediments focusing on treatment of generated effluents from

EKR and recovery of EDTA. *Water Environment Research*, 93(1), 136–147.  
<https://doi.org/10.1002/wer.1369>

Ballesteros, S., Rincón, J. Ma., Rincón-Mora, B., & Jordán, M. M. (2017). Vitrification of urban soil contamination by hexavalent chromium. *Journal of Geochemical Exploration*, 174, 132–139. <https://doi.org/10.1016/j.gexplo.2016.07.011>

Banerjee, S., Ghosh, S., Jha, S., Kumar, S., Mondal, G., Sarkar, D., Datta, R., Mukherjee, A., & Bhattacharyya, P. (2023). Assessing pollution and health risks from chromite mine tailings contaminated soils in India by employing synergistic statistical approaches. *Science of The Total Environment*, 880, 163228. <https://doi.org/10.1016/j.scitotenv.2023.163228>

Benamar, A., Ammami, M. T., Song, Y., & Portet-Koltalo, F. (2020). Scale-up of electrokinetic process for dredged sediments remediation. *Electrochimica Acta*, 352, 136488. <https://doi.org/10.1016/j.electacta.2020.136488>

Benamar, A., & Baraud, F. (2011). Electrokinetic remediation of dredged sediments from Le Havre Harbour. *European Journal of Environmental and Civil Engineering*, 15(2), 215–228. <https://doi.org/10.1080/19648189.2011.9693319>

Benamar, A., Tian, Y., Portet-Koltalo, F., Ammami, M. T., Giusti-Petrucciani, N., Song, Y., & Boulangé-Lecomte, C. (2019). Enhanced electrokinetic remediation of multi-contaminated dredged sediments and induced effect on their toxicity. *Chemosphere*, 228, 744–755. <https://doi.org/10.1016/j.chemosphere.2019.04.063>

Benvenuti, M., Mascaro, I., Corsini, F., Lattanzi, P., Parrini, P., & Tanelli, G. (1997). Mine waste dumps and heavy metal pollution in abandoned mining district of Boccheggiano

(Southern Tuscany, Italy). *Environmental Geology*, 30(3), 238–243.  
<https://doi.org/10.1007/s002540050152>

Bi, R., Schlaak, M., Siefert, E., Lord, R., & Connolly, H. (2011). Influence of electrical fields (AC and DC) on phytoremediation of metal polluted soils with rapeseed (*Brassica napus*) and tobacco (*Nicotiana tabacum*). *Chemosphere*, 83(3), 318–326.  
<https://doi.org/10.1016/j.chemosphere.2010.12.052>

Bolan, N., Kunhikrishnan, A., Thangarajan, R., Kumpiene, J., Park, J., Makino, T., Kirkham, M. B., & Scheckel, K. (2014). Remediation of heavy metal(loid)s contaminated soils – To mobilize or to immobilize? *Journal of Hazardous Materials*, 266, 141–166.  
<https://doi.org/10.1016/j.jhazmat.2013.12.018>

Bunditboondee, C., Lohwacharin, J., Khan, E., & Laohasurayotin, K. (2023). Performance of electrokinetic remediation system for mercury contaminated marine sediment: Roles of electrode spacing and electrode configuration. *Marine Pollution Bulletin*, 194, 115256. <https://doi.org/10.1016/j.marpolbul.2023.115256>

Cai, Z., Sun, Y., Deng, Y., Zheng, X., Sun, S., Romantschuk, M., & Sinkkonen, A. (2021). In situ electrokinetic (EK) remediation of the total and plant available cadmium (Cd) in paddy agricultural soil using low voltage gradients at pilot and full scales. *Science of The Total Environment*, 785, 147277. <https://doi.org/10.1016/j.scitotenv.2021.147277>

Cai, Z., Sun, Y., Deng, Y., Zheng, X., Sun, S., Sinkkonen, A., & Romantschuk, M. (2022). Enhanced Electrokinetic Remediation of Cadmium (Cd)-Contaminated Soil with Interval Power Breaking. *International Journal of Environmental Research*, 16(3), 31.  
<https://doi.org/10.1007/s41742-022-00409-6>

Cameselle, C., Chirakkara, R. A., & Reddy, K. R. (2013). Electrokinetic-enhanced phytoremediation of soils: Status and opportunities. *Chemosphere*, *93*(4), 626–636. <https://doi.org/10.1016/j.chemosphere.2013.06.029>

Cameselle, C., & Gouveia, S. (2020). Removal of Multiple Metallic Species from Sludge by Electromigration. *Journal of Hazardous, Toxic, and Radioactive Waste*, *24*(1), 04019030. [https://doi.org/10.1061/\(asce\)hz.2153-5515.0000470](https://doi.org/10.1061/(asce)hz.2153-5515.0000470)

Cameselle, C., Gouveia, S., & Cabo, A. (2021a). Enhanced Electrokinetic Remediation for the Removal of Heavy Metals from Contaminated Soils. *Applied Sciences*, *11*(4), Article 4. <https://doi.org/10.3390/app11041799>

Cameselle, C., Gouveia, S., & Cabo, A. (2021b). Enhanced Electrokinetic Remediation for the Removal of Heavy Metals from Contaminated Soils. In *Applied Sciences* (Vol. 11, Issue 4). <https://doi.org/10.3390/app11041799>

Cameselle, C., & Pena, A. (2016). Enhanced electromigration and electro-osmosis for the remediation of an agricultural soil contaminated with multiple heavy metals. *Process Safety and Environmental Protection*, *104*, 209–217. <https://doi.org/10.1016/j.psep.2016.09.002>

Cameselle, C., & Reddy, K. R. (2013). Effects of Periodic Electric Potential and Electrolyte Recirculation on Electrochemical Remediation of Contaminant Mixtures in Clayey Soils. *Water, Air, & Soil Pollution*, *224*(8), 1636. <https://doi.org/10.1007/s11270-013-1636-8>

Cang, L., Wang, Q., Zhou, D., & Xu, H. (2011). Effects of electrokinetic-assisted phytoremediation of a multiple-metal contaminated soil on soil metal bioavailability and

uptake by Indian mustard. *Separation and Purification Technology*, 79(2), 246–253.

<https://doi.org/10.1016/j.seppur.2011.02.016>

Chandra, G. V., Golla, S. Y., & Ghosh, P. K. (2024). Review of soil environment quality in India near coal mining regions: Current and future predictions. *Environmental Geochemistry and Health*, 46(6), 194. <https://doi.org/10.1007/s10653-024-01968-7>

Chen, Z., Zhu, B.-K., Jia, W.-F., Liang, J.-H., & Sun, G.-X. (2015). Can electrokinetic removal of metals from contaminated paddy soils be powered by microbial fuel cells? *Environmental Technology & Innovation*, 3, 63–67.

<https://doi.org/10.1016/j.eti.2015.02.003>

Chirakkara, R. A., Reddy, K. R., & Cameselle, C. (2015). Electrokinetic Amendment in Phytoremediation of Mixed Contaminated Soil. *Electrochimica Acta*, 181, 179–191.

<https://doi.org/10.1016/j.electacta.2015.01.025>

Chung, H. I. (2009). Field Applications on Electrokinetic Reactive Pile Technology for Removal of Cu from In-situ and Excavated Soils. *Separation Science and Technology*.

<https://doi.org/10.1080/01496390902983687>

da S Trentin, A. W., Reddy, K. R., Kumar, G., Chetri, J. K., & Thomé, A. (2019). Quantitative Assessment of Life Cycle Sustainability (QUALICS): Framework and its application to assess electrokinetic remediation. *Chemosphere*, 230, 92–106.

<https://doi.org/10.1016/j.chemosphere.2019.04.200>

Deepika, & Haritash, A. K. (2023). Phytoremediation potential of ornamental plants for heavy metal removal from contaminated soil: A critical review. *Horticulture, Environment, and Biotechnology*. <https://doi.org/10.1007/s13580-023-00518-x>

Di Palma, L., Ferrantelli, P., Merli, C., & Biancifiori, F. (2003). Recovery of EDTA and metal precipitation from soil flushing solutions. *Journal of Hazardous Materials*, *103*(1), 153–168. [https://doi.org/10.1016/S0304-3894\(03\)00268-1](https://doi.org/10.1016/S0304-3894(03)00268-1)

Duduković, N., Slijepčević, N., Tomašević Pilipović, D., Kerkez, Đ., Leovac Maćerak, A., Dubovina, M., & Krčmar, D. (2023). Integrated application of green zero-valent iron and electrokinetic remediation of metal-polluted sediment. *Environmental Geochemistry and Health*, *45*(8), 5943–5960. <https://doi.org/10.1007/s10653-023-01609-5>

FAO, U. (2021). *Global Assessment of Soil Pollution: Report*. FAO and UNEP. <https://doi.org/10.4060/cb4894en>

Figuroa, A., Cameselle, C., Gouveia, S., & Hansen, H. K. (2016). Electrokinetic treatment of an agricultural soil contaminated with heavy metals. *Journal of Environmental Science and Health, Part A*, *51*(9), 691–700. <https://doi.org/10.1080/10934529.2016.1170425>

Fu, R., Wen, D., Xia, X., Zhang, W., & Gu, Y. (2017). Electrokinetic remediation of chromium (Cr)-contaminated soil with citric acid (CA) and polyaspartic acid (PASP) as electrolytes. *Chemical Engineering Journal*, *316*, 601–608. <https://doi.org/10.1016/j.cej.2017.01.092>

Gao, M., Zeng, F., Tang, F., Wang, K., Xu, X., & Tian, G. (2020). An increasing Cr recovery from soil with catholyte-enhanced electrokinetic remediation: Effects on voltage

redistribution throughout soil sections. *Separation and Purification Technology*, 253, 117553. <https://doi.org/10.1016/j.seppur.2020.117553>

Ge, X., Song, X., Xie, J., Huang, W., Yuhui, W., Xu, Z., Wang, Y., Hou, X., & Cao, X. (2022). Comparison of the influence of EDTA, nitrilotriacetic acid, diethylenetriamine pentaacetic acid, chitosan, fulvic acid and pine needle extract on the removal of multiple heavy metal by electrokinetic remediation. *International Journal of Electrochemical Science*, 17(10), 221012. <https://doi.org/10.20964/2022.10.08>

Genchi, G., Sinicropi, M. S., Lauria, G., Carocci, A., & Catalano, A. (2020). The Effects of Cadmium Toxicity. *International Journal of Environmental Research and Public Health*, 17(11), Article 11. <https://doi.org/10.3390/ijerph17113782>

Ghobadi, R., Altaee, A., Zhou, J. L., Karbassiyazdi, E., & Ganbat, N. (2021). Effective remediation of heavy metals in contaminated soil by electrokinetic technology incorporating reactive filter media. *Science of The Total Environment*, 794, 148668. <https://doi.org/10.1016/j.scitotenv.2021.148668>

Giannis, A., Gidarakos, E., & Skouta, A. (2008). Transport of cadmium and assessment of phytotoxicity after electrokinetic remediation. *Journal of Environmental Management*, 86(3), 535–544. <https://doi.org/10.1016/j.jenvman.2006.12.003>

Gu, Y., Yeung, A. T., & Li, H. (2018). Enhanced electrokinetic remediation of cadmium-contaminated natural clay using organophosphonates in comparison with EDTA. *Chinese Journal of Chemical Engineering*, 26(5), 1152–1159. <https://doi.org/10.1016/j.cjche.2017.10.012>

Habibul, N., Hu, Y., & Sheng, G.-P. (2016). Microbial fuel cell driving electrokinetic remediation of toxic metal contaminated soils. *Journal of Hazardous Materials*, 318, 9–14. <https://doi.org/10.1016/j.jhazmat.2016.06.041>

Han, J.-G., Hong, K.-K., Kim, Y.-W., & Lee, J.-Y. (2010). Enhanced electrokinetic (E/K) remediation on copper contaminated soil by CFW (carbonized foods waste). *Journal of Hazardous Materials*, 177(1), 530–538. <https://doi.org/10.1016/j.jhazmat.2009.12.065>

Hanfi, M. Y., Mostafa, M. Y. A., & Zhukovsky, M. V. (2019). Heavy metal contamination in urban surface sediments: Sources, distribution, contamination control, and remediation. *Environmental Monitoring and Assessment*, 192(1), 32. <https://doi.org/10.1007/s10661-019-7947-5>

Hassan, I., Mohamedelhassan, E., & Yanful, E. K. (2015). Solar powered electrokinetic remediation of Cu polluted soil using a novel anode configuration. *Electrochimica Acta*, 181, 58–67. <https://doi.org/10.1016/j.electacta.2015.02.216>

He, J., He, C., Chen, X., Liang, X., Huang, T., Yang, X., & Shang, H. (2018). Comparative study of remediation of Cr(VI)-contaminated soil using electrokinetics combined with bioremediation. *Environmental Science and Pollution Research*, 25(18), 17682–17689. <https://doi.org/10.1007/s11356-018-1741-8>

He, X., Cui, G., Zhang, Q., Wang, Z., Tang, T., & Liu, Y. (2021). Application of sulfide-modified nanoscale zerovalent iron electrodes for electrokinetic remediation of chromium-contaminated soil in a three-dimensional electrode system. *Journal of Environmental Chemical Engineering*, 9(6), 106791. <https://doi.org/10.1016/j.jece.2021.106791>



Huang, T., Liu, L., Zhou, L., & Zhang, S. (2018). Electrokinetic removal of chromium from chromite ore-processing residue using graphite particle-supported nanoscale zero-valent iron as the three-dimensional electrode. *Chemical Engineering Journal*, *350*, 1022–1034. <https://doi.org/10.1016/j.cej.2018.06.048>

Hui, L. I. U., Long, C., Xiuzhen, H. A. O., Yuxia, W., & Dongmei, Z. (2016). Field-scale electrokinetic remediation of heavy metal contaminated sites. *Chinese Journal of Environmental Engineering*, *10*(7), 3877–3883.

Iannelli, R., Masi, M., Ceccarini, A., Ostuni, M. B., Lageman, R., Muntoni, A., Spiga, D., Polettini, A., Marini, A., & Pomi, R. (2015). Electrokinetic remediation of metal-polluted marine sediments: Experimental investigation for plant design. *Electrochimica Acta*, *181*, 146–159. <https://doi.org/10.1016/j.electacta.2015.04.093>

Jeon, E.-K., Ryu, S.-R., & Baek, K. (2015). Application of solar-cells in the electrokinetic remediation of As-contaminated soil. *Electrochimica Acta*, *181*, 160–166. <https://doi.org/10.1016/j.electacta.2015.03.065>

Kadhun, S. T., Alkindi, G. Y., & Albayati, T. M. (2022). Remediation of phenolic wastewater implementing nano zerovalent iron as a granular third electrode in an electrochemical reactor. *International Journal of Environmental Science and Technology*, *19*(3), 1383–1392. <https://doi.org/10.1007/s13762-021-03205-5>

Karaca, O., Cameselle, C., & Bozcu, M. (2019). Opportunities of electrokinetics for the remediation of mining sites in Biga peninsula, Turkey. *Chemosphere*, *227*, 606–613. <https://doi.org/10.1016/j.chemosphere.2019.04.059>

Karaca, O., Cameselle, C., & Reddy, K. R. (2017). Acid pond sediment and mine tailings contaminated with metals: Physicochemical characterization and electrokinetic remediation. *Environmental Earth Sciences*, 76(12), 408. <https://doi.org/10.1007/s12665-017-6736-0>

Karachaliou, T., Protonotarios, V., Kaliampakos, D., & Menegaki, M. (2016). Using Risk Assessment and Management Approaches to Develop Cost-Effective and Sustainable Mine Waste Management Strategies. *Recycling*, 1(3), Article 3. <https://doi.org/10.3390/recycling1030328>

Kasemodel, M. C., Sakamoto, I. K., Varesche, M. B. A., & Rodrigues, V. G. S. (2019). Potentially toxic metal contamination and microbial community analysis in an abandoned Pb and Zn mining waste deposit. *Science of The Total Environment*, 675, 367–379. <https://doi.org/10.1016/j.scitotenv.2019.04.223>

Khalid, S., Shahid, M., Niazi, N. K., Murtaza, B., Bibi, I., & Dumat, C. (2017). A comparison of technologies for remediation of heavy metal contaminated soils. *Journal of Geochemical Exploration*, 182, 247–268. <https://doi.org/10.1016/j.gexplo.2016.11.021>

Kim, S.-O., Jeong, J. Y., Lee, W.-C., Yun, S.-T., & Jo, H. Y. (2021). Electrokinetic remediation of heavy metal-contaminated soils: Performance comparison between one- and two-dimensional electrode configurations. *Journal of Soils and Sediments*, 21(8), 2755–2769. <https://doi.org/10.1007/s11368-020-02803-z>

Kim, W.-S., Jeon, E.-K., Jung, J.-M., Jung, H.-B., Ko, S.-H., Seo, C.-I., & Baek, K. (2014). Field application of electrokinetic remediation for multi-metal contaminated paddy soil

using two-dimensional electrode configuration. *Environmental Science and Pollution Research*, 21, 4482–4491.

Kim, W.-S., Kim, S.-O., & Kim, K.-W. (2005). Enhanced electrokinetic extraction of heavy metals from soils assisted by ion exchange membranes. *Journal of Hazardous Materials*, 118(1), 93–102. <https://doi.org/10.1016/j.jhazmat.2004.10.001>

Krishna, A. K., & Govil, P. K. (2007). Soil Contamination Due to Heavy Metals from an Industrial Area of Surat, Gujarat, Western India. *Environmental Monitoring and Assessment*, 124(1), 263–275. <https://doi.org/10.1007/s10661-006-9224-7>

Kumar, A., & Maiti, S. K. (2015). Assessment of potentially toxic heavy metal contamination in agricultural fields, sediment, and water from an abandoned chromite-asbestos mine waste of Roro hill, Chaibasa, India. *Environmental Earth Sciences*, 74(3), 2617–2633. <https://doi.org/10.1007/s12665-015-4282-1>

Kumar, V., Sharma, A., Kaur, P., Singh Sidhu, G. P., Bali, A. S., Bhardwaj, R., Thukral, A. K., & Cerda, A. (2019). Pollution assessment of heavy metals in soils of India and ecological risk assessment: A state-of-the-art. *Chemosphere*, 216, 449–462. <https://doi.org/10.1016/j.chemosphere.2018.10.066>

Lee, S., Yun, J.-M., Lee, J.-Y., Hong, G., Kim, J.-S., Kim, D., & Han, J.-G. (2021). The Remediation Characteristics of Heavy Metals (Copper and Lead) on Applying Recycled Food Waste Ash and Electrokinetic Remediation Techniques. *Applied Sciences*, 11(16), Article 16. <https://doi.org/10.3390/app11167437>

Li, G., Guo, S., Li, S., Zhang, L., & Wang, S. (2012). Comparison of approaching and fixed anodes for avoiding the ‘focusing’ effect during electrokinetic remediation of chromium-contaminated soil. *Chemical Engineering Journal*, 203, 231–238. <https://doi.org/10.1016/j.cej.2012.07.008>

Liu, L., Li, W., Song, W., & Guo, M. (2018). Remediation techniques for heavy metal-contaminated soils: Principles and applicability. *Science of The Total Environment*, 633, 206–219. <https://doi.org/10.1016/j.scitotenv.2018.03.161>

Lu, L., Xie, Y., Yang, Z., & Chen, B. (2023). Sustainable decontamination of heavy metal in wastewater and soil with novel rectangular wave asymmetrical alternative current electrochemistry. *Journal of Hazardous Materials*, 442, 130021. <https://doi.org/10.1016/j.jhazmat.2022.130021>

Luo, J., Cai, L., Qi, S., Wu, J., & Gu, X. W. S. (2018). The interactive effects between chelator and electric fields on the leaching risk of metals and the phytoremediation efficiency of *Eucalyptus globulus*. *Journal of Cleaner Production*, 202, 830–837. <https://doi.org/10.1016/j.jclepro.2018.08.130>

Luo, J., Yang, D., Qi, S., Wu, J., & Gu, X. S. (2018). Using solar cell to phytoremediate field-scale metal polluted soil assisted by electric field. *Ecotoxicology and Environmental Safety*, 165, 404–410. <https://doi.org/10.1016/j.ecoenv.2018.09.031>

Ma, C., Li, J., Xia, W., Ding, Y., Zhang, L., & Xu, Y. (2022). Effect of additives on the remediation of arsenic and chromium co-contaminated soil by an electrokinetic-permeable reactive barrier. *Environmental Science and Pollution Research*, 29(8), 11966–11975. <https://doi.org/10.1007/s11356-021-16357-1>

Mao, X., Han, F. X., Shao, X., Guo, K., McComb, J., Arslan, Z., & Zhang, Z. (2016). Electro-kinetic remediation coupled with phytoremediation to remove lead, arsenic and cesium from contaminated paddy soil. *Ecotoxicology and Environmental Safety*, *125*, 16–24. <https://doi.org/10.1016/j.ecoenv.2015.11.021>

Mohamed Johar, S., & Embong, Z. (2015). The optimisation of electrokinetic remediation for heavy metals and radioactivity contamination on Holyrood-Lunas soil (acrisol species) in Sri Gading Industrial Area, Batu Pahat, Johor, Malaysia. *Radiation Protection Dosimetry*, *167*(1–3), 160–164. <https://doi.org/10.1093/rpd/ncv236>

Moturi, M. C. Z., Rawat, M., & Subramanian, V. (2004). Distribution and Fractionation of Heavy Metals in Solid Waste from Selected Sites in the Industrial Belt of Delhi, India. *Environmental Monitoring and Assessment*, *95*(1), 183–199. <https://doi.org/10.1023/B:EMAS.0000029900.86810.85>

Mulligan, C. N., Yong, R. N., & Gibbs, B. F. (2001). Remediation technologies for metal-contaminated soils and groundwater: An evaluation. *Engineering Geology*, *60*(1), 193–207. [https://doi.org/10.1016/S0013-7952\(00\)00101-0](https://doi.org/10.1016/S0013-7952(00)00101-0)

Naz, A., Chowdhury, A., Mishra, B. K., & Karthikeyan, K. (2018). Distribution of heavy metals and associated human health risk in mine, agricultural and roadside soils at the largest chromite mine of India. *Environmental Geochemistry and Health*, *40*(5), 2155–2175. <https://doi.org/10.1007/s10653-018-0090-3>

Ng, Y.-S., Sen Gupta, B., & Hashim, M. A. (2016). Remediation of Pb/Cr co-contaminated soil using electrokinetic process and approaching electrode technique. *Environmental*

*Science and Pollution Research*, 23(1), 546–555. <https://doi.org/10.1007/s11356-015-5290-0>

O'Connor, C. S., Lepp, N. W., Edwards, R., & Sunderland, G. (2003). The Combined Use of Electrokinetic Remediation and Phytoremediation to Decontaminate Metal-Polluted Soils: A Laboratory-Scale Feasibility Study. *Environmental Monitoring and Assessment*, 84(1), 141–158. <https://doi.org/10.1023/A:1022851501118>

Pamukcu, S., & Kenneth Wittle, J. (1992). Electrokinetic removal of selected heavy metals from soil. *Environmental Progress*, 11(3), 241–250. <https://doi.org/10.1002/ep.670110321>

Pavesi, T., & Moreira, J. C. (2020). Mechanisms and individuality in chromium toxicity in humans. *Journal of Applied Toxicology*, 40(9), 1183–1197. <https://doi.org/10.1002/jat.3965>

Pedersen, K. B., Jensen, P. E., Ottosen, L. M., & Barlindhaug, J. (2018). The relative influence of electrokinetic remediation design on the removal of As, Cu, Pb and Sb from shooting range soils. *Engineering Geology*, 238, 52–61. <https://doi.org/10.1016/j.enggeo.2018.03.005>

Pei, L., Zhang, X., & Yuan, Z. (2023). Iron-Based Amorphous Alloy Enhanced Electrokinetic Method for Remediation of Copper-Contaminated Soil. *Transactions of the Indian Institute of Metals*. <https://doi.org/10.1007/s12666-023-03018-9>

Peng, G., & Tian, G. (2010). Using electrode electrolytes to enhance electrokinetic removal of heavy metals from electroplating sludge. *Chemical Engineering Journal*, 165(2), 388–394. <https://doi.org/10.1016/j.cej.2010.10.006>

Popescu, M., Rosales, E., Sandu, C., Meijide, J., Pazos, M., Lazar, G., & Sanromán, M. A. (2017). Soil flushing and simultaneous degradation of organic pollutants in soils by electrokinetic-Fenton treatment. *Process Safety and Environmental Protection*, *108*, 99–107. <https://doi.org/10.1016/j.psep.2016.03.012>

Prakash, P., Sonal, S., & Mishra, B. K. (2022a). Transportation mechanism of chromium from tannery sludge through an electrokinetic process: Role of electrolytes and operational conditions. *International Journal of Environmental Science and Technology*, *19*(5), 3757–3772. <https://doi.org/10.1007/s13762-021-03278-2>

Prakash, P., Sonal, S., & Mishra, B. K. (2022b). Transportation mechanism of chromium from tannery sludge through an electrokinetic process: Role of electrolytes and operational conditions. *International Journal of Environmental Science and Technology*, *19*(5), 3757–3772. <https://doi.org/10.1007/S13762-021-03278-2/TABLES/7>

Qiu, L. (2020). Study on Electrokinetic Remediation of Cadmium-contaminated Soil. *Agricultural Biotechnology*, *9*(2), 82–88.

Qu, Z., Huang, L., Guo, M., Sun, T., Xu, X., & Gao, Z. (2023). Application of novel polypyrrole/melamine foam auxiliary electrode in promoting electrokinetic remediation of Cr(VI)-contaminated soil. *Science of The Total Environment*, *876*, 162840. <https://doi.org/10.1016/j.scitotenv.2023.162840>

Raffa, C. M., Chiampo, F., & Shanthakumar, S. (2021). Remediation of Metal/Metalloid-Polluted Soils: A Short Review. *Applied Sciences*, *11*(9), Article 9. <https://doi.org/10.3390/app11094134>

Rajendiran, S., Dotaniya, M. L., Coumar, M. V., Panwar, N. R., & Saha, J. K. (2015). Heavy metal polluted soils in India: Status and countermeasures. *JNKVV Res J*, 49(3), 320–337.

Rajić, L., Dalmacija, B., Dalmacija, M., Rončević, S., & Ugarčina Perović, S. (2012). Enhancing electrokinetic lead removal from sediment: Utilizing the moving anode technique and increasing the cathode compartment length. *Electrochimica Acta*, 86, 36–40. <https://doi.org/10.1016/j.electacta.2012.02.029>

Reddy, K. R., Cameselle, C., & Ala, P. (2010). Integrated electrokinetic-soil flushing to remove mixed organic and metal contaminants. *Journal of Applied Electrochemistry*, 40(6), 1269–1279. <https://doi.org/10.1007/s10800-010-0102-1>

Reddy, K. R., & Chinthamreddy, S. (2004a). Enhanced Electrokinetic Remediation of Heavy Metals in Glacial Till Soils Using Different Electrolyte Solutions. *Journal of Environmental Engineering*, 130(4), 442–455. [https://doi.org/10.1061/\(ASCE\)0733-9372\(2004\)130:4\(442\)](https://doi.org/10.1061/(ASCE)0733-9372(2004)130:4(442))

Reddy, K. R., & Chinthamreddy, S. (2004b). Enhanced Electrokinetic Remediation of Heavy Metals in Glacial Till Soils Using Different Electrolyte Solutions. *Journal of Environmental Engineering*, 130(4), 442–455. [https://doi.org/10.1061/\(asce\)0733-9372\(2004\)130:4\(442\)](https://doi.org/10.1061/(asce)0733-9372(2004)130:4(442))

Reddy, K. R., Chinthamreddy, S., & Al-Hamdan, A. (2001). Synergistic Effects of Multiple Metal Contaminants on Electrokinetic Remediation of Soils. *Remediation*, 11(3), 85–109. <https://doi.org/10.1002/rem.1006>



Reddy, K. R., Parupudi, U. S., Devulapalli, S. N., & Xu, C. Y. (1997). Effects of soil composition on the removal of chromium by electrokinetics. *Journal of Hazardous Materials*, 55(1–3), 135–158. [https://doi.org/10.1016/S0304-3894\(97\)00020-4](https://doi.org/10.1016/S0304-3894(97)00020-4)

Reddy, K. R., & Shirani, A. B. (1997). Electrokinetic remediation of metal contaminated glacial tills. *Geotechnical & Geological Engineering*, 15(1), 3–29. <https://doi.org/10.1007/BF00881236>

Reddy, K. R., Xu, C. Y., & Chinthamreddy, S. (2001). Assessment of electrokinetic removal of heavy metals from soils by sequential extraction analysis. *Journal of Hazardous Materials*, 84(2–3), 279–296.

Saleem, M., Chakrabarti, M. H., Irfan, M. F., Hajimolana, S. A., Hussain, M. A., Diya'uddeen, B. H., & Daud, W. M. A. W. (2011). Electrokinetic Remediation of Nickel From Low Permeability Soil. *International Journal of Electrochemical Science*, 6(9), 4264–4275. [https://doi.org/10.1016/S1452-3981\(23\)18326-X](https://doi.org/10.1016/S1452-3981(23)18326-X)

Shariatmadari, N., Weng, C.-H., & Daryaei, H. (2009). Enhancement of Hexavalent Chromium [Cr(VI)] Remediation from Clayey Soils by Electrokinetics Coupled with a Nano-Sized Zero-Valent Iron Barrier. *Environmental Engineering Science*, 26(6), 1071–1079. <https://doi.org/10.1089/ees.2008.0257>

Shen, Z., Chen, X., Jia, J., Qu, L., & Wang, W. (2007). Comparison of electrokinetic soil remediation methods using one fixed anode and approaching anodes. *Environmental Pollution*, 150(2), 193–199. <https://doi.org/10.1016/j.envpol.2007.02.004>

Shen, Z., Jin, F., O'Connor, D., & Hou, D. (2019). Solidification/Stabilization for Soil Remediation: An Old Technology with New Vitality. *Environmental Science & Technology*, 53(20), 11615–11617. <https://doi.org/10.1021/acs.est.9b04990>

Silva, K. N. O., Paiva, S. S. M., Souza, F. L., Silva, D. R., Martínez-Huitle, C. A., & Santos, E. V. (2018). Applicability of electrochemical technologies for removing and monitoring Pb<sup>2+</sup> from soil and water. *Journal of Electroanalytical Chemistry*, 816, 171–178. <https://doi.org/10.1016/j.jelechem.2018.03.051>

Siyar, R., Doulati Ardejani, F., Farahbakhsh, M., Norouzi, P., Yavarzadeh, M., & Maghsoudy, S. (2020). Potential of Vetiver grass for the phytoremediation of a real multi-contaminated soil, assisted by electrokinetic. *Chemosphere*, 246, 125802. <https://doi.org/10.1016/j.chemosphere.2019.125802>

Song, T.-S., Zhang, J., Hou, S., Wang, H., Zhang, D., Li, S., & Xie, J. (2018). In situ electrokinetic remediation of toxic metal-contaminated soil driven by solid phase microbial fuel cells with a wheat straw addition. *Journal of Chemical Technology & Biotechnology*, 93(10), 2860–2867. <https://doi.org/10.1002/jctb.5638>

Song, Y., Ammami, M. T., Benamar, A., Mezazigh, S., & Wang, H. (2016a). Effect of EDTA, EDDS, NTA and citric acid on electrokinetic remediation of As, Cd, Cr, Cu, Ni, Pb and Zn contaminated dredged marine sediment. *Environmental Science and Pollution Research*, 23(11), 10577–10586. <https://doi.org/10.1007/s11356-015-5966-5>

Song, Y., Ammami, M.-T., Benamar, A., Mezazigh, S., & Wang, H. (2016b). Effect of EDTA, EDDS, NTA and citric acid on electrokinetic remediation of As, Cd, Cr, Cu, Ni, Pb

and Zn contaminated dredged marine sediment. *Environmental Science and Pollution Research*, 23(11), 10577–10586. <https://doi.org/10.1007/s11356-015-5966-5>

Song, Y., Benamar, A., Mezazigh, S., & Wang, H. (2018). Citric Acid-Enhanced Electroremediation of Toxic Metal-Contaminated Dredged Sediments: Effect of Open/Closed Orifice Condition, Electric Potential and Surfactant. *Pedosphere*, 28(1), 35–43. [https://doi.org/10.1016/S1002-0160\(18\)60003-7](https://doi.org/10.1016/S1002-0160(18)60003-7)

Song, Y., Cang, L., Xu, H., Wu, S., & Zhou, D. (2019). Migration and decomplexation of metal-chelate complexes causing metal accumulation phenomenon after chelate-enhanced electrokinetic remediation. *Journal of Hazardous Materials*, 377, 106–112. <https://doi.org/10.1016/j.jhazmat.2019.05.055>

Song, Y., Cang, L., Zuo, Y., Yang, J., Zhou, D., Duan, T., & Wang, R. (2020). EDTA-enhanced electrokinetic remediation of aged electroplating contaminated soil assisted by combining dual cation-exchange membranes and circulation methods. *Chemosphere*, 243, 125439. <https://doi.org/10.1016/j.chemosphere.2019.125439>

Souilah, O., Akretche, D. E., & Cameselle, C. (2012). Electroremediation of contaminated soil by heavy metals using ion exchange fibers. *Electrochimica Acta*, 86, 138–141. <https://doi.org/10.1016/j.electacta.2012.04.089>

Sun, H., Song, Y., Liu, W., Zhang, M., Duan, T., & Cai, Y. (2023). Coupling soil washing with chelator and cathodic reduction treatment for a multi-metal contaminated soil: Effect of pH controlling. *Electrochimica Acta*, 448, 142178. <https://doi.org/10.1016/j.electacta.2023.142178>

Sun, R., Gong, W., Chen, Y., Hong, J., & Wang, Y. (2021a). Influence of polarity exchange frequency on electrokinetic remediation of Cr-contaminated soil using DC and solar energy. *Process Safety and Environmental Protection*, *153*, 117–129. <https://doi.org/10.1016/j.psep.2021.07.008>

Sun, R., Gong, W., Chen, Y., Hong, J., & Wang, Y. (2021b). Influence of polarity exchange frequency on electrokinetic remediation of Cr-contaminated soil using DC and solar energy. *Process Safety and Environmental Protection*, *153*, 117–129. <https://doi.org/10.1016/J.PSEP.2021.07.008>

Sun, T. R., & Ottosen, L. M. (2012). Effects of pulse current on energy consumption and removal of heavy metals during electro-dialytic soil remediation. *Electrochimica Acta*, *86*, 28–35. <https://doi.org/10.1016/j.electacta.2012.04.033>

Sun, T. R., Ottosen, L. M., Jensen, P. E., & Kirkelund, G. M. (2013). Effect of pulse current on acidification and removal of Cu, Cd, and As during suspended electro-dialytic soil remediation. *Electrochimica Acta*, *107*, 187–193. <https://doi.org/10.1016/j.electacta.2013.05.138>

Sun, Z., Wu, B., Guo, P., Wang, S., & Guo, S. (2019). Enhanced electrokinetic remediation and simulation of cadmium-contaminated soil by superimposed electric field. *Chemosphere*, *233*, 17–24. <https://doi.org/10.1016/j.chemosphere.2019.05.233>

Suzuki, T., Kawai, K., Moribe, M., & Niinae, M. (2014). Recovery of Cr as Cr(III) from Cr(VI)-contaminated kaolinite clay by electrokinetics coupled with a permeable reactive barrier. *Journal of Hazardous Materials*, *278*, 297–303. <https://doi.org/10.1016/j.jhazmat.2014.05.086>

Tajudin, S. A. A., Azmi, M. A. M., & Nabila, A. T. A. (2016). Stabilization/Solidification Remediation Method for Contaminated Soil: A Review. *IOP Conference Series: Materials Science and Engineering*, 136(1), 012043. <https://doi.org/10.1088/1757-899X/136/1/012043>

Taneja, S., Karaca, O., & Haritash, A. K. (2023a). Combined effects of high voltage gradient and electrolyte conditioning on electrokinetic remediation for chromium (VI)-contaminated soils. *Rendiconti Lincei. Scienze Fisiche e Naturali*, 34(2), 635–646. <https://doi.org/10.1007/s12210-023-01159-z>

Taneja, S., Karaca, O., & Haritash, A. K. (2023b). Treatment of Pb-contaminated soil by electrokinetics: Enhancements by varying voltage, chelant, and electrode material. *Journal of Geochemical Exploration*, 250, 107240. <https://doi.org/10.1016/j.gexplo.2023.107240>

Taneja, S., Karaca, O., & Haritash, A. K. (2024). Electrokinetic remediation: Past experiences and future roadmap for sustainable remediation of metal-contaminated soils. *Journal of Geochemical Exploration*, 259, 107437. <https://doi.org/10.1016/j.gexplo.2024.107437>

Taneja, S., Yadav, S., Pipil, H., Karaca, O., & Haritash, A. K. (2023). Soil–Water Interactions and Arsenic Enrichment in Groundwater. In *Hydrogeochemistry of Aquatic Ecosystems* (pp. 97–120). John Wiley & Sons, Ltd. <https://doi.org/10.1002/9781119870562.ch5>

Tang, J., He, J., Liu, T., Xin, X., & Hu, H. (2017). Removal of heavy metal from sludge by the combined application of a biodegradable biosurfactant and complexing agent in

enhanced electrokinetic treatment. *Chemosphere*, 189, 599–608.  
<https://doi.org/10.1016/j.chemosphere.2017.09.104>

Tang, J., Qiu, Z., Tang, H., Wang, H., Sima, W., Liang, C., Liao, Y., Li, Z., Wan, S., & Dong, J. (2021). Coupled with EDDS and approaching anode technique enhanced electrokinetic remediation removal heavy metal from sludge. *Environmental Pollution*, 272, 115975. <https://doi.org/10.1016/j.envpol.2020.115975>

Tessier, A., Campbell, P. G. C., & Bisson, M. (1979). Sequential extraction procedure for the speciation of particulate trace metals. *Analytical Chemistry*, 51(7), 844–851.  
<https://doi.org/10.1021/ac50043a017>

Tsui, L., Paul, A., Chen, Y.-T., & Tz-Chi, E. (2022). Potential mechanisms contributing to the high cadmium removal efficiency from contaminated soil by using effective microorganisms as novel electrolyte in electrokinetic remediation applications. *Environmental Research*, 215, 114239. <https://doi.org/10.1016/j.envres.2022.114239>

Turer, D., & Genc, A. (2005). Assessing effect of electrode configuration on the efficiency of electrokinetic remediation by sequential extraction analysis. *Journal of Hazardous Materials*, 119(1), 167–174. <https://doi.org/10.1016/j.jhazmat.2004.12.003>

Virkutyte, J., Sillanpää, M., & Latostenmaa, P. (2002). Electrokinetic soil remediation—Critical overview. *Science of The Total Environment*, 289(1), 97–121.  
[https://doi.org/10.1016/S0048-9697\(01\)01027-0](https://doi.org/10.1016/S0048-9697(01)01027-0)

Wang, J., Hou, L., Yao, Z., Jiang, Y., Xi, B., Ni, S., & Zhang, L. (2021). Aminated electrospun nanofiber membrane as permeable reactive barrier material for effective in-situ

Cr(VI) contaminated soil remediation. *Chemical Engineering Journal*, 406, 126822.  
<https://doi.org/10.1016/j.cej.2020.126822>

Wang, J., Yu, Q., Zheng, Y., Li, J., Jiao, B., & Li, D. (2022). Adsorption and reduction from modified polypyrrole enhance electrokinetic remediation of hexavalent chromium-contaminated soil. *Environmental Science and Pollution Research*, 29(29), 44845–44861.  
<https://doi.org/10.1007/s11356-022-18998-2>

Wang, L., Huang, L., Xia, H., Li, H., Li, X., & Liu, X. (2019). Application of a multi-electrode system with polyaniline auxiliary electrodes for electrokinetic remediation of chromium-contaminated soil. *Separation and Purification Technology*, 224, 106–112.  
<https://doi.org/10.1016/j.seppur.2019.05.019>

Wang, Y., Huang, L., Wang, Z., Wang, L., Han, Y., Liu, X., & Ma, T. (2019). Application of Polypyrrole flexible electrode for electrokinetic remediation of Cr(VI)-contaminated soil in a main-auxiliary electrode system. *Chemical Engineering Journal*, 373, 131–139.  
<https://doi.org/10.1016/j.cej.2019.05.016>

Wu, J., Zhang, J., & Xiao, C. (2016). Focus on factors affecting pH, flow of Cr and transformation between Cr(VI) and Cr(III) in the soil with different electrolytes. *Electrochimica Acta*, 211, 652–662. <https://doi.org/10.1016/j.electacta.2016.06.048>

Wuana, R. A., & Okieimen, F. E. (2011). Heavy metals in contaminated soils: A review of sources, chemistry, risks and best available strategies for remediation. *International Scholarly Research Notices*, 2011.  
<https://downloads.hindawi.com/archive/2011/402647.pdf>

Xu, H., Zhang, C., Zhang, H., Qiao, H., Zhang, L., & Zhao, Y. (2022). Enhanced electrokinetic remediation of heterogeneous aquifer co-contaminated with Cr(VI) and nitrate by rhamnolipids. *Journal of Environmental Chemical Engineering*, *10*(5), 108531. <https://doi.org/10.1016/j.jece.2022.108531>

Xu, J., Ma, Q., Chen, C., Wu, Q., & Long, X. (2020). Cadmium adsorption behavior of porous and reduced graphene oxide and its potential for promoting cadmium migration during soil electrokinetic remediation. *Chemosphere*, *259*, 127441. <https://doi.org/10.1016/j.chemosphere.2020.127441>

Xu, Y., Lu, Q., Li, J., Wan, L., Chen, S., & Lu, Y. (2021). Effect of humus on the remediation of arsenic-contaminated soil by electrokinetic technology. *Environmental Technology & Innovation*, *21*, 101297. <https://doi.org/10.1016/j.eti.2020.101297>

Xu, Y., Xu, X., Hou, H., Zhang, J., Zhang, D., & Qian, G. (2016). Moisture content-affected electrokinetic remediation of Cr(VI)-contaminated clay by a hydrocalumite barrier. *Environmental Science and Pollution Research*, *23*(7), 6517–6523. <https://doi.org/10.1007/s11356-015-5685-y>

Xue, F., Yan, Y., Xia, M., Muhammad, F., Yu, L., Xu, F., Shiao, Y., Li, D., & Jiao, B. (2017). Electro-kinetic remediation of chromium-contaminated soil by a three-dimensional electrode coupled with a permeable reactive barrier. *RSC Advances*, *7*(86), 54797–54805. <https://doi.org/10.1039/C7RA10913J>

Yan, Y., Wan, B., Mansor, M., Wang, X., Zhang, Q., Kappler, A., & Feng, X. (2022). Co-sorption of metal ions and inorganic anions/organic ligands on environmental minerals: A



- review. *Science of The Total Environment*, 803, 149918.  
<https://doi.org/10.1016/j.scitotenv.2021.149918>
- Yan, Y., Xue, F., Muhammad, F., Yu, L., Xu, F., Jiao, B., Shiao, Y., & Li, D. (2018). Application of iron-loaded activated carbon electrodes for electrokinetic remediation of chromium-contaminated soil in a three-dimensional electrode system. *Scientific Reports*, 8(1), Article 1. <https://doi.org/10.1038/s41598-018-24138-z>
- Yang, X., Zhou, M., Cang, L., Ji, Q., & Xie, J. (2020). Enhanced Electrokinetic Remediation of Heavy-Metals Contaminated Soil in presence tetrasodium N, N-bis(carboxymethyl) glutamic acid (GLDA) as chelator. *International Journal of Electrochemical Science*, 15(1), 696–709. <https://doi.org/10.20964/2020.01.15>
- Yellishetty, M., Ranjith, P. G., & Kumar, D. L. (2009). Metal concentrations and metal mobility in unsaturated mine wastes in mining areas of Goa, India. *Resources, Conservation and Recycling*, 53(7), 379–385.  
<https://doi.org/10.1016/j.resconrec.2009.02.005>
- Yeung, A. T., Hsu, C., & Menon, R. M. (1997). Physicochemical soil-contaminant interactions during electrokinetic extraction. *Journal of Hazardous Materials*, 55(1), 221–237. [https://doi.org/10.1016/S0304-3894\(97\)00017-4](https://doi.org/10.1016/S0304-3894(97)00017-4)
- Yuan, C., & Chiang, T.-S. (2007). The mechanisms of arsenic removal from soil by electrokinetic process coupled with iron permeable reaction barrier. *Chemosphere*, 67(8), 1533–1542. <https://doi.org/10.1016/j.chemosphere.2006.12.008>

Yuan, L., Li, H., Xu, X., Zhang, J., Wang, N., & Yu, H. (2016). Electrokinetic remediation of heavy metals contaminated kaolin by a CNT-covered polyethylene terephthalate yarn cathode. *Electrochimica Acta*, 213, 140–147. <https://doi.org/10.1016/j.electacta.2016.07.081>

Yuan, S., Zheng, Z., Chen, J., & Lu, X. (2009). Use of solar cell in electrokinetic remediation of cadmium-contaminated soil. *Journal of Hazardous Materials*, 162(2), 1583–1587. <https://doi.org/10.1016/j.jhazmat.2008.06.038>

Zeng, Q. R., Sauvé, S., Allen, H. E., & Hendershot, W. H. (2005). Recycling EDTA solutions used to remediate metal-polluted soils. *Environmental Pollution*, 133(2), 225–231. <https://doi.org/10.1016/j.envpol.2004.06.006>

Zhang, J., Xu, Y., Li, W., Zhou, J., Zhao, J., Qian, G., & Xu, Z. P. (2012). Enhanced remediation of Cr(VI)-contaminated soil by incorporating a calcined-hydrotalcite-based permeable reactive barrier with electrokinetics. *Journal of Hazardous Materials*, 239–240, 128–134. <https://doi.org/10.1016/j.jhazmat.2012.08.039>

Zhang, P., Jin, C., Sun, Z., Huang, G., & She, Z. (2016). Assessment of Acid Enhancement Schemes for Electrokinetic Remediation of Cd/Pb Contaminated Soil. *Water, Air, & Soil Pollution*, 227(6), 217. <https://doi.org/10.1007/s11270-016-2879-y>

Zhang, S., Zhang, J., Cheng, X., Mei, Y., Hu, C., Wang, M., & Li, J. (2015). Electrokinetic remediation of soil containing Cr(VI) by photovoltaic solar panels and a DC-DC converter. *Journal of Chemical Technology & Biotechnology*, 90(4), 693–700. <https://doi.org/10.1002/jctb.4359>

Zhang, T., Zou, H., Ji, M., Li, X., Li, L., & Tang, T. (2014). Enhanced electrokinetic remediation of lead-contaminated soil by complexing agents and approaching anodes. *Environmental Science and Pollution Research*, 21(4), 3126–3133. <https://doi.org/10.1007/s11356-013-2274-9>

Zhang, Y., Boparai, H. K., Wang, J., & Sleep, B. E. (2022). Effect of low permeability zone location on remediation of Cr(VI)-contaminated media by electrokinetics combined with a modified-zeolite barrier. *Journal of Hazardous Materials*, 426, 127785. <https://doi.org/10.1016/j.jhazmat.2021.127785>

Zhao, M., Ma, D., Wang, Q., Wang, Y., & Sun, X. (2022). Electrokinetic remediation of Cd-contaminated soil using low voltage gradients coupled with array adsorption zone and polarity exchange. *Process Safety and Environmental Protection*, 157, 81–91. <https://doi.org/10.1016/j.psep.2021.11.001>

Zhou, D.-M., Deng, C.-F., Cang, L., & Alshwabkeh, A. N. (2005). Electrokinetic remediation of a Cu–Zn contaminated red soil by controlling the voltage and conditioning catholyte pH. *Chemosphere*, 61(4), 519–527. <https://doi.org/10.1016/j.chemosphere.2005.02.055>

Zhou, H., Xu, J., Lv, S., Liu, Z., & Liu, W. (2020). Removal of cadmium in contaminated kaolin by new-style electrokinetic remediation using array electrodes coupled with permeable reactive barrier. *Separation and Purification Technology*, 239, 116544. <https://doi.org/10.1016/j.seppur.2020.116544>



## ANNEXURE 1

### LIST OF PUBLICATIONS

1. Taneja, S., Karaca, O., & Haritash, A. K. (2024). Electrokinetic remediation: Past experiences and future roadmap for sustainable remediation of metal-contaminated soils. *Journal of Geochemical Exploration*, 259, 107437.
2. Taneja, S., Karaca, O., & Haritash, A. K. (2023). Treatment of Pb-contaminated soil by electrokinetics: Enhancements by varying voltage, chelant, and electrode material. *Journal of Geochemical Exploration*, 250, 107240.
3. Taneja, S., Karaca, O., & Haritash, A. K. (2023). Combined effects of high voltage gradient and electrolyte conditioning on electrokinetic remediation for chromium (VI)-contaminated soils. *Rendiconti Lincei. Scienze Fisiche e Naturali*, 34(2), 635-646.
4. Taneja, S., Yadav, S., Pipil, H., Karaca, O., & Haritash, A. K. (2023). Soil-water interactions and arsenic enrichment in groundwater. *Hydrogeochemistry of Aquatic Ecosystems*, 97-120.
5. Radhakrishnan, N., Taneja, S., Ambastha, S., Pipil, H., & Haritash, A. K. (2023). Heavy metal profile, mobility, and source characterization in size-fractionated bed-sediments of River Ganga, India. *Marine Pollution Bulletin*, 188, 114650.
6. Pipil, H., Yadav, S., Chawla, H., Taneja, S., Verma, M., Singla, N., & Haritash, A. K. (2022). Comparison of TiO<sub>2</sub> catalysis and Fenton's treatment for rapid degradation of Remazol Red Dye in textile industry effluent. *Rendiconti Lincei. Scienze Fisiche e Naturali*, 33(1), 105-114.

7. Singh, P., Taneja, S., & Haritash, A. K. (2022). Removal of Nutrients from Simulated Wastewater by Canna-based Wetland Mesocosms. *Environ. We Int. J. Sci. Tech.* 17 (2022) 25-31.

**Book Chapter:**

1. Taneja, S., Yadav, S., Pipil, H., Karaca, O., & Haritash, A. K. (2023). Soil–Water Interactions and Arsenic Enrichment in Groundwater. *Hydrogeochemistry of Aquatic Ecosystems*, 97-120.

**Conference Proceedings:**

1. Taneja, S., Karaca, O., & Haritash, A. K. (2023). Investigating the effect of electrode configuration on pH distribution and conductivity of soil during the Electrokinetic Remediation of multi-metal-contaminated soil. *In proceedings of 4th International Symposium of Engineering Applications on Civil Engineering and Earth Sciences 2023 (IEACES2023), Karabuk, Turkey.* (pp. 366).
2. Taneja, S., Chawla, H., Pipil, H., Yadav, S., Karaca, O., & Haritash, A. K. (2022). Sustainable Treatment of Metal-Contaminated Soil by Electrokinetic Remediation. In *Proceedings of International Conference on Innovative Technologies for Clean and Sustainable Development (ICITCSD–2021)* (pp. 75-84). Cham: Springer International Publishing.

## ANNEXURE II

### CURRICULUM VITAE

#### SONAM TANEJA

House No. 12 Sector- 22, Faridabad, Haryana-121005

[sonamtaneja123@gmail.com](mailto:sonamtaneja123@gmail.com), +91-9971191936

#### EDUCATION BACKGROUND

---

2020-Present	<b>Ph.D. Environmental Engineering</b> Delhi Technological University, Delhi, Çanakkale Onsekiz Mart University, Turkey <i>Dissertation title:</i> Electrokinetic Remediation of Metal-Contaminated Soils
2017-2019	<b>M.Sc. Environmental Sciences</b> J.C. Bose University of Science and Technology, YMCA, Faridabad <i>Dissertation title:</i> Assessment of tree cover change in Shivalik Hills of Punjab using Geospatial Techniques.
2014-2017	<b>B.Sc. Life Sciences</b> Dyal Singh College, University of Delhi

#### PROJECTS AND RESEARCH EXPERIENCE

---

Jan-Dec, 2023	<b>BAP Project, Turkey</b> <ul style="list-style-type: none"><li>Electrokinetic Remediation of Soils Contaminated with Mixed Metals” (Project ID: FHD-2023-4399).</li></ul>
April-Aug, 2024	<b>Consultancy Project</b> <ul style="list-style-type: none"><li>“Inspection of GPIs along the main stem rivers of Ganga and Yamuna for the year 2023-2024” funded by NMCG, Ministry of Jal Shakti, Government of India.</li></ul>
Sept-Dec 2019	<b>Research Intern, <i>The Celestial Earth, Gurgaon</i></b> <ul style="list-style-type: none"><li>Project title “GoI-GEF-UNDP SECURE Himalaya Project on Biodiversity and Ecosystem Services (BDES) evaluation”</li></ul>

and “State Biodiversity Strategy and Action plan (SBSAP) of Ladakh and J&K.”

- Prepared Handbook for Conservation of Snow Leopard in Ladakh and J&K.

Feb- June 2019

**M.Sc. Dissertation, *IORA Ecological Solutions Pvt. Ltd., New Delhi***

- Project title ‘Assessment of Tree cover change in Shivalik Hills of Punjab using geospatial techniques’.
- Prepared Land use and land cover maps using remote sensing and GIS software.

June-July, 2018

**Summer Intern, *NHPC LIMITED, Faridabad***

- Project title ‘Biodiversity and Hydropower Projects (HEPs) in Beas River Basin, Himachal Pradesh’.
- Analysed the impact of HEPs on biodiversity, especially Indus Dolphin, using Environmental Impact Assessment (EIA) studies.

Jan-May, 2018

**Intern, *J.C. Bose University of Science and Technology, YMCA***

- Project title ‘Solid Waste Management- Survey of MSW of 100 Houses and Vermicomposting of Household Waste.’
- Prepared compost using earthworm species *Eisenia foetida*.

## **TRAINING**

---

- Feb, 2023- June 2023 Visiting Scholar at Çanakkale Onsekiz Mart University (ÇOMU), Çanakkale, Turkey (5 months)
- Course on ‘Advanced Biological Nutrient Removal from Wastewater’ at ÇOMU, Turkey (5 months)
- Webinar training on ‘Land-use/Land cover Mapping using QGIS’ conducted by TGIS Lab, Ahmedabad.
- Qualified UGC NET-JRF Environmental Sciences (2020)
- Certificate course on ‘Wastewater Recycling and Treatment’ and ‘Remote Sensing and Digital Image Processing of Satellite Data’, conducted by NPTEL.
- Short course on ‘Climate Change and Sustainable Infrastructure Development’, held by YMCA, Faridabad.



- Organised one-day workshop with The Celestial Earth and UNDP on ‘Biodiversity and Ecosystem Services Valuation in Ladakh.’

## **CONFERENCES ATTENDED**

---

- Presented a paper titled ‘Investigating the effect of electrode configuration on pH distribution and conductivity of soil during the Electrokinetic Remediation of multi-metal-contaminated Soils’ at 4th International Symposium of Engineering Applications on Civil Engineering and Earth Sciences (IEACES, 2023, Karabuk, Turkey).
- Presented a paper titled “Sustainable Treatment of Metal-Contaminated Soil by Electrokinetic Remediation” at International Conference on Innovative Technologies for Clean and Sustainable Development (ITCSD-2020), Chitkara University, Himachal Pradesh and NITTTR, Chandigarh
- Participated in an International Seminar on ‘Sustainable Technologies for Environmental Management (STEM-18)’, Department of Environmental Engineering, Delhi Technological University.

## **PROFICIENCY**

---

- Fluent in English, Hindi, and French (level 1)
- Hands-on experience with software, Microsoft Office Suite (Word, PowerPoint, and Excel), ERDAS 2015, ArcGIS 10, QGIS, and Google Earth Pro
- Hands-on experience with analytical instruments, Atomic Absorption Spectrophotometer (AAS), UV-VIS Spectrophotometer, Flame Photometer, TOC Analyzer, water quality monitoring hand-held instruments.